# The isolation and culture of human ovarian microvascular endothelial cells

Kirsty Elizabeth Ratcliffe

UNIVERSITY OF SOUTHAMPTON

ABSTRACT

FACULTY OF MEDICINE

OBSTETRICS AND GYNAECOLOGY

Doctor of Philosophy

# THE ISOLATION AND CULTURE OF HUMAN OVARIAN MICROVASCULAR ENDOTHELIAL CELLS

by Kirsty Elizabeth Ratcliffe

The development of the corpus luteum is characterised by a period of extensive vascularisation, as the capillaries in the theca layer of the collapsed follicle invade the previously avascular granulosa layer. This invasion of endothelial cells is thought to be mediated by growth factors such as VEGF. In order to study these processes *in vitro* we have developed a model system for the isolation and culture of human ovarian microvascular endothelial cells (HOMEC).

Follicular aspirates, obtained at oocyte recovery for in vitro fertilisation were filtered to obtain fragments of follicle wall. These were set in Matrigel and cultured to allow the growth of cells through the matrix. Cells formed capillary-like structures in association with the Matrigel and upon emergence onto the uncoated surface of the culture flask, formed the characteristic endothelial cell cobblestone monolayer. Immunocytochemistry demonstrated that the cells possessed all of the endothelial cell specific markers, and also constitutively expressed VCAM-1 which is normally associated with stimulated endothelial cells.

The development of an endothelial/granulosa cell co-culture model showed specific cellular architecture. Granulosa cell clusters were linked together by endothelial capillary-like structures. These studies indicate that there is intercellular communication between the cells of the corpus luteum and that these interactions can be modelled *in vitro*.

The presence of both VEGF receptors, flt-1 and KDR, and the endothelial nitric oxide synthase was demonstrated by RT-PCR for HOMEC, therefore, all the constituents for important endothelial mechanisms in relation to VEGF action are in place in these cells. Studies showed a dose dependent increase in HOMEC proliferation in response to VEGF. This proliferative effect in HUVEC could be blocked with an anti-KDR antibody but was not affected by an anti-flt-1 antibody, indicating that the two VEGF receptors have different functions, and that binding of VEGF to KDR elicits the mitogenic effect of VEGF. Furthermore it was shown that the proliferative effect of VEGF on both HOMEC and HUVEC could be blocked with a nitric oxide synthase inhibitor, demonstrating the importance of nitric oxide production on the mitogenic effect of VEGF.

# TABLE OF CONTENTS

CHAPTER 3

CHARACTERISATION OF THE ENDOTHELIAL NATURE OF CELLS GROWN FROM FOLLICULAR FRAGMENTS BY IMMUNOCYTOCHEMISTRY

CHAPTER 7

ENDOTHELIAL CELL PROLIFERATION IN RESPONSE TO VEGF, BFGF, VEGF RECEPTOR BLOCKING ANTIBODIES AND NITRIC OXIDE INHIBITORS

CHAPTER 8

ENDOTHELIAL/GRANULOSA CELL INTERACTIONS IN CO-CULTURE: FORMATION OF SPECIFIC SPATIAL INTER-RELATIONSHIPS



CHAPTER 9

# LIST OF TABLES AND FIGURES

CHAPTER 1



CHAPTER 2



CHAPTER 3

CHAPTER 4

CHAPTER 5



CHAPTER 6

CHAPTER 7



CHAPTER 8

# ACKNOWLEDGEMENTS

I wish to thank the following people for providing me with guidance and support during the completion of this thesis.

I wish to thank all of the members of the department of Obstetrics and Gynaecology, Princess Anne Hospital, Southampton. I would especially like to thank Mr R. W. Stones for managing my project. His continual support, enthusiasm and good humour have made the completion of this thesis possible. A special thank you must also go to Dr. F. W. Anthony and Dr. M. C. Richardson for their knowledge and assistance in the laboratory, as well as their support in the writing of this thesis. Karen Creed and Hazel Hills deserve a special mention for their help in all matters relating to computers. I would like to thank Sister Maggie Barron for the constant supply of umbilical cords and Dr. I. Stewart and Dr. D. Muktar for the use of the time lapse video equipment and their advise on laboratory procedures. Roger Alston's help with the confocal microscope is greatly appreciated as is Anton Paige's assistance with sectioning and electron microscopy. I must say thank you to my colleagues Sarah Morland, Phillippa Neville, Angeliki Komentakis, Pat Engelfield and Joanna Gale for their friendship which has made my time in Southampton so enjoyable.

Finally and most importantly I would like to acknowledge my parents Norma and John Ratcliffe who have always supported me. Their constant encouragement and love have given me the courage to pursue my dreams and ambitions.

# PUBLICATIONS AND PRESENTATIONS

## ORAL PRESENTATIONS

**K. E. Ratcliffe, F. W. Anthony, M. C. Richardson and R. W. Stones.** Ovarian microvascular endothelium: a new culture model. *National Ovarian Workshop* 1998.

**K. E. Ratcliffe, F. W. Anthony, M. C. Richardson and R. W. Stones.** Modelling endothelial/granulosa cell interactions: formation of specific spatial inter-relationships in culture. *National Ovarian Workshop* 1999.

**S. Llewellyn, K. E. Ratcliffe, F. W. Anthony and M. C. Richardson.** Production of vascular endothelial growth factor by luteinised granulosa cells in culture. *National Ovarian Workshop* 1999.

## ABSTRACTS

**K. E. Ratcliffe, F. W. Anthony, M. C. Richardson and R. W. Stones.** (1999) Effects of luteinised granulosa cell products on endothelial cells in culture. *Journal of Reproduction and Fertility* **23**, 69.

## PUBLICATIONS

**K. E. Ratcliffe, F. W. Anthony, M. C. Richardson and R. W. Stones.** (1999) Morphology and functional characteristics of human ovarian microvascular endothelium. *Human Reproduction*, 14, 1549-1554.

**K. E. Ratcliffe, F. W. Anthony, M. C. Richardson and R. W. Stones.** Modelling endothelial/granulosa cell interactions in co-culture: formation of specific spatial inter-relationships in culture. *Manuscript in preparation.*

# ABBREVIATIONS

| | |
|---|---|
| A | Adenosine |
| Ang | Angiopoietin |
| ATP | Adenosine triphosphate |
| bFGF | Basic fibroblast growth factor |
| bp | Base pairs |
| BSA | Bovine serum albumin |
| C | Cytosine |
| °C | Degrees celsius |
| $Ca^{2+}$ | Calcium |
| cAMP | cyclic adenosine monophosphate |
| cDNA | Complementary deoxyribonucleic acid |
| c-fms | Colony stimulating factor-1 receptor |
| c-kit | Stem cell factor receptor |
| cm | Centimeter |
| $CO_2$ | Carbon dioxide |
| dATP | Deoxyadenosine triphosphate |
| dCTP | Deoxycytosine triphosphate |
| dGTP | Deoxyguanidine triphosphate |
| DNA | Deoxyribonucleic acid |
| dNTP | Deoxynucleoside triphosphate |
| dTTP | Deoxythymidine triphosphate |
| ECGS | Endothelial cell growth supplement |
| ECM | Extracellular matrix |
| EGF | Epidermal growth factor |
| ELAM-1 | endothelial leukocyte adhesion molecule |
| eNOS | Endothelial nitric oxide synthase |
| E-selectin | Endothelial-selectin |
| FITC | Fluorescein isothiocyanate |
| flk-1 | Fetal liver kinase-1 |
| flt-1 | fms-like tyrosine kinase receptor-1 |
| FSH | Follicle stimulating hormone |
| g | Grams |
| G | Guanidine |
| GAG | Glycosaminoglycan |
| GAPDH | Glyceraldehyde-3-phosphate dehydrogenase |
| GnRH | Gonadotrophin-releasing hormone |
| HBSS | Hanks balanced salt solution |
| hCG | Human chorionic gonadotrophin |
| HCl | Hydrochloric acid |
| HOMEC | Human ovarian microvascular endothelial cells |
| HIF-1 | Hypoxia inducible factor 1 |
| HUVEC | Human umbilical vein endothelial cells |

| | |
|---|---|
| Ig | Immunoglobulin-like |
| IGF | Insulin-like growth factor |
| IgG | Immuno gamma globulin |
| IgSF | Immunoglobulin superfamily |
| IU | International unit |
| IVF | In vitro fertilisation |
| KCL | Potassium chloride |
| kd | Dissociation constant |
| kDa | Kilodalton |
| KDR | Kinase domain-containing receptor |
| l | Litre |
| LDL | Low density lipoprotein |
| LH | Luteinising hormone |
| L-NAME | $N^{\omega}$-nitro-L-arginine methyl ester |
| L-selectin | Leukocyte-selectin |
| M199 | Media 199 |
| MAP | Mitogen-activated protein kinase |
| mCi | Millicurrie |
| µg | Micrograms |
| mg | Milligrams |
| $MgCl_2$ | Magnesium chloride |
| min | Minutes |
| µl | Microlitre |
| ml | Millilitre |
| µm | Micrometer |
| µmol | Micromoles |
| mmol | Millimoles |
| mm | millimetre |
| MMP | Matrix metalloproteinase |
| mol | Moles |
| mRNA | Messenger ribonucleic acid |
| ng | Nanograms |
| nm | Nanometer |
| nmol | Nanomoles |
| NO | Nitric oxide |
| NOS | Nitric oxide synthase |
| PA | Plasminogen activator |
| PAI | Plasminogen activator inhibitor |
| PBS | Phosphate buffered saline |
| PCR | Polymerase chain reaction |
| PDGF | Platelet derived growth factor |
| PECAM-1 | Platelet endothelial cell adhesion molecule |
| pg | Picograms |
| PIGF | Placenta growth factor |
| PKC | Protein kinase C |
| pmol | Picomoles |
| P-selectin | Platelet-selectin |

| | |
|---|---|
| P450-scc | P450-cholesterol side chain cleavage enzyme |
| RIA | Radioimmunoassay |
| RNA | Ribonucleic acid |
| rpm | Revolutions per minute |
| RT | Reverse transcription |
| RTK | Receptor tyrosine kinase |
| RT-PCR | Reverse transcription-polymerase chain reaction |
| s | Seconds |
| sflt-1 | Soluble fms-like tyrosine kinase receptor-1 |
| T | Tyrosine |
| TGFβ | Transforming growth factor β |
| TIMP | Tissue inhibitors of matrix metalloproteinases |
| Tm | Melting temperature |
| TNFα | Tumour necrosis factor α |
| t-PA | tissue-type plasminogen activator |
| UEA-1 | Ulex Europaeus-1 lectin |
| u-PA | Urokinase-type plasminogen activator |
| uPAr | Urokinase-type plasminogen activator receptor |
| V | Volts |
| VCAM-1 | Vascular cell adhesion molecule |
| VEGF | Vascular endothelial growth factor |
| VPF | Vascular permeability factor |
| VRP | Vascular endothelial growth factor related protein |
| VVO | Vesicular-vacuolar organelles |
| vWF | Von Willebrand factor |
| w/v | Weight/volume |
| x g | Times gravity |
| 3β-hsd | 3β-hydroxysteroid dehydrogenase |

# Chapter 1.

# Introduction.

## 1.1 The structure of the mature ovary.

The ovary is suspended from the uterus by the ovarian ligament attached to its medial end and in the reproductive era is 3-5 cm in length and weighs 5-8 g.
The aim of the ovarian cycle is the release of a single mature oocyte every month during the female reproductive years. The surface of the ovary is covered by a single layer of cuboidal epithelium, the cortex contains a large number of oogonia surrounded by follicle cells which become granulosa cells and the remainder of the ovary consists of mesenchymal core. Most of the oocytes in the cortex never reach an advanced stage of maturation, and become atretic early in follicular development (Fortune, 1994).

## 1.2 Follicular development in the ovary.

During reproductive life, groups of primordial follicles, generated no later than six months postpartum mature and ovulate. Primordial follicles consist of a primary oocyte surrounded by a single layer of flattened pre-granulosa cells. Primordial follicles can remain dormant for the entire reproductive life of the female, and as yet it is not clear what factors initiate the development of these follicles, or why one primordial follicle is stimulated over another (Fortune, 1994).

The first stage of follicular development is the preantral growth phase, this stage is characterized by enlargement of the oocyte and proliferation of the surrounding granulosa cells. Stromal cells immediately surrounding the follicle begin to differentiate into spindle-shaped cells and form the outer theca layer (Gougeon, 1996). A fluid filled space develops within the granulosa cells, and a clear layer of gelatinous material

collects around the oocyte, forming the zona pellucida. The innermost layers of granulosa cells known as cumulus cells adhere to the oocyte and form the corona radiata (Gougeon, 1996). This development of the primordial follicle increases the diameter of the follicle from 30-60 μm to 75-80 μm. The granulosa cells also develop follicle stimulating hormone (FSH), oestrogen and androgen receptors. Further thecal cells are recruited as the follicle grows and compresses the surrounding stroma. This growth of the theca layer is also associated with the acquisition of a follicular blood supply by outgrowth of capillaries supplied by branches of the ovarian artery (McClure *et al.*, 1994).

As the follicular cells continue to increase in number, fluid filled cavities begin to form between the granulosa cells. These cavities fuse to form one large fluid filled space called the antrum which is surrounded by a thin layer of granulosa cells, thickened at one pole to encompass the oocyte and cumulus granulosa cells. At this stage of development the theca cells around the follicle become differentiated into two layers, forming the theca interna and theca externa. The follicle has now reached the antral stage and is about 200 μm in diameter (Gougeon, 1996).

Although many follicles reach the antral stage only one follicle will develop further, whilst the others become atretic. The selected follicle now becomes considerably larger as FSH continues to increase cell number and the follicular antrum takes up fluid from the surrounding tissues and expands to a diameter of about 2 mm. The oocyte becomes eccentrically placed, and the Graafian follicle assumes its classical mature form. As the follicle enlarges, it bulges towards the surface of the ovary and the area under the germinal epithelium thins out. The oocyte, with its surrounding investment of granulosa cells, escapes through this area at the time of ovulation (Gougeon, 1996).

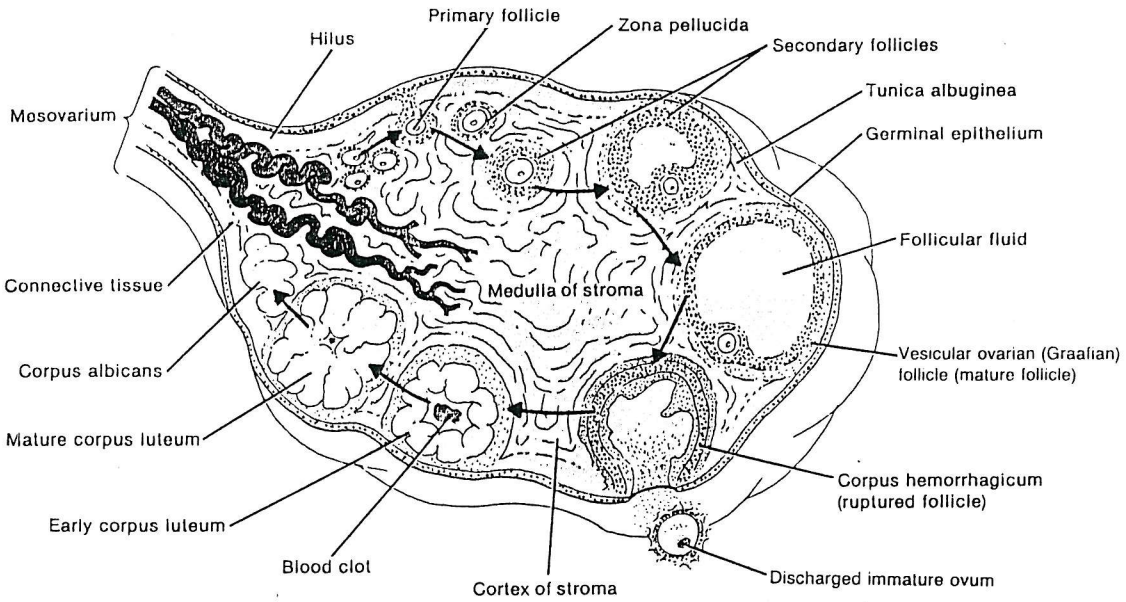


**Figure 1.1 The development of a follicle from a primordial precursor to a corpus albicans.** Follicle at all stages of development can be seen in the ovary during the reproductive years (Tortora and Anagnostakos, 1987, p719).

### 1.2.1 Hormonal control of folliculogenesis.

The maturation of oocytes, ovulation and the endometrial changes of the menstrual cycle are regulated by a series of interactive hormonal changes. The process is initiated by the release of gonadotrophin-releasing hormone (GnRH), which is a major neurosecretory product of the hypothalamus. GnRH, in turn, stimulates the release of follicle-stimulating hormone (FSH) and luteinizing hormone (LH) by the anterior pituitary gland. In the earliest stages of follicle development FSH is the dominant hormone and binds exclusively to granulosa cells (Midgley, 1973). For this reason it is thought the FSH is responsible for increasing granulosa cell numbers.

In the preantral stages of follicle growth, the actions of FSH and LH stimulate the follicles to produce oestrogen, and this increase in oestrogen stimulates the repair of

the endometrium in anticipation of ovulation, fertilization and implantation. The increased levels of oestrogen in turn increase the uptake of FSH, thereby increasing the sensitivity of the follicle to FSH action. By the midfollicular phase, one follicle has become dominant. High levels of FSH have induced the expression of LH receptors on the granulosa cells. Granulosa cells in the preantral stage have been shown to bind LH in negligible quantities. LH binding at this stage of development is confined to theca cells (Bortolussi *et al.*, 1977). However, in antral follicles, granulosa cells appear capable of binding both FSH and LH (Amsterdam *et al.*, 1975; Rajaniemi *et al.*, 1977). *In vivo* and *in vitro* treatment with FSH has shown the induction of LH receptor expression in granulosa cells (Ericson *et al.*, 1979).
The theca cells surrounding the dominant follicle selectively take up more LH than the other non-dominant follicles (DiZerega *et al.*, 1980; Zeleznik *et al.*, 1981) and the vascularity of the theca of the dominant follicle is also greater than that of other follicles. This increased vascularity leads to increased delivery of LH and FSH and substrates for steroid biosynthesis.

Just prior to ovulation, the high levels of oestrogens that develop during the preovulatory phase inhibit GnRH production by the hypothalamus. This, in turn, inhibits FSH secretion by the anterior pituitary via a negative feedback cycle. Concurrently, the high levels of oestrogen act in a positive feedback cycle to cause the anterior pituitary to release a surge of LH which initiates ovulation (Knobil, 1973; Spies and Niswender, 1971).

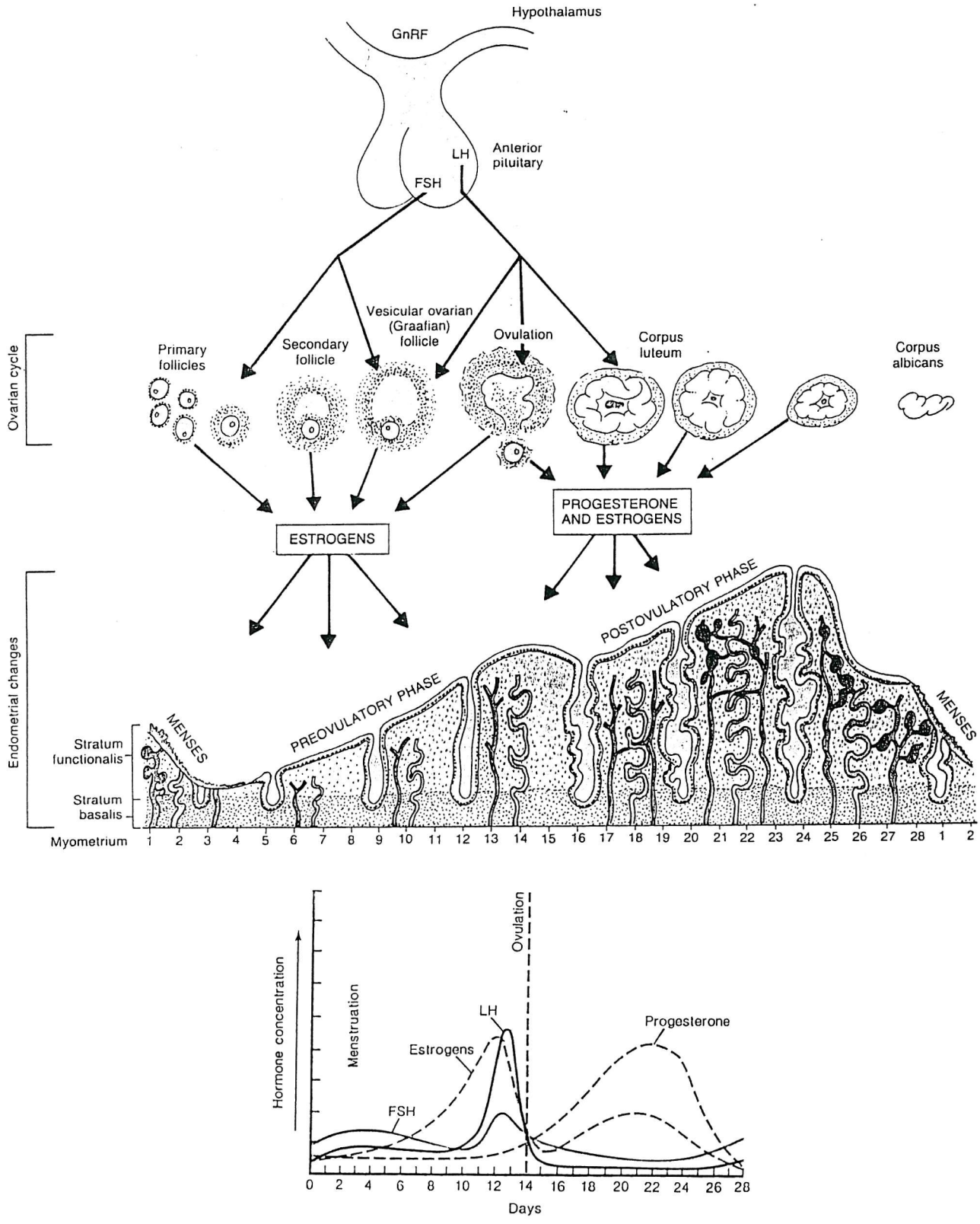


**Figure 1.2 Gonadotrophin control of folliculogenesis,** showing the levels of gonadotrophins throughout the cycle, oestrogen level biosynthesis and development of the follicle in relation to gonadotrophin expression (Tortora and Anagnostakos, 1987, p725).

### 1.2.2 Oestrogen biosynthesis during folliculogenesis.

The biosynthesis of oestrogen requires cooperation between the granulosa cells and their thecal neighbours. The participation of these two cell types and of the two gonadotrophins, FSH and LH, in ovarian oestrogen biosynthesis underlies the two cell/two gonadotrophin hypothesis shown in figure 1.3.

Thecal cells produce androgens, mainly androstenedione when stimulated with LH. This production is catalysed by the 17 α-hydroxylase enzyme. The androgens are transferred across the basement membrane of the follicle to the granulosa cells where they are aromatized to oestrogens (Hillier, 1985).

Studies have shown that granulosa cells are incapable of producing oestrogens without the presence of the precursor hormones as granulosa cells are unable to synthesise androgens themselves. In a similar manner, theca cells can only produce the precursor androgens and not oestrogen as they lack the P450 aromatase enzyme responsible for aromatisation of the androgens to oestrogen (Conley *et al.*, 1995).
Therefore, the biosynthesis of oestrogens in the developing follicles requires the co-operation of the two neighbouring cell types.

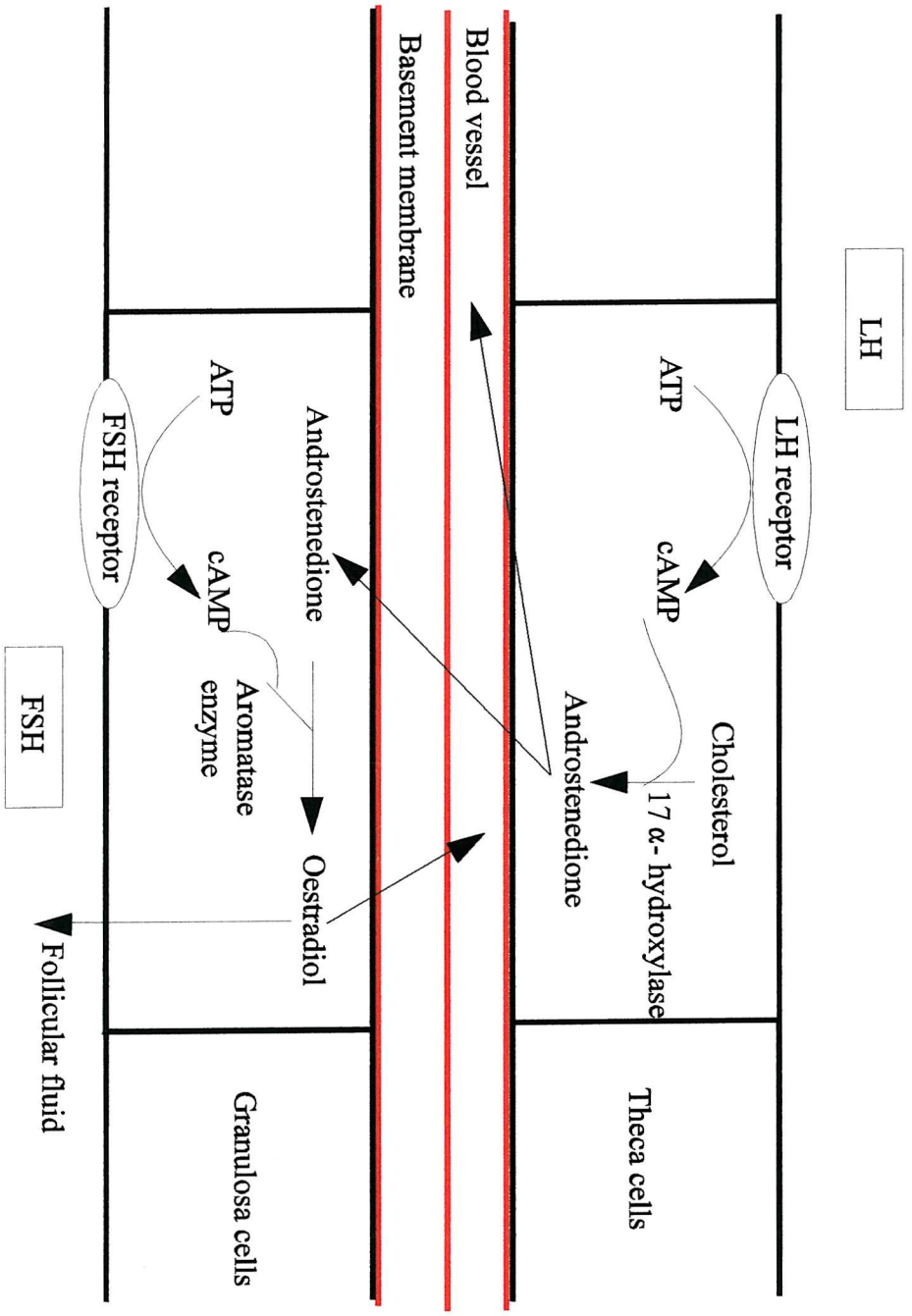


**Figure 1.3 Two cell/two gonadotrophin hypothesis.**

## 1.3 Ovulation.

Increasing amounts of oestrogen produced by the dominant follicle elicit the LH surge. This dramatic increase in the level of LH has many actions on the follicle including, resumption of meiosis of the oocyte, luteinization of the granulosa and theca cells and ovulation (Tsafriri *et al.*, 1993).

Ovulation is preceded by rapid follicular enlargement. This enlargement is thought to be caused by edema as a result of increased capillary permeability of the capillaries that surround the follicle (Bassett, 1943; Burr and Davies, 1951; Damber *et al.*, 1987). Ultimately, the rupture of the follicle results in the expulsion of the oocyte-cumulus complex. Endoscopic visualisation of the ovary around the time of ovulation has revealed that preceding rupture there is an elevation of a conical stigma on the surface of the protruding follicle (Doyle, 1951). Rupture of this stigma is accompanied by gentle, rather than explosive expulsion of the oocyte and antral fluid, suggesting that the latter is not under high pressure (Espey and Lipner, 1963; Blandau and Rumery, 1963).

As for the mechanisms of rupture of the follicle wall, a proteolytic enzyme, plasminogen activator, has been localised in increasing concentrations in the wall of the rat ovarian follicle just before ovulation (Beers *et al.*, 1975). Plasminogen activator, a serine protease, stimulates the conversion of plasminogen (a follicular fluid component) to the proteolytic enzyme plasmin. Plasmin is known to activate collagenase, presumably an obligatory element in the dissolution of the basal membrane and the perifollicular stroma in the course of ovulation. *In vitro* studies have shown that granulosa cells contribute 80-90% of the total follicular plasminogen activator activity in the human ovary (Reich *et al.*, 1986) and thus may initiate ovulation. Further studies have shown that treatment with inhibitors of serine proteases prevented ovulation in vivo (Reich *et al.*, 1985) highlighting the essential proteolytic cascade involved in follicle rupture.

## 1.4 The corpus luteum.

The transformation of ovarian follicles into a corpus luteum was first described in 1672 by Regnier de Graaf (Jocelyn and Setchell, 1972). Since that time, ovarian follicles have been shown to constitute the fundamental functional unit of the ovary. These traverse a developmental track that propels primordial follicular units into a highly differentiated preovulatory stage.

The corpus luteum is a temporary endocrine gland that forms in the ruptured follicle following ovulation. The cavity of the follicle often fills with blood and the cells reorganise themselves to form a functional gland. The granulosa cells and the theca interna cells undergo changes in a process called luteinisation, becoming filled with yellow carotenoid material and developing steroid producing capabilities. Capillaries and fibroblasts from the surrounding stroma proliferate and penetrate the basal lamina. This rapid vascularisation has been proposed to be guided by angiogenic factors readily detected in follicular fluid (Klagsbrun and D'Amore, 1991).

The physiological role of the corpus luteum is the secretion of products that are indispensable for the establishment and maintenance of pregnancy. Luteal products include progesterone, androgens, relaxin, oxytocin, inhibin, eicosanoids, cytokines and growth factors. Progesterone is the principal hormone secreted by the corpus luteum, and its main function is to alter the morphology and function of the endometrium, preparing the uterine environment for implantation of the blastocyst (Behrman *et al.*, 1993; Groome *et al.*, 1996).

The development of the corpus luteum reaches its peak approximately 7 days after ovulation, and the functional lifespan of the corpus luteum is approximately 14 days. Thereafter, the corpus luteum regresses by functional and structural luteolysis unless implantation occurs. This degeneration is characterized by a decrease in progesterone synthesis, increased vacuolization of the granulosa cells and increased quantities of fibrous tissue in the centre of the corpus luteum, which finally develops into a white

scar known as the corpus albicans (Behrman *et al.*, 1993).

### 1.4.1 Cellular composition of the corpus luteum.

The corpus luteum is made of several cell types which contribute to its structural and functional characteristics. These include luteal cells, endothelial cells, immune cells, pericytes and fibroblasts (Bassett, 1943; Burr and Davies, 1951; Damber *et al.*, 1987).

It is now accepted that the luteal cells are derived from both the granulosa and theca cells of the follicle (Pederson, 1951) with the theca derived cells characterized as small luteal cells and granulosa derived cells characterised as large lutein cells (Behrman *et al.*, 1991). In the human these are clearly evident with the theca lutein cells at the periphery and cortical infoldings and the granulosa lutein cells internal to this area. The cellular distinction of granulosa and theca lutein cells is not possible morphologically in other species such as the rat, yet both cells contribute to luteal tissue in these species (Pederson, 1951). In the human, there are reported to be about twice as many large luteal cells than small luteal cells and this pattern of cell number does not appear to change during the early, mid or late luteal phases, or during pregnancy (Lei *et al.*, 1991). It has also been shown that in the human corpus luteum there are more non-luteal cells than luteal cells, this is also true of the bovine corpus luteum (Lei *et al.*, 1991). However, in the rat corpus luteum it has been shown that luteal cells account for over 65% of the gland (Pederson, 1951).

Rapid angiogenesis results in a large number of endothelial cells present in the corpus luteum. The corpus luteum has an extremely rich blood supply which forms shortly after ovulation (Dharmarajan *et al.*, 1985; Dharmarajan *et al.*, 1986; Morris and Sass, 1966). The capillaries are highly fenestrated to permit the transport of large molecules (Enders, 1973). It has been estimated that in the rat, 22% of the total cells are endothelial (Dharmarajan *et al.*, 1985), in the guinea pig almost 75% are endothelial (Azmi *et al.*, 1984) whilst in the human the number is estimated at >50% (Lei *et al.*, 1991). The capillary network of the mature corpus luteum is so extensive that the

majority of luteal cells are adjacent to one or more capillaries (Dharmarajan *et al.*, 1985; Zheng *et al.*, 1993). This is not surprising following studies showing that up to 85% of the proliferating cells in the corpus luteum are endothelial (Jablonka-Shariff *et al.*, 1993; Reynolds *et al.*, 1994; Christenson and Stouffer *et al.*, 1995; Nicosia *et al.*, 1995).

An interesting characteristic of ovarian endothelial cells was shown by Ghinea *et al.*, (1994) whose studies revealed that endothelial cells of the porcine ovarian vasculature bind and transport hCG to the underlying endocrine cells, whereas endothelial cells in other organs do not appear to display this characteristic. This specialised function of ovarian endothelial cells maybe important for the hCG mediated rescue of the corpus luteum if conception occurs.

### 1.5 Luteinisation.

Following the preovulatory surge, granulosa cells go through a process of luteinisation. This is the process by which the granulosa cells acquire the ability to produce progesterone. Until ovulation, the granulosa cells mainly produce oestrogen by the aromatization of androgens produced in the theca cells (Hillier, 1994).

Luteinisation increases the size of granulosa cells by about 250%, increasing lipid droplets and cellular organelles such as smooth endoplasmic reticulum and mitochondria. These mitochondria have lamellar cristae which are characteristic of steroidogenic cells.

Luteinisation increases the mRNA and protein levels of P450-cholesterol side chain cleavage enzyme (P450-scc) and 3β-hydroxysteroid dehydrogenase (3β-hsd) which catalyse the conversion of low-density lipoprotein (LDL) derived cholesterol into progesterone (Hillier, 1988).

Granulosa cells in culture have been shown to spontaneously luteinise (Hillier, 1981) and under stimulation from hCG produce sustained levels of progesterone in culture media (Richardson *et al.*, 1992).

## 1.6 Extracellular matrix.

As well as the cells and vascular component of the corpus luteum, the extracellular matrix (ECM) serves as the glue to hold the structure together, a store for growth factors and probably contributes to the functional activity of the gland.
The ECM is a highly organised meshwork made of various proteins and polysaccharides. Most of the extracellular space is filled with a network of glycosaminoglycan (GAG) chains which form a hydrated gel complex. GAGs are negatively charged polysaccharide chains which are linked to protein to form proteoglycan molecules. They provide mechanical support to tissues while still allowing the rapid diffusion of nutrients, metabolites and hormones between the blood and tissue cells, as well as the migration of cells. Various types of proteoglycans can form gels with different pore sizes to act as selective sieves to regulate the traffic of molecules. Proteoglycans are also thought to play a major role in chemical signalling between cells due to their ability to bind secreted signalling molecules, such as growth factors (Cohen *et al.*, 1995). In addition to the GAG chains, the matrix also contains fibrous proteins such as the structural collagen which provides strength and helps to organise the matrix, and the rubber-like elastin fibres which provide elasticity. Adhesive proteins such as fibronectin and laminin help cells to attach to the appropriate part of the ECM.

Endothelial cells secrete ECM components during angiogenesis. These include fibronectin, type V collagen and small amounts of laminin and type IV collagen (Tonnesen *et al.*, 1985; Nicosia and Madri, 1987). As the growing vessels mature, laminin and collagen type IV accumulate in the sub-endothelial space forming a basement membrane (Nicosia and Madri, 1987).

Remodelling of the ECM is an essential part of many physiological processes including follicular growth, ovulation and the formation and regression of the corpus luteum. During the early stages of angiogenesis, activated endothelial cells create gaps in the basement membrane through which they sprout into the surrounding tissue. Matrix

components are degraded by extracellular proteolytic enzymes which are secreted locally by cells. There are two main classes of proteolytic enzymes: plasminogen activators (PAs) and matrix metalloproteinases (MMPs). PAs trigger a proteinase cascade which results in generation of high local concentrations of plasmin and active MMPs which have a broad spectrum of proteolytic activity. (McIntush and Smith, 1998). Figure 1.4 shows the cascade of proteolytic activation.

### 1.6.1 Plasminogen activators.

Also known as serine proteinases, PAs form plasmin by the hydrolysis of the inactive plasminogen which is present in plasma. There are two main forms of PA, tissue-type PA (t-PA) and urokinase-type PA (u-PA), which can both be synthesised by endothelial cells (Loskutoff and Edington, 1979; Pepper *et al.*, 1991).
Plasmin functions directly by degrading non collagenous components of the ECM such as fibronectin, laminin and the protein core of proteoglycans (Liotta *et al.*, 1981; Mignatti and Rifkin, 1993) or indirectly by activating MMP-1, which in turn digests interstitial collagen (Gross *et al.*, 1982).
u-PA binds to its receptor, uPAr, at the sites of proteolysis (Loskutoff and Edington, 1979) and has been demonstrated to generate high levels of plasmin at the tips of growing microvessels (Bacharach and Keshet, 1992).
As with all proteolytic enzymes, the PAs have inhibitors to stop uncontrolled matrix dissolution. The inhibitors of PAs are part of a multigene family and are called serine proteinase inhibitors (serpins) or plasminogen activator inhibitors (PAI) (Bacharach and Keshet, 1992).
Angiogenic factors such as bFGF and VEGF induce the upregulation of both u-PA and PAI (Moscatelli and Rifkin, 1988, Pepper *et al.*, 1991).

### 1.6.2 Matrix metalloproteinases.

The MMPs are a family of zinc-dependent proteinases which are secreted in an inactive

form and activated extracellularly. There are a range of enzymes characterised in the family that degrade different collagen types, laminin, fibronectin, elastin and the protein core of proteoglycans (Mignatti and Rifkin, 1993; Moscatelli and Rifkin, 1988). There are four groups of MMPs which are classified by their substrate specificity: 1) Interstitial collagenases; collagenase-1 (MMP-1), collagenase-2 (MMP-8) and collagenase-3 (MMP-13) (Freije *et al.*, 1994; Quinn *et al.*, 1990).
2) Type IV collagenases; 72-kDa gelatinase (MMP-2) and 92-kDa gelatinase (MMP-9) (Goldberg *et al.*, 1986; Wilhelm *et al.*, 1989).
3) Stromelysins; stromelysin-1 (MMP-3), stromelysin-2 (MMP-10), stromelysin-3 (MMP-11) and matrilysin (MMP-7) (Chin *et al.*, 1985; Nicholson *et al.*, 1989; Wilhelm *et al.*, 1987).
4) Membrane-type MMP; MMP-14 which has the unique property of activating the proenzyme form of MMP-2 (Sato *et al.*, 1994; Cao *et al.*, 1995).

These different groups of MMPs have different substrate specificities within the ECM. For example: interstitial collagenases degrade collagen types I, II, III, VII and X (Miller *et al.*, 1976; Schmid *et al.*, 1986). Type IV collagenases degrade collagen types I, IV, V, VII and X as well as gelatins and fibronectins (Wilhelm *et al.*, 1989; Collier *et al.*, 1988; Aimes and Quigley, 1995). Stromelysins degrade fibronectins, laminin, elastin and the protein core of proteoglycans as well as collagen types I, IV, VIII and IX (Chin *et al.*, 1985; Wilhelm *et al.*, 1987; Murphy *et al.*, 1993).

The action of MMPs is regulated by the tissue inhibitors of matrix metalloproteinases (TIMPs) (Ray and Stetler-Stevenson, 1994). TIMP-1, TIMP-2 and TIMP-3 have all been shown to be produced in the corpus luteum by the granulosa cells (Nothnick et al., 1995). TIMPs bind noncovalently to MMPs in a 1:1 molecular ratio (Baragi *et al.*, 1994; Murphy *et al.*, 1992). As with u-PA, growth factors can induce the expression of MMPs. MMP-1 is induced by both bFGF and VEGF (Unemori *et al.*, 1992; Kennedy *et al.*, 1997). However, growth factors are not the only stimuli that induce MMPs. Changes in cell shape, as well as cell-cell and cell-matrix interactions influence MMP production (Woessner, 1994).

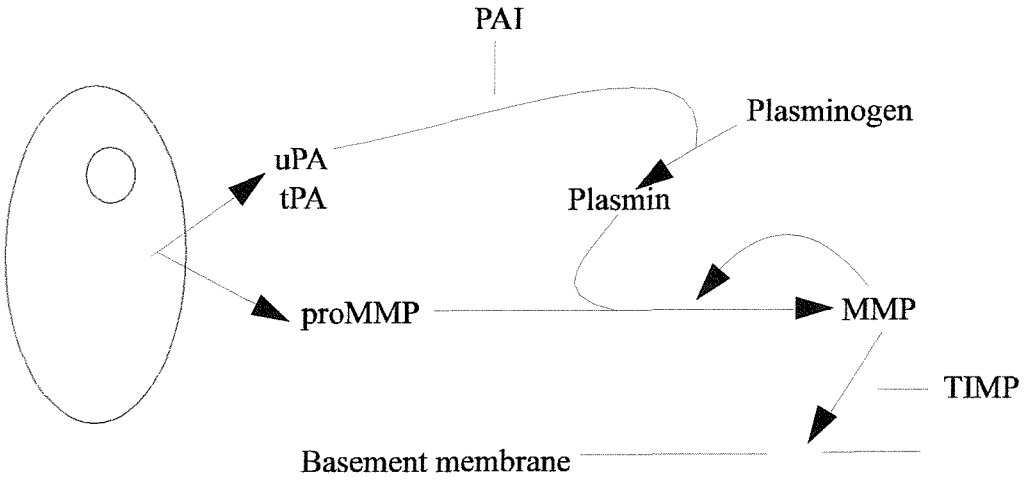


**Figure 1.4 Proteolytic cascade of activation of PA and MMP.**

### 1.6.3 Proteolysis in ovarian function.

The growth of the follicle during folliculogenesis requires remodelling as the follicle grows from 0.1 mm in the primordial follicle to 19 mm at the point before ovulation. MMP-1 expression has been shown at all points of follicular growth and is thought to play a vital role in the expansion of the follicle (Tadakuma *et al.*, 1993). Proteolysis of the ECM has also been shown to release growth factors stored in the ECM that are required for the development of the follicle (Flaumenhaft and Rifkin, 1992).

The preovulatory gonadotrophin surge has been shown to initiate a cascade of proteolytic activity that can be compared to that of an immune response (Espey, 1992, 1994). Following the gonadotrophin surge, ovarian collagenase activity increases (Curry *et al.*, 1985; Hirsch *et al.*, 1993). The stigma formed at the apex of the follicle wall is the site of proteolytic degradation of collagen fibres. This leads to a weakness in

the wall which eventually ruptures to release the oocyte (Murdoch and McCormick, 1992, Espey, 1994).

MMP activity appears to be essential for follicle rupture whereas PA activity is not. This was demonstrated by Carmeliet *et al.*, (1994) who demonstrated that ovulation still occurred in the absence of PAs but not in the absence of MMPs where follicular rupture was blocked. MMP-1, MMP-2 and MMP-9 have all been implicated in follicular rupture (Curry *et al.*, 1992; Russell *et al.*, 1995; Hurwitz *et al.*, 1993) and are all thought to play an important role.

Formation of the corpus luteum involves extensive remodelling of the ECM to accommodate the rapid vascularisation and growth of the gland (Jablonka-Shariff *et al.*, 1993).

It has also been reported that ECM components enhance luteinisation of follicular cells and that loss of ECM results in cell death. Laminin and fibronectin have been shown to be important for luteinisation (Aten *et al.*, 1995) and that the process can be blocked with antibodies that block cell-ECM interactions.

## 1.7 Angiogenesis.

The corpus luteum has one of the highest blood flow rates in the body (Bruce and Moor, 1976). The extensive capillary network is the result of rapid angiogenesis following ovulation and is coincident with luteinisation to ensure that the newly developed lutein cells receive the substrates for progesterone synthesis, particularly LDL.

Angiogenesis is under the control of angiogenic growth factors and consists of three main processes; 1) fragmentation of the existing basement membrane, 2) migration of endothelial cells and 3) proliferation of endothelial cells in response to angiogenic stimuli (Folkman, 1985).

Following ovulation, capillaries located in the theca layer invade the previously

avascular granulosa layer and move towards the centre of the ruptured follicle (Reynolds *et al.*, 1992). New vessels originate as sprouts from small capillaries. The basement membrane is broken down by proteolytic enzymes and the endothelial cells migrate as a cord towards the angiogenic stimulus. The cord then begins to form a lumen, mitosis begins and growth occurs just behind the tip of the advancing vessel. Formation of the vessel is completed by the laying down of a basement membrane (Folkman, 1985; Tsang *et al.*, 1995; Liu *et al.*, 1996).

There are many angiogenic growth factors and cytokines which have been implicated in the vascularisation of the corpus luteum. However, there is no single factor which is thought to be solely responsible and it is thought that a combination of growth factors are required (Klagsbrun and D'Amore, 1991; Gordon *et al.*, 1996). These include platelet derived growth factor (PDGF; Bagavandos and Wilks, 1991), insulin-like growth factor (IGF; Jones and Clemmons, 1995), epidermal growth factor (EGF; Huang *et al.*, 1995; Tamura *et al.*, 1995), transforming growth factor β (TGFβ; Tamura *et al.*, 1995) and tumour necrosis factor α (TNFα; Behrman *et al.*, 1993). More recently Angiopoietin-1 and -2 (Ang-1, Ang-2) were identified as angiogenic factors thought to play a role in corpus luteum vascularisation (Maisonpierre *et al.*, 1997).

*In vitro* studies of corpus luteum angiogenesis suggest that the principal angiogenic regulators are basic fibroblast growth factor (bFGF) and vascular endothelial growth factor (VEGF; Reynolds *et al.*, 1992; Redmer and Reynolds, 1996; Redmer *et al.*, 1996). A recent study by Ferrara *et al.*, (1998) has shown for the first time that the formation of the vasculature of the corpus luteum is VEGF dependent, and this will be discussed later.

### 1.8 Basic fibroblast growth factor.

bFGF is a member of a heparin-binding family of growth factors with potent angiogenic activity. There are to date nine members of the family with four receptors (Moses *et al.*, 1995; Gorlin, 1997). Endothelial cells have been shown to produce

bFGF as well as expressing the receptors (Schweigerer *et al.*, 1987; Hughes *et al.*, 1993).

bFGF is not a specific endothelial mitogen and has been shown to enhance the proliferation and migration of fibroblasts and smooth muscle cells as well as endothelial cells (Root and Shipley, 1991; Lindner, 1995). In response to injury, vascular and smooth muscle cells express elevated levels of bFGF mRNA and its receptor FGFR-1 (Lindner and Reidy, 1993).

bFGF is stored intercellularly and in the basement membrane where it binds to the heparan sulphate proteoglycans (Lindner and Reidy, 1993). Immunohistochemical studies have shown bFGF to be stored in the cytoplasm of endothelial cells and smooth muscle cells of the rat aorta (Villaschi and Nicosia, 1993). Treatment with anti bFGF antibodies caused a 40% inhibition of the angiogenic response of bFGF in rat aortic cultures, as well as an inhibition of the angiogenic effect of endogenous bFGF in cultures of human chorionic vessels and bovine capillary endothelial cells (Brown *et al.*, 1996; Sato *et al.*, 1991).

### 1.9 Angiopoietin.

The angiopoietins are a newly discovered family of growth factors which have been shown to play a critical role in the development of the vessel wall during embryogenesis. Ang-1 and Ang-2 bind to the Tie-2 receptor found on endothelial cells, which, as with many other growth factor receptors, is a tyrosine kinase receptor (Sato *et al.*, 1995; Davis *et al.*, 1996; Maisonpierre *et al.*, 1997).

Ang-1 phosphorylates the Tie-2 receptor on endothelial cells but does not appear to induce proliferation or migration of endothelial cells (Suri *et al.*, 1996). It has been proposed that Ang-1 stimulates endothelial cells to secrete factors which contribute to the differentiation of the vessel wall (Suri *et al.*, 1996) due to the fact that vessels formed in the absence of Ang-1 fail to fully differentiate (Puri *et al.*, 1995; Sato *et al.*, 1995; Suri *et al.*, 1996). Ang-2 appears to be a natural inhibitor of Ang-1 and competes for binding of the Tie-2 receptor with Ang-1 (Maisonpierre *et al.*, 1997). Recently, Ang-1 and Ang-2 have been shown to be expressed in a cyclical fashion in

the rat ovary, this finding suggests a role in the regulation of growth and remodelling of the corpus luteum vasculature.

### 1.10 Vascular endothelial growth factor.

Vascular permeability factor (VPF) was originally purified from guinea pig ascites and tumour cell culture media as a factor that increases the permeability of blood vessels (Senger *et al.*, 1983). Independently, a new growth factor, called VEGF, specific to endothelial cells was reported in conditioned media of bovine pituitary folliculostellate cells (Ferrara and Henzel, 1989).
Molecular characterisation of VEGF and VPF led to the conclusion that they were in fact the same protein generated from a single gene (Leung *et al.*, 1989; Keck *et al.*, 1989; Ferrara *et al.*, 1991). This finding was followed by the identification of specific VEGF receptors which formed a new subfamily of tyrosine-kinase receptors (Terman *et al.*, 1992; Millauer *et al.*, 1993; Quinn *et al.*, 1993).

#### 1.10.1 Structure of VEGF.

The human VEGF gene has recently been localised on chromosome 6 (Vincenti *et al.*, 1996). It is composed of eight exons, separated by seven introns and its coding region spans approximately 14 kilobases (Tisher *et al.*, 1991). Sequence analysis of the cDNA of a variety of human VEGF clones has indicated that VEGF exists as one of four different molecular species or isoforms (Houck *et al.*, 1991; Ferrara *et al.*, 1991). These have a 121, 165, 189 or 206 amino acid composition in the VEGF monomer and arise from alternate exon splicing of the single VEGF gene and are referred to as $VEGF_{121}$, $VEGF_{165}$, $VEGF_{189}$ and $VEGF_{206}$ respectively. The VEGF itself is composed of two identical subunits which form a dimer. The alternate splicing is shown in figure 1.5.

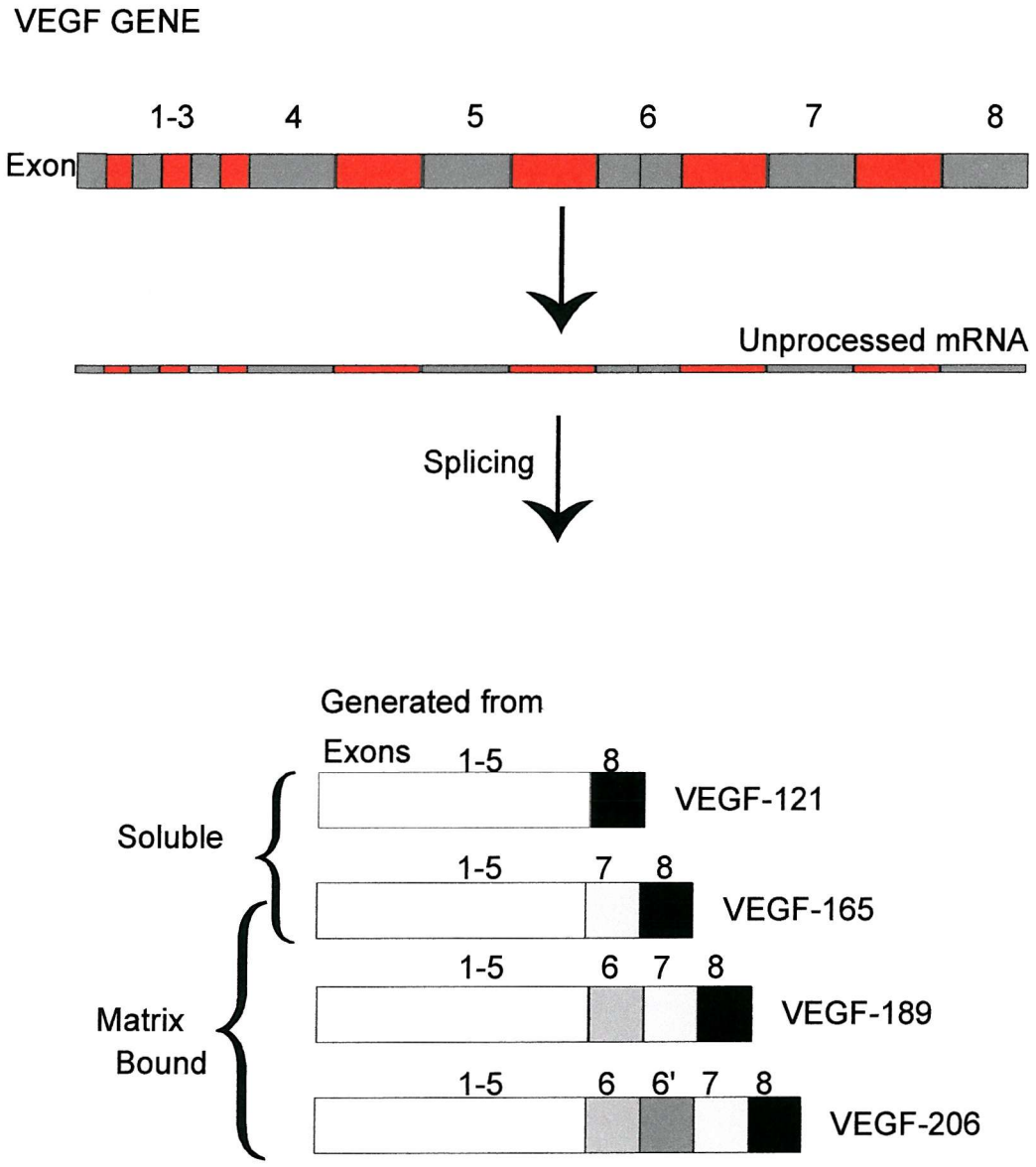


**Figure 1.5 An overview of the alternative splicing of VEGF gene products** to generate four VEGF splice variants.

All subtypes of VEGF share the amino terminal 141 amino acid residues including a signal peptide encoded by exons 1-5, which contains 8 cysteine residues that contribute to dimer formation and the carboxyl terminal 6 amino acids encoded by exon eight. $VEGF_{165}$ lacks the residues encoded by exon 6, while $VEGF_{121}$ lacks the residues encoded by exons 6 and 7. $VEGF_{165}$ is the predominant isoform produced by a variety of normal and transformed cells. $VEGF_{121}$ and $VEGF_{189}$ are also generally detected in the majority of cells expressing $VEGF_{165}$ but are present in lower amounts. In contrast, $VEGF_{206}$ is a less common form of VEGF which was initially only identified in a human fetal liver cDNA library (Houck *et al.*, 1991). In reality, it is probably present in more tissues and a more sensitive method is required for its detection. $VEGF_{145}$ is a further alternative spliced variant which has only rarely been detected in some tissues since the levels of expression of this form are considerably lower than any of the other isoforms (Charnock-Jones *et al.*, 1994). The bioactivity of all of these spliced variants of VEGF could be regulated by the degree of alternative splicing.

All of these variants differ in efficiency of secretion, heparin binding ability (Cohen *et al.*, 1995) and potency of vascular permeability and mitogenic activity (Boocock *et al.*, 1995). The heavier species of VEGF ($VEGF_{206}$ and $VEGF_{189}$) are basic like FGF and are almost completely sequestered in the extracellular matrix, whereas the lighter forms ($VEGF_{165}$ and $VEGF_{121}$) are weakly acidic and are readily secreted in the soluble form. As the size of the VEGF increases so does the affinity by which the species bind heparin. $VEGF_{121}$ unlike the others does not possess heparin binding ability (Cohen *et al.*, 1995) suggesting different biological functions of VEGF subtypes *in vivo*. $VEGF_{165}$ can be cleaved by plasmin to yield the first 110, $NH_2$-terminal amino acids of VEGF, $VEGF_{110}$ which is equipotent to $VEGF_{121}$ with respect to mitogenic activity on endothelial cells (Houck *et al.*, 1992; Keyt *et al.*, 1996). In addition, the product of plasmin cleavage of $VEGF_{189}$ generates a dimeric 32 kDa molecule exhibiting VEGF activity (Houck *et al.*, 1992). Therefore, generation of bioactive VEGF products and their availability to other cells occurs either by the release of the free $VEGF_{165}$ and $VEGF_{121}$ or by protease activation and cleavage of the longer isoforms of VEGF. These longer cell-bound forms of VEGF are essentially a 'stored' VEGF which are

released on demand by partial cleaving (Houck *et al.*, 1992). However, the loss of heparin binding ability by cleavage of the longer isoform $VEGF_{165}$ to the smaller $VEGF_{121}$ or $VEGF_{110}$ has been shown to vastly reduce the potency of the mitogenic actions of VEGF (Keyt *et al.*,1996). These results suggest that VEGF may have the ability to produce a graded response through its structural and functional heterogeneity.

### 1.10.2 Other members of the VEGF family.

Recently the original VEGF has sometimes been referred to as VEGF-A, as other growth factors with very similar structures have been discovered which either react with one of the receptors of VEGF or stimulate endothelial mitogenesis.

Placenta growth factor (PIGF) was cloned from a human placenta cDNA library (Maglione *et al.*, 1991) and was found to be closely related to VEGF. There is 40% amino acid homology between VEGF and PIGF in the core region encoded from exons 1-5 of VEGF with all eight cysteine regions conserved. Like VEGF, the two existing forms of PIGF (PIGF-1 and PIGF-2) are generated by an alternative splicing mechanism (Maglione *et al.*, 1993). PIGF is a dimeric glycoprotein with growth stimulatory effects on endothelial cells. Its similarity to VEGF includes it in the VEGF family.

There are continual encounters of novel proteins with structural similarity to VEGF being characterised and associated with the growing VEGF family. VEGF-C, cloned from human prostatic carcinoma cells (Joukov *et al.*, 1996), shows homology to VEGF but contains a pattern of extra cysteine residues at its C-terminal end. VEGF-C is also known as vascular endothelial growth factor-related protein (VRP) which was isolated from cDNA clones from a human glioma cell line that encoded a secreted protein with 32% amino acid identity to VEGF (Lee *et al.*, 1996).
VRP/VEGF-C elicits a migratory response in bovine capillary endothelial cells in collagen gel (Joukov *et al.*, 1996) and was found to have a mitogenic effect on human

lung endothelial cells (Lee *et al.*, 1996). The mRNA for this protein was detected in several human tissues including adult heart, placenta, ovary and small intestine and in fetal lung and kidney (Lee *et al.*, 1996). VEGF-C has also been reported to be a lymphangiogenic factor (Oh *et al.*, 1998 ) and is thus thought to have a dual role.

Another growth factor for endothelial cells, VEGF-B has been identified (Olofsson *et al.*, 1996) along with a second isoform (Olofsson *et al.*, 1996). They again bear structural resemblance to VEGF and PIGF, form cell surface-linked homodimers and heterodimers with VEGF and have a role in angiogenesis and endothelial cell growth. VEGF-B binding to flt-1 on endothelial cells results in increased expression and activity of u-PA and PAI (Olofsson *et al.*, 1998). This suggests a role for VEGF-B in the regulation of extracellular matrix degradation, cell adhesion and migration.

VEGF-D was first cloned by Orlandini *et al.*, (1996) and is most closely related to VEGF-C. VEGF-D has been shown to be mitogenic for microvascular endothelial cells (Achen *et al.*, 1998) and in adult tissues VEGF-D mRNA is most abundant in lung, heart, skeletal muscle, colon and small intestine (Achen *et al.*, 1998; Yamada *et al.*, 1997).

### 1.10.3 Functions of VEGF.

VEGF has been shown to be a specific mitogen for endothelial cells *in vitro* but is devoid of consistent and appreciable mitogenic activity in other cell types (Connolly *et al.*, 1989; Ferrara and Henzel, 1989; Leung *et al.*, 1989).

Originally the Miles assay demonstrated the ability of VEGF to induce permeability in tumour cells (Senger *et al.*,1983). The effective concentration of VEGF found to induce blood vessel permeability was 1 nmol/l, which is about 100-1000 fold more potent than that of histamine and bradykinin (Connolly *et al.*, 1989). It was proposed that an increase in vascular permeability was of prime importance in the process of angiogenesis associated with tumours and wounds (Dvorak, 1986). These and other

findings suggest that VEGF may have a significant role in mechanisms involving angiogenesis such as wound healing and neovascularisation.

VEGF has a possible migratory function indicated by its ability to induce PAs and PAIs in cultured microvascular endothelial cells (Pepper *et al.*, 1991). Furthermore, VEGF increases the production of MMP-1 that degrades interstitial collagen in human umbilical vein endothelial cells (Unemori *et al.*, 1992). These migratory characteristics may facilitate the process of angiogenesis in the degradation of the extracellular matrix and the sprouting of new blood vessels.
$VEGF_{165}$ has been shown to induce the MMP-1 interstitial collagenase, both at mRNA and protein levels, in HUVEC, but not in dermal fibroblasts (Unemori *et al.*, 1992). Also, VEGF has been found to induce the serine proteases u-PA and t-PA, both at mRNA and protein levels, and also PAI in microvascular endothelial cells (Pepper *et al.*, 1991)

Recently, VEGF has been reported to be involved in the functioning of other cells apart from endothelial cells. In support of the reported migratory responses elicited by VEGF, Barelon *et al.*, (1996) showed that VEGF stimulates the migration of human mononuclear cells, an effect which is inhibited by antibodies to VEGF. VEGF has also been implicated in the activation of monocytes and their chemotaxis across collagen membranes and endothelial cell monolayers (Clauss *et al.*, 1990). Another finding reported VEGF receptor mRNA in haematopoietic cells and VEGF was found to enhance colony formation of mature subsets of granulocyte macrophage progenitor cells that had been treated with a colony stimulating factor (Broxmeyer *et al.*, 1995).

VEGF induces the formation of fenestrations in blood vessels (Esser *et al.*, 1998; Roberts and Palade, 1997) and the formation of vesiculo-vacuolar organelles that form channels through which blood-bourne proteins can extravasate (Dvorak *et al.*, 1996). This leads to the formation of an extravascular fibrin gel which provides a matrix that supports the growth of endothelial cells and tumour cells and allows invasion of stromal cells into the developing tumour (Dvorak *et al.*, 1992).

### 1.10.4 Regulation of VEGF production.

Hypoxia is a major stimulator of VEGF expression (Shweiki *et al.*, 1992).
Hypoxia has been shown to activate signal transduction pathways involving the Src proto-oncogene family which upregulate VEGF production (Mukhopadhyay *et al.*, 1995). Levy *et al.*, (1996) have shown that the increase in VEGF mRNA associated with hypoxia results not only from increased transcription but also from increased stability of VEGF mRNA due to its binding with hypoxia induced proteins, many of which are still unknown.
However, the production of other VEGF family members such as VEGF-B, VEGF-C and PIGF does not seem to be potentiated by hypoxia even though some of these factors such as VEGF-C are strong angiogenic factors in their own right (Jeltsch *et al.*, 1997; Enholm *et al.*, 1997).
Hypoxia-induced transcription of VEGF mRNA is apparently mediated, at least in part, by the binding of hypoxia-inducible factor 1 (HIF-1) to an HIF-1 binding site located in the VEGF promoter (Levy *et al.*, 1995; Lui *et al.*, 1995).
Several growth factors or cytokines have been shown to influence VEGF mRNA expression and/or the release of the protein. There is an increase in the level of expression of VEGF mRNA when human kidney keratinocytes are exposed to epidermal growth factor (EGF), transforming growth factor-β (TGF-β) or keratinocyte growth factor (Frank *et al.*, 1995). Furthermore, the addition of TGF-β to cultured human fibroblasts or epithelial cell lines resulted in an increase in the VEGF message and protein, indicating that VEGF may function in a paracrine fashion as a mediator for angiogenic factors such as TGF-β (Pertovaara *et al.*, 1994).

Cytokines, growth factors and gonadotrophins which do not stimulate angiogenesis directly can modulate angiogenesis by modulating VEGF expression in specific cell types, and thus exert an indirect angiogenic or anti-angiogenic effect. Factors that can potentiate VEGF production include fibroblast growth factor 4 (Deroanne *et al.*, 1997), PDGF (Finkenzeller *et al.*, 1997), tumour necrosis factor α (Ryuto *et al.*, 1996), and TGF-β (Pertovaara *et al.*, 1994). Thus VEGF may act as a paracrine

mediator for indirectly acting angiogenic agents such as TGF-β (Petrovarra *et al.*, 1994)

### 1.11 The VEGF receptors.

Two classes of high-affinity binding sites for VEGF were first identified on the surface of bovine endothelial cells (Plouet and Moukadiri, 1990; Vaisman *et al.*, 1990). They were originally reported to have dissociation constants (kd) of 10 pmol and 100 pmol and molecular masses in the range of 180-220 kDa. The DNA sequences encoding these two VEGF receptors have been cloned and expressed (DeVries *et al.*, 1992; Millauer *et al.*, 1993; Terman *et al.*, 1994) and are known as the fms-like tyrosine kinase receptor-1, or flt-1, and the kinase domain-containing receptor, or KDR, also known as flk-1 (fetal liver kinase).

The VEGF receptors are in the sub-group of receptors called the receptor tyrosine kinases (RTKs) since they contain a tyrosine kinase insert domain in their intracellular region. Because of their large extracellular domains comprising seven instead of five immunoglobulin-like loops (as with the platelet derived growth factor receptors) and high sequence homologous tyrosine kinase domains, the flt-4, flt-1 and KDR/flk-1 receptors comprise a distinct novel subfamily of the RTKs. A further common feature of these receptors is that all three are expressed on endothelial cells showing both overlapping and diverse patterns of expression (Kaipainen *et al.*, 1993).

The flt family that encodes these receptor proteins belongs to the class III RTKs (Ullrich and Schlessinger, 1990). This group of genes includes two protooncogenes (c-fms and c-kit), the genes for the α and β chains of the platelet derived growth factor receptors (PDGFR) and the flt-3/flk-2 gene. PDGF is closely related to VEGF since the core region of VEGF encoded by exons 1-5 is conserved in PDGF. The amino terminal two thirds of PDGF-A and -B are homologous to that of VEGF. The similarity includes the distribution of the eight cysteine residues and the exon-intron organisation.

Two separate domains of VEGF interact with flt-1 and KDR. These binding domains are located at opposite ends of the VEGF monomer. In the mature VEGF dimer, the monomers are linked in a head to tail fashion with a large overlap by disulphide bridges so that the main flt-1 binding domains are at opposite ends of the molecule, as are the main KDR binding domains (Keyt *et al.*, 1996; Muller *et al.*, 1997). This spatial arrangement is in agreement with observations indicating that mutations within the flt-1 binding site of VEGF have a minimal effect on the binding of VEGF to KDR, and that mutants effecting the KDR binding site of VEGF do not affect the binding of VEGF to flt-1 (Keyt *et al.*, 1996). This is shown in figure 1.6

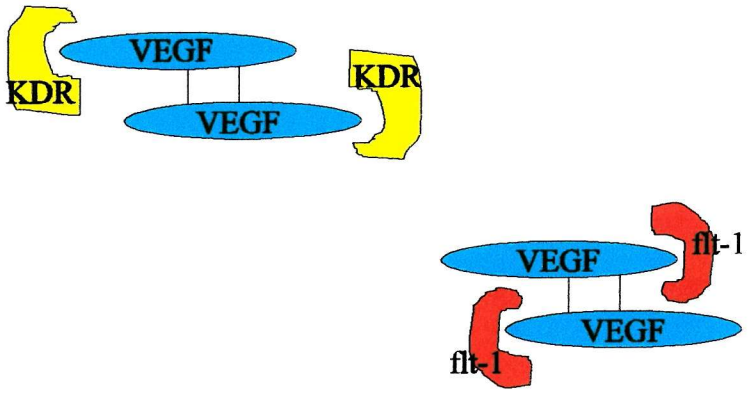


**Figure 1.6 The binding of VEGF to its receptors flt-1 and KDR.** Binding of flt-1 does not interrupt binding to KDR and visa versa.

Activation of the KDR receptor by VEGF in cells devoid of flt-1 results in a mitogenic response, while the activation of flt-1 by VEGF in cells lacking KDR does not induce cell proliferation (Seetharam *et al.*, 1995; Waltenberger *et al.*, 1994). However, activation of flt-1 by VEGF does induce cell migration, a response that is also induced as a result of KDR activation by VEGF (Barleon *et al.*, 1996; Yoshida *et al.*, 1996; Soker *et al.*, 1998). These results indicate that the signal transduction cascades induced by flt-1 and KDR are somewhat different. The information regarding the signalling cascades induced by each of these receptors is limited, and it is not completely clear why flt-1 does not induce cell proliferation in response to VEGF while KDR does. VEGF promoted MAP kinase activation in porcine aortic endothelial cells expressing recombinant KDR. In contrast MAP kinase was not activated by VEGF in cells expressing recombinant flt-1 in two separate studies (Seetharam *et al.*, 1995; Kroll *et al.*, 1997). It is therefore possible that flt-1 does not induce cell proliferation because it does not activate the MAP kinase.

A cDNA coding an alternatively spliced soluble form of flt-1 (sflt-1), lacking the seventh Ig-like domain, the transmembrane sequence and the cytoplasmic domain, has been identified in HUVEC (Kendall *et al.*, 1996). This sflt-1 receptor binds VEGF with high affinity, is soluble and can inhibit VEGF induced mitogenesis. It may be a physiological negative regulator of VEGF's action. (Kendall *et al.*, 1996).

### 1.11.1 Flt-1.

A tyrosine kinase sequence was used as a probe to screen a human genomic DNA library in an attempt to isolate new receptor tyrosine kinases that might have been involved in carcinogenesis (Shibuya *et al.*, 1990). An exon encoding a novel receptor type tyrosine kinase was obtained and was found to be expressed in low levels in normal tissue. An 8 kb cDNA corresponding to this gene was isolated from a normal human placental cDNA library and was found to be distantly related to the structures of c-fms (colony stimulating factor-1 receptor) c-kit (stem cell factor receptor) and

PDGF receptor. Thus this gene was designated as flt-1 (fms-like tyrosine kinase; Shibuya *et al.*, 1990).

flt-1 consists of 1338 amino acid residues which are divided into seven immunoglobulin-like domains in its extracellular region, a 22 amino acid transmembrane region which is followed by a cluster of basic amino acids and a 558 amino acid cytoplasmic region containing a tyrosine kinase domain as shown in figure 1.7 (Shibuya *et al.*, 1990). flt-1 binds all 4 splice variants of VEGF with high affinity (kd=1-20 pmol; DeVries *et al.*, 1992; Waltenberger *et al.*, 1994) resulting in autophosphorylation of the receptor which in turn results in the phosphorylation of other proteins (Myoken *et al.*, 1991). PIGF also binds flt-1 but with lower affinity than VEGF (kd=170 pmol; Sawano *et al.*, 1996).

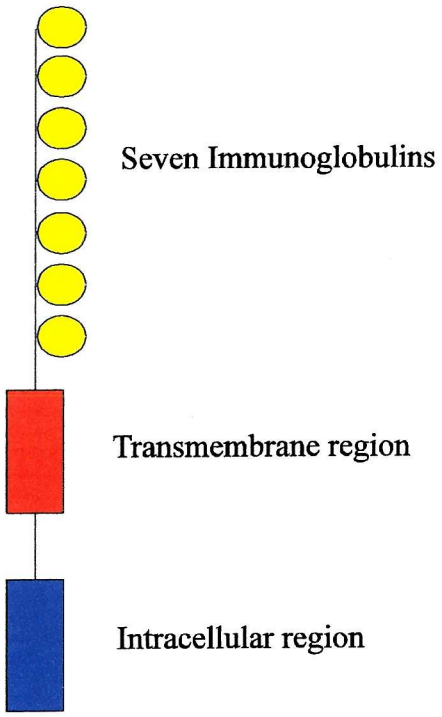


**Figure 1.7 Structure of the flt-1 receptor** with the seven immunoglobulin-like domains, a transmembrane region and an intracellular domain.

The flt-1 gene that encodes this RTK maps to chromosome 13q along with flk-2/flt-3. This gene also seems to encode two isoforms as cDNA clones putatively encoding flt-1 molecules with different C-terminals that have been isolated (DeVries *et al.*, 1992). In addition, the flt-4 gene encodes a long and short form by alternative processing making this a common feature of this receptor subtype in humans (Pajusola, 1993). This characteristic may have possible consequences on the associated mechanisms of signal transduction.

**Signal transduction of the flt family.**

In general, signal transduction from receptor-type tyrosine kinases is proposed to be as follows (Schlessinger and Ullrich 1992; Egan *et al.*, 1993) 1. Dimerisation and oligomerization of the receptors through ligand binding, 2. Activation of tyrosine kinases and autophosphorylation of the receptor, 3. Association of signal transducers and other tyrosine kinases, 4. Tyrosine phosphorylation of these associated molecules, 5. Translocation to the cell membrane, 6. Activation of RAS, 7. Activation of MAP kinase cascade.

### 1.11.2 KDR.

After the isolation of the flt-1 gene, a receptor closely related to flt-1 the kinase domain containing receptor (KDR) was detected in a human endothelial cell cDNA library (Terman *et al.*, 1991; Terman *et al.*, 1992) and from a mouse fetal cDNA library (fetal liver kinase-1, flk-1; Matthews *et al.*, 1991). Since the two are derived from the same gene but from different species, the receptor is known as the KDR/flk-1. flt-1 and KDR are most structurally related on the basis of the kinase insert sequence (about 50% identity). Chromosomal mapping of the KDR gene shows that the flk-1, c-kit and PDGFα genes are closely linked (Matthews *et al.*, 1991).
An original report showed that the affinity of VEGF for the KDR receptor was approximately 100 pmol. However, KDR has been reported to have varying affinities

for VEGF. Although PIGF is a ligand for flt-1 it is not a ligand for KDR (Sawano *et al.*, 1996)

### 1.11.3 Neuropilin.

Endothelial cells also contain VEGF receptors possessing a lower mass than either flt-1 or KDR (Gitay-Goren *et al.*, 1992). It was subsequently found that these smaller VEGF receptors of the endothelial cells are isoform specific and bind to $VEGF_{165}$ but not to $VEGF_{121}$ . It was therefore recognised that these receptors are not related to the flt-1 or KDR receptors that bind to both VEGF isoforms. The receptors were revealed to be neuropilin-1 (Soker *et al.*, 1998). In addition, a second closely related gene was discovered, neuropilin-2 (Soker *et al.*, 1998; He *et al.*, 1997).
The neuropilins have a short intracellular domain and are therefore unlikely to function as independent receptors. Indeed, no responses to $VEGF_{165}$ were observed when cells expressing neuropilin-1 but no other VEGF receptors were stimulated with $VEGF_{165}$ (Soker *et al.*, 1998). Nevertheless, gene disruption studies indicate that neuropilin-1 is probably an important regulator of blood vessel development as mouse embryos lacking a functional neuropilin-1 gene die because their cardiovascular system fails to develop properly (Kitsukawa *et al.*, 1997). It is therefore likely that neuropilin-1 is a $VEGF_{165}$ co-receptor. This assumption is supported by experiments showing that KDR binds $VEGF_{165}$ more efficiently in cells expressing neuropilin-1, and this potentiating effect is subsequently translated into a better migratory response to $VEGF_{165}$ as compared to the migratory response of cells expressing KDR but no neuropilin-1 (Soker *et al.*, 1998). However there is no evidence of neuropilin-1 being a co-receptor for flt-1.

Neuropilin-1 is the same receptor that nerve axons use to detect semaphorin III, a protein that helps steer axons to their proper destinations in the developing nervous system. The receptors dual role raises the possibility that angiogenesis , far from being random, is in fact as highly scripted as axonal pathfinding. Neuropilins role in angiogenesis seems to be different from its role in axonal guidance, however. When

Semaphorin III binds to the receptor on the growing tips of neurons, it repels the cells, keeping them from getting off track. But on developing blood vessels, neuropilin-1 seems to work in concert with KDR to stimulate vessel growth toward a VEGF source (Roush, 1998).

### 1.11.4 Receptors for other VEGF related proteins.

Flt-4 is not a receptor for VEGF or PIGF but rather binds a recently identified member of the VEGF family, VEGF-C (Joukov *et al.*, 1996).

The 4.5 and 5.8 kb flt-4 mRNAs encode polypeptides diverging in their C-terminal due to alternative splicing (Pajusola, 1993). The long flt-4 form contains 65 additional amino acid residues in its C-terminus in comparison to the short one. The mature form of flt-4 differs from the other two receptors in that it undergoes proteolytic processing by glycosylation and proteolytic cleavage. In contrast flt-1 and KDR receptors are expressed as intact polypeptides of about 200 kDa (Vaisman *et al.*, 1990).

Flt-3 (Rosnet *et al.*, 1991) is homologous to flt-1 and possibly encodes a receptor for VEGF but as yet no VEGF binding has been detected (Sander *et al.*, 1997). Figure 1.8 shows all of the VEGF receptors and the forms of VEGF which activate them.

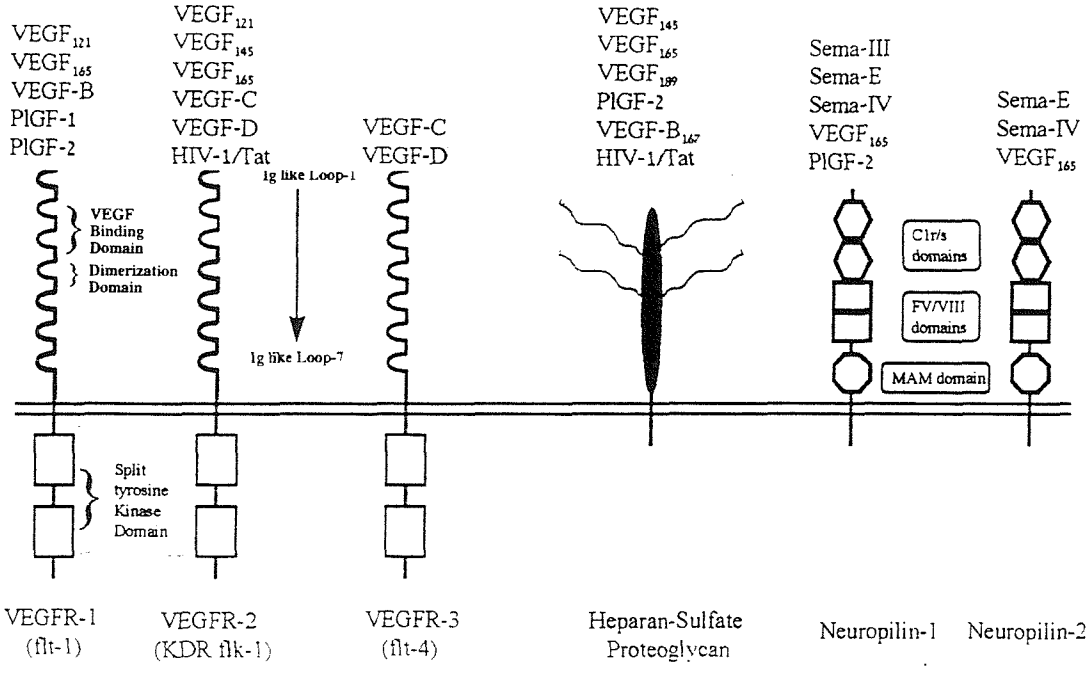


**Figure 1.8 Different VEGF receptors** and the isoforms of VEGF which activate them (Neufeld *et al.*, 1999, p10).

## 1.12 Nitric oxide production in response to VEGF.

VEGF receptor stimulation has been found to lead to receptor autophosphorylation and tyrosine phosphorylation of various cellular proteins. These events result in the transient accumulation of intracellular $Ca^{2+}$, inositol 1,4,5-triphosphate (Waltenberger *et al.*, 1994; Brock *et al.*, 1991) and endothelial nitric oxide synthase (eNOS) activation by a mechanism that is inhibited by the tyrosine kinase inhibitor genistein (Ku *et al.*, 1993). Morbidelli *et al.*, (1996) have shown that VEGF's activity in inducing growth of coronary vein endothelial cells requires NOS activity. They also demonstrated that NOS is persistently activated by VEGF and therefore that it could be involved in subsequent stages of VEGF-induced signalling of mitogenesis. Recently, NOS activity has also been shown to be required for VEGF's permeability enhancing effects in an isolated microvessel preparation (Wu *et al.*, 1996). Nitric oxide (NO) contributes to the blood vessel-permeabilizing effects of VEGF and to the VEGF stimulated vasodilation (Tuder *et al.*, 1995; Chin *et al.*, 1997; Murohara *et al.*, 1998). The production of NO is consistently shown to be up-regulated by VEGF, indicating that it is an important signalling molecule for VEGF (Dembinskakiec *et al.*, 1997; Hood *et al.*, 1998).

NOS activity has also been shown to be required for VEGF induced neovascularization in the rabbit cornea model for angiogenesis *in vivo* (Ziche *et al.*, 1997).

It has been suggested that VEGF's effects in increasing permeability are mediated by increased transcytotic transport due to the formation of numerous interconnected membrane invaginations termed vesicular-vacuolar organelles (VVOs; Kohn *et al.*, 1992). Plasma membrane caveolae have recently been shown to have a similar elaborate structure, with a large percentage clustered around larger 'vacuoles' in a rosette/bunch of grapes formation (Parton *et al.*, 1994; Robinson *et al.*, 1992). It is likely therefore, that VVOs and caveolae represent the same organelle. Caveolae were originally described as intracellular compartments involved in endocytotic and transcytotic transport (Montesano *et al.*, 1982). They are now recognised as having the additional functions of concentrating and internalising small molecules by a process called potocytosis and serve as signal transduction organising centres for segregating

and concentrating membrane receptors with downstream effectors (Anderson *et al.*, 1993; Lisanti *et al.*, 1994; Parton *et al.*, 1996).
Recent work has shown that eNOS is targeted to caveolae (Garcia-Cardena *et al.*, 1996; Feron *et al.*, 1996; Shaul *et al.*, 1996; Venema *et al.*, 1996) and that eNOS activity is regulated by protein-protein interactions with the structural protein caveolin-1 (Ju *et al.*, 1997). Thus, eNOS activity within the caveolae may have an important role in mediating VEGF's effects in increasing endothelial cell permeability.

**1.13 VEGF signal transduction.**

Although the significance of VEGF and its receptors is well established, the signal transduction cascades activated by VEGF and their involvement in mediating the mitogenic response of endothelial cells to VEGF are incompletely characterised.

VEGF induces an increase in intracellular free calcium concentration. A distal step in the $Ca^{2+}$ signalling pathway is the activation of the $Ca^{2+}$ and phospholipid-dependent kinase, protein kinase C (PKC). PKC is activated by an increase in $Ca^{2+}$ and the generation of diacylglycerol (DAG; Nishizuka *et al.*, 1993). Activation of PKC plays a prominent role in the growth response of endothelial cells (Montesano *et al.*, 1992). Hu and Fan, (1995) also reported previously that incubation with PKC inhibitors can significantly decrease the proliferation of endothelial cells. It has been reported that PKC isoforms $\alpha$ and $\zeta$ are important for VEGF's angiogenic effects. (Wellner *et al.*, 1999).

In mammalian cells, ligand binding to receptor tyrosine kinases trigger the activation of downstream signalling enzymes, including mitogen-activated protein (MAP) kinase, phosphatidylinositol 3-kinase (PI 3-kinase), p70 S6 kinase and PLC$\gamma$ (Marshall *et al.*, 1995). Activation of these signalling intermediates transduces extracellular signals to the nucleus and ultimately regulates gene expression and cellular responses such as cell proliferation, migration, differentiation and apoptosis.

Recent studies by Yu *et al.*, (1999) have shown that in HUVEC, extracellular signal-regulated protein kinase (ERK), PI 3-kinase and p70 S6 kinases are all essential for VEGF induced HUVEC proliferation.

### 1.14 VEGF in the formation of the corpus luteum.

A rich capillary plexus progressively develops in the theca layer surrounding the avascular granulosa layer and, following ovulation, the vessels proliferate further, penetrate into the granulosa layer and form the corpus luteum.
The expression of VEGF has been detected in the corpora lutea of humans (Kamat *et al.*, 1995) and mammals (Philips *et al.*, 1990; Ravindranath *et al.*, 1992).

The expression of VEGF in the theca and granulosa cells was examined during the course of follicular development and corpora lutea formation in human ovaries by Yamomoto *et al.*, (1997b). The granulosa cells in the primordial and primary follicles were VEGF negative, but at the preantral stage, the granulosa cells showed weakly positive immunostaining for VEGF. However, the VEGF immunostaining in the granulosa cells was weak throughout folliculogenesis. In contrast, the theca interna cells of developing follicles showed strong staining for VEGF. In atretic follicles, the granulosa and theca cells were negative for VEGF. In the corpora lutea, VEGF was strongly expressed in both granulosa and theca cells in the early luteal phase, but the VEGF staining in these cells became weak in the mid- and late luteal phases (Yamomoto *et al.*, 1997b).
These results are in contrast to the expression of bFGF which showed strong expression in the luteinised thecal cells and atretic follicles (which were negative for VEGF). In the corpora lutea, the immunostaining pattern was almost identical to that of bFGF, except that the thecal cells of the corpora lutea in the late luteal phase and during regression expressed bFGF but not VEGF (Yamomoto *et al.*, 1997a).
These findings suggest that drastic differentiation of granulosa cells into large lutein cells after the LH surge and ovulation is associated with the increase in VEGF

expression, which is presumably involved in angiogenesis during corpus luteum development.

VEGF expression has been reported to be enhanced by LH or hCG in cultured bovine (Garrido *et al.*, 1993) and human (Neulen *et al.*, 1995) granulosa cells. High levels of VEGF have also been reported in both granulosa cells and theca cells of patients with polycystic ovary syndrome (Kamat *et al.*, 1995) which is characterised by hypersecretion of LH. These findings indicate that the expression of VEGF in granulosa cells is regulated by gonadotrophins, especially LH/hCG.

A recent study has shown that VEGF is essential for the development of the corpus luteum (Ferrara *et al.*, 1998). Treatment with a truncated soluble flt-1 receptor consisting of the first three immunoglobulin-like domains of the human flt-1 fused to a Fc-IgG resulted in virtually complete suppression of corpus luteum angiogenesis in a rat model of hormonally induced ovulation. This effect was associated with inhibition of corpus luteum development and progesterone synthesis. Failure of maturation of the endometrium was also observed. Areas of ischemic necrosis were demonstrated in the corpora lutea, however, no effect on the pre-existing ovarian vasculature was observed (Ferrara *et al.*, 1998).

### 1.15 Regression of the corpus luteum.

There are two main mechanisms of corpus luteum regression or luteolysis which were first described by Malvern, (1969), based on observations in the rat. Functional luteolysis refers to the suppression of progesterone production and is the first stage. Structural luteolysis follows and is the process by which the corpus luteum degenerates (Malvern, 1969; Malvern, 1966; Wang *et al.*, 1993). In the human, functional and structural luteolysis appear to be separate events as the corpora lutea of previous cycles are present within the ovary.

### 1.15.1 Functional luteolysis.

Several features have been reported which characterise the functional luteolysis of the corpus luteum. Progesterone secretion decreases due to the abrogation of action by LH, which interrupts the trophic support of luteal function. The process resembles the effects of LH withdrawal, but in natural luteal luteolysis LH secretion is not decreased. It seems that it is the luteal responsiveness to LH that is decreased as luteolysis approaches (Behrman, 1979). One of the mechanisms for this decrease in LH responsiveness is the uncoupling of the LH receptor from adenylate cyclase, blocking the production of cAMP. Thus binding of LH to its receptors has no effect (Eyster *et al.*, 1985; Rojas *et al.*, 1989).

### 1.15.2 Structural luteolysis.

Structural luteolysis is defined as involution of the corpus luteum. This process has been studied in many species such as the cow, sheep and rat (Zheng *et al.*, 1994) and is characterised by the release of cellular blebs referred to as apoptotic bodies, nuclear condensation and phagocytosis (Kerr *et al.*, 1972; Wyllie *et al.*, 1980; Yuan and Giudice, 1997). However, there is very little evidence for apoptosis in the regression of the human or primate corpus luteum (Fraser *et al.*, 1999).

Matrix remodelling is also a major factor in structural luteal regression. Matrix proteolysis is normally controlled by TIMPs. However, at the time of luteolysis there is a decrease in the level of TIMP expression (Tanaka *et al.*, 1992). It has been proposed that LH is necessary for TIMP synthesis because receptors for this gonadotrophin are inactivated during functional luteolysis (Eyster *et al.*, 1985). Certainly *in vitro*, LH and hCG stimulate TIMP expression in granulosa cells (Mann *et al.*, 1991; O'Sullivan *et al.*, 1997).

### 1.16 Rescue of the corpus luteum.

If conception occurs rescue of the corpus luteum from functional luteolysis is vital for the maintenance of pregnancy. The corpus luteum is essential for the production of progesterone during the first six weeks of pregnancy until the placenta assumes this role. In the primate, hCG is known to extend the functional life of the corpus luteum. And hCG can be detected in maternal serum nine days after ovulation in the conception cycle in women. The mechanism of hCG rescue is at this point unknown, but administerisation of hCG to women is known to increase progesterone secretion and to extend luteal function.

# Hypothesis.

Human ovarian microvascular endothelial cells have their own unique identity in culture and are most responsive to angiogenic related compounds released by luteinising granulosa cells.

# Aims of the study.

1. The development of a reproducible and convenient method for the isolation and culture of human ovarian microvascular endothelial cells and to determine their morphological and functional characteristics.

2. Determine the stimulatory effects on the HOMEC by VEGF and investigate which VEGF receptor is responsible for proliferation. Investigate possible mechanisms whereby VEGF exerts its effects, such as through nitric oxide production.

3. Assess the interactions between different cells of the corpus luteum by culturing endothelial cells in granulosa cell conditioned media and determining the effect on endothelial cell proliferation.

4. Develop a co-culture model to show cellular interactions and formations of vascular structures similar to those of the corpus luteum.

# Chapter 2.

# Development of a model culture system for the isolation and culture of human ovarian microvascular endothelial cells from follicular fragments.

## 2.1 Introduction.

The belief that endothelial cells are a homogenous cell population has in more recent years been challenged. There is now a vast amount of evidence which shows that endothelial cells from different tissues and vessel types are morphologically, biochemically and functionally diverse (Fajardo, 1989).

This finding of endothelial cell heterogeneity has led researchers to question which type of endothelial cells they utilise for *in vitro* studies. Human umbilical vein endothelial cells (HUVEC) were first isolated by Jaffe *et al.* in 1973. They have been one of the favoured endothelial cell types over the past two decades for *in vitro* studies looking at angiogenesis and vascular function. HUVEC have the benefit of being easy to isolate and culture from umbilical veins and have the advantage that supply of human tissue is not usually a limiting factor. However, the question of whether HUVEC, which are isolated from large vessels provide the most accurate model for studies of the microvasculature has been asked. Spontaneously transformed endothelial cell lines have also been widely used but how reflective these cells are of the *in vivo* situation must be questioned. Transformed cell lines, as there name suggests, have lost many of the natural control mechanisms governing the behaviour of normal endothelial cells.

Endothelial cells have recently been isolated from many tissues of various species as researchers have found that the most reliable endothelial cells for studying a particular organ are those derived from the organ in question. Endothelial cells have been isolated from the primate corpus luteum and the porcine ovary, however, there were no models for culturing human ovarian microvascular endothelial cells when this project was undertaken.

## 2.2 Endothelial cell heterogeneity.

Recent evidence has shown that endothelial cells of the testicular and ovarian vasculature bind and transport human chorionic gonadotrophin (hCG) to the underlying endocrine cells, whereas endothelial cells in other organs do not display this capacity (Ghinea *et al.*, 1994). Current culture models for microvascular endothelium have shown that in the bovine corpus luteum there are five separate microvascular endothelial phenotypes which show differences in their actin cytoskeleton, as well as their responsiveness to growth factors (Fenyves *et al.*, 1993). Microvascular endothelial cells isolated from mouse brain are unable to form capillary-like structures on Matrigel (Morbidelli *et al.*, 1995), whilst in sheep they are the only microvascular cells to demonstrate tight junctions (Craig *et al.*, 1998). Cultured placental villous microvessels do not form cobblestone monolayers in culture (Kacemi *et al.*, 1996). Endothelial cells isolated from the porcine fetus display cobblestone morphology with the exception of testicular endothelium, while the myocardial endothelium showed very low binding of von Willebrand factor (vWF) (Plendl *et al.*, 1996). VEGF appears to have a survival effect on sinusoidal endothelial cells of rat liver. Even in the presence of FGF and high serum concentration, these cells are unable to grow or survive without VEGF. The rat sinusoidal cells express high levels of flt-1 and KDR mRNA, and the cells display differences in their morphology in the absence or presence of VEGF. Therefore, the activated flt-1 and KDR receptors may modulate the cytoskeletal organisation of the sinusoidal endothelial cells.

None of the endothelial cell lines established so far have been shown to be solely

dependent on exogenously added VEGF for their growth, and hence all of the endothelial cells shown to respond to VEGF are primary cultures. Why do endothelial cell lines lose their responsiveness to VEGF? One of the reasons for this could be due to a decrease in the expression of the VEGF receptors and the acquisition of VEGF-independent growth-stimulatory mechanism, since the levels of flt-1 and KDR transcripts are very low in endothelial cell lines examined so far (Hughes *et al.*, 1996; Shibuya, 1995).

## 2.3 Model development.

The evidence presented above shows that the study of the development of the human corpus luteum requires cultures of human ovarian microvascular endothelial cells. Endothelial cells have been isolated from the primate corpus luteum (Christenson and Stouffer, 1996). However, previous attempts to isolate endothelial cells from the human corpus luteum in this laboratory proved unsuccessful due to difficulties in complete separation of the tissue.
Another major problem in isolating endothelial cells from the human corpus luteum is the availability of tissue. For tissue to be of any use, surgery would have to be performed at the correct stage of the patients cycle. Current medical opinion is that it is preferable not to remove the ovaries from younger women due to the associated hormonal problems. Another factor is the ethical considerations of using such tissue. These problems in obtaining human corpora lutea meant that human ovarian tissue from other sources would have to be used.

Women undergoing in vitro fertilisation treatment have to have their oocytes from developed follicles removed manually. A double lumen needle is inserted into each developed follicle via transvaginal ultrasound guidance. As this needle is inserted into the follicle it removes a small fragment of the follicle wall. The follicles are aspirated just before they would spontaneously ovulate. The follicles are mature and so the fragments will contain the inner granulosa cells and the outer theca cells which are

richly vascularised (figure 2.1). These fragments of the richly vascularised theca layer should contain capillary fragments from which it was proposed to grow endothelial cells.
As the follicles are aspirated these follicular fragments are collected and following the removal of the oocytes, would normally be discarded.

Evidence already shows that capillary fragments can be used to generate cultures of endothelial cells. Brown *et al.*, (1996) developed an *in vitro* system for human angiogenesis by embedding fragments of human placental blood vessels in a fibrin gel. These fragments were found to give rise to complex networks of microvessels within 7-21 days in culture. These microvessel outgrowths stained positively for the endothelial cell marker von Willebrand factor. Electron microscopy also clearly identified Weibel Palade bodies identifying them as endothelial.

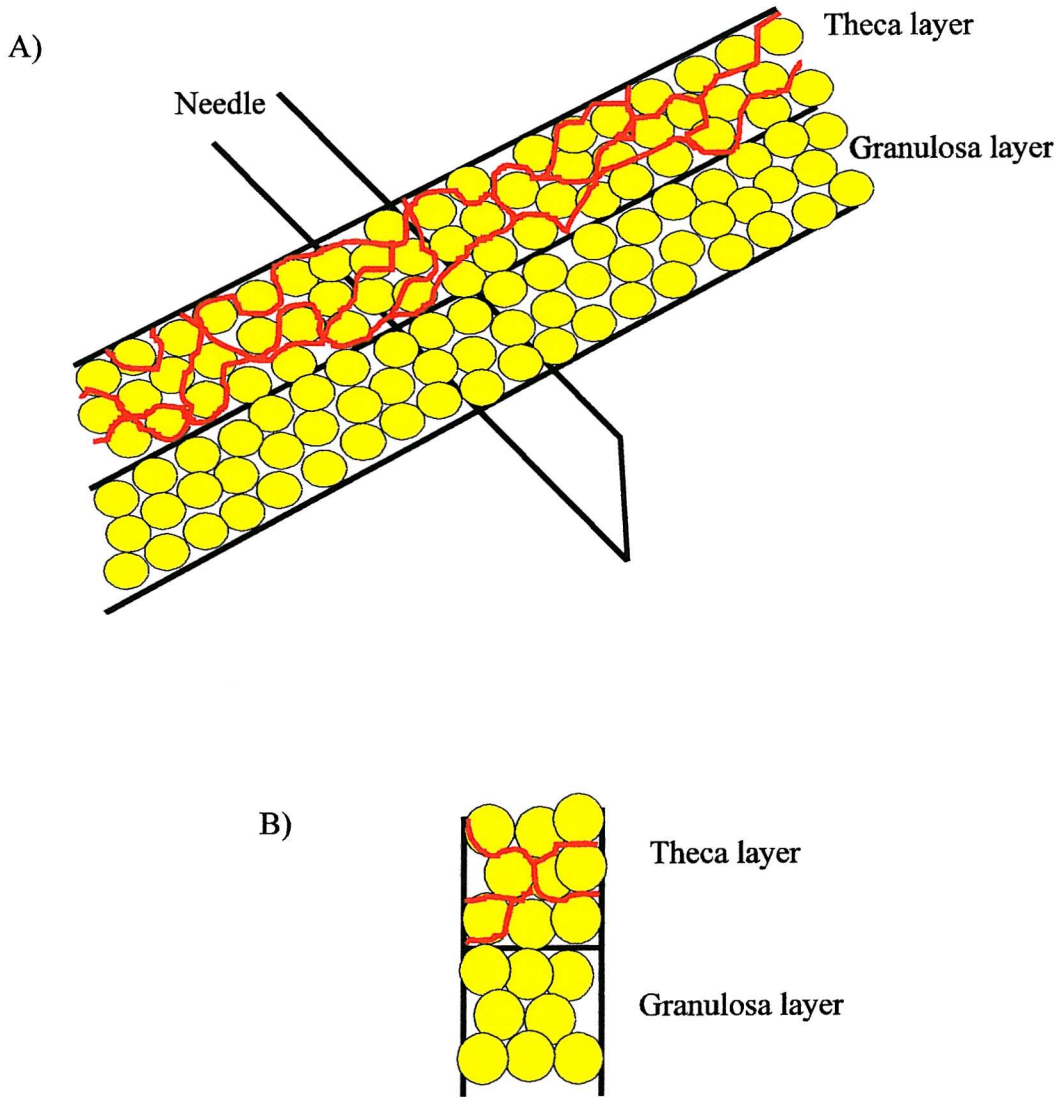


**Figure 2.1 Aspiration procedure and removal of a fragment of the follicle wall.** A) shows the needle inserted into the follicle during oocyte collection and B) shows the fragment of follicle wall removed during this procedure with the granulosa layer and the theca layer containing capillary fragments.

## 2.4 Materials and Methods.

Ethical approval for the use of human tissue in these studies was obtained.

### 2.4.1 IVF protocol.

Follicular aspirates were obtained at ooctye collection for IVF according to a procedure approved by our local ethical committee. The treatment protocol, adapted from a previously described method by Jenkins *et al.*, (1991), involved down-regulation of pituitary function with gonadotrophin releasing hormone analogue (Nafarelin: 400 μg intranasally twice daily) started in the luteal phase of the preceding cycle. From day 4 of the IVF cycle, 150-600 IU FSH (doses were tailored to individual patients) was administered daily to stimulate multifollicular development. When the leading two follicles had a diameter of >18 mm and serum oestradiol concentration was >300 pmol/l for each follicle >14 mm in diameter, human chorionic gonadotrophin (hCG; 100 IU) was given and oocytes were collected 34 hours later under transvaginal ultrasound guidance. Follicles aspirated were >15 mm in diameter. Figure 2.2 shows a schematic diagram of how the follicles were aspirated.

### 2.4.2 Media.

All cell cultures in this chapter were maintained in a basic Media 199 (M199) supplemented with 10% fetal calf serum (heat inactivated), penicillin (100 units/ml), streptomycin (100 μg/ml), amphotericin B (2.5 μg/ml) and L-glutamine (2 μmol/ml), all from Life Technologies, Paisley, UK. Any other supplements added to specific cultures are detailed in the relevant section.

All additions were sterile filtered through a 0.44 μm sterile filter followed by a 0.22 μm sterile filter (Sartorius AG, Goettingen, Germany) before addition to the Media. Supplemented media were stored at 4°C and kept for no longer than 10 days following supplementation.

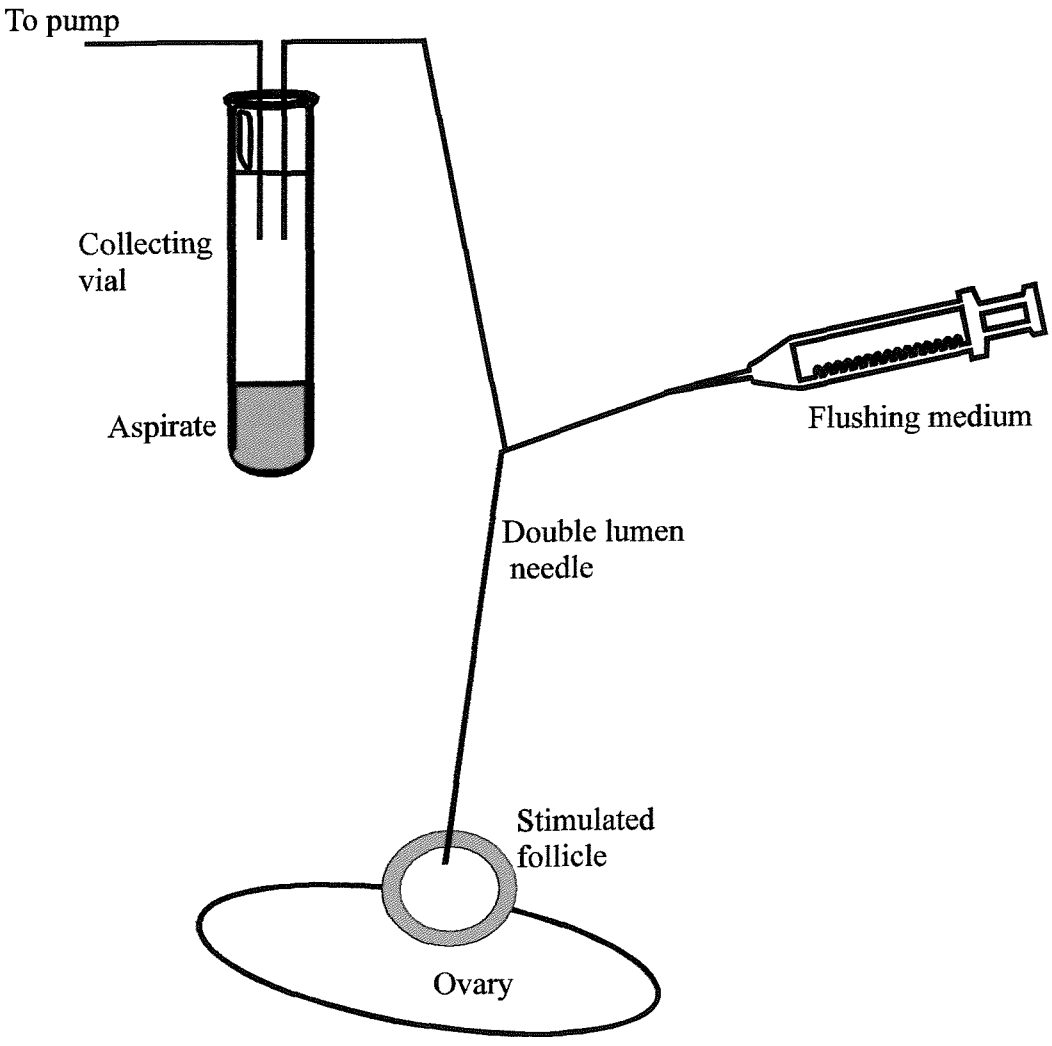


**Figure 2.2 Process of follicular aspiration during oocyte collection for IVF.**

## 2.4.3 Human ovarian microvascular endothelial cell (HOMEC) isolation and culture.

Follicular aspirates and washes were combined for each patient undergoing oocyte collection for IVF. The aspirates were filtered through 70 µm nylon cell strainers (Falcon, Becton Dickinson Labware, Bedford, UK) to retain any fragments of tissue which were removed from the edge of the follicle during the procedure. The filters were backwashed with M199 using a fine tipped pastette. The tissue pieces in suspension were transferred to a conical tipped centrifuge tube and the tissue was washed by settling of the fragments for 20-30 min followed by resuspension in M199. The washing process was performed 2-3 times further, depending on the amount of blood and mucus in the aspirate. The tissue fragments were then centrifuged at 1000 x g for 10 min to yield a small pellet. The fragments were chilled for 15 min before resuspension in 0.5 ml of Matrigel (Cat No. 40234, Collaborative Biomedical Products, Becton Dickinson Labware). Aliquots (50-100 µl) of this mixture were dispensed onto the surface of uncoated 25 $cm^2$ flasks and allowed to set (figure 2.3 shows the aliquots in the culture flask).

Cultures were maintained in supplemented M199 with additional endothelial cell growth supplement (ECGS; 150 µg/ml; Sigma Chemicals Co., Poole, UK) and VEGF (6.25 ng/ml; Cat No. 293-VEGF-010, R and D Systems, Abingdon, UK) using 5% $CO_2$ in air at 37°C. Culture medium was changed every 3-4 days and cultures were monitored for growth daily by phase contrast microscopy.

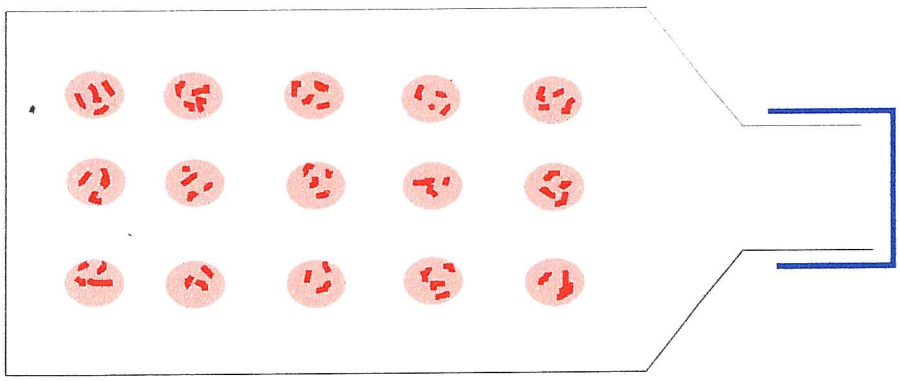

**Figure 2.3 Arrangement of Matrigel aliquots in the culture flask.**

Cultures which did not show any signs of development or cultures which appeared to be mainly producing cells exhibiting fibroblast morphology were discarded. Cultures which showed patches of cells with a cobblestone morphology were preserved by eliminating any other areas of contaminating cell types. This was achieved by removal of Matrigel blobs within these cultures which were not showing signs of producing cobblestone areas of cells and other patches of non-endothelial cells. The unwanted Matrigel blobs were removed using a combination of a sterile cotton bud inserted into the end of a normal tipped pastette (figure 2.4). These could be inserted into the culture flask and manouvered fairly skilfully to remove only certain areas.

**Figure 2.4 Tool constructed for removal of unwanted material within the HOMEC cultures.** The tool is made from a sterile cotton bud inserted into the end of a normal pastette.

Cell scrapers proved not to be as efficient for this procedure as they did not remove areas completely. The area of interest was circled using a lab-marker and a microscope to ensure the endothelial-like cells were left untouched (figure 2.5). The cultures were washed with Hanks balanced salt solution (HBSS; Sigma Chemicals Co.) several times to ensure all of the waste was removed from the culture. These cultures were treated as before and any further areas of contaminated cells which developed were removed.

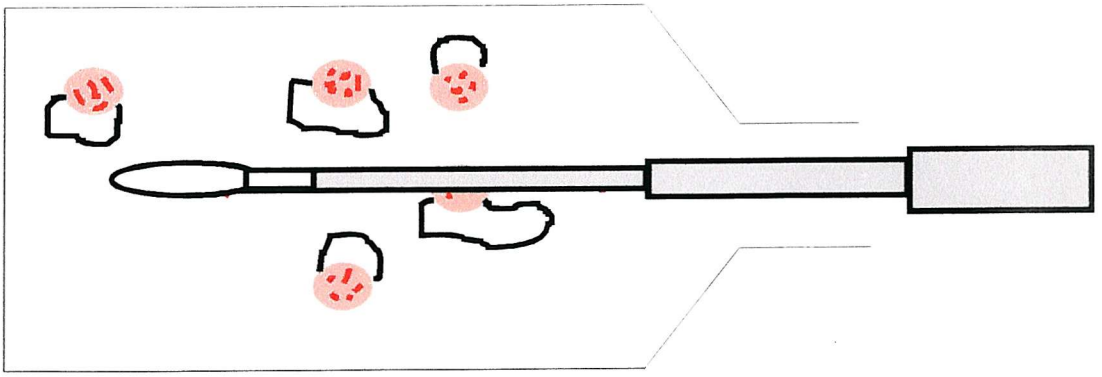

**Figure 2.5 Clearing of unwanted material in the HOMEC cultures.** Patches of cobblestone cells were identified and circled using a light microscope. Material in the flasks not producing these endothelial-like cells were removed along with patches of cells of a fibroblast morphology.

## 2.4.4 Corpus luteum endothelial cell isolation and culture model.

Corpora lutea were removed from patients during hysterectomy and were delivered to the laboratory as soon as possible. The corpus luteum was cut into eight small pieces with two scalpels. Two of the smaller pieces were then shredded further and resuspended in M199. The protocol for the HOMEC follicular aspirate cultures was then followed as regard to washing the tissue by settling and resuspension to remove as many of the red blood cells as possible. The pieces were embedded in Matrigel and aliquoted onto the surface of a culture flask. Cultures were maintained as before and checked for development with phase contrast microscopy daily.

## 2.4.5 ECV304 cell culture.

The ECV304 cell line, a spontaneously transformed HUVEC cell line, was obtained from the European Collection of Animal Cell Cultures (ECACC, Centre for Applied Microbiology and Research, Salisbury, UK). The cells were dispatched as a growing medium at passage 136 and were confluent on arrival. The cells were immediately subcultured and a stock of the cell line was frozen as a back up.

## 2.4.6 Subculture of Cells.

Confluent cell monolayers were washed with a pre-warmed (37°C) solution of HBSS (Sigma) and incubated with 3 ml of a 1 x trypsin EDTA solution (Gibco BRL) for a 25 $cm^2$ culture flask for approximately 5-10 minutes until the cell monolayer began to lift off the culture surface. The trypsin was then neutralised by the addition of 6 ml of fresh M199, transferred to a centrifuge tube and spun at 1000 x g for 10 minutes. The cell pellet was then resuspended in Fresh M199 and transferred to 3 new 25 $cm^2$ flasks.

## 2.4.7 Cell Freezing and Thawing.

ECV304 cells and fibroblasts were the only cell types that were frozen during these studies. All other cultures were isolated and used immediately.

### 2.4.7a Freezing.

The cells were harvested in the same manner used for routine subculture. Following centrifugation, the cell pellet was resuspended in 1 ml of freeze medium (9 ml fetal calf serum: 1 ml dimethyl sulphoxide cryoprotectant). The cell suspension was transferred to a cryopreservation vial and stored at -70°C overnight in a Nalgene Cryo 1°C freezing container. The cryopreservation vial was then snap frozen by immersion in liquid nitrogen and stored in a nitrogen storage vessel.

### 2.4.7b Thawing.

The cryopreservation vial was removed from liquid nitrogen storage and the cap loosened immediately to avoid the risk of explosion of the vial. Sterility was maintained at all times. The vial was thawed in water at 37°C. Cells were removed from the vial and added to 10 ml of fresh M199. The protocol for routine subculture was then followed for centrifugation and plating.

The viability of the cells subjected to the freeze/thaw process did not appear to be affected as there were no problems in generating new cultures which were of the same appearance as those cells not processed in this way.

## 2.4.8 Human umbilical vein endothelial cell (HUVEC) isolation and culture.

HUVEC were harvested from fresh, human umbilical cords obtained at Caesarean section in the Princess Anne Hospital, Southampton using the method of Jaffe *et al.*, 1973. Cords were processed as soon as possible after delivery and cords left for more than 4 hours following delivery were not used.

All surgical instruments were autoclaved and glass ware incubated at 140°C in an oven before use to maintain sterility. The umbilical cord was checked for any signs of damage or piercing and excess blood washed away with HBSS. All solutions used were pre-warmed to 37°C.

The umbilical vein was identified from the two capillaries and cannulated with a blunted gauge 12 needle. The needle was held in place with a sterile double-grip umbilical cord clamp (Hollister Incorporated, Illinois, USA). The vein was flushed with 20 ml HBSS to expel any excess blood or fluid with a syringe. The free end of the cord was then clamped with a cord clamp and the vein was gently perfused with 0.1% (w/v) collagenase type 1A (Cat. No. c-9891, Sigma). The collagenase was added until the vein had become as dilated as possible without rupture. The needle and syringe were left in the vein to prevent leakage of the collagenase and the cord was placed in HBSS at 37°C for 10-15 minutes. Longer incubation times generally resulted in contamination of cultures with fibroblasts. The effluent was flushed through with 20 ml of HBSS and centrifuged at 1000 x g for 10 min. The cells were resuspended in M199, cultures were grown to confluence on 1% (w/v) gelatin-coated 25 $cm^2$ flasks. Cultures were maintained in supplemented M199 with additional endothelial cell growth supplement (ECGS; 150 µg/ml) using 5% $CO_2$ in air at 37°C. Culture medium was changed every 3-4 days and cells were used up to and including passage 4.

The efficiency of this cell preparation with respect to the average number of HUVEC collected from each cord varies greatly depending on several factors. The length of the cord, the cord's morphology (eg, some cords were straight and easily cannulated and some were more coiled making cannulation difficult) and length of collagenase incubation were the major factors involved.

## 2.4.9 Fibroblast culture.

Human foreskin fibroblasts were kindly supplied by the Department of Medical Oncology, Southampton General Hospital. The cell cultures were maintained in the

supplemented M199 with no additional growth factors, in 5% $CO_2$ in air at 37°C. Culture medium was changed every 3-4 days and cells were used up to and including passage 10.

## 2.4.10 Histochemistry.

In order to confirm the ovarian origin of fragments obtained by follicle aspiration, histochemical staining for the steroidogenic marker 3β-hydroxysteroid dehydrogenase (3βhsd) was carried out.
HOMEC cultures exhibiting cell morphology consistent with endothelial cobblestone growth and the original tissue fragment in Matrigel that the cells had grown out from, were stained according to the method described by Aldred and Cooke, (1983). Cultures were washed with HBSS and incubated at 37°C for 2 hours with a mixture of 100 µl 5α-androstan-3β-ol-17-one (epiandrosterone) in dimethyl formamide (2 mg/ml), 1 ml nitroblue tetrazolium (1.6 mg/ml), 800 µl $NAD^+$- free salt (3 mg/ml) and 4 ml of phosphate buffered saline (PBS; Life Technologies). Cultures were incubated at 37°C for 1-2 hours. The presence of staining for 3βhsd was observed by light microscopy.

Steroidogenic cells produce progesterone from pregnenolone though the 3βhsd enzyme. As a model for this reaction 5α-androstan-3β-ol-17-one (standing in for pregnenolone) acts as a substrate for the 3βhsd enzyme generating NADH from NAD. NADH and the dehydrogenase enzyme then reduce the nitroblue tetrazolium causing the colour change (Aldred and Cooke, 1983).

## 2.5 Results of HOMEC culture model development.

The cultures of follicular fragments embedded in Matrigel showed signs of cellular development from approximately day 6 of culture. Figure 2.6 shows a Matrigel blob at day 2 of culture. The follicular fragments are clearly visible embedded within the Matrigel. Figure 2.7 shows a culture at day 6 of culture. Here we can clearly see the original tissue fragments but there are now cells growing from these fragments through the Matrigel towards the edge of the Matrigel blob. The cells which developed had a branch-like structure and did not form into monolayers at this point. These branch-like structures became very extensive and in some cultures took over a large proportion of the original blob, as shown in figure 2.8. The branch-like structures grew outwards to the periphery as they divided. This development continued until the cells reached the edge of the blob, at this point they emerged from the Matrigel and moved onto the uncoated surface of the flask between the separate blobs. Figure 2.9 shows this emergence onto the uncoated surface. These cells, which had emerged from the blobs, continued to proliferate and the patches of cells became denser until their elongated appearance became polygonal as they formed a contact inhibited monolayer which had a cobblestone appearance similar to that seen in HUVEC cultures. These areas were small and did not appear from every blob. Only a limited number of fragments within each blob showed this kind of cellular growth leading to cobblestone areas. As the cultures were allowed to progress other cellular morphology was seen within these cultures. Figure 2.10 shows one of these late cultures at day 20 of culture. At this stage we can still clearly see the early branch-like structures, and the cobblestone areas of cell growth outside the original Matrigel, but we can also see the appearance of capillary-like structures on the surface of the Matrigel. These capillary-like structures are at a different level in the culture than the monolayer and thus not in focus.

These were not the only type of cells produced by the follicular fragments in culture. Fibroblasts proved to be a significant problem in the development of this culture model. Fibroblasts are very prolific and take over a culture very rapidly, contaminating the cobblestone areas. For this model to be viable areas of these cobblestone cells had

to be isolated so further studies could be performed on pure cells with no or little contamination from other cell types.

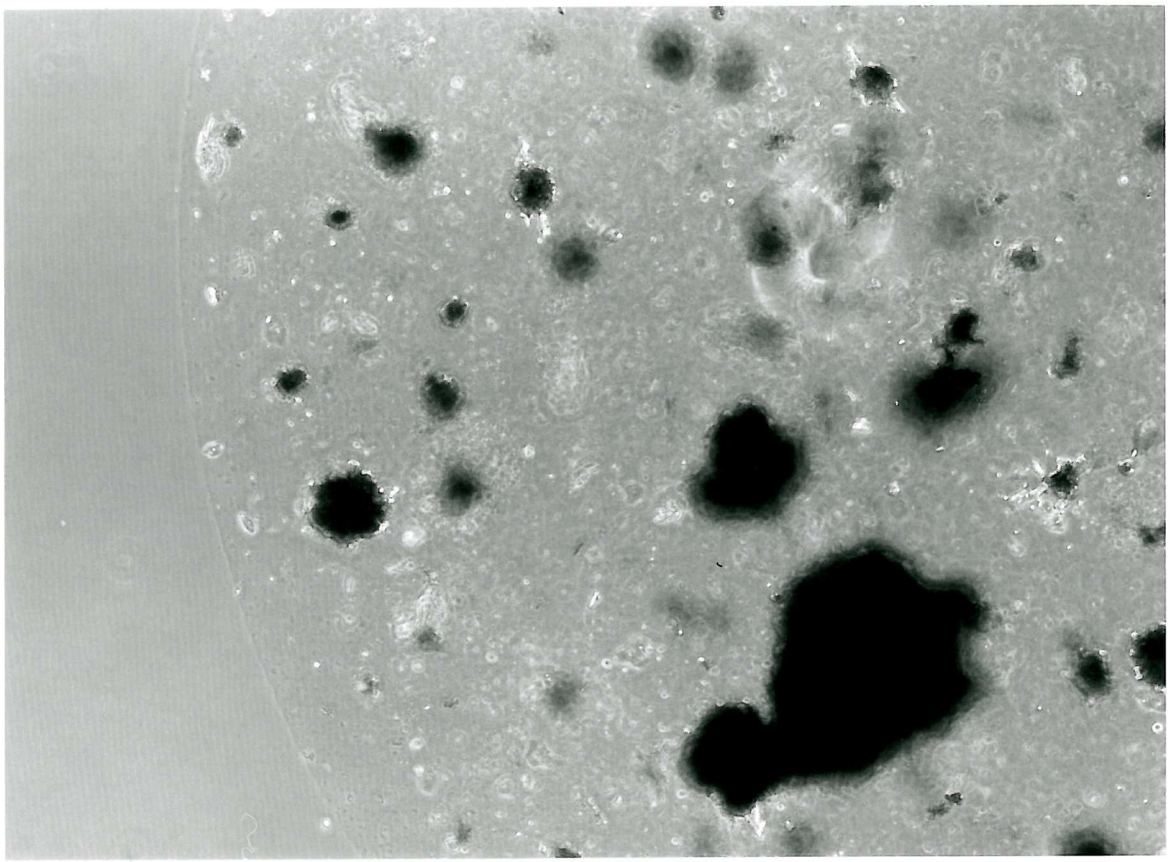

**Figure 2.6 HOMEC culture at day 2.** Follicular material can be seen embedded within the Matrigel although there is no sign of endothelial cell development.

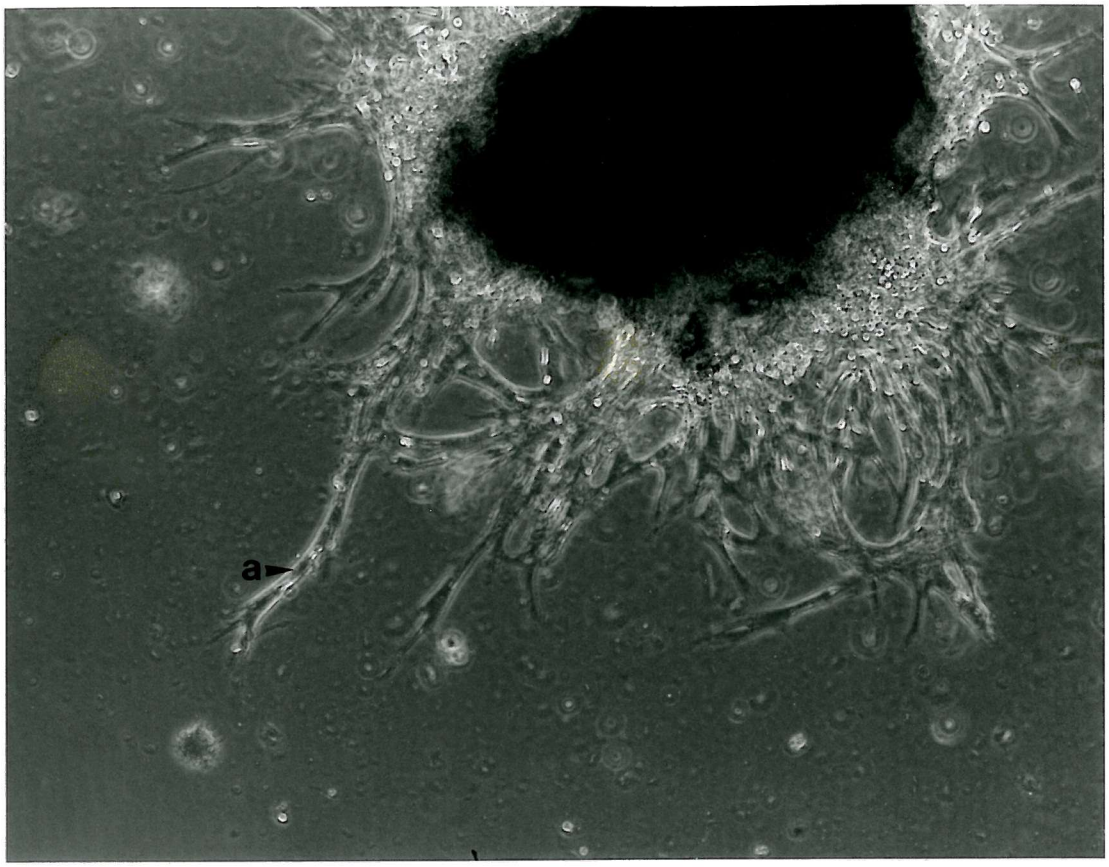


**Figure 2.7 HOMEC culture at day 6.** Branch-like cellular structures (a) can be seen growing from the follicular material.

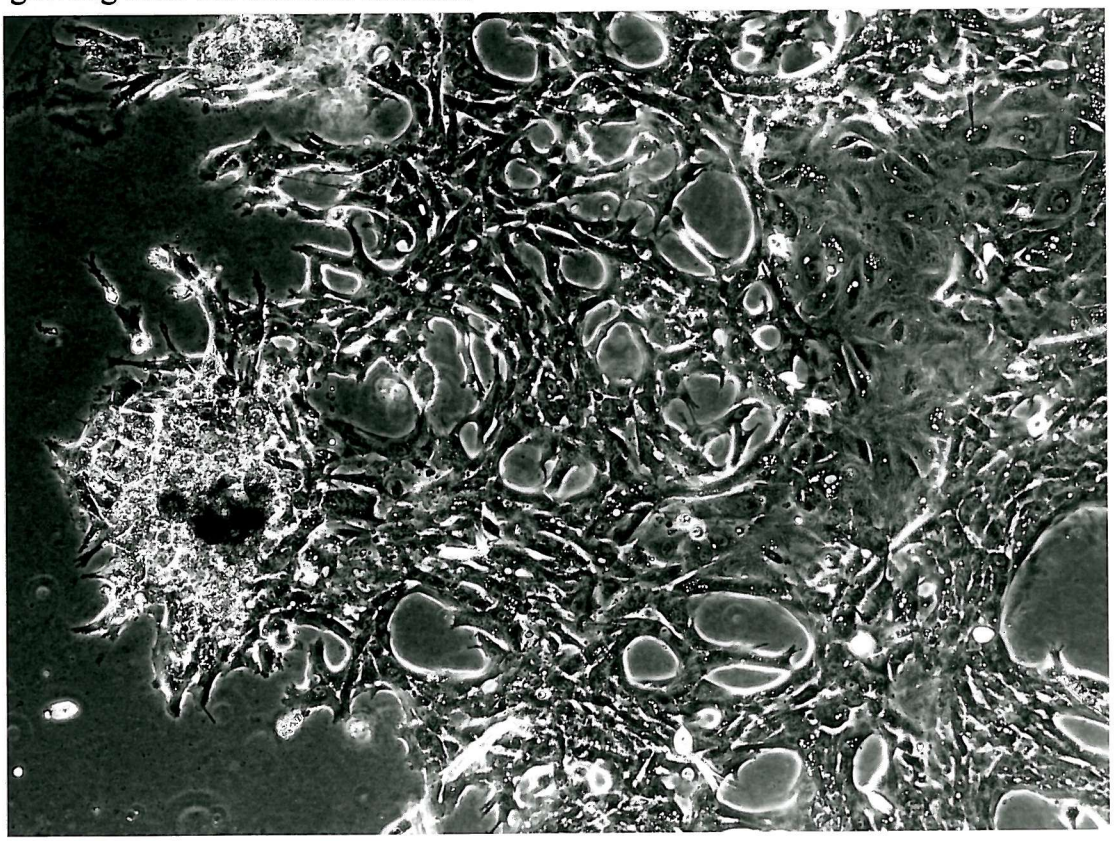

**Figure 2.8 HOMEC culture at day 10.** Extensive branch-like cellular structures can be seen to have occupied most of the Matrigel.

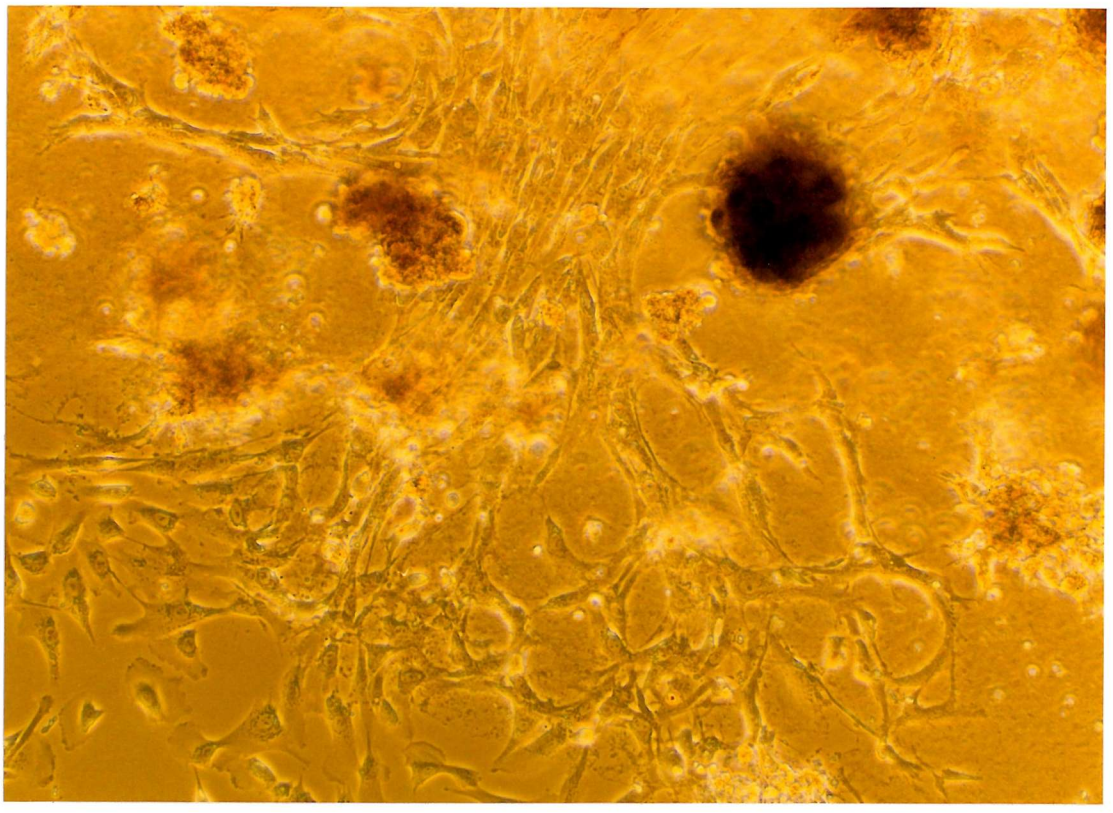

**Figure 2.9 HOMEC culture at day 12.** The cells forming the branch-like structures have emerged from the Matrigel onto the uncoated surface of the flask.

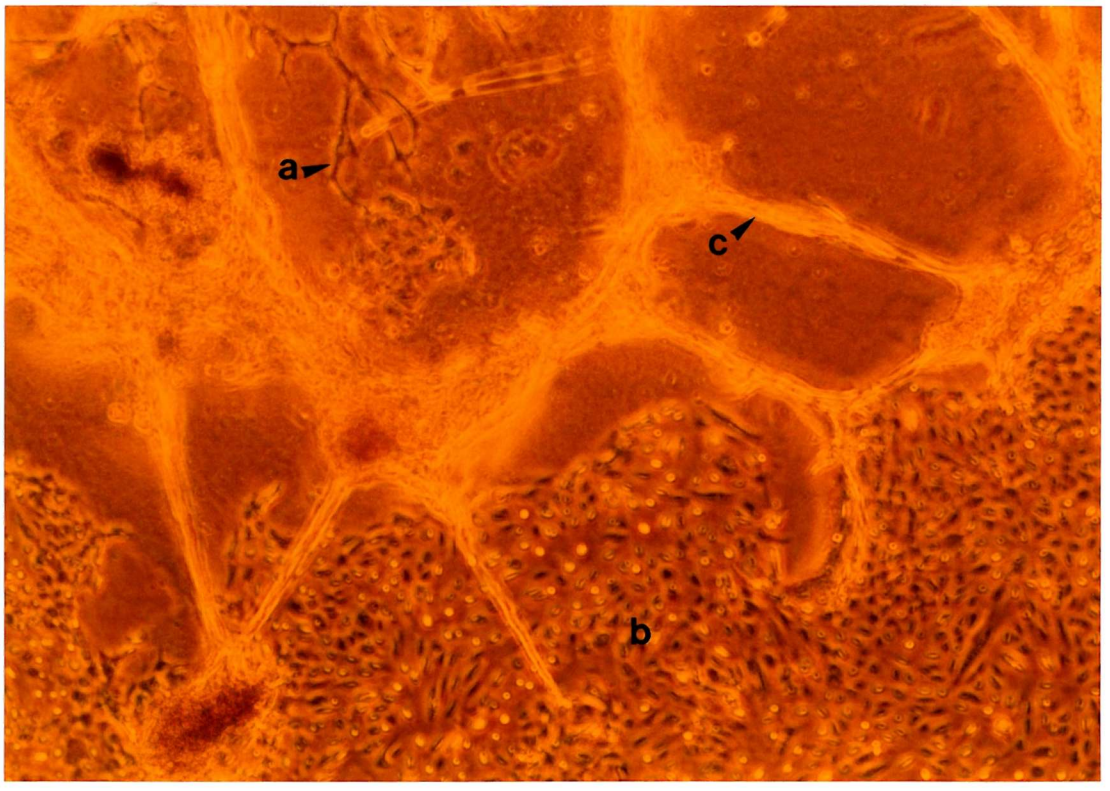


**Figure 2.10 HOMEC culture at day 20.** Showing a) original branch-like structures within the Matrigel, b) cobblestone monolayer on uncoated surface, c) capillary-like structure in association with Matrigel.

Several modifications to the model were produced throughout the development of the work to ensure that studies could be performed on only the cells of interest without significant contamination. Firstly, it was observed that fewer follicular fragments in each Matrigel blob allowed much clearer observation of the cell type developing from the fragments at an early stage. The endothelial cells formed branch-like structures as already described. Fibroblasts also formed a similar branch-like network. However, with experience in studying these cultures, it became apparent which type of cell was making up these structures at an early stage of development. Those blobs in which fibroblasts were developing could then be removed from the culture before a large number of these contaminating cells could multiply. Patches of cells on the uncoated culture surface which were not showing the cobblestone morphology, whether they were large flat cells or fibroblasts, were removed before they were a problem. Many cultures which showed predominantly non-endothelial cell development were discarded at an early stage. The removal of unwanted cells as described in section 2.4.3 proved vastly to increase the number of cultures from which endothelial cells could be subcultured without the contaminating cell types.

Figure 2.11a shows in more detail the cobblestone appearance of the cells growing from the follicular fragments. Figure 2.11b shows a confluent HUVEC culture in which again there is a cobblestone appearance to the cell monolayer. This cobblestone appearance is a well documented characteristic of endothelial cells. Figure 2.11c shows a fibroblast culture. It is clear that the cells developing from the follicular fragments in figure 2.11a (suspected as being endothelial cells) have a morphology not consistent with fibroblasts. Areas of cells with a fibroblast morphology which developed in the follicular fragment cultures were removed if possible or the culture discarded.

When the areas of cobblestone cells were removed from the primary culture and replated, they once again formed a cobblestone monolayer on the surface of the culture flask. Cells which were plated on to Matrigel formed complex capillary-like networks. These networks were also seen when HUVEC were plated on Matrigel and are a well documented characteristic of endothelial cells. Fibroblasts when plated on Matrigel form aggregates of cells rather than the complex networks of endothelial cells.

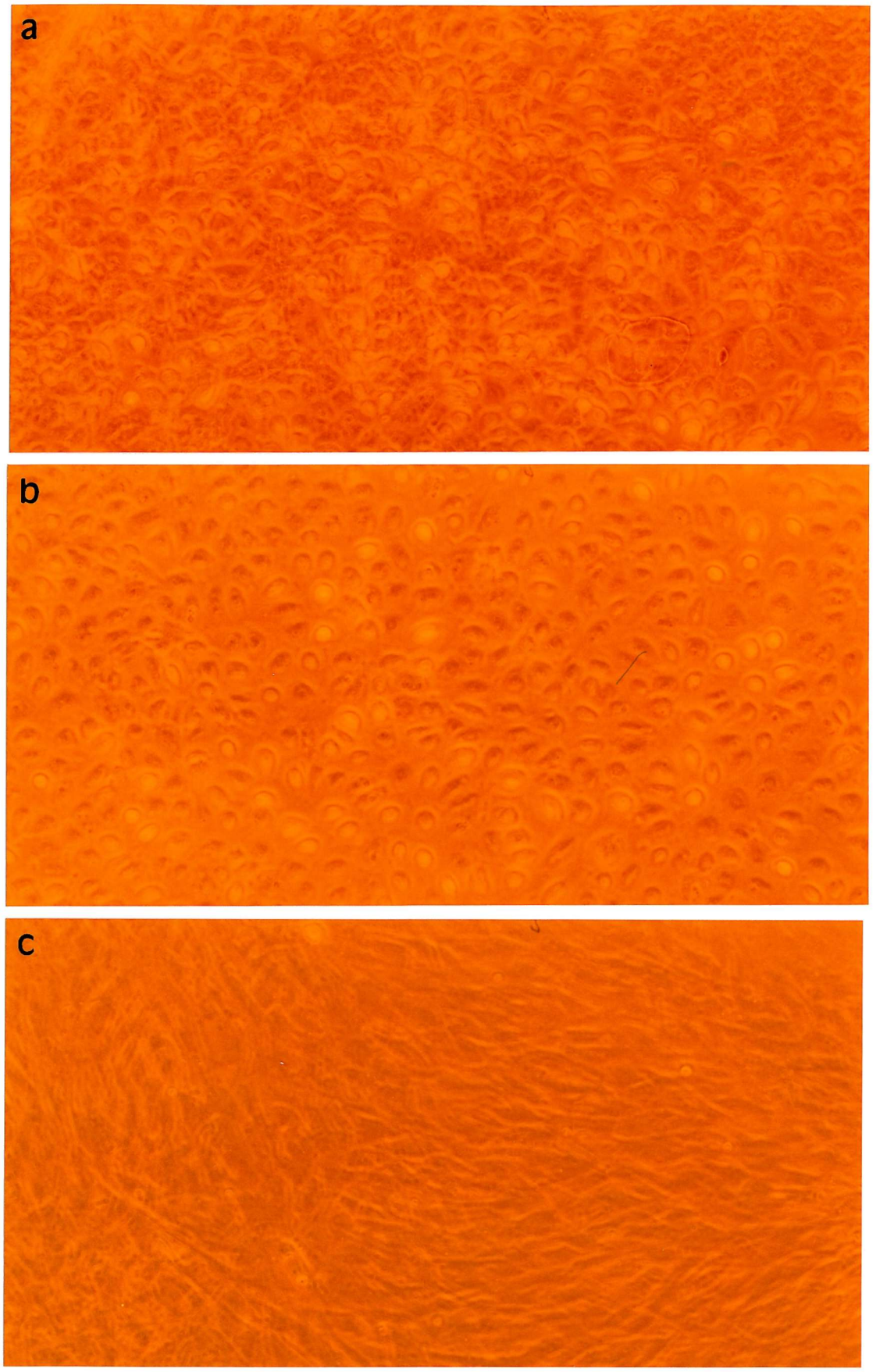


**Figure 2.11 Characteristic endothelial cell cobblestone monolayers.** a) HOMEC cobblestone monolayer, b) HUVEC cobblestone monolayer, c) fibroblast monolayer without cobblestone appearance.

Shredded corpus luteum embedded in Matrigel again showed the development of branch-like structures emerging from the tissue (figure 2.12). The development of the cultures was similar to that of the follicular fragment cultures with the exception that there were many more contaminating cells. Cobblestone patches grew on the uncoated surface of the culture flask and capillary-like structures grew on the surface of the Matrigel. Isolation of the endothelial like cells proved more difficult but was possible, however the availability of this tissue severely restricted this study.

This method of isolation of endothelial cells is not as efficient due to the large number of cell types within the corpus luteum. The fragments that are embedded in the Matrigel will have a very mixed cell population as opposed to the IVF fragments which are predominantly steroidogenic and vascular cells.

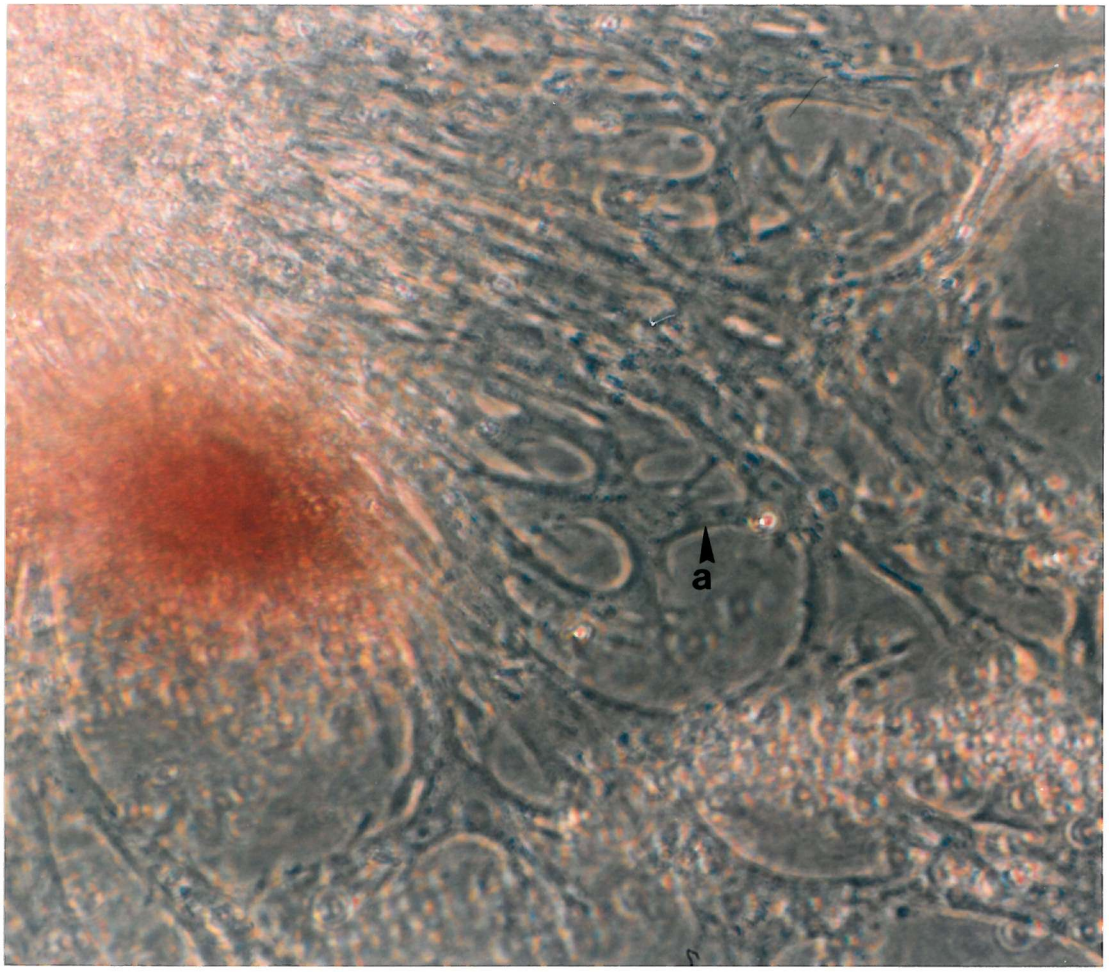


**Figure 2.12 Corpus luteum culture at day 6.** Branch-like cellular structures (a) can be seen growing from the tissue material.

## 2.6 Results of histochemical analysis.

Histochemical staining for 3βhsd was seen within some of the tissue fragments of the follicular aspirates and in some of the specimens endothelial cells were seen to be growing out from positively stained fragments indicating an origin in a tissue layer containing steroidogenic cells. Results shown in figure 2.13 show positively stained tissue pieces stained a dark blue/black colour whilst non steroidogenic tissue remained unstained. If compared to figure 2.9 (unstained), the staining is very conclusive.
The analysis was performed to ensure that the endothelial cells were developing from capillary fragments in the steroidogenic tissue and not capillary fragments removed from elsewhere in the reproductive system.

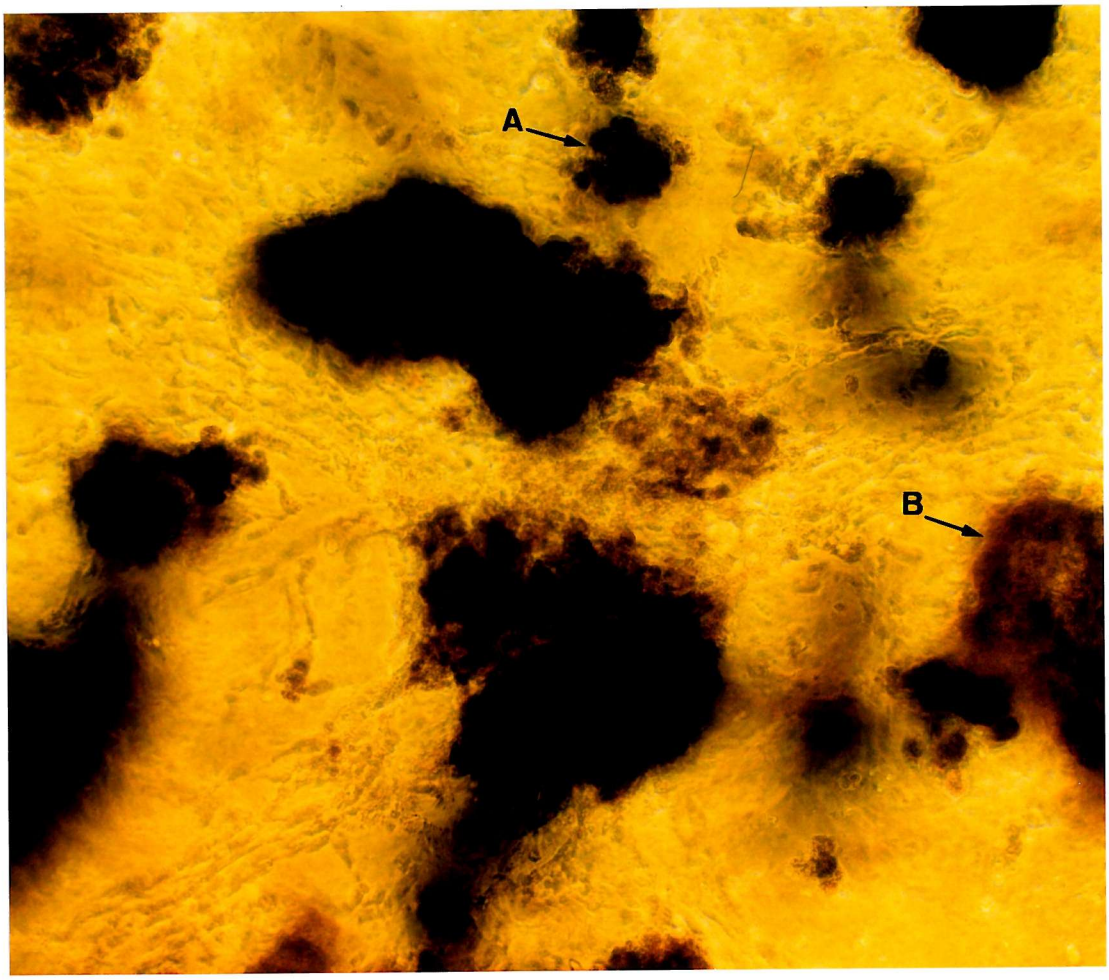


**Figure 2.13 Histochemical staining for 3βhsd.** Showing steroidogenic tissue from which endothelial cells developed. A) shows a positively stained fragment, B) shows an unstained fragment.

## 2.7 Discussion.

The model culture system developed in this chapter has shown that it is possible to generate cultures of cells from follicular fragments isolated during oocyte collection from patients undergoing in vitro fertilization treatment.

Areas of cells growing were seen to exhibit several endothelial cell characteristics and cellular morphology that is consistent with documented vascular endothelial cell culture models. Firstly, cells grew out of the Matrigel and formed contact inhibited cell monolayers when cells reached confluence on the uncoated surface of the culture flasks. This characteristic pattern of cells is consistent with HUVEC monolayers and other published endothelial cell culture models (Kubota *et al.*, 1996; Koolwijk *et al.*, 1996).

Secondly, the ability of HOMEC to rapidly form capillary-like architecture on the artificial matrix preparation Matrigel, is consistent with other cells including HUVEC and ECV304 cells. Ovarian endothelial cells isolated from the porcine fetus have also demonstrated this organisation (Plendle *et al.*, 1996).

# Chapter 3.

# Characterisation of the endothelial nature of cells grown from follicular fragments by immunocytochemistry.

## 3.1 Introduction.

Chapter 2 describes the method for isolating and culturing cells exhibiting endothelial cell morphology from fragments of the follicle wall removed during oocyte collection in the IVF treatment process. Although the isolated cells have the cobblestone appearance of cultured endothelial cells and behave on Matrigel as endothelial cells, further evidence is required to demonstrate their endothelial nature.

Immunocytochemistry is now one of the most widely used tools for characterising specific cell types by the use of antibodies specific for the cell of interest. Provided that good antibodies of high specificity and avidity are available, the number of problems to which the method is applicable is unlimited.

This chapter details the use of immunocytochemistry with endothelial cell specific antibodies to add further evidence of the endothelial phenotype of the cells grown in culture in chapter 2.

Recent studies have shown that vascular endothelial cells in different anatomical compartments of the liver, lung and kidney expressed different patterns of surface antigens (Page *et al.*, 1992). Therefore we are looking for any specific antigen expression in the follicular cultures as well as further endothelial characterisation.

## 3.2 Introduction to Immunocytochemistry.

Albert H. Coons and colleagues were the first group to label an antibody with a fluorescent dye and use it to identify an antigen in tissue sections.
Following the early work and as better, more specific antibodies to more cellular markers became commercially available, the technique has been enormously expanded and developed. The direct method as used by Coons (figure. 3.1) has generally now been replaced by the indirect method. These improvements have greatly enhanced the quality and reliability of the results that can be obtained. The indirect method (figure. 3.2) uses a primary antibody which is not directly conjugated to a fluorophore as used by Coons. Rather, following incubation with the primary antibody, a second layer is added which consists of an antibody raised to the γ-globulin of the species which donated the primary antibody, conjugated with a fluorophore such as fluorescein isothyocyanate (FITC).

This indirect method has many advantages over the direct method such as;

- More than one labelled anti-immunoglobulin molecule can bind to each primary antibody molecule, thus increasing the sensitivity of the reaction. This is helpful when expression of a particular antigen is very low.
- Non-specific fluorescence is reduced.
- A single fluorescent second layer antibody can be used to stain any number of first-layer antibodies to different antigens, provided they have all been raised in the same species.

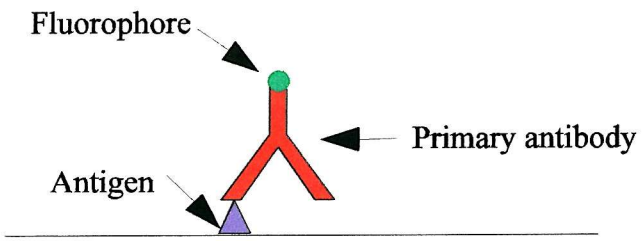


**Figure 3.1 Direct method of immunocytochemistry** where the primary antibody is conjugated with a fluorophore such as fluorescein.

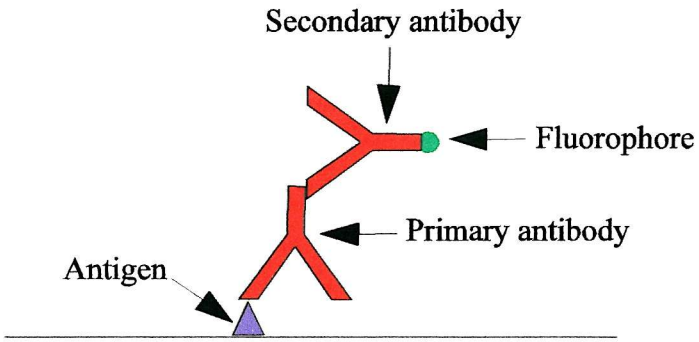


**Figure 3.2 Indirect method of immunocytochemistry** where the primary antibody binds to the antigen, and a secondary antibody, conjugated with a fluorophore, binds to the primary antibody.

Greater specificity of binding has more recently been improved by further developments in immunocytochemistry, which have led to the modification of the indirect method (figure 3.3). Avidin is a large glycoprotein from egg white which has a very high affinity (four binding sites per molecule) for biotin, a vitamin of low molecular weight found in egg yolk. Biotin can easily be coupled to antibodies in a high molecular proportion. Avidin, too, may be labelled to fluorescein, which can then bind the biotin coupled antibody. The use of the biotin/avidin system increases the sensitivity of the reaction as many more fluorophore molecules become bound to the cell marker being studied.

For example, the first layer is rabbit anti-antigen. The second layer is biotinylated goat anti-rabbit IgG. The third layer is a complex of avidin and FITC. The substitution for avidin by streptavidin, derived from streptococcus avidini, is a more recent development. The streptavidin molecule is uncharged relative to animal tissue, unlike avidin which has an isoelectric point of 10, and therefore electrostatic binding to tissue is eliminated, thus reducing non-specific binding. In addition, streptavidin does not contain carbohydrate groups which might bind to tissue lectins, again reducing the risk of non-specific binding. In other respects the molecule behaves in a similar way to avidin (Coggi *et al.*, 1986).

It is the three step biotin/streptavidin method described above that has been used for these studies (figure 3.3).

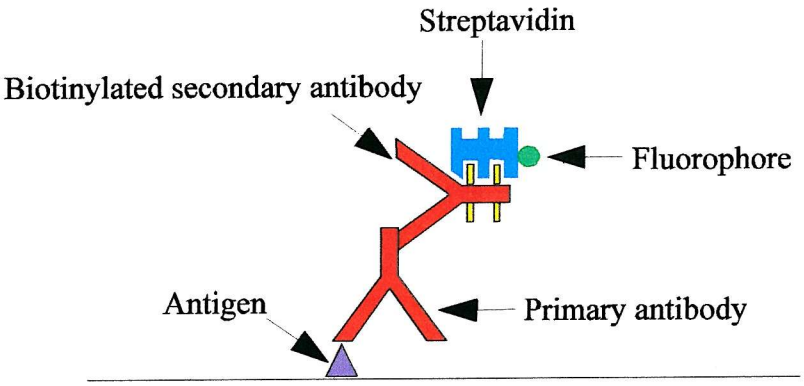


**Figure 3.3 Three step indirect immunocytochemistry** where the primary antibody binds to the antigen, a secondary biotinylated antibody binds to the primary antibody, and finally streptavidin conjugated with FITC binds to the secondary antibody.

### 3.3 Specificity problems and essential controls.

In immunocytochemistry a positive-appearing result may not always be genuine, there are risks of non-specific reactions which must be eliminated before the result can be accepted. There are many procedures and essential controls which must be followed in immunocytochemistry to reduce non-specific binding of antibodies and ensure that the observed results are accurate and not a result of autofluorescence or cross-reactivity.

**Essential controls**

Positive control:

1. Known positive control tissue included each time

Negative controls:

2. Test tissue can be treated in a number of ways
    a. With non-immune serum as first layer
    b. With inappropriate antiserum as first layer
    c. Omitting first layer

    All of these controls should be negative.

Preliminary immunocytochemistry experiments often give poor results with very high

background fluorescence and non-specific binding. There are numerous ways to remedy this, as shown below.

**Remedies**

1. Dilute primary and/or secondary antibody further
2. Block with normal serum from donor of second layer prior to staining with first layer
3. Absorb primary and secondary antibodies with albumin or tissue powder from species to be stained

These controls and refinements lead to very specific binding of antibodies to their antigens and allows accurate results to be obtained.
Fluorescence preparations have the disadvantage that they are impermanent and should be photographed within a few days of preparation. Storage of the slides in the dark helps to prevent fading, and addition of an anti-fade agent is also helpful in this respect.

## 3.4 Imaging.

Immunofluorescent preparations must be viewed with a microscope that provides light of the correct wavelength to give maximum excitation of the fluorescent label used. Fluorescein compounds emit a bright green fluorescence when excited at a wavelength of 490 nm whereas the excitation wavelength of the red fluorescence of rhodamine is 530 nm. In order to view both of these compounds the microscope has to be fitted with two sets of interchangeable filters.
The development of the confocal microscope and computer software which enables digital manipulation of images to be performed has allowed the field of immunocytochemistry to progress further.

## 3.5 Confocal microscopy.

In conventional light microscopy two dimensional images of the object are formed only in the X and Y planes, generally parallel to the plane of sectioning. This is also true of confocal microscopy but here, each image represents only a part of the thickness of the sample. Confocal microscopy allows the production of a series of images at different positions through the thickness of the object i.e: a series of X-Y images at different Z positions. These series of images form a three dimensional representation of the object which can be recombined digitally to produce a three dimensional picture. This is the main feature and major advantage of confocal microscopy over conventional microscopy.

The major optical difference between a normal microscope and a confocal microscope is the confocal pinhole which allows only light from the plane of focus to reach the detector which produces the series of images to be collected without parts of the specimen which are out of focus clouding the image, as is the case with conventional microscopy. Figure 3.4 shows a basic diagram of the confocal microscope and the principle of the pinholes.

The confocal principle is most effectively implemented when combined with a point scanning system using a laser light source. This builds up an image by scanning a point of laser light across the sample in the X and Y directions in a raster pattern. In the case of a laser scanning system, the detector is usually a photomultiplier tube. An image is displayed by using a computer to store the intensity value of each point from the detector, and then presenting these in the correct order on a high resolution video monitor. To collect a series of images the computer then shifts the focus by a fixed amount and the object is scanned again to produce the next image at a different Z position (figure 3.5.1A). This image is stored and the process repeated and the resulting data combined to build the 3D image (figure 3.5.1B).

Figure 3.5.2 shows how the two channels, red and green are combined after being generated, to form the final image.

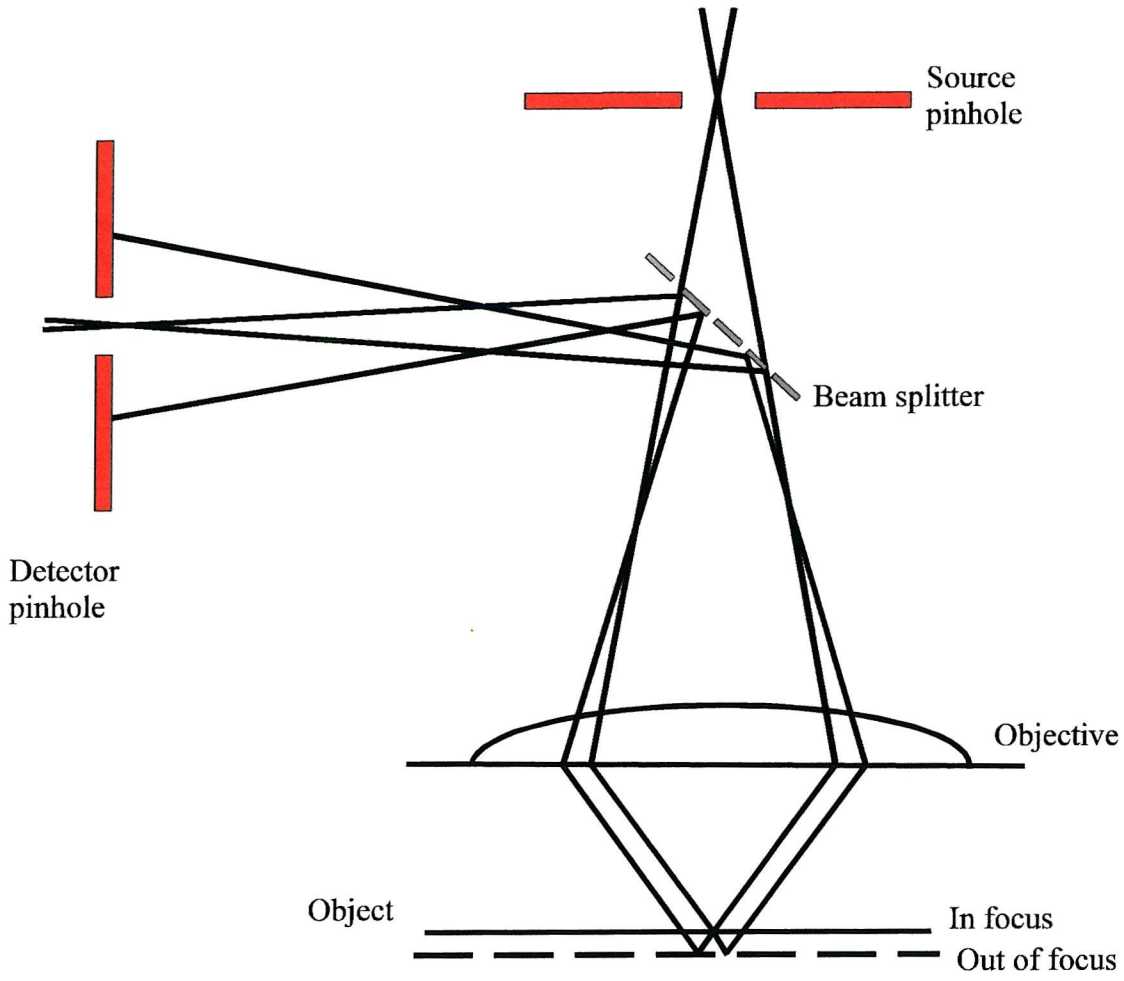


**Figure 3.4. Diagram of the principal of a confocal microscope** showing the light pathways and pinholes which allow only the section of the image in focus to be seen.

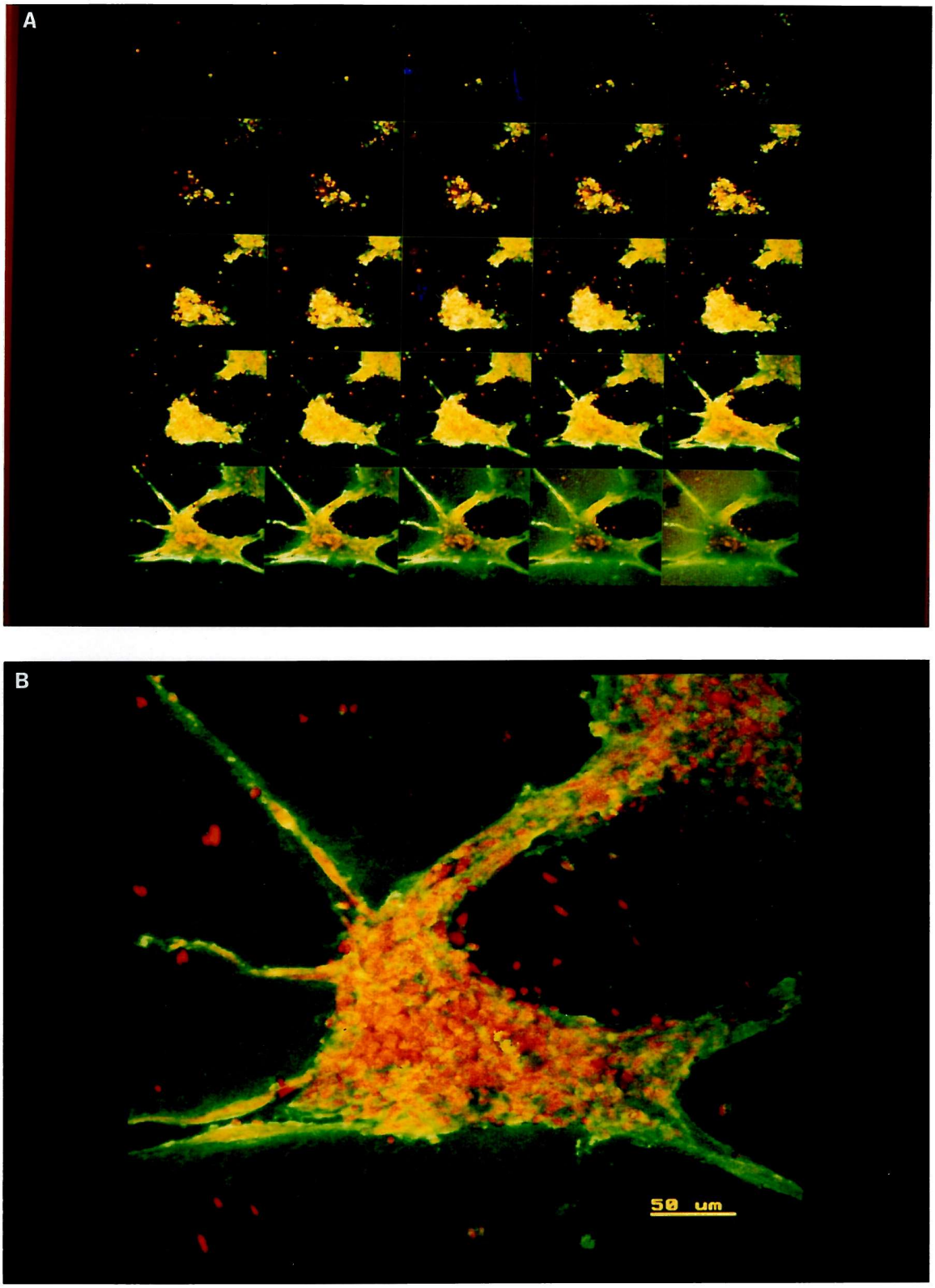


**Figure 3.5.1 Confocal series and 3D image.** A; shows the series of images collected as the object is sectioned in different Z positions. B; shows the digitally combined series of images shown in 3.5.1A to produce a 3D combined image. Specimen is a HUVEC capillary-like structure positively stained for CD31.

**Figure 3.5.2 Combined confocal image.** Red and green images are formed separately from the scanning. A; shows combined images in the green channel. B; shows combined images in the red channel. C; shows the combined images from both the red and green channels. Specimen is ECV304 positively stained for vimentin.

## 3.6 General advantages of laser scanning confocal microscopy.

**Optical sectioning-** of thick samples up to 150 μm is possible removing most of the out-of-focus information which would make conventional microscopy unusable. 3D information is collected in this way.

**Resolution-** may be up to 1.4 x that achievable in conventional microscopy.

Specimen bleaching- the scanning system reduces the exposure of each point to the strong light used for exciting fluorophores.

**Sensitivity-** the photomultipliers can image low light levels.

**Digital scanning-** allows easy manipulation of stored images.

## 3.7 The Leica TCS 4D confocal microscope.

The Lecia TCS 4D confocal microscope is illuminated by epi-illumination using a mercury vapour light source.

It is generally acknowledged that fluorescence is most efficient seen by epi-illumination, in which the incident light passes through the objective lens, which thus acts as a condenser, and is focused on the specimen. There are a number of advantages if the objective is used to both illuminate the sample and to collect the light emitted from it. These include the precise and limited illumination of only a small area of interest and loss of light which is not absorbed by the sample (greatly increasing the relative strength of the fluorescent signal). The light source for viewing immunofluorescence is usually a mercury vapour or xenon arc lamp and light of the wavelength providing for a maximum excitation of the fluorophore passes through appropriate filters to the specimen.

## 3.8 Endothelial cell markers.

### 3.8.1 Cell adhesion molecules.

For an efficient stepwise immune response to be mounted there has to be communication between the cells of the immune system and those of the blood and tissue barrier. This communication is in part by the direct interaction between cells via cell to cell contact and is facilitated by a number of cell surface molecules called the cellular adhesion molecules. The main cell adhesion molecule families are integrins, the immunoglobulin superfamily and cadherins.

In the early phase of inflammation, leukocytes migrating through the body adhere to the endothelial cells lining the blood vessels of the damaged or infected area. This adherence is due to the expression of adhesion molecules by both the endothelial cells and leukocytes. This initial weak adherence is caused by selectins expressed on the activated endothelial cells binding to carbohydrate sequences on the leukocytes. These weakly bound circulating leukocytes slow down and roll in contact with the endothelial cells of the blood vessel. This process triggers the release of other factors and adhesion molecules which bind to their respective receptors. Leukocytes then migrate to the extravascular damaged or infected tissue (figure 3.6).

The expression of adhesion molecules by microvascular endothelial cells is known to play roles in certain pathological conditions eg, multiple sclerosis, haemorrhagic shock, cerebral ischemia, rheumatoid arthritis and atherosclerosis (McCarron *et al.*, 1995).

## Selectins.

The selectins, a family of Ca2+-dependent-carbohydrate-binding proteins, mediate the initial attachment of flowing leucocytes to the blood vessel wall during the capture and rolling step of the inflammatory adhesion mechanism. Selectins recognise fucosylated carbohydrate ligands, especially structures containing sLe. There are 3 closely related members of the selectin family, namely L(leucocyte)-, P(platelet)- and E(endothelial)-Selectin.

All selectins consist of three protein domains: a calcium dependent lectin binding domain at the N-terminus, a domain structure similar to epidermal growth factor (EGF), and a domain with a varying number of repeat sequences similar to those found in complement regulatory proteins. It appears each member of the selectin family recognises a number of different ligands which show differential cellular distribution and may have different binding characteristics (Ruco *et al.*, 1992).

## E-Selectin (CD62E).

The CD62E antigen (115 kDa), also known as E-selectin or endothelial leukocyte adhesion molecule-1 (ELAM-1), is expressed at sites of inflammation. The initial binding of leukocytes by CD62E is thought to trigger the recruitment and activation of other adhesion molecules. CD62E antigen expression is upregulated on vascular endothelium at sites of inflammation in a variety of disease states where neutrophil infiltration is evident (Ruco *et al.*, 1992; DeLisser *et al.*, 1993).

## The Immunoglobulin Superfamily.

The Immunoglobulin Superfamily (IgSF) is the most abundant family of cell surface molecules, accounting for 50% of leucocyte surface glycoproteins. Certain members are also present on the surface of other cell types, particularly endothelial cells. Leucocyte firm adherence to blood vessels, which occurs during inflammation, involves ICAM-1, ICAM-2 and VCAM-1 (CD106). ICAM-1 and ICAM-2 are surface ligands for the integrin LFA-1, whereas VCAM-1 is a ligand for integrin VLA-4. Transendothelial migration of leucocytes, which proceeds firm adherence, involves IgSF members PECAM-1 (CD31). PECAM-1 is expressed predominantly on endothelial cells and platelets (DeLisser *et al.*, 1993).

The immunoglobulin superfamily is the largest group of adhesion molecules and includes more than 70 members. Their functions and roles are diverse but they have in common some control over cell behaviour. Such control is exerted by molecules acting as signal transducing receptors, intracellular adhesion molecules or both. All members of the family share a common ancestral structure, termed the immunoglobulin fold. The evolutionary pressure to maintain such a structure is thought to result from the

conformation being protease resistant and therefore able to survive the hostile extracellular environment. The family members are involved in two main areas: development, particularly development of the nervous system, and regulation of the immune system (Ruco *et al.*, 1992).

**CD31 (PECAM-1).**

This molecule has been implicated in a number of cellular phenomena, including vascular wound healing and angiogenesis, and transendothelial migration of inflammatory responses. Anti CD31 reacts with a 130 kDa glycoprotein gpIIa, also known an PECAM-1. CD31 has a wide tissue distribution and is expressed on platelets, monocytes, granulocytes and in high amounts on endothelial cells.
The molecule has an extracellular domain that contains six Ig-like homology units of C2 subclass, typical of cell to cell adhesion molecules. This domain-mediated endothelial cell-to-cell adhesion, plays a role in endothelial cell contact and may serve to stabilize the endothelial cell monolayer. The CD31 molecule also has a cytoplasmic domain with potential sites for phosphorylation after cellular activation. The properties of CD31 antigen suggest that it is involved in interactive events during angiogenesis, thrombosis and wound healing (DeLisser *et al.*, 1993).

## VCAM-1.

Our antibody reacts with human VCAM-1. The antigen is present on activated endothelial cells and dendritic cells (Wellicome, 1993).

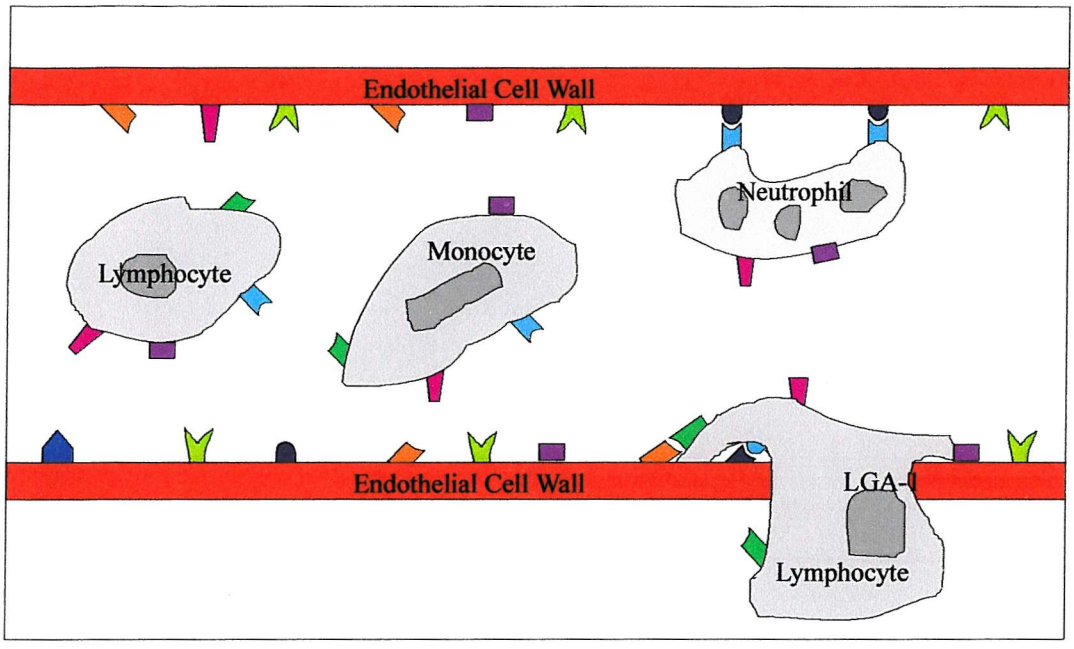


Key

- P-selectin
- VCAM-1
- ICAM-2
- PECAM-1
- LGA-1
- VLA-4
- ICAM-1
- E-selectin

**Figure 3.6 Cell adhesion molecules** in a section of a capillary. The diagram represents the triggering of an immune response where a leukocyte is migrating to the extravascular tissue.

## 2.8.2 von Willebrand Factor (vWF).

Human vWF also known as factor VIII is a multimeric plasma glycoprotein that mediates platelet adhesion to injured vessel walls. Endothelial cells synthesize and store vWF within Weibel-Pallade bodies (Hendrick *et al.*, 1988). Decreased levels of vWF in the circulation results in the severe bleeding disorder Haemophilia.
Anti vWF/factor VIII reacts specifically with the cytoplasm of human endothelial cells of normal, reactive and neoplastic blood and lymphatic vessels. It also reacts with human endocardium, platelets and megakaryocytes. Factor VIII R:Ag endocytosed by other cells may also react. Endothelium from several mammalian species can also be stained (Hendrick *et al.*, 1988).

## 3.8.3 Ulex Europaeus-I Lectin (UEA-I).

UEA-I lectin reacts strongly with endothelial cells in all tissues. It appears that the binding sites of UEA-I lectins are structural α-fucosyl containing glycocompounds specific for endothelial cells in which the fucose residues are readily accessible for UEA-I lectin. Although the chemical nature of the compounds carrying these determinants in the cytoplasm and at the cell surface of endothelial cells is not known, they seem to be shared by all endothelial cells in human tissues (Holthofer *et al.*, 1982).
UEA-I reacts with human blood group O erythrocytes, human endothelial cells and a variety of human and animal epithelial cells.

## 3.8.4 Vimentin.

The antibody against vimentin reacts with 57 kDa intermediate filament protein present in cells of mesenchymal origin. In normal tissues, cell types which express vimentin

include endothelial cells, fibroblasts, smooth muscle cells and lymphoid cells. The antibody shows a broad interspecies cross reactivity (Olah *et al.*, 1992).

### 3.8.5 Fibroblast 5B5.

The antibody against fibroblast 5B5 reacts with the active site of the prolyl 4-hydroxylase enzyme that has been reported to be specific for fibroblasts. The enzyme is an $alpha_2$ $beta_2$ heterotetramer which is essential for the co-translational and post-translational hydroxylation of proline in position 4 during collagen synthesis and triple helix formation (Konttinen *et al.*, 1989).

## 3.9 Materials and Methods.

### 3.9.1 Cell culture/slide preparation.

HUVEC, HOMEC, ECV304 and fibroblast cells were cultured as previously described in chapter 2.

20,000 cells (Cell numbers were calculated as shown in section 3.9.2) of each type were plated in individual wells of eight well chamber slides. Cells were incubated overnight in the appropriate media at 37°C in 5% $CO_2$ in air to allow adherence to the culture surface.

HOMEC capillary-like structures were also prepared in wells of eight well chamber slides. Wells were coated with 60 µl of Matrigel before the addition of 40,000 cells/well. These cells were allowed to form into capillary-like structures overnight in the appropriate media at 37°C in 5% $CO_2$ in air.

### 3.9.2 Cell counting.

The Haemocytometer slide was thoroughly washed in Virkon, swabbed liberally with 95% ethanol and allowed to air dry. The coverslip and haemocytometer were moistened and held together until Newton's rings appeared.

Cells were removed from their culture flasks following the subculture method (section 2.4.6) using trypsin and centrifuged to form a pellet. The pellet was thoroughly resuspended in 1 ml of fresh media and a small drop of the cell suspension was transferred to the haemocytometer slide by gentle addition down the side of the coverslip.

The slide was viewed under the microscope and cells located in the centre grid were counted, only cells touching the north and east margins were included. Those touching the west and south margins were discarded.

### 3.9.3 Immunocytochemistry.

Cells and capillary-like structures were fixed in the chamber wells with 300 µl of ice-cold methanol for 30 minutes. Methanol was removed from the wells and cells were washed with phosphate buffered saline (PBS; Gibco BRL) containing 0.1% Triton to permeabilize the cell membranes. The cells were washed twice more in 10% serum of the host animal of the secondary antibody, diluted in PBS (for example the secondary antibody for VCAM-1 is horse anti mouse, therefore 10% horse serum was used for all the washing steps of this particular antibody). This thorough washing removed all of the Triton and blocked the cells to reduce non specific binding. Cells were incubated overnight with primary antibodies diluted according to the manufacturers instructions at room temperature. A list of all antibodies, host animal, serum for blocking and concentrations of use are detailed in table 3.1.

The primary antibody was excluded from negative controls which were incubated with 10% serum diluted with PBS. Following the overnight incubation, cells were washed with 10% serum in PBS for a total of three washes of five minutes. Biotinylated secondary antibodies (Vector Laboratories) were incubated at a concentration of 7.7 µg/ml at room temperature for one hour (such as biotinylated anti-mouse IgG for VCAM-1). Cells were again washed with 10% serum in PBS for three washes of five minutes. Cells were then incubated with Fluorescein isothiocyanate conjugated streptavidin (FITC; 20 µg/ml; Vector Laboratories) for 1 hour at room temperature. cells were again washed with PBS for three washes of five minutes to remove all unbound FITC. Propidium iodide (0.01 mg/ml; Sigma) was used as the nuclear counter stain and incubated for no longer than 2 minutes. Cells were not washed again following propidium iodide incubation, the excess solution was removed with a fine tipped pastette. Wells of the slides were then carefully removed to leave a slide which was layered with Moviol (Harlow chemicals Ltd) and a coverslip positioned on top. Slides were stored wrapped in foil at 4°C in the dark until imaging. Results shown are representative of a minimum of three independantly stained cell cultures.

| Antibodies/ Lectin | Antibody Source | Type of Antibody | Stock Concentration (mg/ml) | Dilution | Serum for blocking |
|---|---|---|---|---|---|
| **Von Willebrand Factor** (vWF) | Sigma Chemicals Co. (F-3520) | Rabbit IgG | 12 | 1:2500 | Goat |
| **Anti-Ulex Europaeus agglutinin-1 Lectin** (UEA-1) | Sigma Chemicals Co. (L-4889) | - | 1 | 1:10 | |
| **Platelet Endothelial Cell Adhesion Molecule-1** (PECAM-1) CD31 | Dako, Bucks,UK (M-0823) | Mouse IgG | 3.5 | 1:40 | Horse |
| **Vascular Cell Adhesion Molecule-1** (VCAM-1) CD106 | Serotec, Oxford, UK (MCA1131) | Mouse IgG | 0.02 | 1:10 | Horse |
| **E-Selectin** CD62E | R & D Systems (BBA16) | Mouse IgG | 1 | 1:10 | Horse |
| **Vimentin** | Dako (M7020) | Mouse IgG | 0.05 | 1:100 | Horse |
| **Fibroblast 5B5** | Sigma Chemicals Co. (F4771) | Mouse IgG | 0.2 | 1:500 | Horse |

**Table 2.1Table of primary antibodies used for immunocytochemical characterisation** of cells grown from follicular aspirates (HOMEC), HUVEC, ECV304 cells and fibroblasts. Host animal, serum for blocking, stock concentrations and dilutions for use are listed.

### 3.9.4 Confocal microscopy.

Immunofluorescence was detected with epifuorescence using a Lecia TSC 4D confocal microscope.

## 3.10 Results of immunocytochemistry.

Immunocytochemical studies on the cells isolated from the follicular aspirates were performed using HUVEC and ECV304 cells as positive endothelial control cells for certain cellular markers, and fibroblasts as negative controls. Controls were also performed where the procedure was followed without primary antibody. These controls with no primary antibody were negative for immunofluorescence in all cases. Results of the immunocytochemical studies can be seen in table 3.2.

The cells isolated from the cobblestone areas of follicular cultures showed positive immunofluorescence for all of the endothelial cell markers used. Whereas fibroblasts showed no immunofluorescence for these endothelial cell specific markers.

Figure 3.7 shows the results for the endothelial specific von Willebrand factor. Both HOMEC and HUVEC demonstrate the same level of positive immunofluorescence for this marker. However, the ECV304 cell line and fibroblasts do not show any positive immunofluorescence for von Willebrand factor.

Figure 3.8 shows positive immunofluorescence for anti-Ulex Europaeus agglutinin-1 Lectin for all of the endothelial cell types stained. Staining was stronger with HOMEC and HUVEC than that of ECV304. The fibroblasts showed no immunofluorescence for this lectin as expected. The bright green flecks which can be seen in the HOMEC picture are a result of small particles in the FITC.

Figure 3.9 shows positive immunofluorescence for both HOMEC and HUVEC with platelet endothelial cell adhesion molecule-1. Both ECV304 and fibroblasts show no immunofluorescence for this marker.

Figure 3.10 shows positive immunofluorescence for only HOMEC with Vascular cell adhesion molecule-1 although this is at a low level. All of the other cell types show no immunofluorescence for this marker.

Figure 3.11 shows positive immunofluorescence for all of the cell types with the intermediate filament vimentin. The level of immunofluorescence is similar for all cell types but with the ECV304 cells showing a different arrangement of filaments.

| | Cell Type | | | | |
|---|---|---|---|---|---|
| **Antibodies/ Lectin** | **Ligand** | **HOMEC** | **HUVEC** | **ECV304** | **Fibroblast** |
| **Von Willebrand Factor** (vWF) | Cytoplasm of human endothelial cells. Weibel pallade bodies | +++ | +++ | - | - |
| **Anti-Ulex Europaeus agglutinin-1 Lectin** (UEA-1) | Sugar lectin on vascular endothelium | +++ | +++ | ++ | - |
| **Platelet Endothelial Cell Adhesion Molecule-1** (PECAM-1) CD31 | 100 kDa glycoprotein in endothelial cells | +++ | +++ | - | - |
| **Vascular Cell Adhesion Molecule-1** CD106 | Integrins | + | - | - | - |
| **E-Selectin** CD62E | Sialyated, fucosylated molecules | +++ | +++ | - | - |
| **Vimentin** | Intermediate filament protein in cells | +++ | +++ | +++ | +++ |
| **Fibroblast 5B5** | Prolyl 4-hydroxylase enzyme | +++ | +++ | +++ | +++ |

**Table 2.2 Results of immunocytochemical characterisation** of cells grown from follicular aspirates (HOMEC), compared with HUVEC, ECV304 cells and fibroblasts.

**Figure 3.7 Immunocytochemistry using the von Willebrand factor antibody.** A; positive immunofluorescence in HOMEC. B; positive immunofluorescence in HUVEC. C; negative immunofluorescence in ECV304 cells. D; negative immunofluorescence for fibroblasts.

## Von Willebrand Factor

HOMEC

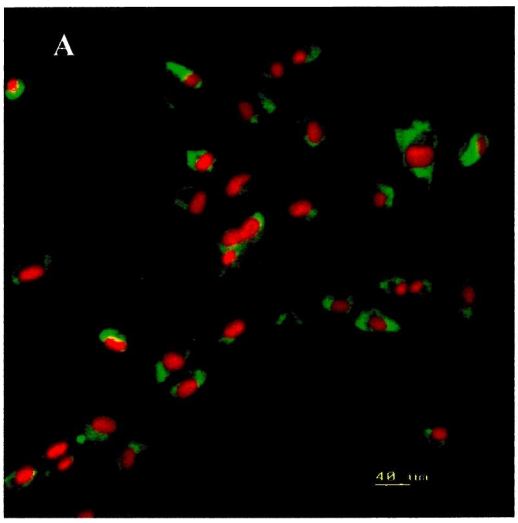


HUVEC

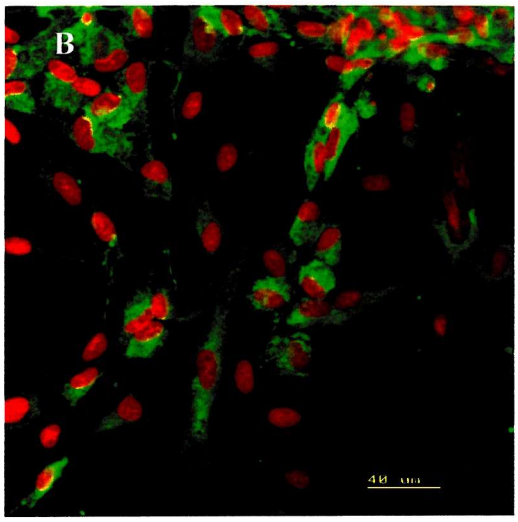


ECV304

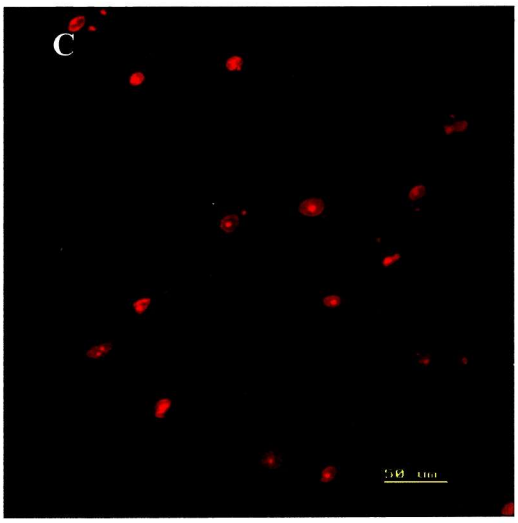


Fibroblast

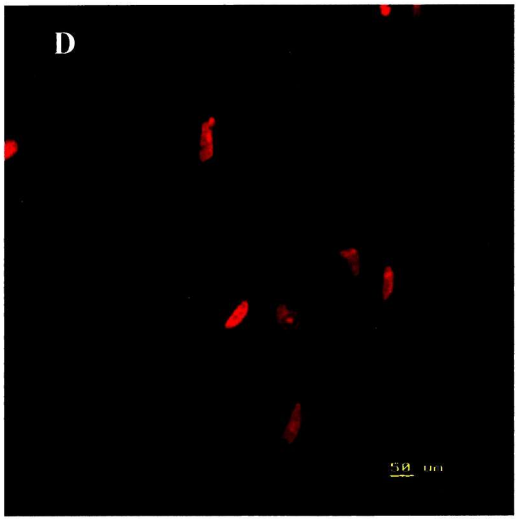

**Figure 3.8 Immunocytochemistry using the anti-Ulex Europaeus agglutinin-1 Lectin.** A; positive immunofluorescence in HOMEC. B; positive immunofluorescence in HUVEC. C; shows positive immunofluorescence in ECV304 cells. D; negative immunofluorescence in fibroblasts.

## Anti-Ulex Europaeus agglutinin-1 Lectin

HOMEC

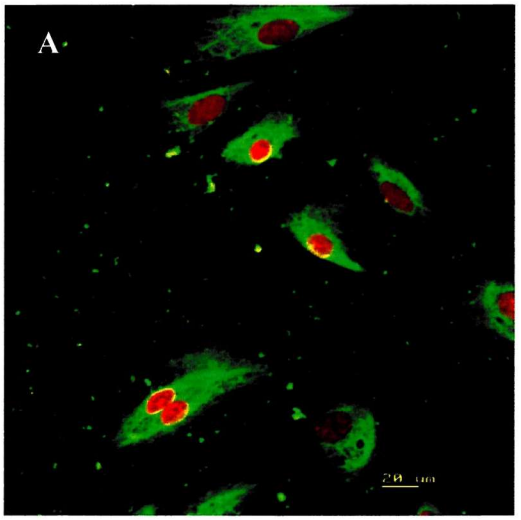


HUVEC

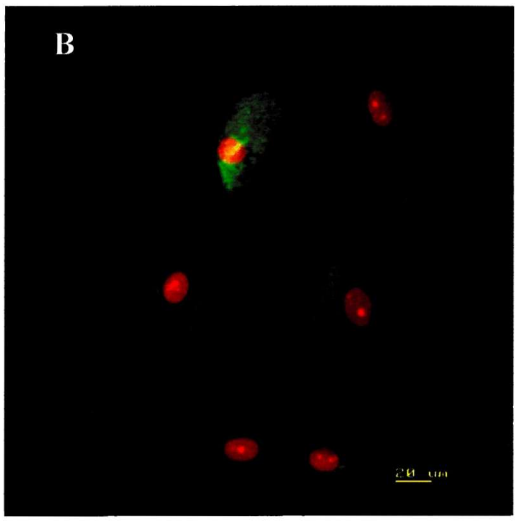


ECV304

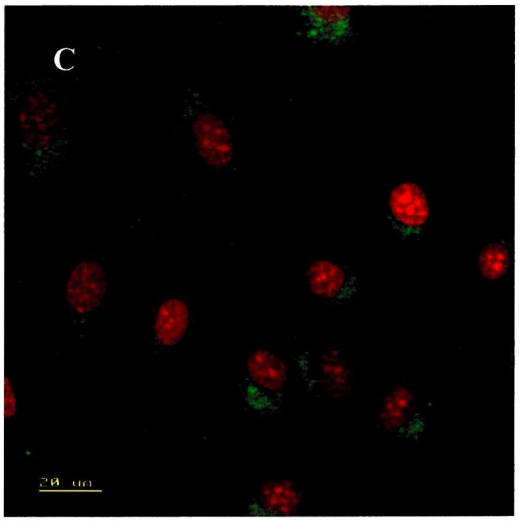


Fibroblast

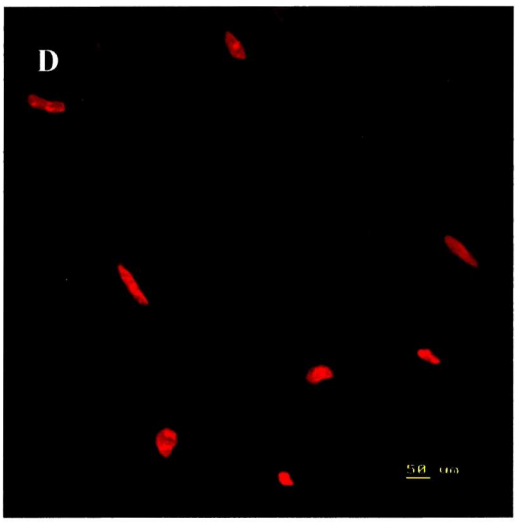

**Figure 3.9 Immunocytochemistry using the Platelet Endothelial Cell Adhesion Molecule-1 antibody.** A; positive immunofluorescence in HOMEC. B; positive immunofluorescence in HUVEC. C; negative immunofluorescence in ECV304 cells. D; negative immunofluorescence in fibroblasts.

# Platelet Endothelial Cell Adhesion Molecule-1

HOMEC

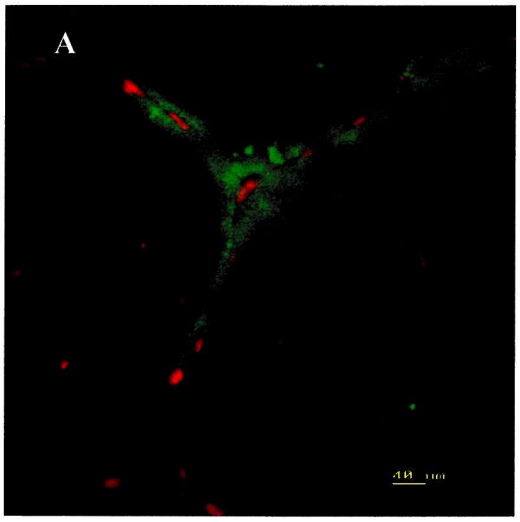


HUVEC

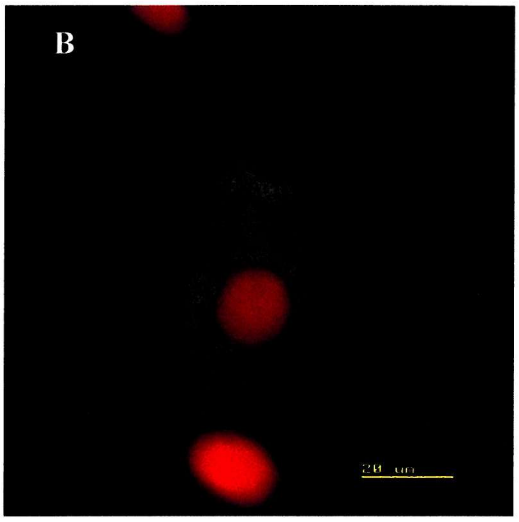


ECV304

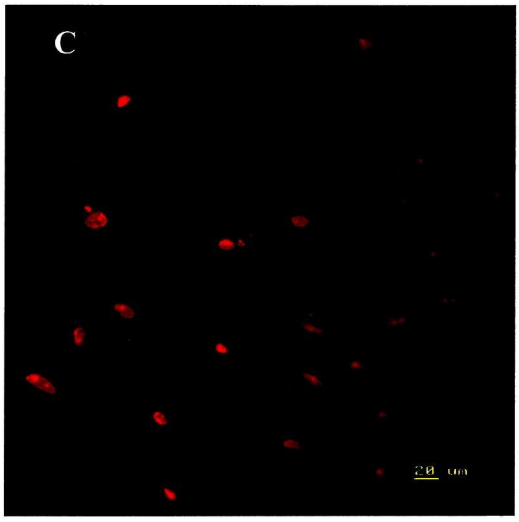


Fibroblast

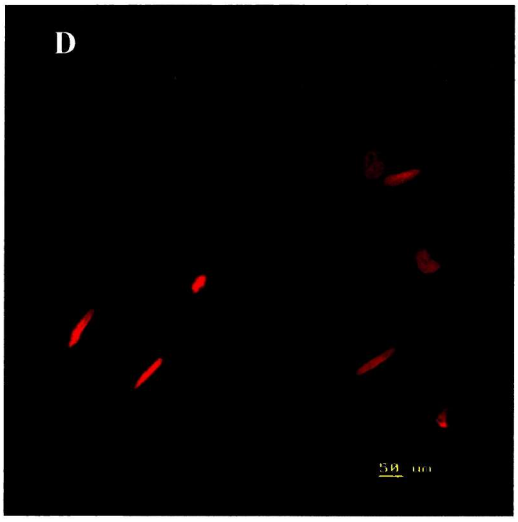

**Figure 3.10 Immunocytochemistry using the Vascular Cell Adhesion Molecule-1 antibody.** A; positive immunofluorescence in HOMEC. B; negative immunofluorescence in HUVEC. C; negative immunofluorescence in ECV304 cells. D; negative immunofluorescence in fibroblasts.

## Vascular Cell Adhesion Molecule-1

HOMEC

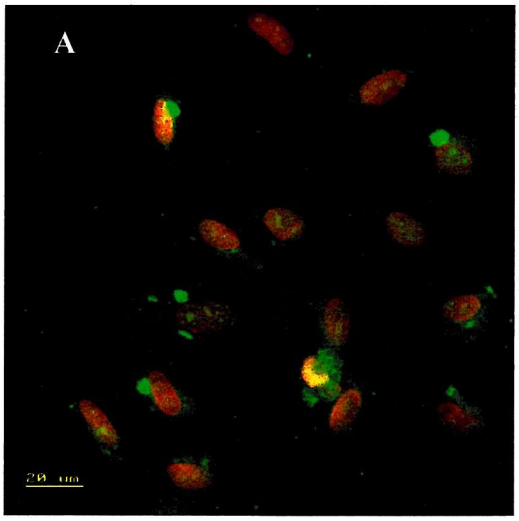


HUVEC

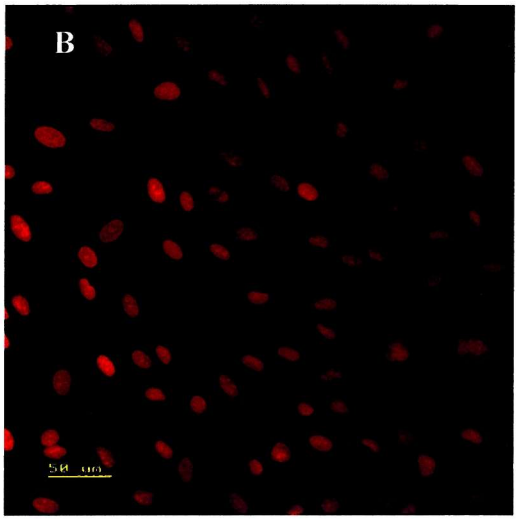


ECV304

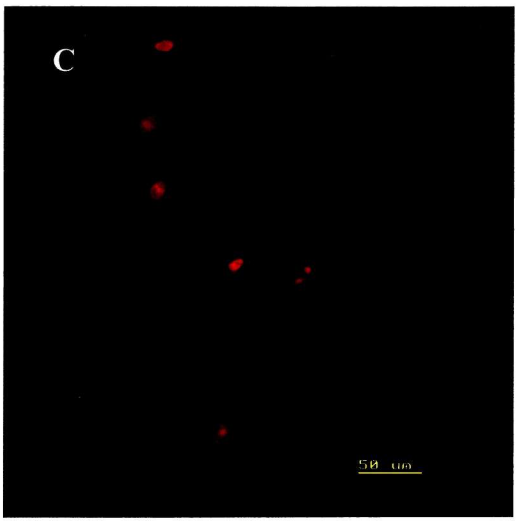


Fibroblast

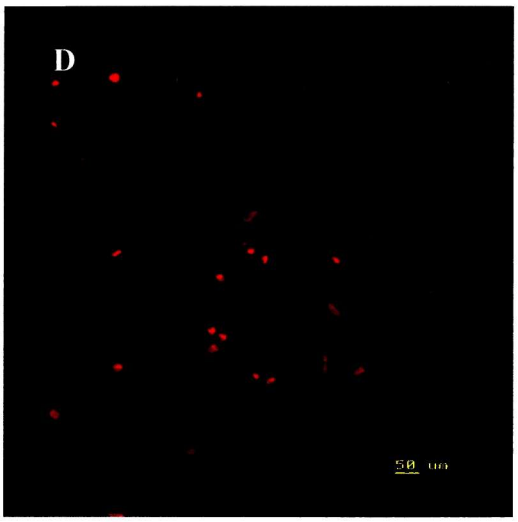

**Figure 3.11 Immunocytochemistry using the Vimentin antibody.** A; positive immunofluorescence in HOMEC. B; positive immunofluorescence in HUVEC. C; positive immunofluorescence in ECV304 cells. D; positive immunofluorescence in fibroblasts.

**Vimentin**

HOMEC

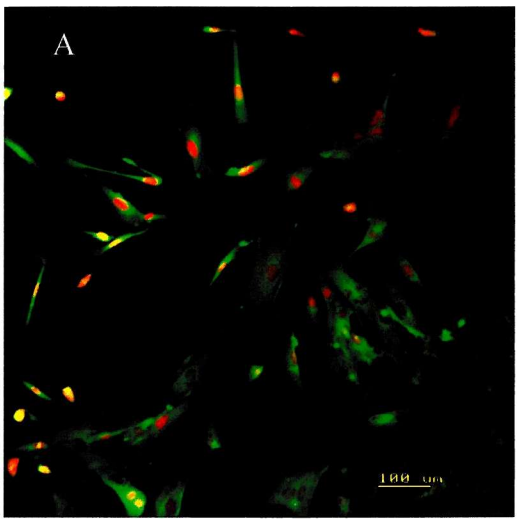


HUVEC

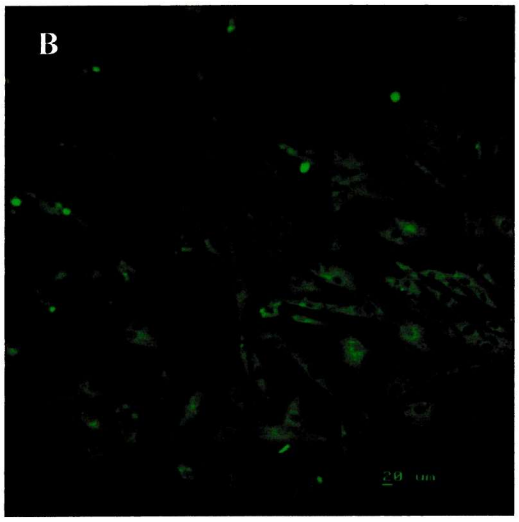


ECV304

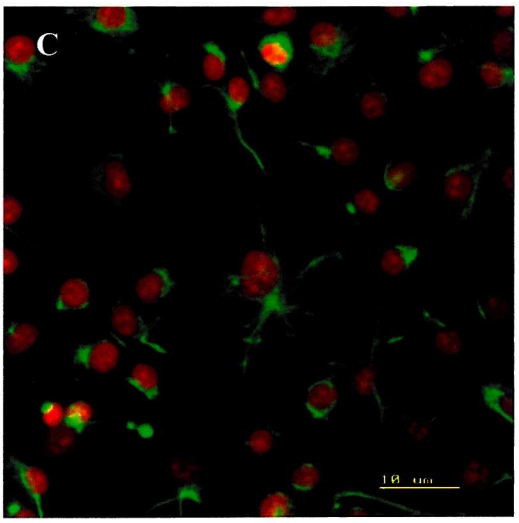


Fibroblast

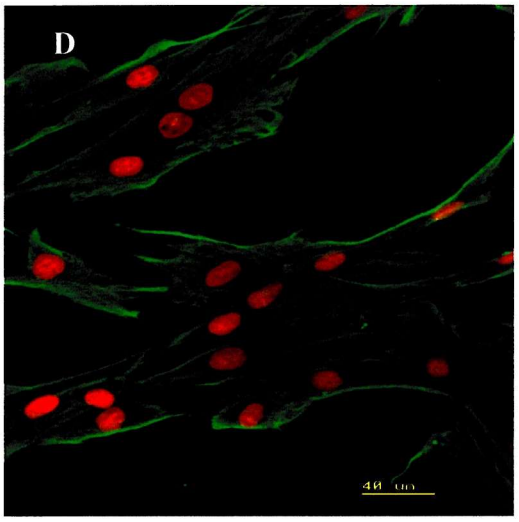

**Figure 3.12 Immunocytochemistry using the Fibroblast 5B5 antibody.** A; positive immunofluorescence in HOMEC. B; positive immunofluorescence in HUVEC. C; positive immunofluorescence in ECV304 cells. D; positive immunofluorescence in fibroblasts.

## Fibroblast 5B5

HOMEC

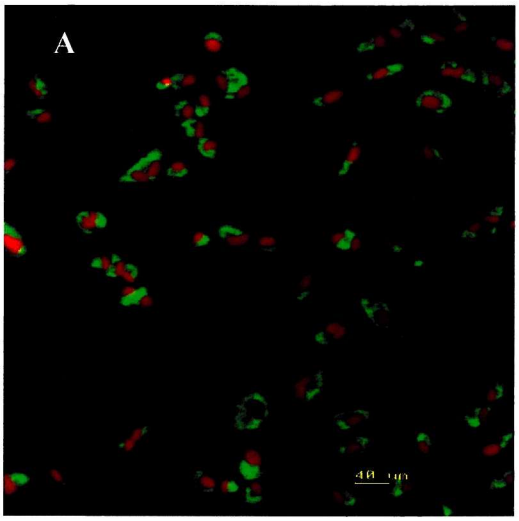


HUVEC

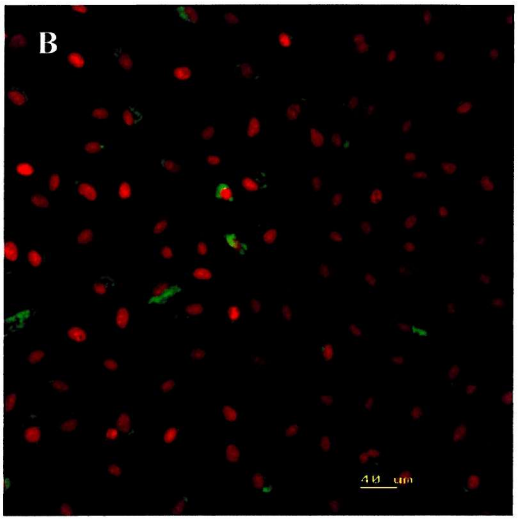


ECV304

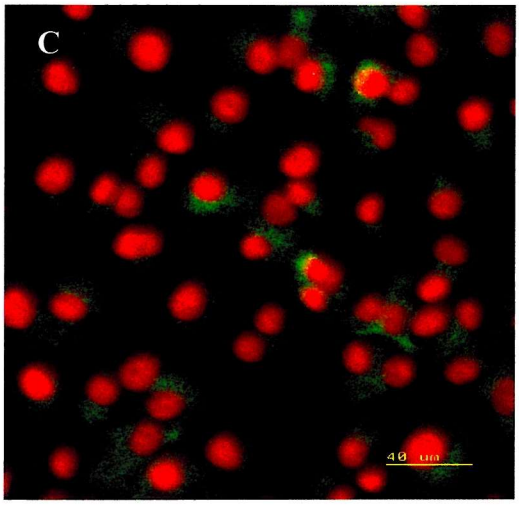


Fibroblast

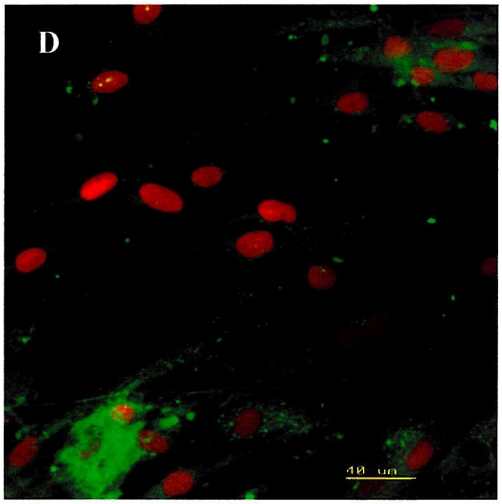

**Figure 3.13 Immunocytochemistry using Platelet Endothelial Cell Adhesion Molecule-1 antibody in HOMEC capillary-like structures.** A; positive immunofluorescence in the early HOMEC branch-like structures growing from the original follicular fragment. B; positive immunofluorescence of a HOMEC capillary-like structure at high magnification. C; positive immunofluorescence in a HOMEC capillary-like structure. D; positive immunofluorescence in HOMEC capillary-like structures and cell aggregates when seeding density was very high.

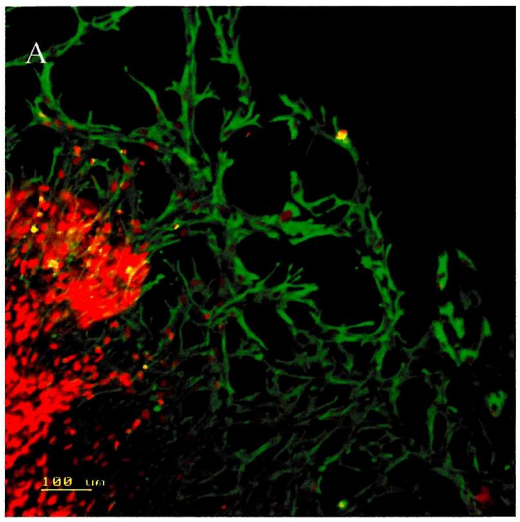
A
100 um

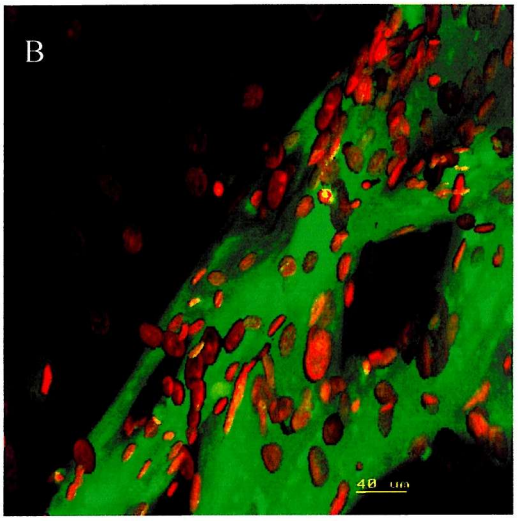
B
40 um

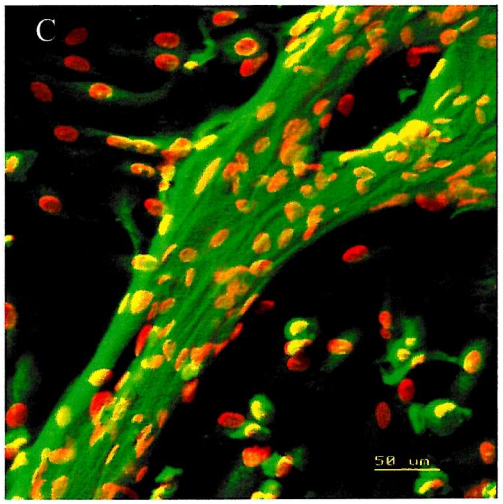
C
50 um

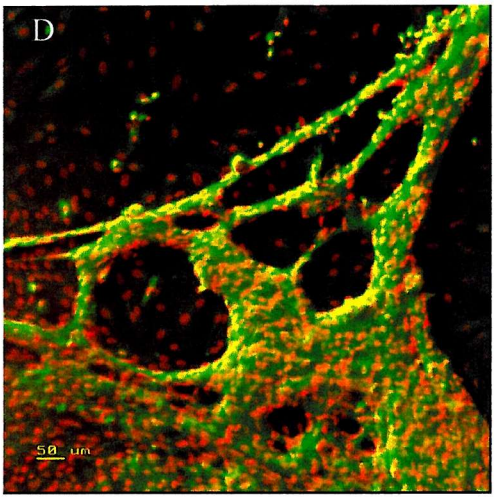
D
50 um

Figure 3.12 shows positive immunofluorescence of all cell types for the fibroblast 5B5 molecule. Although this marker is reported to be fibroblast specific it has been shown to bind to other cell types rather than just fibroblasts (Schwachula *et al.*, 1994).

Positive immunofluorescence was also seen in HOMEC cultures which were allowed to form capillary-like structures on Matrigel before immunocytochemical characterisation. Figure 3.13-A shows a primary HOMEC culture showing positive immunofluorescence for PECAM-1, the area can be compared to that in Figure 2.7 where the endothelial cells are beginning to move out from the original tissue fragment and move through the Matrigel toward the uncoated culture surface. The cells seen in the figure are all still within the Matrigel and the large red area to the left of the picture is the nuclei of the cells comprising the original tissue fragment.

Figure 3.13-C shows a section of a HOMEC capillary-like structure which was formed following subculture of HOMEC from the primary culture and plating onto Matrigel. The cells are showing positive immunofluorescence for PECAM-1 where they are in the capillary-like structure and also those which are not involved. This particular picture has been manipulated with the confocal microscopy computer software, where an imaginary light source is used to show shadowing. This manipulation does not change the positive immunofluorescence in any way, merely the quality of the final picture. The same result was observed when the computer manipulation was not performed.

Figure 3.13-D shows positive immunofluorescence for PECAM-1 of HOMEC where the cells were plated on Matrigel in a high seeding density and have formed a large flat aggregation as well as the finer capillary-like structures at the periphery.

Figure 3.13-B shows positive immunofluorescence for PECAM-1 in a HOMEC capillary-like structure under high magnification. The figure shows branching of the structure with a gap in the middle.

## 3.11 Discussion.

Following the morphological appearance of the follicular aspirate derived cells exhibiting endothelial cell characteristics the data presented in this chapter provides further evidence of their endothelial nature. The immunocytochemical analysis has shown the HOMEC to posses all of the endothelial specific markers (von Willebrand Factor, UEA-1, PECAM-1 and E-selectin) with at least the same level of positive immunofluorescence as that seen in HUVEC. The constitutive expression of VCAM-1 by HOMEC and not HUVEC is of particular interest. VCAM-1 expression is more typically seen in endothelial cells stimulated by cytokines (Haraldsen *et al.*, 1996). Its expression in unstimulated HOMEC in the present study may reflect the special role of these cells in interacting with luteal cells and the tissue matrix during the rapid formation of the corpus luteum *in vitro*. In contrast the ECV304 cell line appears to have lost most of the endothelial cell specific markers which has also been shown to be the case in other studies performed by Hughes, (1996). The fact that the cell line has lost most of the endothelial cell specific markers is not unexpected as these cells are a spontaneously transformed cell line and so have lost many of the natural endothelial cell characteristics. Fibroblasts did not react with any of the endothelial cell specific markers as expected. Fibroblasts showed positive immunofluorescence for the intermediate filament vimentin but this was expected. The positive immunofluorescence of all cell types for fibroblast 5B5 can be accounted for by the revelation that this antibody has been shown to be non-specific and that endothelial cells exhibit positive immunofluorescence for this antibody (Schwachula *et al.*, 1994). This finding is not as surprising as it would first appear. The prolyl 4-hydroxylase enzyme that is the target for fibroblast 5B5 plays an important role in the synthesis of collagen. Collagen, although mainly synthesised by fibroblasts has also been demonstrated to be produced by endothelial cells (Nicosia and Madri, 1987).

These studies also showed that the cultures of HOMEC were very pure as there are very few cells in any of the immunocytochemical studies which did not show positive immunofluorescence for the endothelial cell specific markers. This fact of purity gave

several advantageous features for the pending experiments, the most outstanding of which being the homogeneity of the cultures. This study has shown that it is possible to successfully culture HOMEC after carrying out a relatively simple culture model using readily available human tissue. The similarity of the HOMEC and HUVEC expression of endothelial cell specific markers indicate that the HUVEC are a suitable control for study of the endothelium of the human ovary. However, the HOMEC obviously provide a much better reflection of the cells of the corpus luteum *in vitro*. The ECV304 cell line has lost most of its endothelial cell markers and the question of its usefulness as a representative model for further studies of the human corpus luteum can be questioned.

# Chapter 4.

# Reverse transcription of flt-1, KDR and eNOS messenger ribonucleic acid and polymerase chain reaction amplification.

## 4.1 Introduction.

Very high levels of VEGF mRNA have been shown to accompany the follicular growth preceding ovulation (Neeman *et al.*, 1997). VEGF expression levels have also been shown to vary throughout the oestrous cycle (Redmer *et al.*, 1996). Furthermore, recent evidence obtained from a rat model demonstrated that the development of the corpus luteum is actually VEGF dependent (Ferrara *et al.*, 1998). This evidence suggests that the human ovarian microvascular endothelial cells are influenced by VEGF produced in the local environment.

VEGF binds to the flt-1 and KDR receptor complexes which are expressed almost exclusively on endothelial cell surfaces. Binding of VEGF to its receptors, activates endothelial cells to generate mitotic signals for angiogenesis (Shibuya *et al.*, 1995). Complementary DNA (cDNA) encoding the two VEGF receptors, flt-1 and KDR has been cloned and expressed (DeVries *et al.*, 1992, Millauer *et al.*, 1993, Terman *et al.*, 1992) and the message for the receptors has been shown to be expressed in vascular endothelial cells using reverse transcription and the polymerase chain reaction (RT-PCR).

VEGF has also been shown in some circumstances to stimulate endothelial cells to produce nitric oxide (Ziche *et al.*, 1997). Nitric oxide is produced by the nitric oxide synthase enzyme (eNOS) which is constitutively expressed in endothelial cells.

This chapter investigates the expression of the messages for the VEGF receptors KDR and flt-1 as well as the eNOS enzyme using the sensitive technique of RT-PCR in the cultured HOMEC.

## 4.2 Introduction to reverse transcription-polymerase chain reaction.

Numerous techniques have been developed to measure gene expression in tissue and cells. These include northern blotting, RNAse protection assays, in situ hybridisation, dot blot and S1 nuclease assay. However, these methods lack the sensitivity needed for investigation of rare transcripts or RNA present in low abundance. The adaptation of the PCR methodology to the investigation of RNA provided researchers with a method featuring speed, efficiency, specificity and sensitivity.

Since RNA cannot serve as a template for PCR, reverse transcription was combined with PCR to make RNA into a cDNA suitable for PCR. The combination of both techniques is colloquially referred to as RT-PCR. The technique can be used to determine the presence or absence of a transcript, to estimate expression levels and to clone cDNA products without the necessity of constructing and screening a cDNA library. RT-PCR can be used where small amounts of tissue are available. In cases where there are low amounts of RNA the sensitivity of analytical techniques used in their detection is of prime importance. Individual RNA molecules can be amplified by use of reverse transcription followed by polymerase chain reaction (RT-PCR). RT-PCR has been shown to be 1,000 to 10,000 times more sensitive than traditional RNA blot techniques therefore enabling detection of mRNA's of rare abundance and in small amounts of tissue.

RNA transcripts that exist at levels lower than those detectable by conventional analytical techniques can be detected by RT-PCR. This involves the primary extraction of RNA, it's separation from protein and DNA in solution and its conversion into cDNA by the enzyme reverse transcriptase. Two oligonucliotide (primer) sequences are synthesised to bind to complementary positions on the cDNA flanking a desired sequence of DNA. The positioned oligonucleotides encapsulate this defined region of

DNA giving exclusive amplification during the polymerase chain reaction. The principle of the RT-PCR technique is shown in Figure 4.1.

PCR was invented in 1985 by Kary Mullis (Saiki *et al.*, 1985) who was awarded the 1993 Nobel prize for chemistry. PCR is a powerful technique for rapid amplification of short DNA segments (generally less than 5 kb) from single or double stranded DNA. The reaction involves three stages;

1) denaturation of the double stranded template (or opening of initial cDNA template),
2) annealing of the primers to their complementary sequence on the single stranded DNA template,
3) extension of the desired sequence by the enzyme Taq polymerase to generate more double stranded product.

By subsequent repetition (cycles) of these three stages, high levels of amplification can be achieved. RT-PCR is now a conventional technique using one pair of oligonucleotide primers. PCRs of around 30 cycles are frequently used to investigate RNA levels of low amounts in tissue and cell cultures due to the high sensitivity following amplification.

## 4.3 GAPDH.

Constitutive control genes are frequently employed to show that if a gene is not present, it is not due to a failure of the RT-PCR. Such house-keeping genes are β-actin, β-microglobulin and cyclophillin. In this study we have used glyceraldehyde-3-phosphate dehydrogenase (Dissen *et al.*, 1994; Dveksler *et al.*, 1992; Golay *et al.*, 1991; Leonard *et al.*, 1993). Glyceraldehyde-3-phosphate dehydrogenase (GAPDH) is a glycolytic enzyme that catalyses the conversion of glyceraldehyde-3-phosphate to 1,3-diphosphoglycerate (Ercolani *et al.*, 1998). GAPDH has an essential role in glycolysis and is therefore known as a house-keeping gene. The GAPDH was used as a reference standard for investigation of flt-1, KDR and eNOS expression in this study.

The natural GAPDH product of 428 bp yielded the expected 3 fragments of 194, 190 and 44 bp after Sau 3aI restriction enzyme digest confirming its authenticity.

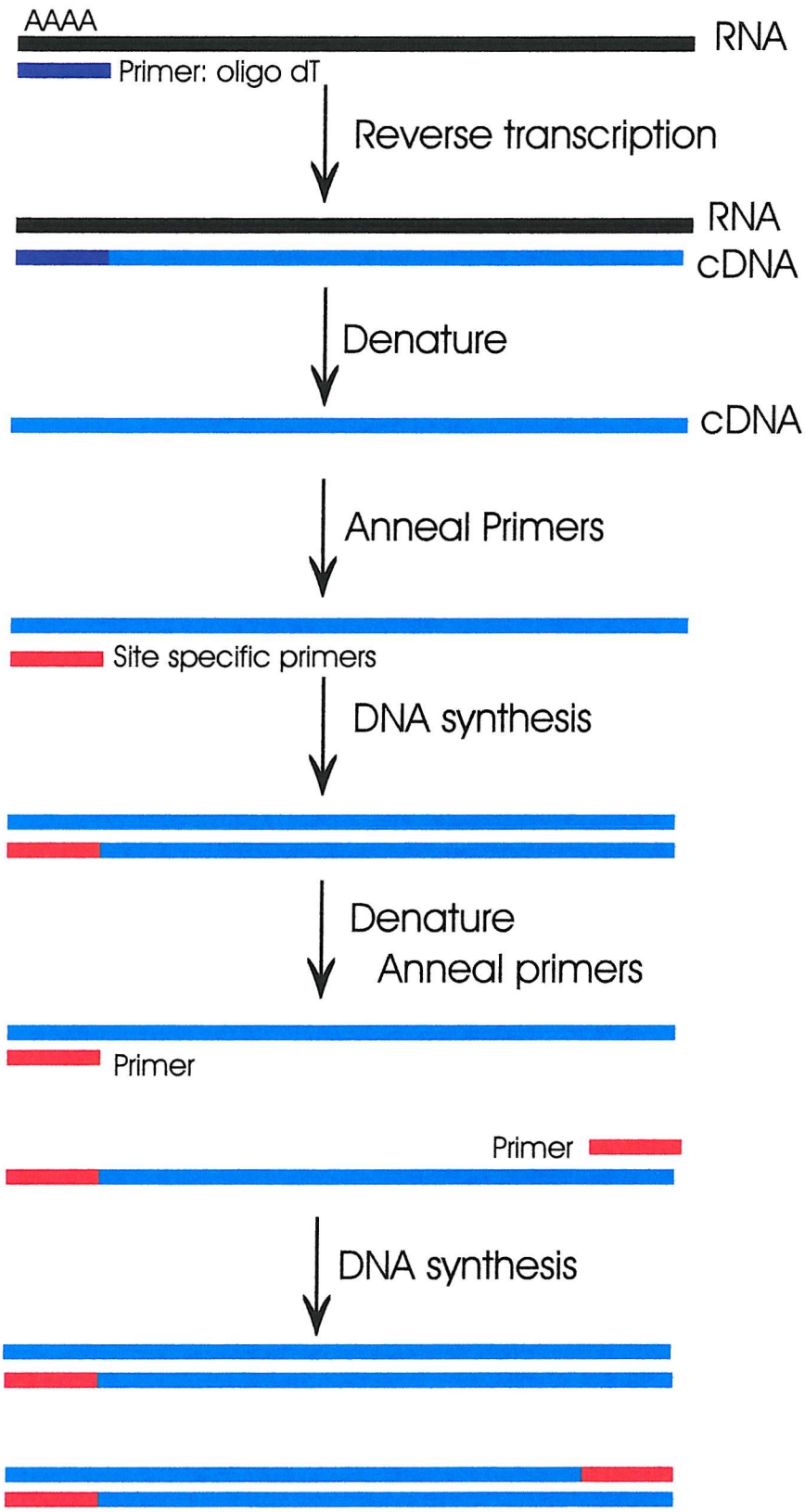


**Figure 4.1 Principle of RT-PCR.**

## 4.4 Materials and Methods.

### 4.4.1 Cell culture.

HOMEC, HUVEC and the ECV304 cell line were cultured according to the methods detailed in chapter 2. HUVEC were effective as a control cell culture as they have been demonstrated to express both of the VEGF receptors (Keyt *et al.*, 1996).

### 4.4.2 RNA Extraction.

**I. Cell Lysis and RNA extraction.**

RNA was solubilized by the addition of 1 ml of RNAzol B (Biogenesis Ltd., Bournmouth, UK) per $5x10^6$ cells. The lysate was mixed through a pipette and 10% of the final volume of chloroform was added. The mixture was vortexed for fifteen seconds, placed on ice for five minutes and then spun at 12,000 x g at room temperature for ten minutes. The upper aqueous phase containing the RNA was separated from the organic phase and interphase which contained the protein and DNA.

**II. RNA Precipitation.**

The aqueous phase was carefully removed and an equal volume of isopropanol was added. This was stored on ice for a minimum of fifteen minutes and subsequently spun at 12,000 x g at room temperature for fifteen minutes in order to collect a precipitate of RNA. After removal of the supernatant, the precipitated pellet was washed with 75% ethanol, vortexed and then spun at 7500 x g at room temperature for eight minutes. The supernatant was then carefully removed and the pellet was allowed to dry for approximately fifteen minutes in a Laminar flow cabinet. The dried pellet of RNA was resuspended in 38 µl nuclease free water.

### 4.4.3 Complementary DNA Synthesis.

Prior to the reverse transcription it was necessary to determine the amount of RNA present since the RT reaction was optimised for 5-10 μg of RNA. The absorbance of the RNA suspension was measured at 260 nm in a spectrophotometer where 40 μg of RNA gave an absorbance of 1 through a 1cm deep cuvette. From this reading the amount of RNA present in each tube could be calculated and if necessary, reduced to the optimum concentration for reverse transcription. The purity of the RNA in the samples could also be estimated by reading the sample absorbency at 280 nm; the purer the sample the closer the ratio of the reading 260:280 nm was to 1:8.

Complementary DNA was synthesised from 5-10 μg of the extracted total RNA using the Stratagene first strand synthesis kit (Stratagene Ltd., Cambridge, UK). 3 μl of random primers (100 ng/ml) were added to each 38 μl aliquot of RNA. The mixture was gently vortexed, heated to 65°C for five minutes and then allowed to cool slowly at room temperature to enable annealing of the primers to the template RNA. The following reagents were added in the stated order; 10 x first strand buffer (5 μl); RNase block Ribonuclease Inhibitor 2 (1 μl); 25 mmol/l deoxyribonucleoside triphosphates mixture (dNTP, 2 μl); 20 U/μl Moloney Murine Leukaemia Virus reverse transcriptase (1 μl). The total reagents for the reverse transcription were made up in a 500 μl microcentrifuge tube as a master mix. A fixed amount of master mix was added to each of the sample tubes to ensure equal concentrations of each reagent. The mixture was vortexed and incubated at 37°C for sixty minutes in order to generate the cDNA. The tubes were subsequently stored at -20°C.

It was possible that the RNA extracted could have been contaminated by DNA from the lower organic phase during their separation. Any contaminating DNA can interfere with the RT and PCR reactions generating non-specific products. Furthermore, contaminating DNA could give misleading results from the PCR giving products arising from DNA and not reverse transcribed RNA. This would not give an accurate estimation of the level of a particular mRNA in the cell. The homogeneity of the RNA

was determined by introducing the extracted RNA into this reverse transcription reaction without the presence of the reverse transcriptase enzyme. This control for each sample was run in the following PCRs for flt-1, KDR and eNOS to verify that products generated arose from the amplification of the RNA extracted and was not of genomic origin.

### 4.4.4 Optimisation of the Polymerase Chain Reaction.

Development of a PCR involved the evaluation of variables to obtain optimum amplification for detection of the PCR product. Parameters that were manipulated for the PCR were primer design, annealing temperature and cycle number.

**I. Primer Synthesis.**

The correct design of oligonucleotides is of paramount importance in the success of the PCR. The primer sequences for flt-1 are shown in figure 4.2A. These sequences are directed against a portion of the transmembrane region of the flt-1 receptor (based on the work of DeVries *et al.*, 1992). The primer sequences for eNOS were designed in this laboratory previously. A list of all primer sequences used are shown in table 4.1. Sense and antisense primers are synthesised to match as closely as possible with respect to their melting points and %GC content. Detrimental features of the primers such as the complementarity between primer pairs at their 3' ends, runs of three or more cytosine residues at the 3' end to reduce mispriming rate in regions of high G+C content, and palindromic sequences are minimised. All oligonucleotide primers used in the PCR were synthesised by the department of Molecular Microbiology, University of Southampton.

**II. Annealing Temperature.**

The annealing temperature is the temperature at which the primers specifically anneal to the primer template on the single stranded cDNA. This temperature is dependant on the base composition, length and concentration of the primers. The annealing

temperatures for the PCRs in this study are based on the theory that the recommended annealing temperature is generally 5°C below the melting point of the primers (Innis *et al.*, 1990).

The primer annealing step is an important parameter in optimizing the specificity of PCR. If the annealing temperature is too high, it will reduce the amount of product generated. If it is too low, it will allow non-specific binding with subsequent generation of multiple products. The annealing temperature and time required for optimal annealing of the primers to their template is dependant upon the base composition, length and concentration of primers. Many laboratories use annealing temperatures of 3-5°C below the Tm (melting temperature) at which the DNA is 50% melted as a starting point for PCR optimisation experiments. The most commonly used formula for calculating Tm is [(number of A+T) x 2°C + (number of G+C) x 4°C], but this is inaccurate with primers longer than 20 nucleotides. However, suitable annealing temperatures are only approximately related to the Tm and the calculated Tms only act as a reference point to begin experimentation. The ideal annealing temperatures may actually be 3-12°C higher than the calculated Tm. If a routine PCR of a particular target is planned, then the optimum annealing temperature should be determined empirically. The highest annealing temperature which gives the best PCR products should be used (Newton and Graham, 1994). The deliberate use of low annealing temperatures in an initial study can indicate the presence of the desired product, but this is generally impeded by excessively low specificity. By subsequently increasing the annealing temperature, the specificity of the reaction can be augmented by a reduction in mispriming and the misextension of incorrect nucleotides at the 3' ends of the primers (Innis *et al.*, 1990).

**III. Cycle Number.**

The cycle number was chosen with respect to the relative abundances of the RNA molecules in question. It is important to create the appropriate amount of product for detection following gel electrophoresis especially when looking at molecules of low expression. A PCR of 30 cycles was sufficient for detection of the message for GAPDH. However, 30 cycles was found to be inadequate for detection of the

messages of flt-1, KDR and eNOS in all of the cell types. The PCR was repeated for 35 and 40 cycles, the message for flt-1, KDR and eNOS being detectable only after 40 cycles. It was essential not to increase the number of cycle further than necessary due to the plateau phase of product generation in a PCR. If this plateau phase is extended by increasing the number of cycles it would allow the amplification of non-specific products which may reach their plateau later on in the reaction.

During PCR amplifications, the first extension products from the original DNA template do not have a distinct length as the DNA polymerases will continue to synthesise new DNA until it either stops or is interrupted by the next cycle. The second extension products are also of indeterminate length; however, at the third cycle, fragments of target sequence are synthesised which are of defined length corresponding to the positions of the primers on the original template. From the fourth cycle onwards the target sequence is amplified.
Despite being initially exponential in nature, product generation in PCR amplification eventually plateaus, at which point a maximum level is reached. If a situation arises where non-specific products are also generated, these may in fact reach their plateau phase at a later number of cycles than the desired product. Therefore, in these circumstances, increasing the cycle number would have no beneficial effect on the product of interest, but would lead to the accumulation of high levels on non-specific products.
Too many cycles will cause non-specific products, and too few cycles will give low product yield. In this study it was found that 40 cycles were needed for the amplification of flt-1, KDR and eNOS.

### 4.4.5 Standard Reaction Conditions.

Preliminary PCRs were performed based on suggested parameters recommended by Innis *et al.*, (1990). Magnesium concentrations were maintained at a constant value of 15 mmol/l as recommended for optimal efficiency with the manufacturers Taq

polymerase 10 x reaction buffer (Promega, Southampton, UK).

**I. Reaction mixture.**

A master mix of reagents was used for one round of PCR of 30 or 40 cycles depending on the product under investigation. This ensured that each PCR tube received equal concentrations of reagents and allowed a direct comparison of samples during the exponential phase of amplification.

The master mix was made up in a 500 µl microcentrifuge tube and consisted of the following reagents: 10 x reaction buffer consisting of 500 mmol/l KCL, 100 mmol/l Tris-HCl (pH 9.0 at 25°C), 15 mmol/l $MgCl_2$ (10 µl per PCR reaction); 25 µmol/l dNTP mixture consisting of 25 µmol/l each of dATP, dTTP, dCTP and dGTP (0.8 µl per PCR reaction; Boehringer Mannheim., Lewes, UK); 20 µmol/l outer primers (2 µl of each per PCR reaction); 5 U/µl Thermus aquaticus (Taq) polymerase (2.5 U; 0.5 µl per PCR reaction; Promega).

The master mix was mixed vigorously and spun to collect the reagents at the bottom of the tube. The composite mix was equally divided into reaction tubes (15.3 µl per tube) ensuring identical reaction mixtures in each tube. 2 µl of each cDNA sample was added to each tube which allowed an estimated comparison of the cDNA samples. Nuclease-free water gave a final aqueous volume of 100 µl which was layered with 100 µl of mineral oil (Sigma). A negative control was formulated for each PCR performed. This consisted of an equal volume of the master mix without any sample cDNA to verify that products detected by the PCR were generated from the sample and not from contaminants present in the master mix.

**II. Thermal cycling.**

PCR was carried out on a Hybaid thermal cycler (Hybaid, Teddington, UK) for 30 cycles for GAPDH or 40 cycles for flt-1, KDR and eNOS. The reaction temperature was monitored with an intra-tube thermocouple. The full program was as follows;

1) 91°C for 30s (to denature template complexes)

2) X°C for 30s (primer/template annealing)

3) 72°C for 30s (extension)
91°C for 30s (denaturing)
X°C for 30s (annealing)
(Y cycles)

4) 72°C for 600s (to maximise strand completion)

The annealing temperature X and cycle number Y varied with each PCR.
The optimum annealing temperature value for eNOS, KDR and flt-1 primers was found to be 55°C.

### 4.4.6 Precautions.

Due to the sensitivity of the polymerase chain reaction, caution is needed and essential steps were taken to prevent contamination. If a contaminant was to enter a reaction false positive sources of template would be generated. Thus the risk of contamination was minimised by applying rigid rules to the technique and the laboratory practise surrounding the procedure.
These rules were as follows;

1. One laboratory was allocated for the RT-PCR, the surfaces of which were frequently swabbed with ethanol to eliminate any contaminating dust particles.
2. All tubes used for RT-PCR were autoclaved and the tips used contained filters to exclude any aerosol effect from the pipettes.
3. The pipettes were not removed from the laboratory.
4. All manipulations with nucleic acids were carried out using positive displaceable pipettes (Alpha Laboratories., Eastleigh, UK). The design of these allowed immediate disposal of tips after each use so that the tips were easily changed after contact was made with each sample of nucleic acid.
5. During all stages of the PCR, latex gloves were used and regularly changed on handling of the reagents.

### 4.4.7 Analysis of PCR Products.

PCR products were identified by their ability to move through an agarose gel. Products were fractionated by their molecular weights through electrophoresis on an 8 x 7 cm 1.5% TBE agarose gel (Sigma). A 20 µl aliquot of PCR product along with 5 µl of Blue/Orange loading buffer (Promega) was run across the gel with constant applied voltage of 100 V. 1 µl of a 100 bp ladder was used to allow determination of the product size (Gibco BRL). Gels were stained with ethidium bromide (0.5 µg/ml) for 10 min. The gels were subsequently visualised on a 312 nm UVP ultraviolet transilluminator (Genetic Research Instrumentation Ltd., Dunmow, UK) and photographed using a D.S.34 Polaroid camera and hood and Polaroid 667 film (Genetic Research Instrumentation Ltd.).

Results shown are representative of analysis of two independent RNA extractions from each cell type.

| mRNA | Primers 5'-3' | | Product size | Reference |
|---|---|---|---|---|
| | sense | antisense | | |
| GAPDH | ATCC GCTTGTCATCAATGGAA | CAGGGATGATGTTCTGG A | 428 bp | Ercolani *et al,*. 1988. |
| flt-1 | GTCACAGAAGAGGATGAA GGTGTCTA | CACAGTCCGGCACGTAG GTGATT | 414 bp | DeVries *et al.*, 1992. |
| KDR | CATCATATCCACTGGTAT TGG | GCCAAGCTTGTACCATGT GAG | 404 bp | Charnock-Jones *et al.*, 1994. |
| eNOS | GTGATGGCGAAGCGAGTG AA | ACATCTCCATCAGGGCA GCT | 244 bp | Janssens *et al.*, 1992. |

**Table 4.1** Summary of sense and antisense primers used for RT-PCR with the product size generated following PCR amplification

## Flt-1 primer sequence.

Sense: 5' GTCACAGAAGAGGATGAAGGTGTCTA 3'

Antisense: 5' CACAGTCCGGCACGTAGGTGATT 3'

5'
TACAACAAGAGCCTGGAATTATTTTAGGACCAGGAAGCAGCACGCT
GTTTATTGAAAGAGTCACAGAAGAGGATGAAGGTGTCTATCACTGC
AAAGCCACCAACCAGAAGGGCTCTGTGGAAAGTTCAGCATACCTCA
CTGTTCAAGGAACCTCGGACAAGTCTAATCTGGAGCTGATCACTCT
AACATGCACCTGTGTGGCTGCGACTCTCTTCTGGCTCCTATTAACCC
TCCTTATCCGAAAAATGAAAAGGTCTTCTTCTGAAATAAAGACTGA
CTACCTATCAATTATAATGGACCCAGATGAAGTTCCTTTGGATGAGC
AGTGTGAGCGGCTCCCTTATGATGCCAGCAAGTGGGAGTTTGCCCG
GGAGAGACTTAAACTGGGCAAATCACTTGGAAGAGGGGCTTTTGGA
AAAGTGGTTCAAGCATCAGCATTTGGCATTAAGAAATCACCTACGT
GCCGGACTGTGGCTGTGAAAATGCTGAAGAGGGGGCCACGGCCAG
CGAGTACAAAGCTCTGATGACTGAGCTAAAAATCTTGACCCACATT
GGCCACCATCTGAACGTGGTTAACCTGGCTGGGAGCCTGCACCAAG
CAAGGAGGGCCTCTGATGGTGATTGTTGAATACTGCAAATATGGAA
ATCTCTCCAACTACCTCAAGAGCAAACGTGACTTATTTTTCTCAAC
AAGGATGCAGCACTACACATGGAGCCTAAGAAAGAAAAAATGGAG
CCAGGCCTGGAACAAGGCAAGAAACCAAGACTAGATAGCGTCACCA
GCAGCGAAAGCTTTGCGAGCTCCGGCTTTCAGGAAGATAAAAGTCT
GAGTGATGTTGAGGAAGAGGA 3'

**Figure 4.2 A sequence of the transmembrane region of human flt-1 mRNA and oligonucleotide primer sequence.** Features shown are primer sequences sense and antisense (red) and primer binding region for the antisense and region which is complementary to the binding region for the sense oligonucleotides (blue, underlined) these primers together span the transmembrane region of the flt-1 receptor.

## GAPDH primer sequences.

Sense: 5' GCTTGTCATCAATGGAAATCC 3'

Antisense: 5' CAGGGATGATGTTCTGGA 3'

5'
GTTTACATGTTCCATATGATTCCACCCATGGCAAATTCCATGGCACC
GTCAAGGCTGAGAACGGGAAGCTTGTCATCAATGGAAATCCCATCA
CCATCTTCCAGGAgtgagtggaagacagaatggaagaaatctgctttggggaggcaaaccccggt
agGCGAGATCCCTCCAAAATCAAGTGGGGCGATGCTGGCGCTGAGT
ACGTCGTGGAGTCCACTGGCGTCTTCACCACCATGGAGAAGGCTGG
Ggtgagtgcaggagggcccgcgggaggggaagctgactcagccctgcaaaggcaggacaagggttcata
actgtctgcttctctgtgtagGCTCATTTGCAGGGGGGAGCCAAAAGGGTCATCA
TCTCTGCCCCCTCTGCTGATGCCCCCATGTTCGTCATGGGTGTGAAC
CATGAGAAGTATGACAAACGCCTCAAGATCATCAGgtgaggaaggcagggc
ccgtggagaagcggccagcctggcaccctatggacacgctcccctgacttgcgccccgctccctctttctttgc
agCAATGCCTCCTGCACCACCAACTGCTTAGCACCCCTGGCCAAGGT
CATCCATGACAACTTTGGTATCGTGGAAGGACTCATGgtatgagagctggg
gaatgggactgaggctcccacctttctcatccaagactggctcctccctgctggggctgcgtgcaaccctggg
gttgggggttctggggactggctttcccataatttcctttcaaggtggggagggaggtagaggggtgatgtggg
gagtacgctgcagggcctcactcctttgcagACCAACAGTCCATGCCATCACTGCCA
CCCAGAAGACTGTGGATGGCCCCTCCGGGAAACTGTGGCGTGATGG
CCGCGGGGCTCTCCAGAACATCATCCCTGCCTCTACTGGCGCTGCCA
AGGCTGTGGGCAAGGTCATCCCTGAGCTGAACGGGAAGCTCACTGG
CATGGCCTTCCGTGTCCCCACTGCCAACCTGTCAGTGGTGGACCTGA
CCTGCCGTCTAGAAAAACCTGCCAAATATGATGACATCAAGAAGGT
GGTGAAGCAGGCGTCGGAGGGCCCCCTCAAGGGCATCCGGGCTACA
CTGAGCACCAGGTGGTCTCCTCTGACTTCAACAGCGACACCCACCCT
CCACCTTTGACGCTGGGGCTGGCATTGCCCTCAACGACCACTTTGTC
AAGCTCATTTCCTG 3'

**Figure 4.3 Sequence of the human GAPDH gene and the primers used to amplify exons four and eight.** Features shown are exons 4-8 (upper case), introns (green, lower case), sense and antisense primers (red) and primer binding sites (blue, underlined).

## 4.5 Results of RT-PCR for GAPDH, VEGF receptors flt-1 and KDR, and eNOS.

Using the amplification conditions described in section 4.4.5, figure 4.4 shows that the correct size PCR products for GAPDH were detected in HOMEC, HUVEC and ECV304 cells. These results show that the reverse transcription was performed correctly and successfully, and that the cDNA could be used for further studies and provide accurate results of the mRNA present in the cells at the time of extraction. These observations of GAPDH expression were not due to genomic DNA since the negative controls from reverse transcription reactions without the reverse transcriptase enzyme were subjected to the same PCRs for each sample and no products were generated from these.

Figure 4.5 shows the results for the PCR products for the VEGF receptors flt-1 and KDR in HOMEC, HUVEC and ECV304 cells. The correct size double stranded product for flt-1 was present in both HOMEC and HUVEC but not ECV304 cells. Expression of the KDR receptor was also only seen in HOMEC and HUVEC, ECV304 cells again showed no expression. The presence of GAPDH in ECV304 proves that this lack of VEGF receptor expression in ECV304 cells was not due to a failure of the RT, but in fact due to no expression. Negative controls for HOMEC and HUVEC did not show any PCR product.

The apparent conclusion that HUVEC express both receptors in greater abundance under the same reaction conditions cannot be drawn since no quantitative studies were performed. These results only show the presence of the receptors in both cell types and the apparent difference in quantity may be a result of many contributing factors rather than expression levels. The appearance of a more intense band in HUVEC for GAPDH compared to that for HOMEC can also be seen.

The PCR for eNOS demonstrated the presence of mRNA in only HOMEC and HUVEC as shown in figure 4.6. Once again ECV304 cells were negative for expression. These results for ECV304 cells show that the cells have lost both of the VEGF receptors and eNOS expression. Whereas HOMEC have both of the VEGF

receptors and eNOS activity in a similar way to those of HUVEC.

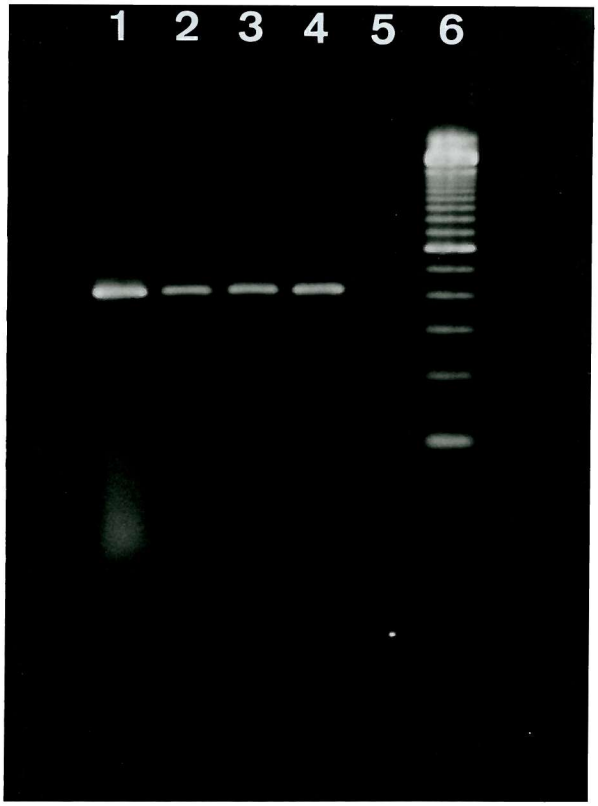


**Figure 4.4 Electrophoretic pattern of the RT-PCR products for GAPDH in HOMEC, HUVEC and ECV304 cells.** The PCR examines the message for the GAPDH housekeeping gene in HOMEC, HUVEC and ECV304 cells. Lane 1, HUVEC. Lanes 2+3, HOMEC. Lane 4, ECV304. Lane 6, 100 bp ladder.

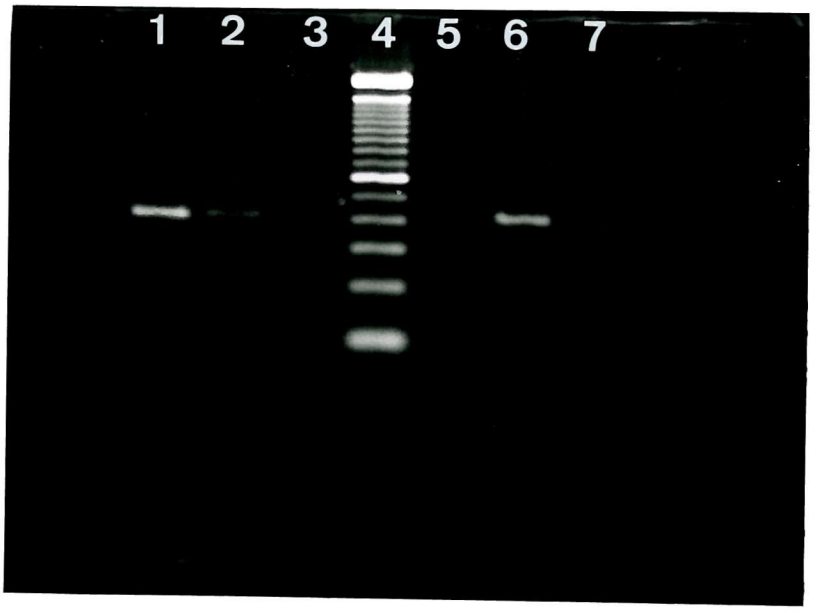


**Figure 4.5 Electrophoretic pattern of the RT-PCR products for the VEGF receptors flt-1 and KDR in HOMEC, HUVEC and ECV304 cells.** Electrophoresis is used to show the presence or absence of flt-1 and KDR in HOMEC, HUVEC and ECV304 cells.
KDR specific primers: Lane 1, HUVEC. Lane 2, HOMEC. Lane 3, ECV304.
flt-1 specific primers: Lane 5, ECV304. Lane 6, HUVEC. Lane 7, HOMEC.
Lane 4, 100 bp ladder.

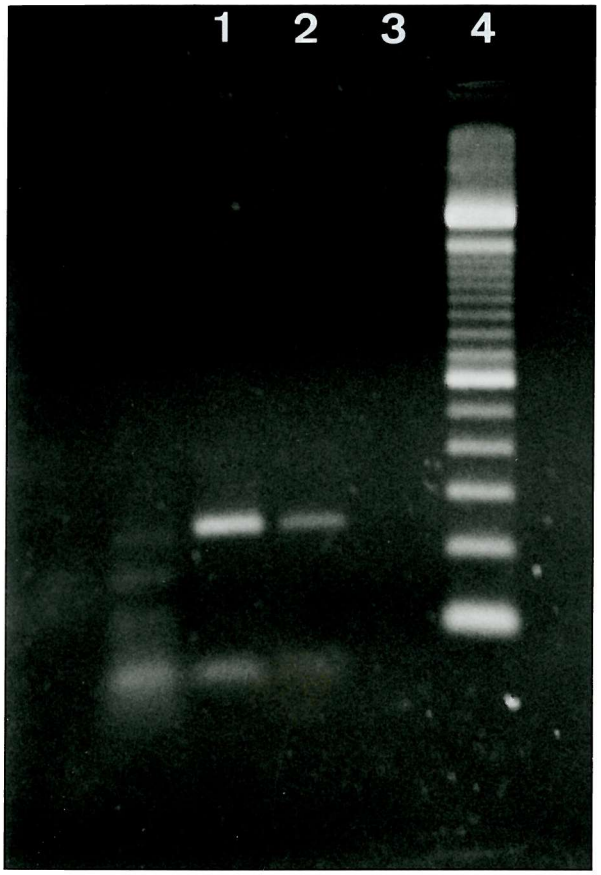


**Figure 4.6 Electrophoretic pattern of the RT-PCR products for eNOS in HOMEC, HUVEC and ECV304 cells.** The electrophoresis patterns are shown for HOMEC, HUVEC and ECV304 cell expression of eNOS. Lane 1, HUVEC. Lane 2, HOMEC. Lane 3, ECV304. Lane 4, 100 bp ladder.

## 4.6 Discussion.

This chapter has described the development of RT and PCRs for the detection of the messages for the VEGF receptors flt-1 and KDR, and eNOS in HOMEC, HUVEC and ECV304 cells. The PCR products for all of the messages were readily detected after 40 cycles in both HOMEC and HUVEC but not in ECV304 cells.

The implication of the presence of these messages in HOMEC adds further evidence of their endothelial nature as eNOS is specific to endothelial cells and the VEGF receptors are also almost exclusively found on endothelial cells (Charnoch-Jones *et al.*, 1994).

The failure of any detection, or at least in levels measurable in this study with ECV304 cells is not a complete surprise. The fact that the ECV304 cells are a transformed cell line implies that they have lost many of the regulating mechanisms of normal endothelial cells. Response to VEGF is not a requirement of these cells whose proliferation is more rapid, and therefore the expression of VEGF receptors is not needed in these cells.

VEGF has been shown to play an important role in corpus luteum formation in a number of species and the present study shows that its effects could be mediated by either or both of the main VEGF receptors, flt-1 and KDR, which are being expressed by HOMEC. The activation of flt-1 has been shown to mobilise calcium ions which are important for eNOS activity (Morbidelli *et al.*, 1996). As eNOS was also shown to be expressed in HOMEC, the constituents for important endothelial mechanisms in relation to VEGF action are in place in these cells. The present observations are qualitative in nature and further studies are required to establish the role of these mechanisms. Survival of microvascular endothelium under serum-free conditions has been demonstrated and it has been postulated that VEGF may act as a survival factor for microvascular endothelial cells under these conditions (Gupta *et al.*, 1997). The proliferative activity of microvascular luteal cells isolated from the primate corpus luteum has been shown to be stimulated by VEGF (Christenson *et al.*, 1996). Taken together, the available evidence thus suggests that VEGF has an important role in controlling the function of microvascular endothelium in the ovary.

# Chapter 5.

# Endothelial cell ultrastructure and matrix interactions.

## 5.1 Introduction.

A special characteristic of endothelial cells is their ability to form capillary-like structures when plated on the artificial basement membrane preparation Matrigel. This capillary-like structure formation is a well documented phenomenon and has been reported in most of the recently isolated types of endothelial cells including human cerebral microvascular endothelial cells (Lamszuz *et al.*, 1999), rat KMT-17 fibrosarcoma-derived endothelial cells (Utoguchi *et al.*, 1995), human dermal microvascular endothelial cells (Kraling and Bischoff, 1998), the endothelial-derived cell line EA hy926 (Jones *et al.*, 1998) and Schlemm's canal endothelial cells (Stamer *et al.*, 1998). The exception to this capillary-like structure formation are microvascular endothelial cells isolated from mouse brain (Morbidelli *et al.*, 1995).
A cell line prepared from the murine embryonic yolk sac 10 years ago which has been successfully cultured since, was recently plated on to Matrigel to see if it still had the ability to form these structures. The cells formed a complete network of capillary structures within 12 hours (Li *et al.*, 1999).

*In vivo*, this formation of blood vessels is dependent on matrix degradation and remodelling. This chapter investigates the capillary-like structure formation with matrix remodelling and cell-matrix interactions being of particular interest.

## 5.2 Matrix degradation during angiogenesis.

During capillary formation, endothelial cell migration and organisation have been shown to be critically dependent on surrounding basement membrane proteins. These proteins serve as a physical support and are also thought to provide signals which regulate the migration and organisation of cells (Williams *et al.*, 1996).

In the initial stages of capillary formation the microvascular endothelial cells of pre-existing blood vessels locally degrade the underlying basal lamina and invade into the stroma of the tissue to be vascularised. This process has been shown to require numerous degradative enzymes such as the plasminogen activator (PA)-plasmin system and the matrix metalloproteinase (MMP) family. PAs trigger a proteinase cascade that results in the generation of high local concentrations of plasmin and MMP's. This increase in proteolytic activity has three major consequences: 1) it permits endothelial cell mediated degradation of the vessel basal lamina, 2) generates extracellular matrix (ECM) degradation products that are chemotactic for endothelial cells, and 3) activates and mobilises growth factors localised in the ECM. PA and MMP activities are modulated in endothelial cells by complex mechanisms, including transcriptional regulation by a variety of growth factors and cytokines with angiogenic activity, extracellular control of the proteolytic activities by tissue inhibitors, and interaction with binding sites on the cell membrane and ECM (Mignatti and Rifkin, 1996).

The ability of endothelial cells to form capillary-like structures is a specialised function of this cell type. Understanding the mechanisms responsible for the control of capillary-like structure formation, as well as regression, are of importance considering the central role of angiogenesis in development, inflammation, repair and cancer. (Ilan *et al.*, 1998).

In this study we have used the complete ECM in the form of Matrigel as well as the individual components to look at capillary-like structure formation.

## 5.3 Matrix components.

### 5.3.1 Matrigel.

Matrigel Basement Membrane Matrix is a solubilised basement membrane preparation extracted from the Engelbreth-Holm-Swarm (EHS) mouse sarcoma, a tumour rich in extracellular matrix proteins. Matrigel has been shown to be effective for the attachment and differentiation of vascular endothelial cells and provides the substrate necessary for the study of angiogenesis. Its major matrix component is laminin, followed by collagen IV, heparan sulfate proteoglycans, entactin and nidogen. It also contains TGF-beta, fibroblast growth factor, tissue plasminogen activator, and other growth factors which occur naturally in the EHS tumour. Table 5.1 shows the composition of Matrigel. Matrigel is also available in a growth factor reduced formulation, this is achieved by including two high salt precipitations that reduce endogenous growth factors in the preparation of the Matrigel. Table 5.2 shows the concentrations of growth factors present in growth factor reduced Matrigel compared to that in the original Matrigel. The total protein content and ECM composition remain unchanged in the growth factor reduced Matrigel, but the levels of growth factors are greatly reduced with the exception of TGF-beta. This growth factor has been shown to be tightly bound to collagen IV (and possibly other ECM components) in its latent form (Kleinman *et al.*, 1982).

### 5.3.2 Rat tail collagen type I.

Collagen I is found in most tissues and organs, but is most plentiful in dermis, tendons and bones. The type I molecule is a heterotrimer of 300 nm length being composed of two $alpha_1$ chains and one $alpha_2$ chain. Collagen binding integrin receptors are $alpha_1$, $beta_1$, and $alpha_3beta_1$. When used as a gel, collagen facilitates successful adaptation in *in vitro* culture and enhances expression of cell-specific morphology and function. Collagen may also be used in a thin layer to promote attachment. The concentration of collagen in the gel influences the clarity, consistency and gel behaviour (Kuhn, 1987).

| Composition of Matrigel matrix vs. GFR Matrigel matrix | | |
|---|---|---|
| **Compound** | **Amount in Matrigel (%)** | **Amount in GFR Matrigel (%)** |
| Laminin | 56% | 61% |
| Collagen IV | 31% | 30% |
| Entactin | 8% | 7% |
| HSPG | 5% | 2% |

**Table 5.1** The major components found in standard and growth factor reduced Matrigel.

| Amounts of growth factors present in Matrigel matrix vs. GFR Matrigel matrix | | |
|---|---|---|
| **Growth Factor** | **Average concentration in Matrigel matrix** | **Average concentration in GFR Matrigel** |
| EGF | 0.7 ng/ml | <0.5 ng/ml |
| bFGF | not applicable | not determined |
| NGF | not applicable | <0.2 ng/ml |
| PDGF | 12 pg/ml | <5 pg/ml |
| IGF-1 | 16 ng/ml | 5 ng/ml |
| TGF-β | 2.3 ng/ml | 1.7 ng/ml |

**Table 5.2** The average concentrations of growth factors found in standard and growth factor reduced Matrigel.

### 5.3.3 Fibronectin.

Fibronectin is a broad range natural cell adhesion factor. It is a 440-500 kDa dimeric glycoprotein consisting of two similar 220-250 kDa subunits linked by disulfide bonds. It is found as a dimer in plasma and in multimeric form in the extracellular matrix and on cell surfaces. Its primary function is related to cell adhesion to the extracellular matrix. Fibronectin may also be involved in interactions with collagen, heparin and other cell surface glycosaminoglycans. The conformation and orientation of adsorbed fibronectin is also important and has an effect on cell spreading and strength of adhesion of endothelial cells. Fibronectin addition to serum free medium promotes cell adhesion (Aota *et al.*, 1991).

### 5.3.4 Laminin.

Laminin, a major structural component of basement membranes, is a glycoprotein composed of three polypeptide chains with a multi-domain structure. Laminin has many and varied functions that are mediated by cell surface integrins binding to various components of the basement membrane. As a cell attachment factor it promotes migration, growth, morphology and adhesion, all of which are important functions in tissue repair (Beck *et al.*, 1990).

The laminins belong to a family of trimeric basement membrane glycoproteins with multiple domains, structures and functions. Endothelial cells bind laminin-1 and form capillary-like structures when plated on a laminin rich basement membrane Matrigel. Laminin-1 is composed of 3 chains: alpha-1, beta-1 and gamma-1. Laminin has multiple active sites in its three polypeptide chains, including the pentapeptides IKVAV in the A chain and YIGSR in the $\beta 1$ chain, as well as an RGD side in the $\alpha$ chain. A number of laminin-binding cellular proteins have been characterised, including a variety of cell surface integrins that mediate the interactions of cells with laminin. Because laminin-1 is known to contain multiple biologically active sites a recent study screened the entire laminin gamma-1 chain for potential angiogenic sequences of which they found several which had angiogenic activity (Ponce *et al.*, 1999).

## 5.4 Materials and Methods.

### 5.4.1 Cell culture.

HOMEC, HUVEC, ECV304 cells and fibroblasts were isolated and cultured as previously described in chapter 2.

### 5.4.2 Electron microscopy of HOMEC and HUVEC capillary-like structures.

HOMEC and HUVEC capillary-like structures were grown on Matrigel covered Thermanox coverslips.
The coverslips were embedded in araldite to form blocks. Following embedding, the blocks were transversely cut to give 5 micron sections which were mounted, stained with 1% toluidine blue in borax and viewed under a microscope. Once the block had been cut to a depth where a cross section of a capillary-like structure was visible, 1 micron sections were prepared for transmission electron microscopy.

### 5.4.3 Capillary-like structure formation on Matrigel, fibronectin, collagen, laminin and glass.

#### 5.4.3.1 Matrigel.

Wells of 8-well Lab-Tek II chamber slides were coated with 100 µl of Matrigel, both standard and growth factor reduced (Becton Dickinson).
40,000 HOMEC or HUVEC were added to individual wells and incubated in M199 with additional endothelial cell growth supplement (150 µg/ml) using 5% $CO_2$ in air at 37°C. Cultures were left overnight.
In an attempt to inhibit capillary-like structure formation, cultures were incubated with

excess VEGF (100 ng/ml) or with anti human and anti mouse VEGF neutralising antibodies (500 ng/ml; R and D Systems).

**5.4.3.2 Collagen.**

Wells of 8-well Lab-Tek II chamber slides were coated with a thin layer or a thick 3D gel of collagen I (Becton Dickinson).

40,000 HOMEC or HUVEC were added to individual wells and incubated in M199 with additional endothelial cell growth supplement (150 µg/ml). Half of the wells were also supplemented with VEGF (12 ng/ml). Cultures were left overnight in 5% $CO_2$ in air at 37°C.

**5.4.3.3 Fibronectin.**

Wells of 8-well Lab-Tek II chamber slides were coated with a thin layer of fibronectin (Becton Dickinson).

40,000 HOMEC or HUVEC were added to individual wells and incubated in M199 with additional endothelial cell growth supplement (150 µg/ml). Half of the wells were also supplemented with VEGF (12 ng/ml). Cultures were left overnight in 5% $CO_2$ in air at 37°C.

**5.4.3.4 Laminin.**

Wells of 8-well Lab-Tek II chamber slides were coated with a thin layer of laminin (Becton Dickinson).

40,000 HOMEC or HUVEC were added to individual wells and incubated in M199 with additional endothelial cell growth supplement (150 µg/ml). Half of the wells were also supplemented with VEGF (12 ng/ml). Cultures were left overnight in 5% $CO_2$ in air at 37°C.

**5.4.3.5 Glass.**

40,000 HOMEC or HUVEC were added to individual wells and incubated in M199 with additional endothelial cell growth supplement (150 µg/ml). Half of the wells were

also supplemented with VEGF (12 ng/ml). Cultures were left overnight in 5% $CO_2$ in air at 37°C.

### 5.4.4 Time lapse video microscopy of HOMEC and HUVEC capillary-like structure formation on Matrigel.

Individual wells of 24 well plates were separated using a heated scalpel. These single wells were then coated with 200 µl of standard Matrigel.
40,000 HOMEC or HUVEC cells were added to individual wells and the wells were transferred to a 50 $cm^2$ culture flask and gassed for 2 min with 5% $CO^2$ in air. The flask was sealed and transferred to the time lapse apparatus. This consisted of a microscope with a heated stage (37°C) linked to a JVC BR-9000 time lapse video recorder and monitor. Frames were taken over a period of time up to 60 hours.

### 5.4.5 Immunocytochemistry of HOMEC and HUVEC capillary-like structures for laminin β1 chain.

Cultures were prepared in Lab-Tek II chamber slides as detailed in section 5.4.3.1 on standard Matrigel.
Following formation of capillary-like structures, the cultures were fixed in ice-cold methanol for 10 min and washed with PBS followed by a 30 min wash with 10% goat serum in PBS. A dilution of the primary antibody, anti-laminin β1 chain (Catalogue number, MAB1928; Stratech Scientific Ltd, Luton, UK) was incubated overnight at room temperature. After 3 ten minute washes with 0.2% BSA in PBS, cultures were incubated with a fluorescein isothyocyanate conjugated anti-mouse secondary antibody (20 µg/ml; Stratech) for 1 hour. Three further ten min washes with 0.2% BSA in PBS were followed by incubation with the nuclear counterstain propidium iodide (0.01 mg/ml). The chamber slides were disassembled to leave the bottom surface. The samples were then mounted with moviol and imaged under ultraviolet light on an

Olympus microscope. Photographs were taken with an Olympus camera using Ektachrome 400 film.

### 5.4.6 Spontaneous formation of HOMEC and HUVEC capillary-like structures.

Cultures of HOMEC, HUVEC and ECV304 cells and fibroblasts were prepared as described in chapter 2. Once the cells had reached confluence they were kept at 37°C in 5% $CO_2$ in air but the media was no longer replaced every 3-4 days and the cells were not subcultured. Cultures were observed daily with the microscope.

## 5.5 Results of endothelial cell ultrastructure and matrix interactions.

When capillary-like structures formed by endothelial cells on Matrigel were examined in the 5 micron sections under the light microscope, small clusters of cells were apparent (figure 5.1). Figure 5.1a shows HOMEC and 5.1b shows HUVEC. Both figures show a small cluster of cells in the centre of the picture. In both cases the cells (a) are sitting on top of the Matrigel which can be seen in the area indicated by (b). There appears to be a space within the centre of the capillary-like structure which could signify the presence of a lumen. Areas where the section has folded during the preparation of the slide are shown (c). The reason for the folds is that the Thermanox coverslips and araldite are different forms of plastics and therefore when the section is heated to adhere it to the glass slide the two types of plastic contract at different rates and folds are introduced into the section. The HUVEC capillary-like structure appears to be much more elongated than the HOMEC capillary-like structure, however both are made up of several cells.

Further analysis by electron microscopy of the structures shown in figure 5.1a+b has shown with much more clarity the presence of a lumen within the structures. Figure 5.2a shows the HOMEC capillary-like structure and figure 5.2b shows the HUVEC capillary-like structure. Both structures show that they are made up of several cells, and the presence of a large 'gap' in the centre of the structure which in a functional capillary would be the lumen. The HOMEC structure is partially obscured by the grid used to mount the specimen, although all of the important parts can still be seen. There are lots of mitochondria within both structures which indicates that the cells are very active. The golgi, nucleus and other cellular organelles can also be seen. The HUVEC structure can clearly be seen to be composed of five separate cells one of which is necrotic, there is also a central 'Y' shaped lumen and figure 5.2c shows the presence of a gap junction. This gap junction between two adjoining cells indicates intercellular communication between cells that are comprising the structure.

**Figure 5.1 Capillary-like structures on Matrigel transversely cut in 5 micron sections.** A) HOMEC capillary-like structure, B) HUVEC capillary-like structure. Both showing, a) capillary-like structures, b) Matrigel, c) folds introduced during slide preparation. Two independent capillary-like structure were sectioned for each cell type.


A
c
a
b
c

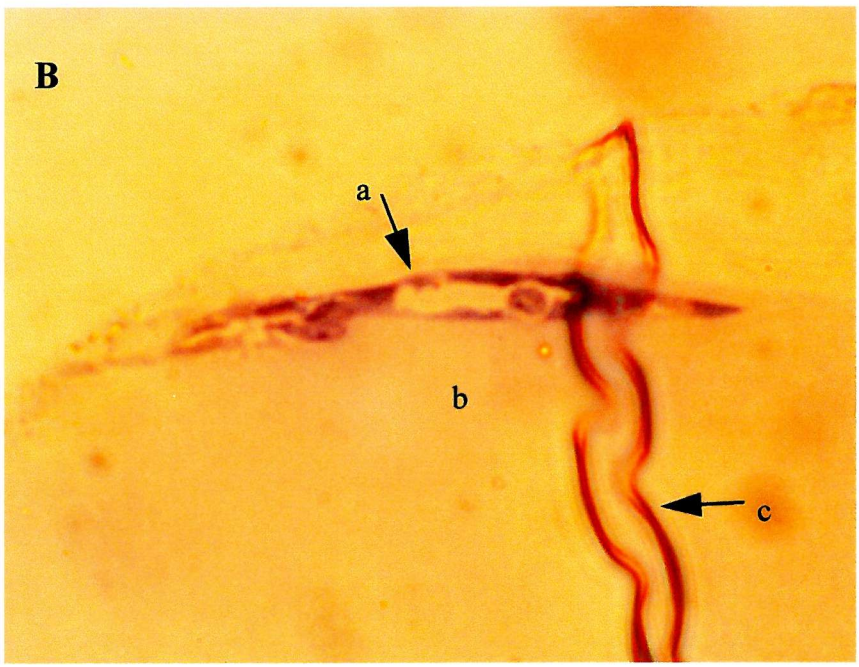
B
a
b
c

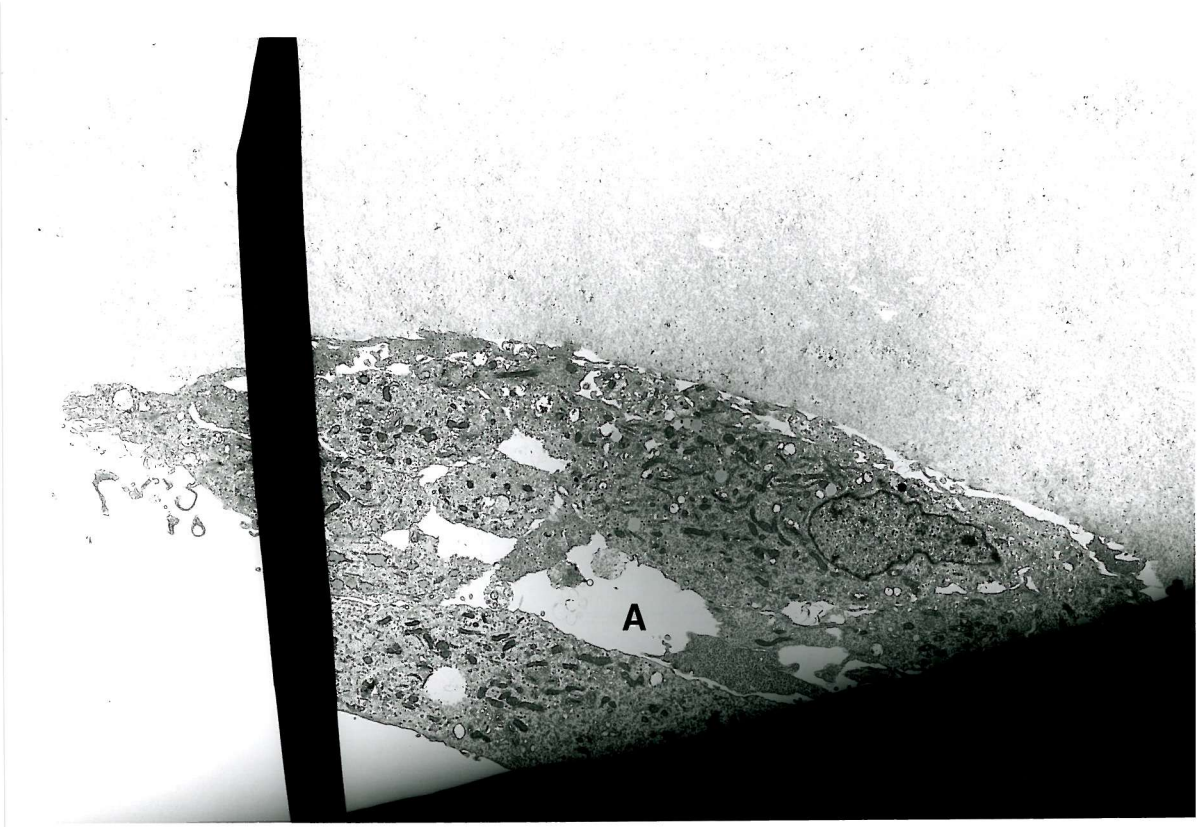


**Figure 5.2a Electron microscopy of HOMEC capillary-like structure.** There is a large gap in the centre of the structure (A) comparable to a lumen in a capillary. EM Magnification x 1500.

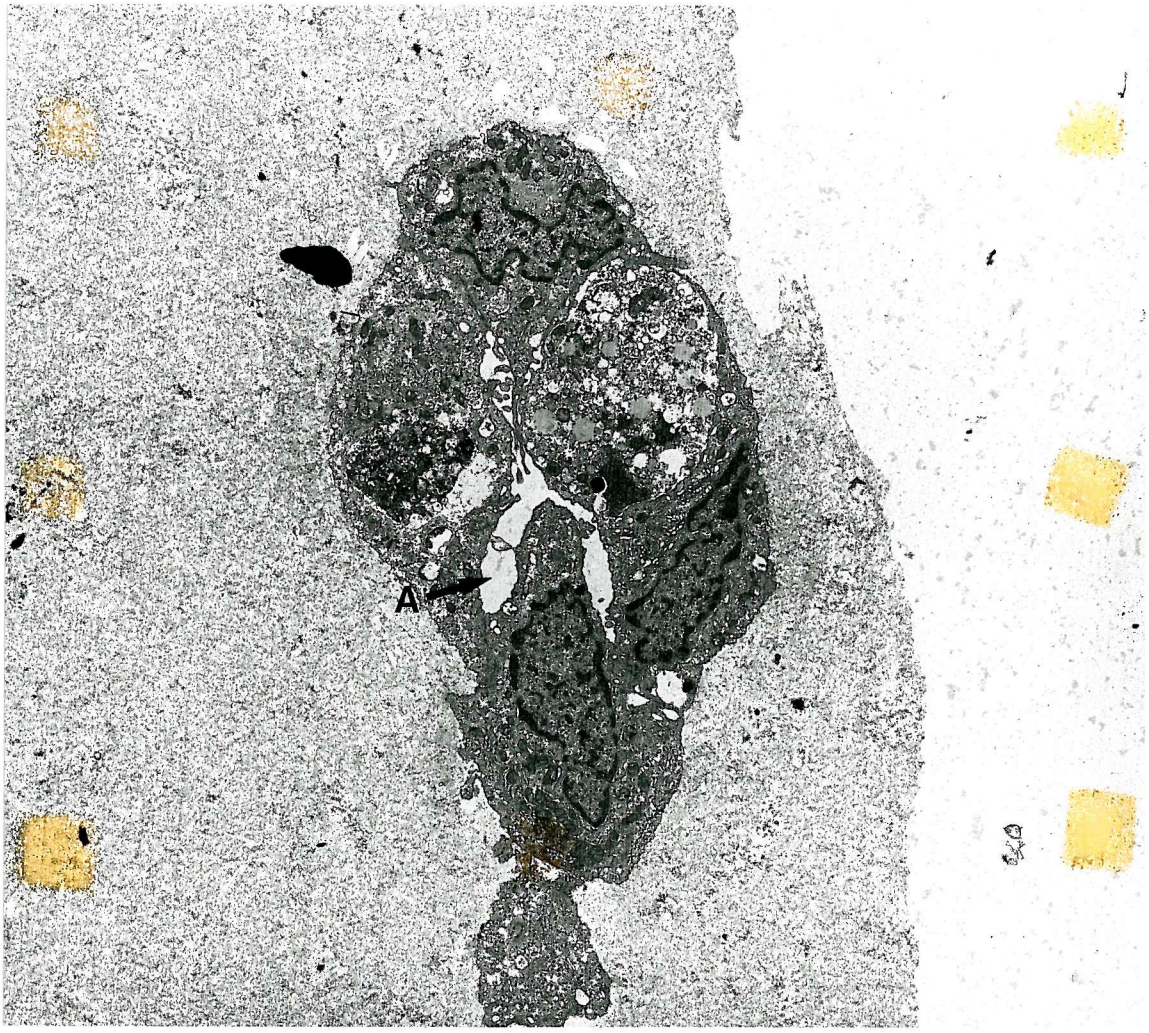


**Figure 5.2b Electron microscopy of HUVEC capillary-like structure.** There is a large gap in the centre of the structure (A) comparable to a lumen in a capillary. EM Magnification x 3000.

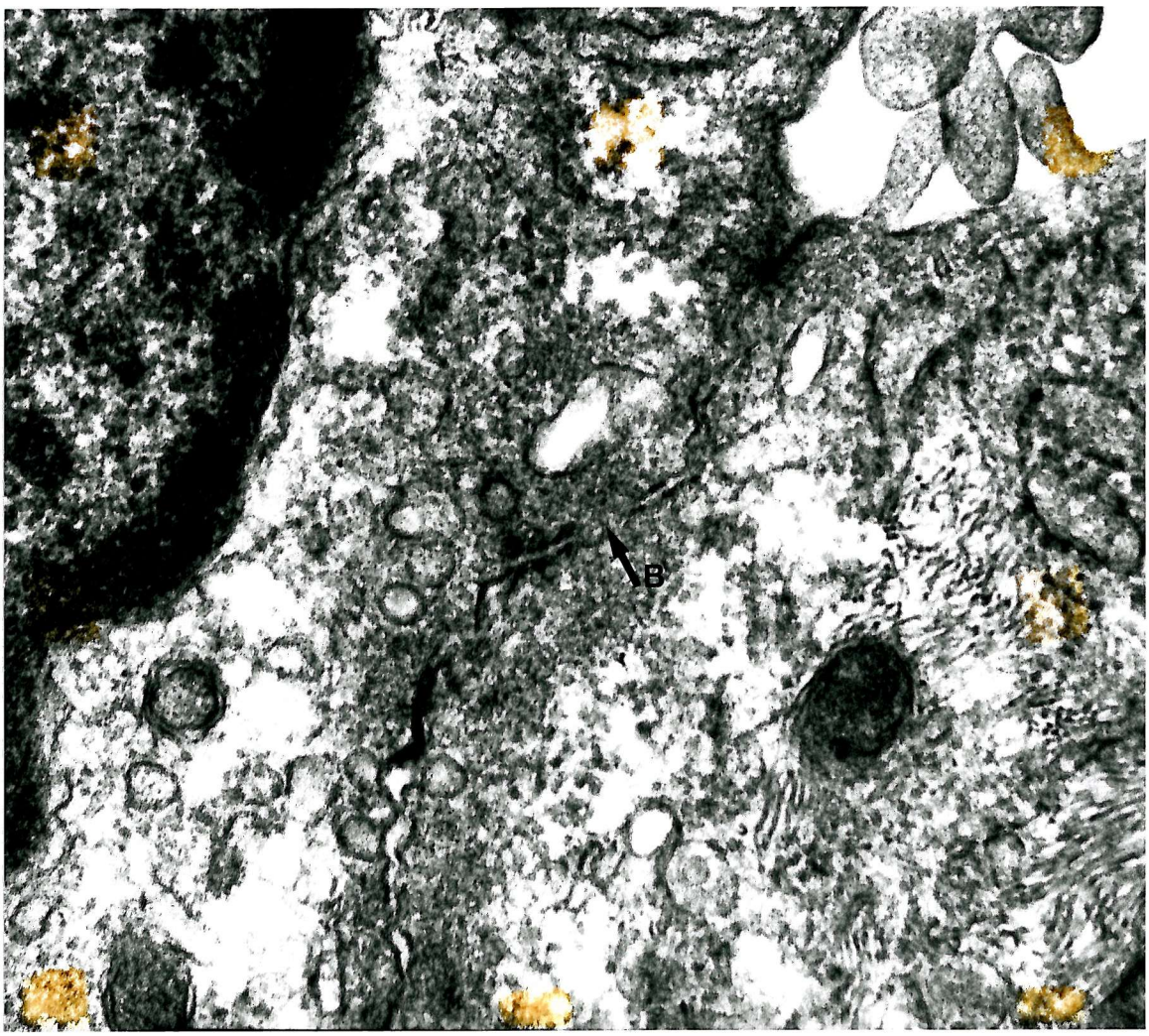


**Figure 5.2c Electron microscopy of a gap junction.** B) shows a gap junction which has formed between two adjoined HUVEC cells in a capillary-like structure. EM Magnification x 40,000.

The formation of capillary-like structures on matrices other than Matrigel was of particular interest. HUVEC and HOMEC plated on both Matrigel and growth factor reduced Matrigel formed capillary-like structures. Where excess VEGF or blocking antibodies to VEGF were used, no inhibition of the formation of capillary-like structures was observed. The only time capillary-like structures did not form was when cell seeding density was too low or the Matrigel was not applied in a thick enough layer. No growth factors had to be added to the media to stimulate formation of capillary-like structures for either cell type. Figure 5.3 shows capillary-like structures at a different magnification so that the complexity of the networks formed can be clearly seen.

HUVEC and HOMEC plated on 3D collagen type I gels did not survive well, the cells did not organise into capillary-like structures and most of the cells died within 4 days of plating. However, the addition of VEGF to the cultures appeared to have a survival effect on the cells. Figure 5.4a shows a HUVEC culture on collage gel in the presence of VEGF, figure 5.4b shows an identical culture without VEGF. The culture with VEGF present shows healthy cells which continued to proliferate, but no capillary-like structures formed. The culture without VEGF shows that most of the cells have died and again there is no sign of capillary-like structure development. An interesting finding was that on thin layer collagen coated flasks neither HOMEC nor HUVEC required the presence of VEGF to survive. However, the rate of cellular proliferation was considerably increased with cells reaching confluence much quicker than those on normal culture surfaces and VEGF further increased the rate of proliferation. There were no capillary-like structure formations with this culture system either.

The results of HOMEC and HUVEC plated on to laminin (figure 5.5) and fibronectin coated culture surfaces, and uncoated glass showed only the development of cell monolayers. The effect of VEGF in these cultures again increased the rate of proliferation but had no effect on the development of capillary-like structures. None of these culture matrices had any adverse effect on the cells, such as apoptosis.

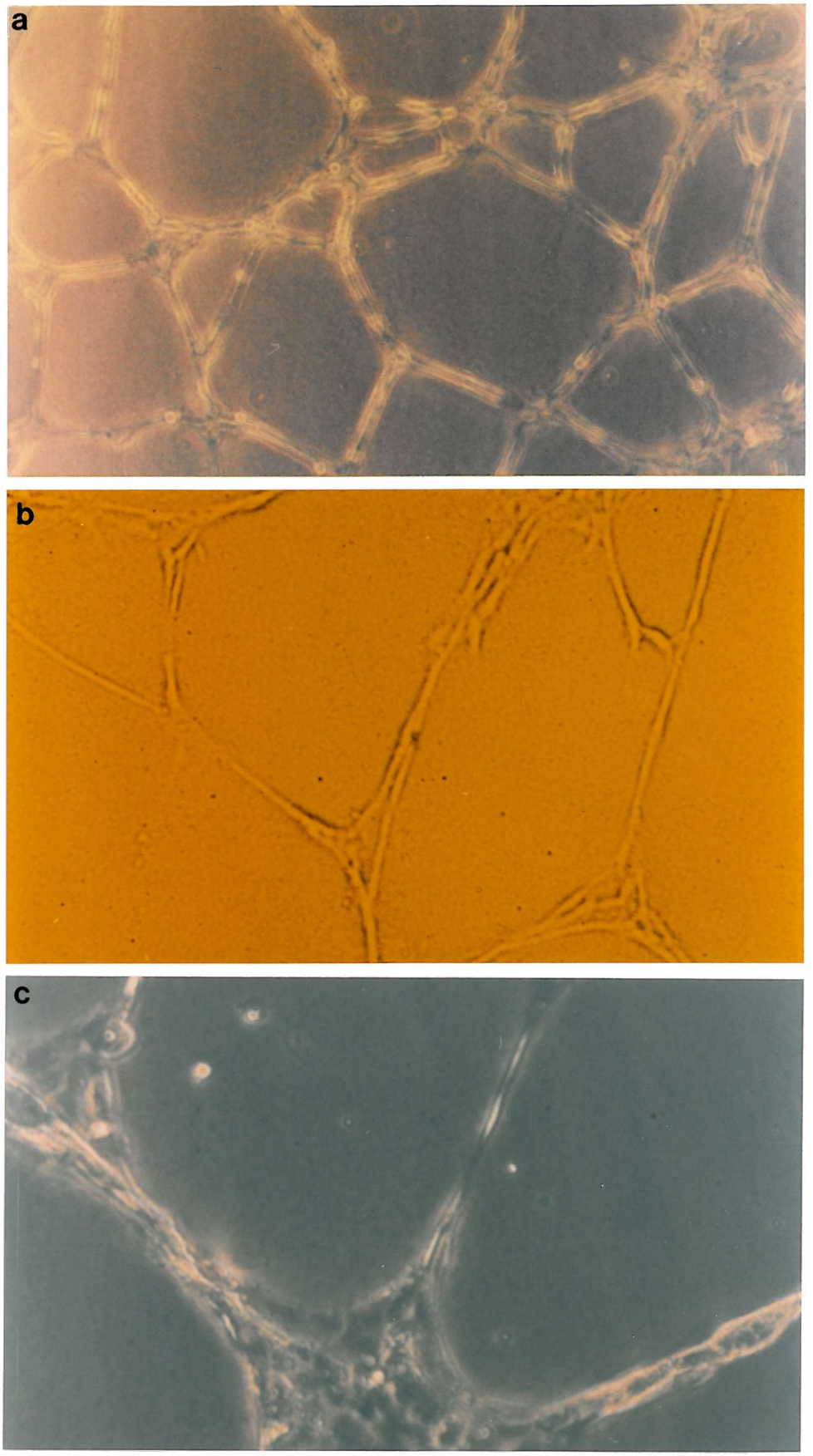


**Figure 5.3 HOMEC capillary-like structures on Matrigel.** Objective magnification; a) x4, b) x10, c) x20.

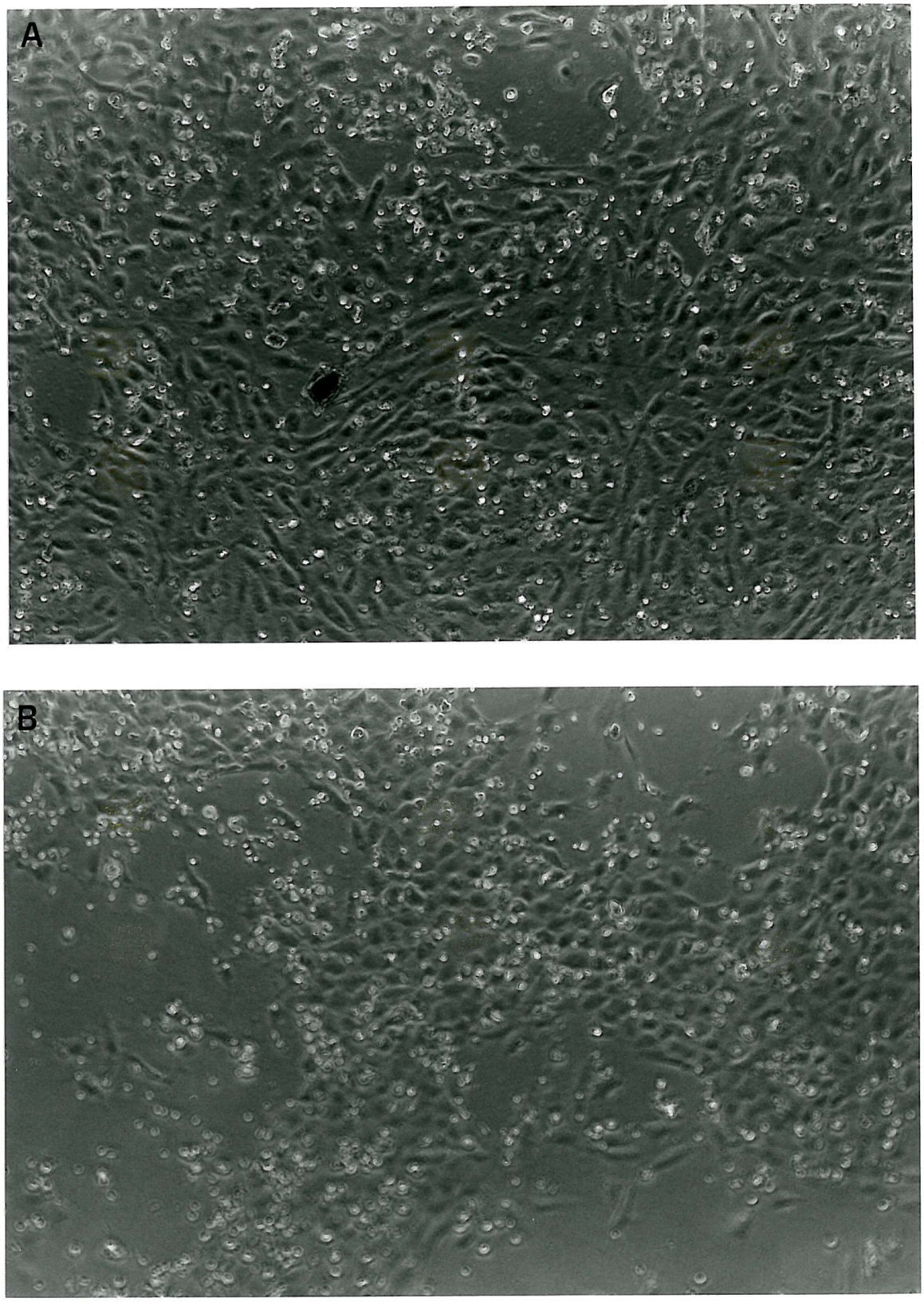


**Figure 5.4 HOMEC plated on collagen type I 3D gels.** A) shows cells in the presence of VEGF, where the cells have formed a monolayer, B) shows cells without the presence of VEGF, where most of the cells have died.

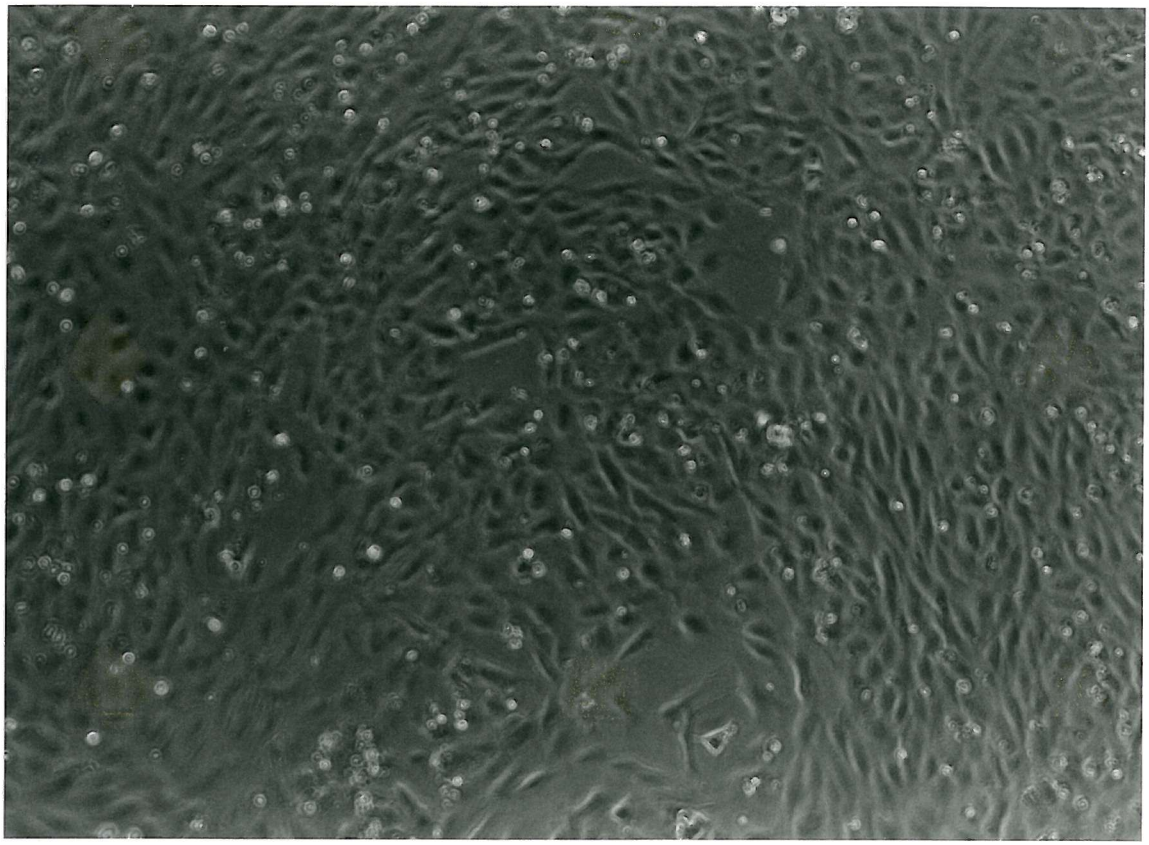

**Figure 5.5 HOMEC plated on laminin coated slides.**

An interesting feature of HUVEC and HOMEC cultures when culture was continued after confluence had been reached, but the media was no longer changed was that, although most of the cells died and floated off from the culture surface, the spontaneous formation of capillary-like structures was seen (figures 5.6a+b). These structures were similar in size to those which developed on Matrigel although they had a much flatter appearance and the cells did not knit together to form smooth capillaries. Shaking of the flasks could dislodge areas of these networks and they did not appear to be viable cells. These structures did not form in ECV304 cells (figure 5.6c) or fibroblast cultures that were left in the same way. ECV304 cells carried on proliferating and began to grow on top of each other. Thus their ability to form contact inhibited monolayers would appear to be another trait that they have lost. Eventually the cells died but no sign of capillary-like structures were seen at any point.

**Figure 5.6a HOMEC capillary-like structures**, which spontaneous developed when cultures were left.

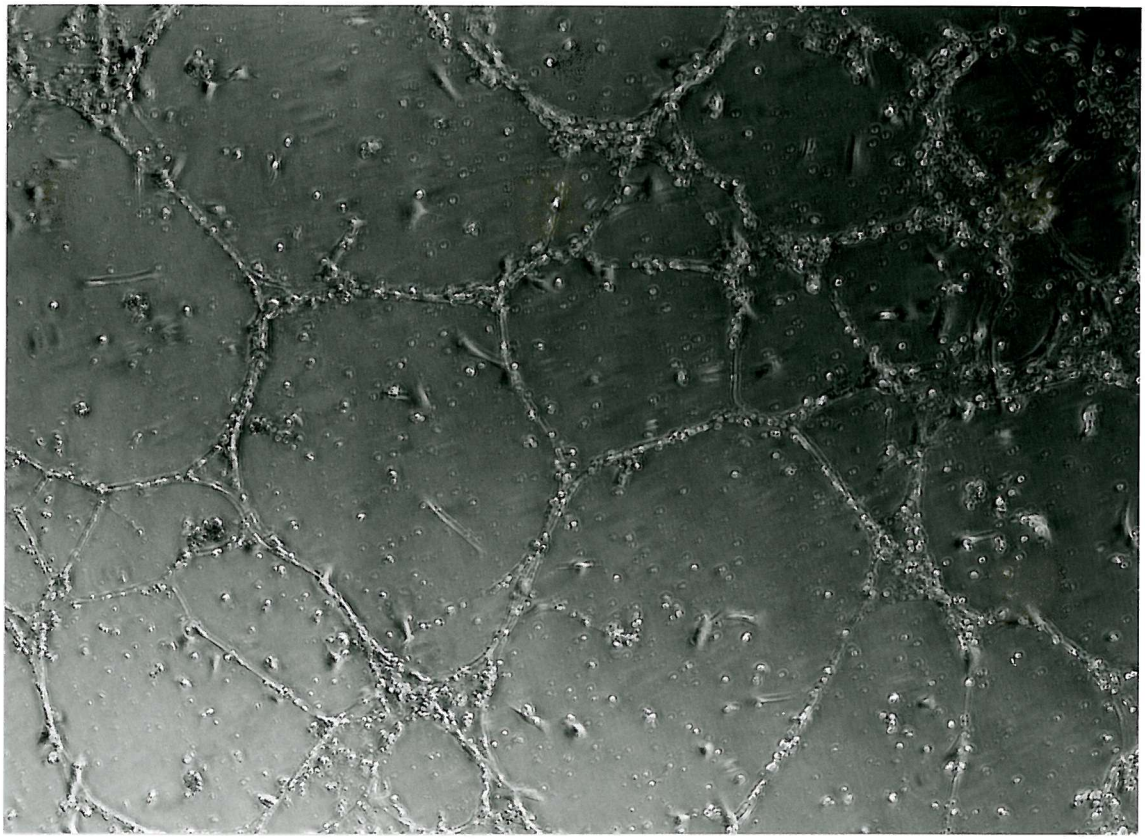

**Figure 5.6b HUVEC capillary-like structures**, which spontaneously developed when cultures were left.

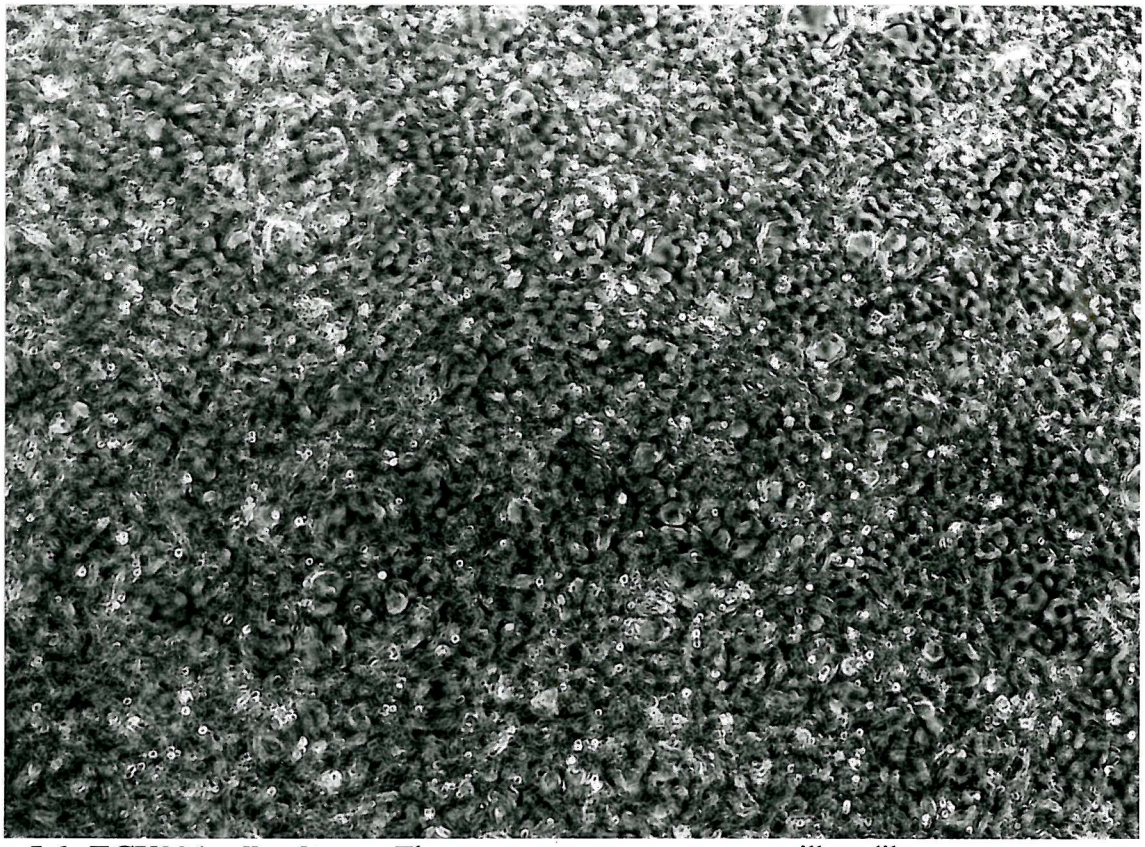

**5.6c ECV304 cell cultures**. There were no spontaneous capillary-like structure formations when cultures were left.

Analysis of how the HUVEC capillary-like structures form on Matrigel can be seen in figure 5.7. This shows the progression of the structure formation with stills taken from the time lapse video at hourly intervals. Within two hours of plating, the cells were nearly all adhered to the Matrigel and moved towards each other to form small aggregates. By three hours the cells were beginning to align and the basis for the final network could be seen. These crude early alignments were refined over time and by 5 hours a comprehensive network could easily be distinguished. This was still further refined with capillary-like structures becoming more elongated and the clusters of cells at the meeting place of two or more capillaries becoming smaller. The network between 5-14 hours was not greatly changed although by 22 hours there had been further refinement of the model and the network was much more well defined.
Figure 5.8 shows the same development of capillary-like structures formed by HOMEC plated on Matrigel. The images have been recorded at a much higher magnification than those in figure 5.7. The time recorded in the left hand corner of the images is actually 30 minutes earlier than the time of plating. These results show that the cells adhered and started to form clusters within 30 minutes of plating. The clusters then began to join together by cells migrating from their clusters to others nearby, these cells formed capillary-like structures between clusters by becoming very elongated and spindle-like, in complete contrast to the cobblestone shape exhibited in culture on plastic surfaces. The cells continue to remodel the network throughout the 10 hours of recording. The final networks were seen to be the same for both HOMEC and HUVEC.
Figure 5.9 shows the remodelling that is performed by the capillary-like structures following the original formations. Stills taken from 18 hours after plating show a fully developed capillary-like structure network. This network is slightly modified over the next 20 hours as one of the capillary-like structures at the top of the network is remodelled to rejoin the cell aggregate in the centre of the picture. This cell aggregate then reduces in size as the cells comprising it migrate along the capillary-like structures to other areas of the network.

**Figure 5.7 Time lapse video microscopy of HUVEC capillary-like structure formation.** Frames of the time lapse video are shown at hourly intervals to show the process of capillary-like structure formation in HUVEC on Matrigel.

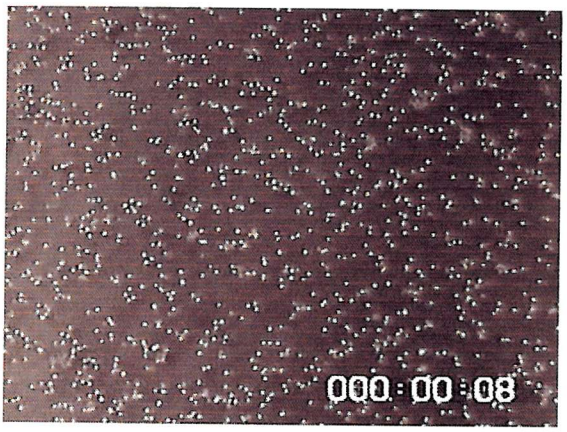
000:00:08

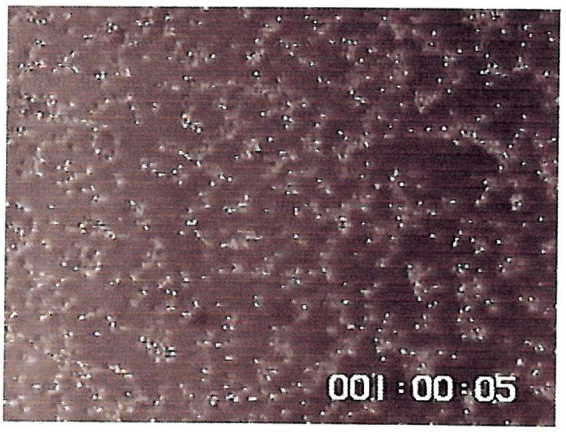
001:00:05

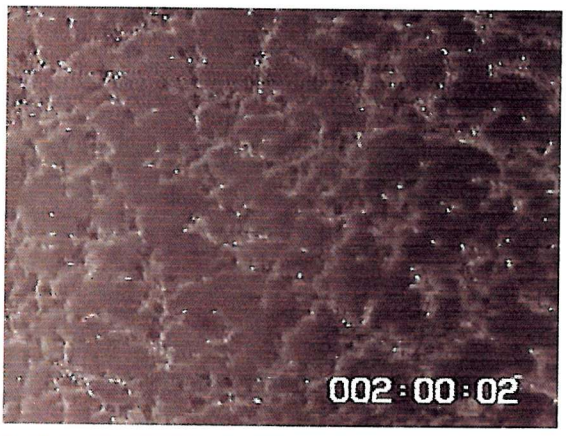
002:00:02

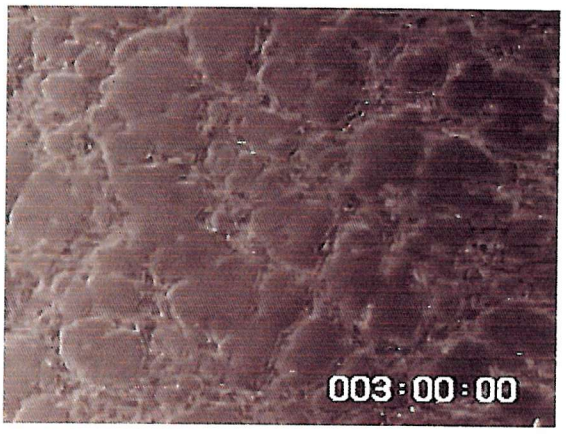
003:00:00

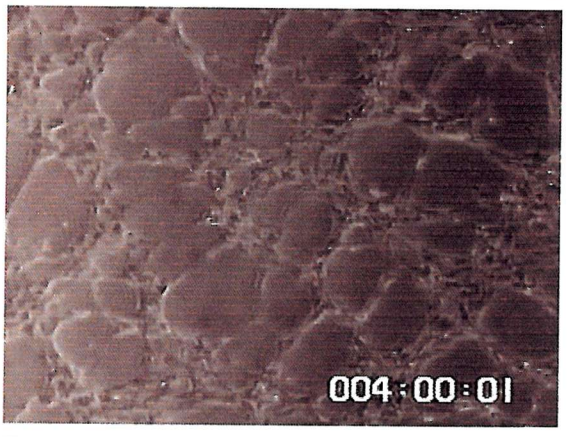
004:00:01

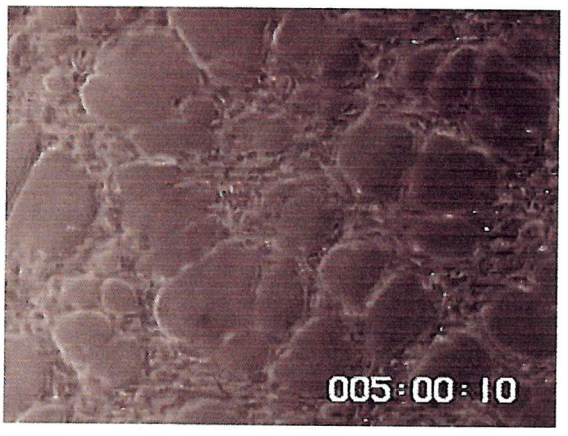
005:00:10

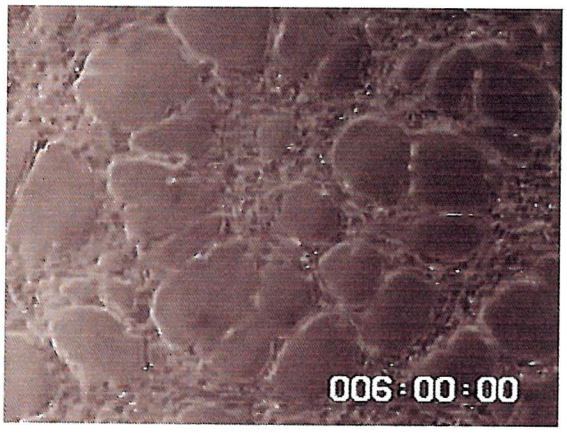
006:00:00

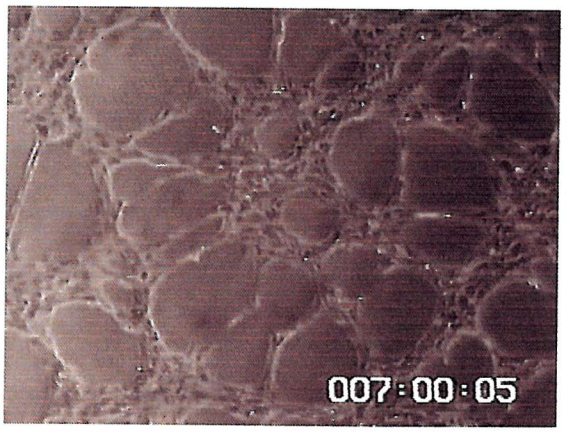
007:00:05

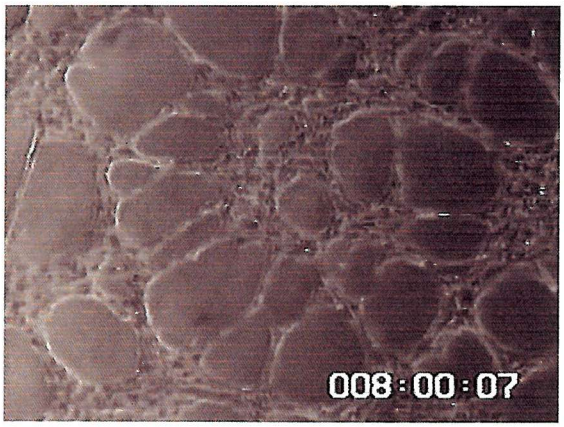
008:00:07

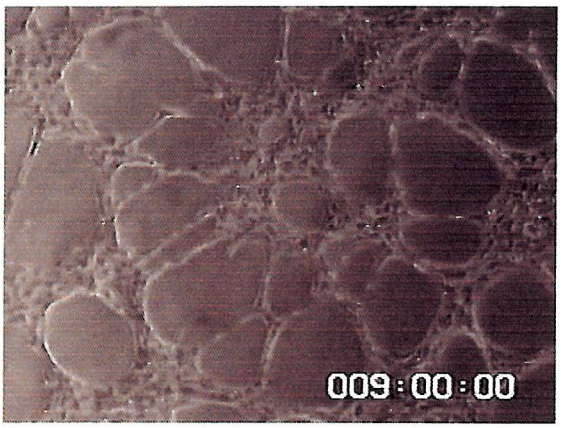
009:00:00

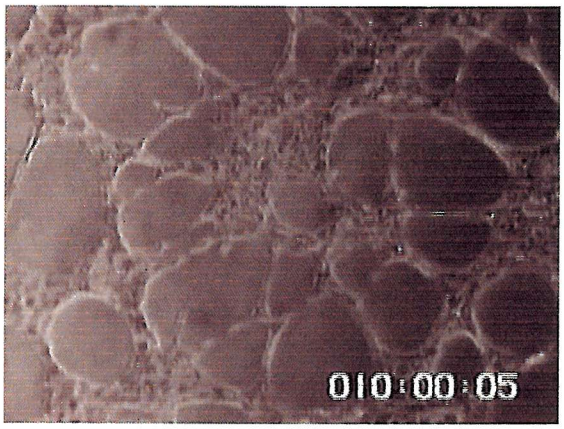
010:00:05

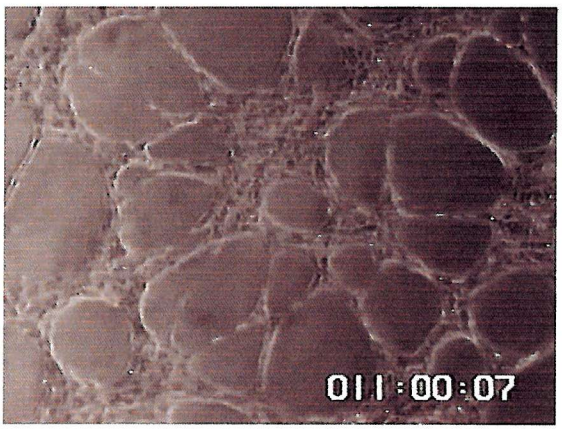
011:00:07

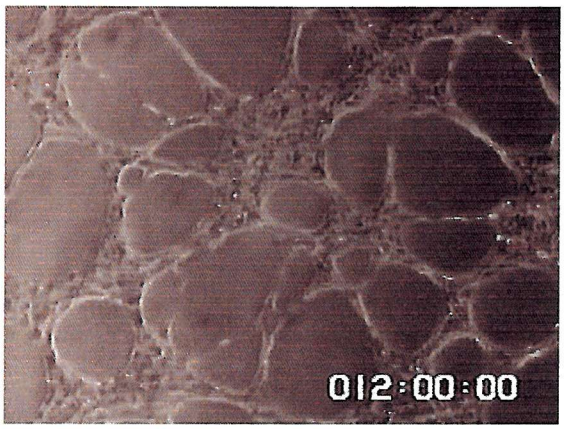
012:00:00

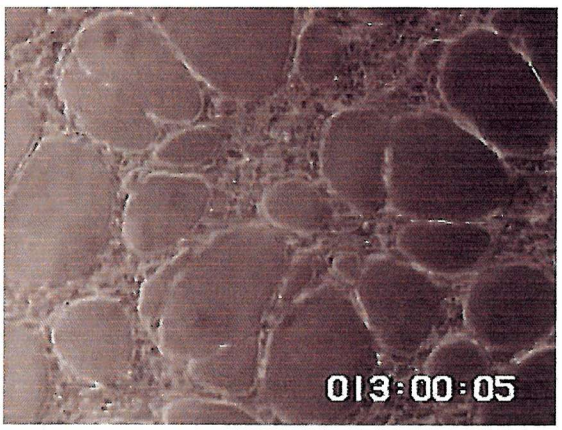
013:00:05

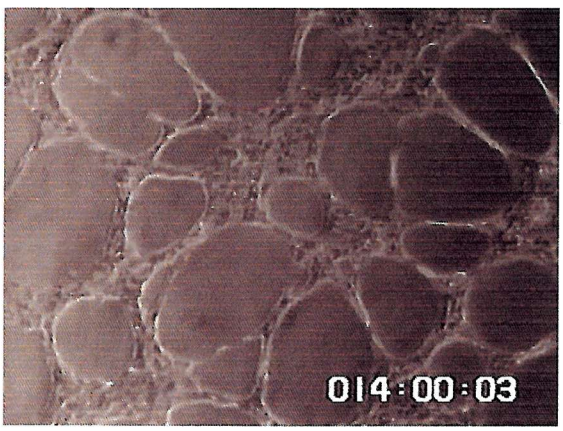
014:00:03

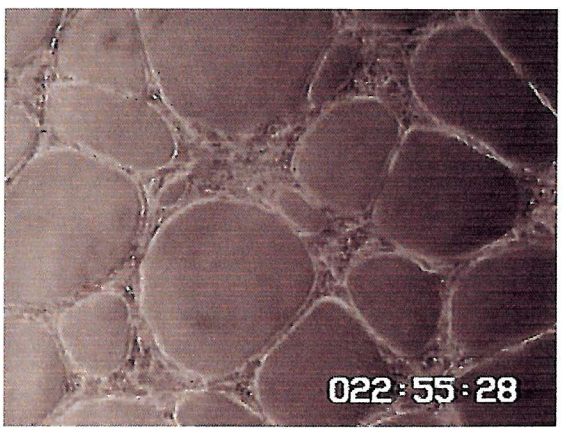
022:55:28

**Figure 5.8 Time lapse video microscopy of HOMEC capillary-like structure formation.** Frames of the time lapse video are shown at hourly intervals to show the process of capillary-like structure formation in HOMEC on Matrigel.

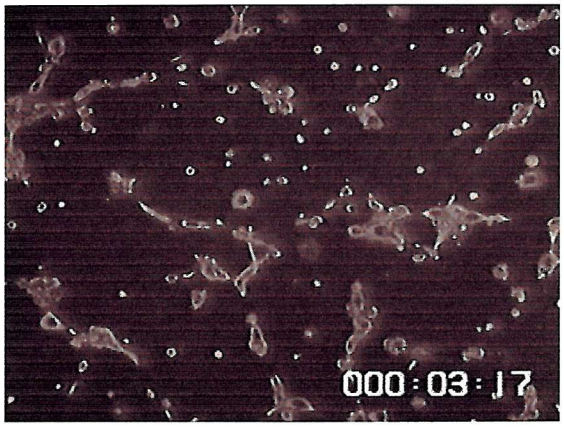
000:03:17

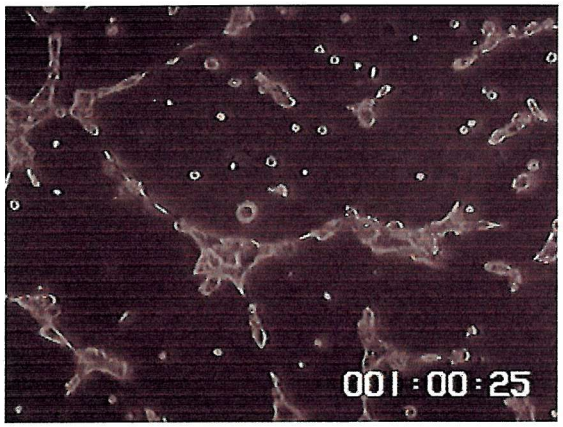
001:00:25

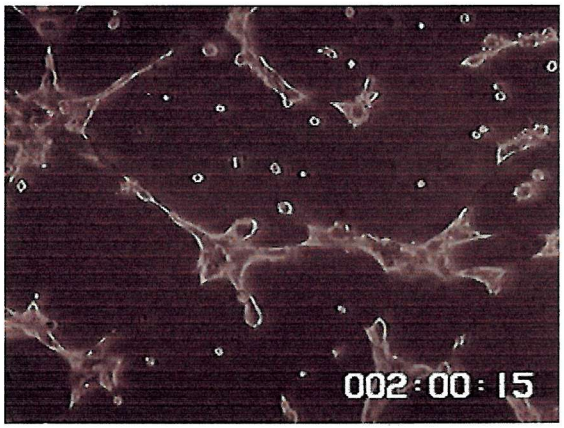
002:00:15

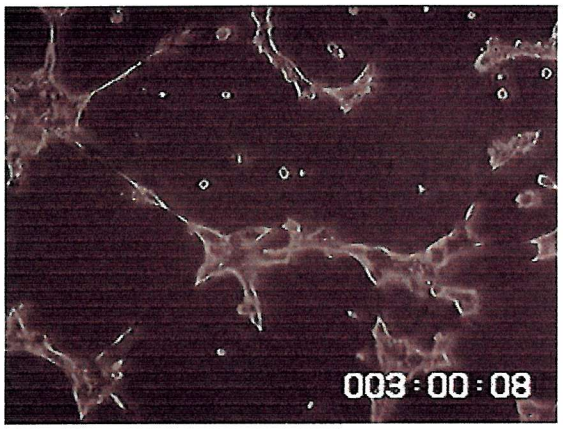
003:00:08

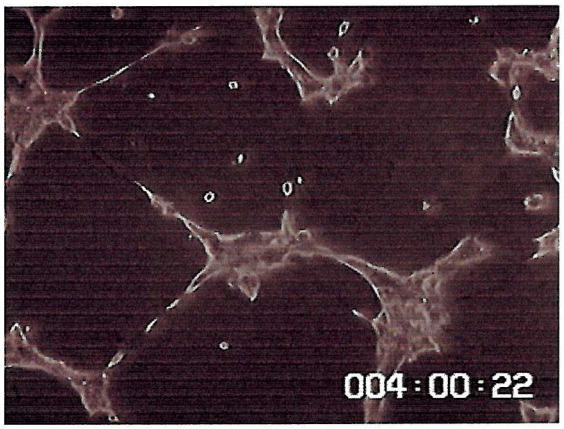
004:00:22

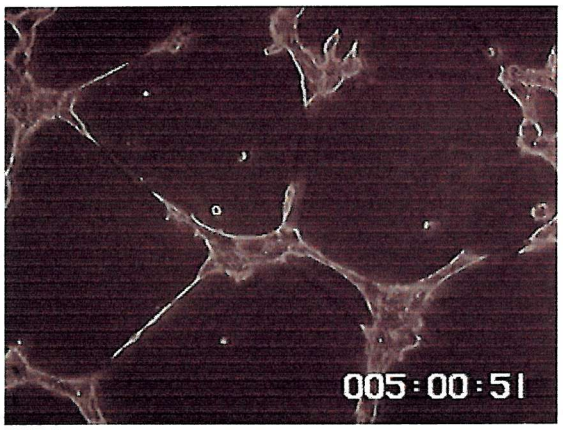
005:00:51


006:00:24


007:00:38


008:00:44


009:00:33


010:00:42

**Figure 5.9 Time lapse video microscopy of HUVEC capillary-like structure remodelling.** Frames of the time lapse video are shown at hourly intervals to show the process of capillary-like structure remodelling in HUVEC on Matrigel.

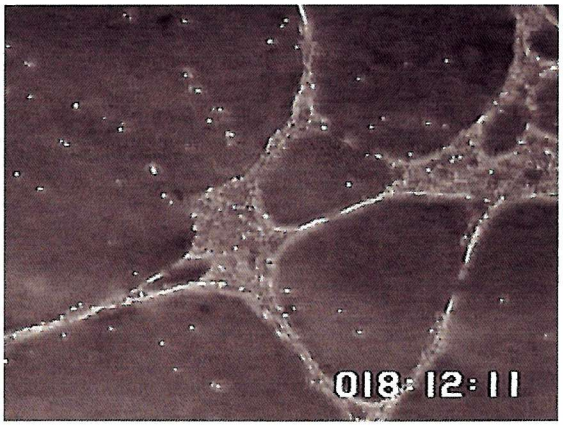
018:12:11

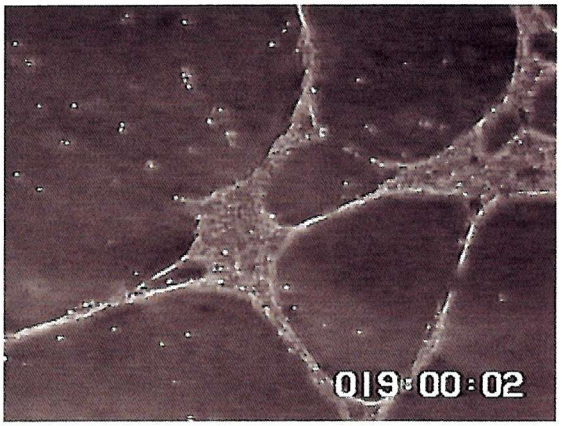
019:00:02

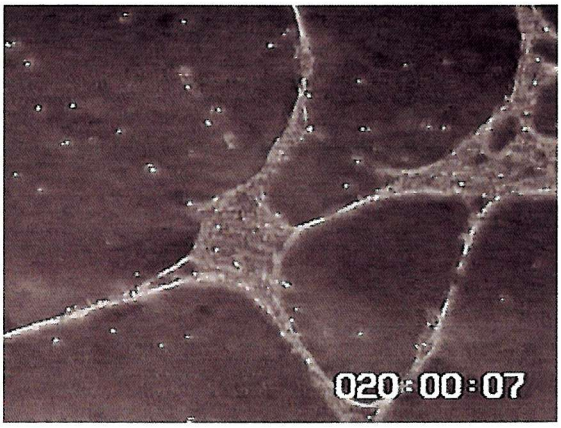
020:00:07

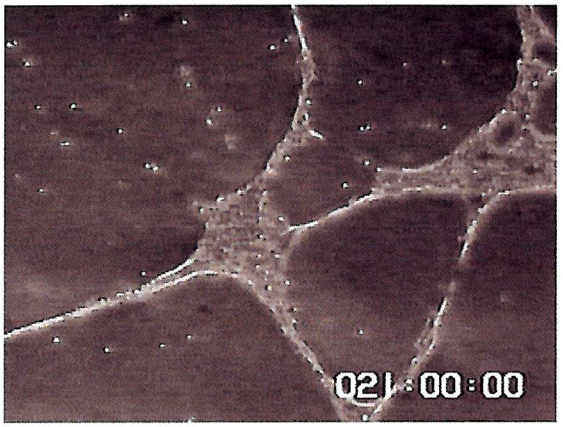
021:00:00

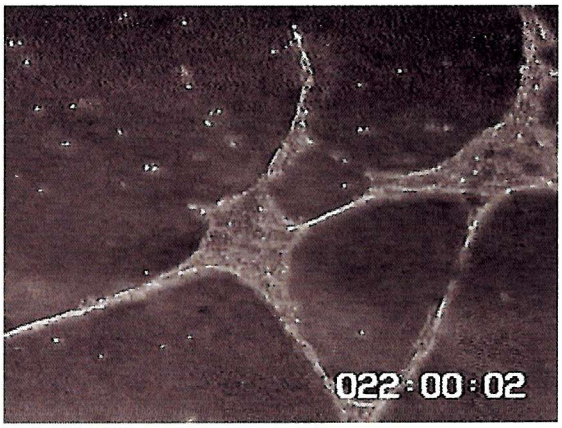
022:00:02

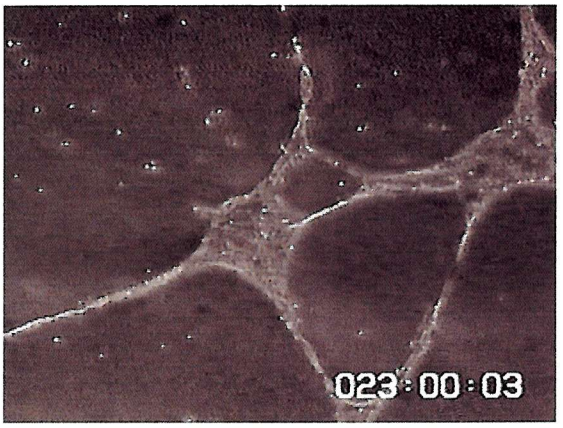
023:00:03

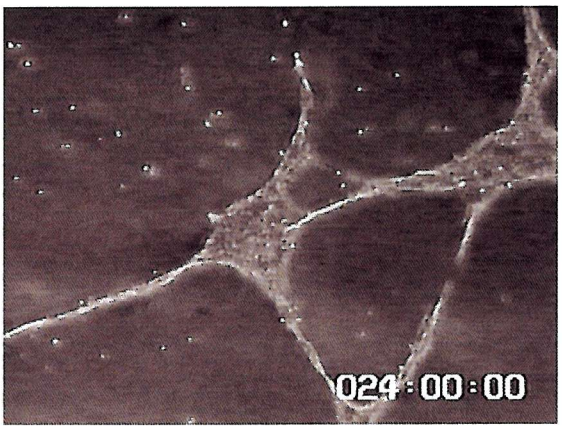
024:00:00

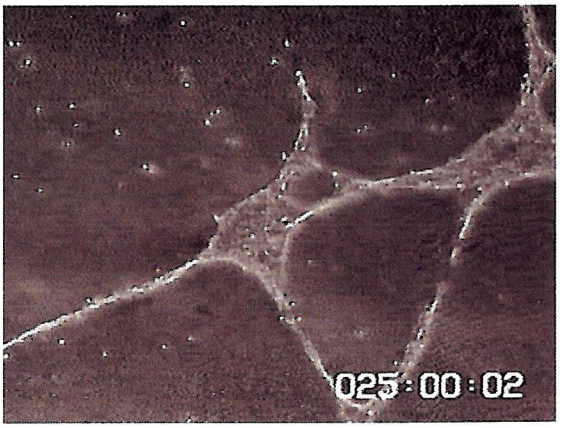
025:00:02

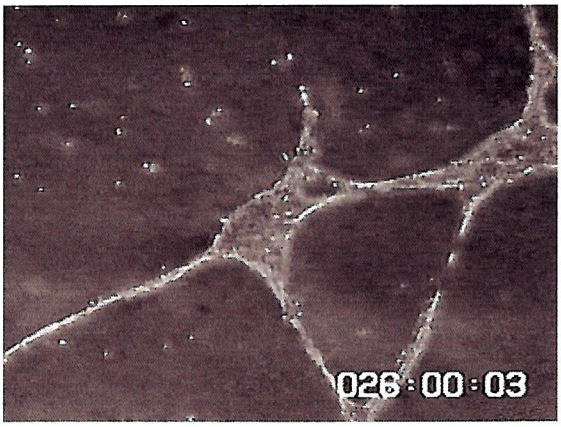
026:00:03

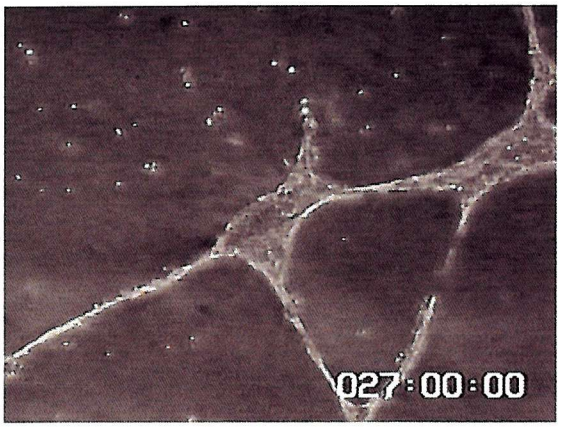
027:00:00

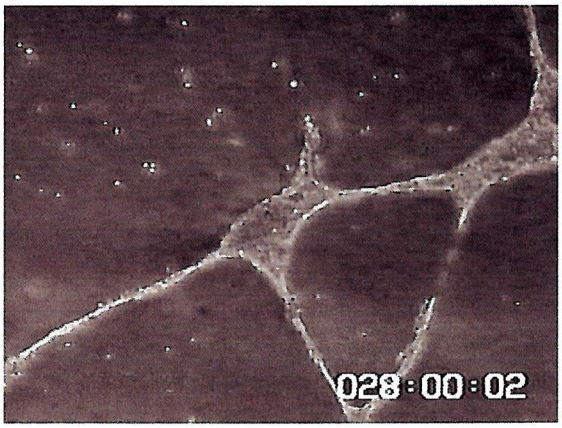
028:00:02

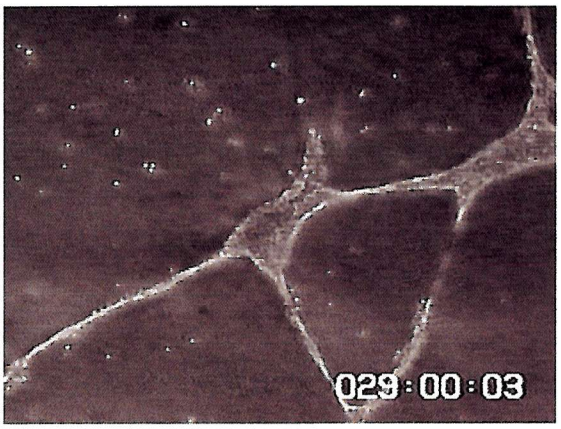
029:00:03

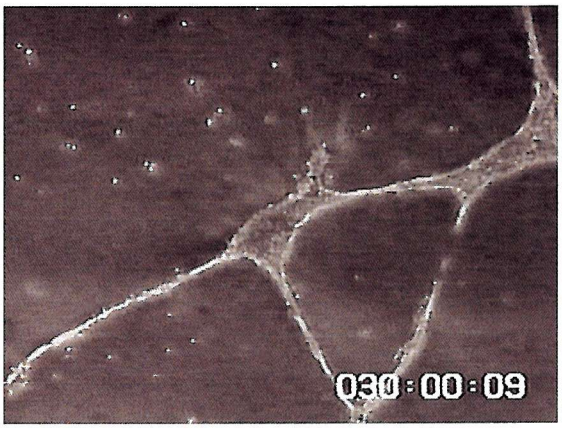
030:00:09

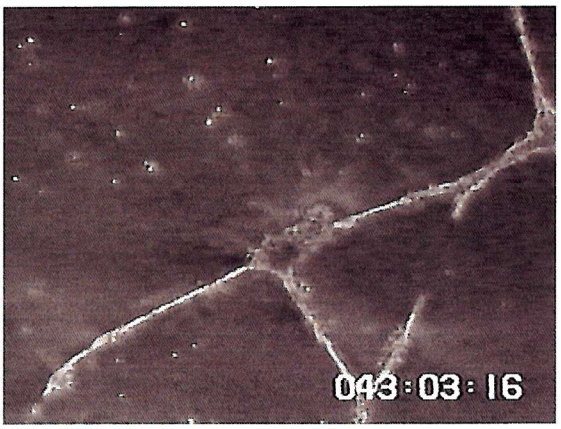
043:03:16

## Results of immunocytochemical analysis of capillary-like structures.

The major component of Matrigel is laminin, therefore immunocytochemistry was performed with an antibody to laminin beta-1 chain. The results shown in figure 5.10 show the capillary-like structures which are stained yellow/red by the propidium iodide nuclear stain. The laminin component of the Matrigel is showing as positive immunofluorescence (green) and can be clearly seen. The Matrigel was applied to the flask as a uniform layer, this layer has been remodelled during formation of the capillary-like structures and shows areas where there is no laminin left, these areas appear as black circles. Light microscopy showed that there were no gaps in the Matrigel coincident with these areas containing no laminin which suggests that only the laminin component of the Matrigel has been remodelled.

Matrigel applied to the culture surface without the addition of any cells and stained with the antibody to the laminin beta-1 chain showed a uniform distribution of laminin. There were no areas where the laminin component of Matrigel was absent as shown by c) in figure 5.10.

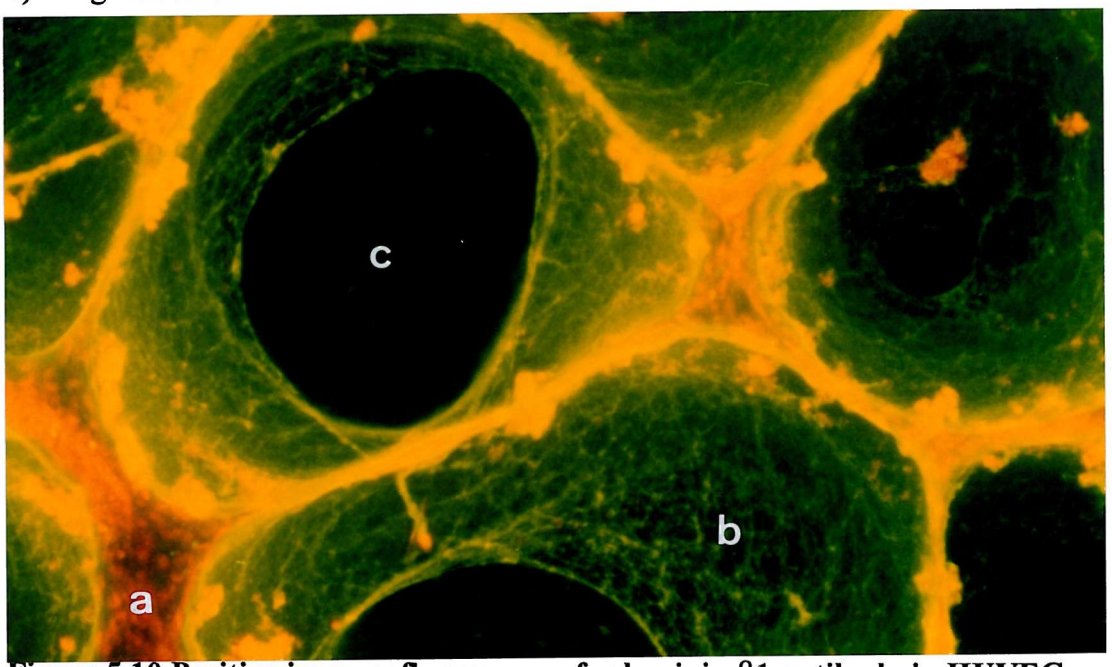


**Figure 5.10 Positive immunofluorescence for laminin β1 antibody in HUVEC capillary-like structure cultures.** Showing a) capillary-like structure stained with propidium iodide, b) positive immunofluorescence of laminin, c) area of culture where all of the laminin has been removed.

Figure 5.11 shows computed analysis from the confocal images of the laminin staining. This figure shows the capillary-like structure, represented as the black channel in the centre of the picture and the laminin as the coloured area to either side. The colours change as in a contour map with brighter colours showing areas with deeper laminin content.

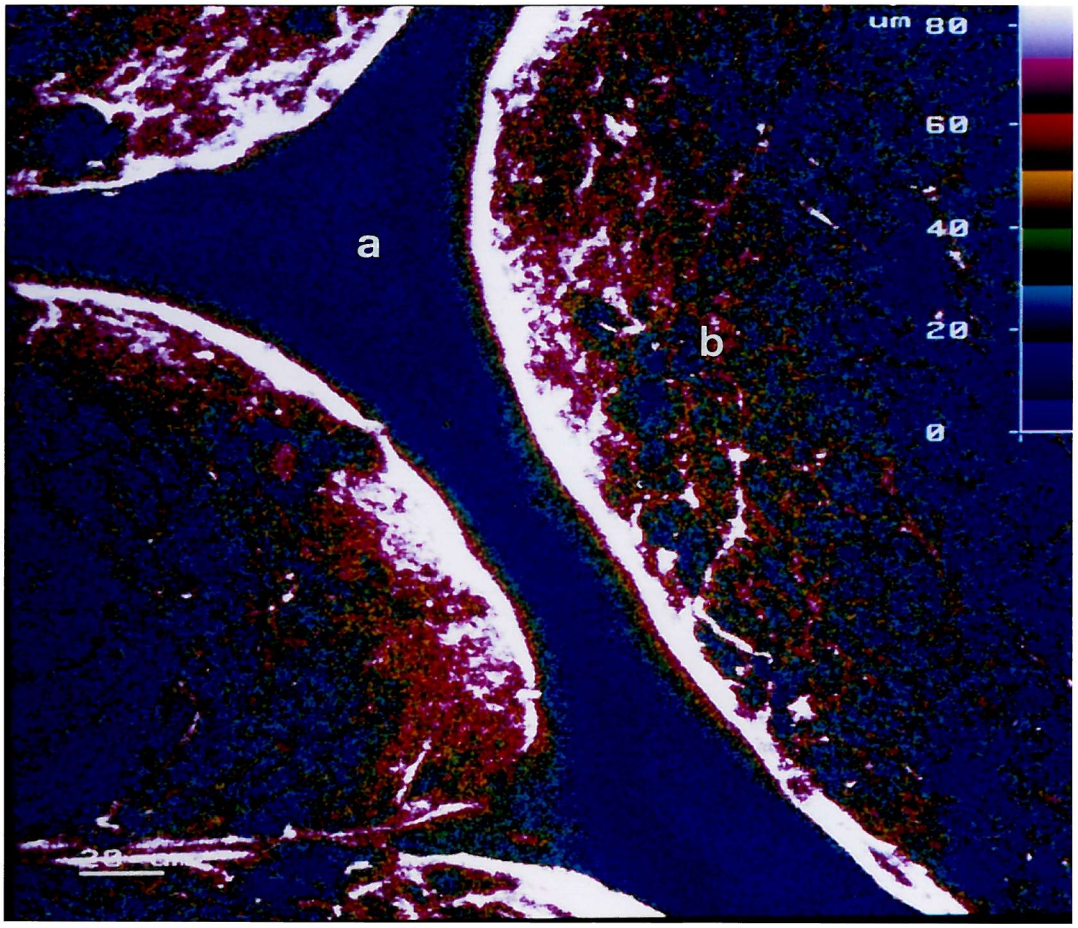


**Figure 5.11 Confocal microscopy analysis of laminin remodelling.** Showing a) HOMEC capillary-like structure, b) laminin build up at the edges of the capillary-like structure.

## 5.6 Discussion.

The results of the electron microscopy show that both HOMEC and HUVEC form capillary-like structures on Matrigel and that these possess a channel in the centre which can be compared to a lumen in capillaries *in vivo*. The cells making up these structures are very active, which is shown by the very high number of mitochondria present. The presence of desmosomes which have formed between the cells indicates that there is a degree of intercellular communication involved in the formation of these structures. The necrotic cell present in the HUVEC capillary-like structure is very interesting. Studies by Kim *et al.*, (1999) have shown very similar results to those here. They also showed the abundance of cellular organelles and intercellular junctions in endothelial cell capillary-like structures on Matrigel.

The formation of these capillary-like structures has been proposed to be mediated by interaction of adhesive proteins of endothelial cells and ECM components. Studies have shown that the pre-treatment of HUVEC with Cdw49 and CD29 beta-1 integrin antibodies inhibits the formation of significant capillary-like structures (Kubota *et al.*, 1996). CD44 antibodies also inhibit the formation of these structures (Trochan *et al.*, 1996).

The apoptosis seen when HOMEC and HUVEC were cultured on 3D collagen type I gels has also recently been observed by other groups (Ilan *et al.*, 1998; Goto *et al.*, 1998). However, confluent endothelial cells on this matrix have been shown to form capillary-like structures within 4-6 hours when overlayed with collagen type I gel (Richard *et al.*, 1998). A combination of VEGF and bFGF in the culture media has also been shown to induce capillary-like structure formation (Goto *et al.*, 1998) as has the presence of phorbol myristate acetate which also increased a transient induction of mmp-2 activity (Ilan *et al.*, 1998). The formation of capillary-like structures can also be inhibited by treatment of cultures with mmp inhibitors (Haas *et al.*, 1998) and thrombospondin-1 (Tolsma *et al.*, 1997), a naturally occurring molecule that is likely to play a key role in maintaining the quiescence of the normal vasculature (Folkman *et al.*, 1995; Bouck *et al.*, 1996).

The immunocytochemical analysis showed that the laminin component of the Matrigel

is remodelled during the formation of capillary-like structures. The computed analysis showed that the endothelial cells did not gather the laminin all around themselves as they moved because no laminin was shown to be present of the surface of the capillary-like structures as shown in figure 5.11, all of the laminin is gathered along the sides of the capillary-like structure. Rather the cells moved across the surface of the Matrigel dragging the laminin with them.

# Chapter 6.

# Granulosa cell isolation, culture and analysis of the production of VEGF in response to hCG stimulation.

## 6.1 Introduction.

Granulosa cells are one of the major cell types which make up the corpus luteum. Following ovulation the granulosa cells undergo a process of luteinisation which involves cell enlargement and increased progesterone production. Coincident with this process, the endothelial cells located in the richly vascularised theca layer begin to invade the granulosa layer to form a rich capillary network. This rapid infiltration of endothelial cells is thought to be mediated by angiogenic growth factors including VEGF, which is produced by the granulosa cells (Kamat *et al.*, 1994; Ferrara *et al.*, 1998). The release of VEGF by granulosa cells has been proposed to be stimulated by hCG, due to the central role of this hormonal stimulation in maintaining corpus luteum function.

Granulosa cells in culture have been shown to produce VEGF in response to culture with hCG (Tao *et al.*, 1995). The presence of hCG in granulosa cell cultures has also been reported to have a survival effect on the cells, with cultures containing hCG having a much longer life span. Granulosa cells cultured without gonadotrophin rapidly decrease their level of VEGF production and cell viability is greatly reduced. It has therefore been proposed that hCG acts on the cells in the same manner as *in vivo* where this hormone rescues the corpus luteum during early pregnancy, avoiding luteal regression which will occur in a non-conception cycle.

The interaction of endothelial and granulosa cells has only been studied in relation to intercellular communication through secreted factors. Spanel Borowski *et al*, (1994) showed that in co-culture, granulosa cells secreted VEGF which increased the rate of endothelial cell proliferation. However the two cell types were separated by a membrane and were not in direct contact. This co-culture model is designed to study the direct intercellular interactions between endothelial and granulosa cells.

## 6.2 Materials and methods.

### 6.2.1 Media D.

Granulosa cell cultures were maintained in Medium D which consisted of 1:1 Dulbecco's modified Eagle's medium and Hams Nutrient Mixture F12. The media were supplemented with $ITS^+$ (providing insulin at 6.23 mg/l, transferrin at 6.25 mg/l, selenious acid at 6.25 µg/l, bovine serum albumin at 1.25 g/l and linoleic acid at 5.35 mg/l), penicillin (100 units/ml), streptomycin (100 µg/ml), amphotericin B (2.5 µg/ml) and L-glutamine (2 µmol/ml), ($ITS^+$ was purchased from Stratech, Luton, UK, and all other additions were from Life Technologies, Paisley, UK).
All additions were filtered through a 0.2 µm sterile filter before addition to the media. Supplemented media was stored at 4°C and kept for no longer than 10 days following supplementation.

### 6.2.2 IVF aspirate collection.

The IVF treatment protocol and oocyte collection procedure are detailed in chapter 2, section 2.4.1.

## 6.2.3 Granulosa cell isolation.

Granulosa cells were isolated using a method which was modified from one previously described by Richardson *et al.*, 1992.

Follicular aspirates and washes were combined for each patient undergoing ovum collection for IVF. The aspirates were filtered through nylon 70 µm cell strainers (Falcon, Becton Dickinson Labware, Bedford, UK) and the filtrate collected in centrifuge tubes (Falcon, Becton Dickinson). The filtrate was centrifuged at 1200 x g for 10 minutes to collect a cell pellet consisting of blood cells, vaginal cells and steroidogenic cells. Pellets were combined for each patient and resuspended in a small amount of medium D. The resuspended cells were layered on to a mixture of, 1 ml 10 x F-12, 9 ml Percoll (Pharmacia, St. Albarn, UK) and 10 ml of medium D to separate the granulosa cells from the red blood cells. 1-4 Percoll tubes were used for each patient depending on the amount of cellular material collected for the patient. The best results were obtained when no more than 10 ml of cellular material was layered into each tube. The tubes were centrifuged for 30 min at 1200 x g. Granulosa Cells which were trapped on the interface were carefully removed with a pastette and were resuspended in fresh medium D. The cells were washed twice in medium D to remove any Percoll which would have detrimental effects in culture.

The viability of cells isolated in this way was found to be >90% by trypan blue.

## 6.2.4 Granulosa cell cluster formation on extracellular matrix.

### 6.2.4.1 Matrigel.

Wells of 8-well Lab-Tek II chamber slides (Life Technologies) were coated with 100 µl of Matrigel or growth factor reduced Matrigel (Becton Dickinson).

60,000 freshly isolated granulosa cells in suspension were added to individual wells in 500 µl final volume medium D, with additional hCG (100 ng/ml; Sigma). Cultures were incubated at 37°C in 5% $CO_2$ in air.

#### 6.2.4.2 Laminin.

Wells of 8-well Lab-Tek II chamber slides were coated with a thin layer of laminin (Becton Dickinson).

60,000 freshly isolated granulosa cells were added to individual wells in 500 µl final volume medium D, with additional hCG (100 ng/ml). Cultures were incubated at 37°C in 5% $CO_2$ in air.

#### 6.2.4.3 Collagen type I 3D gel.

Wells of 8-well Lab-Tek II chamber slides were coated with a 3D collagen type I gel (Becton Dickinson).

60,000 freshly isolated granulosa cells were added to individual wells in 500 µl final volume medium D, with additional hCG (100 ng/ml). Cultures were incubated at 37°C in 5% $CO_2$ in air.

#### 6.2.4.4 Glass.

60,000 freshly isolated granulosa cells were added to individual wells in 500 µl final volume medium D, with additional hCG (100 ng/ml). Cultures were incubated at 37°C in 5% $CO_2$ in air.

### 6.2.5 Immunocytochemistry of granulosa cell clusters on Matrigel for laminin β1 chain.

Cultures were prepared in Lab-Tek II chamber slides as detailed in section 6.2.4.1 on standard Matrigel.

Following formation of granulosa cell clusters, cultures were fixed in ice-cold methanol for 10 min and washed with PBS followed by a 30 min wash with 10% goat serum in PBS. A dilution of the primary antibody anti-laminin β1 was incubated overnight at room temperature. After 3 ten minute washes with 0.2% BSA in PBS, cultures were incubated with a fluorescein isothiocyanate conjugated secondary antibody (20 µg/ml) for 1 hour. Three further ten min washes with 0.2% BSA in PBS were followed by

incubation with the nuclear counterstain propidium iodide (0.01 mg/ml). The chamber slides were disassembled to leave the bottom surface which was mounted with moviol and imaged under ultraviolet light on a Olympus microscope. Photographs were taken with a Olympus camera using Ektachrome 400 film.

### 6.2.6 VEGF radioimmunoassay.

The assay is a competitive binding radioimmunoassay (RIA). It depends on competition between VEGF present in the sample and $^{125}$I-labelled VEGF tracer for a fixed number of binding sites on a polyclonal rabbit anti-VEGF antiserum. An anti-rabbit antibody is then allowed to react with the anti-VEGF complex. As the anti-rabbit antibody is attached to cellulose particles, the rabbit antibody-bound VEGF fraction can be separated by centrifugation of the mixture and subsequent decantation of the supernatant. The amount of $^{125}$I-labelled VEGF bound is inversely proportional to the concentration of VEGF present in the sample under investigation.

The assay was performed using the protocol described by Anthony *et al.*, 1997.
Media D, which had been incubated with granulosa cells plated on glass slides with no additional matrix and cultured in the presence of hCG was collected from several patients and combined.
Recombinant human $VEGF_{165}$, usually the most abundant form of VEGF, was used for the standard and tracer. VEGF was labelled to a specific activity of 35 mCi/mg with $^{125}$I using a modified chloramine T method of iodination. 100 µl aliquots of standard (0.2 to 50 µg/l in 5% BSA). Controls and the conditioned media were assayed with 200 µl of radioactive tracer (30,000 c.p.m. in 0.2% BSA in phosphate buffer containing 200 µg/ml heparin) and 200 µl of rabbit polyclonal antiserum (diluted 1:20,000 in 0.2% BSA in phosphate buffer). Following overnight incubation, 100 µl of Sac-cel donkey anti-rabbit coated cellulose suspension were added to all samples and standards, which were incubated for a further 30 min. 1 ml of distilled water was then added and the tubes centrifuged at 1500 x g for 15 min. After decantation, the

radioactivity of the pellets was counted and analysed by computer using the RIA-CALC, LKB-Wallac package.
No cross-reactivity was found with the closely related PIGF or bFGF. No significant interference was shown with $\alpha_2$-macroglobulin.

## 6.2.7 Affinity chromatography.

0.5 ml of VEGF antiserum (Cymbus Biotech, Chandlers Ford, Southampton, UK) was precipitated by the addition of an equal amount of a concentrated sodium sulphate solution (360 g/l in 0.05 mol/l phosphate buffer, pH 7.4). The precipitate was centrifuged at 3000 rpm for 5 min to form a pellet and the supernatant discarded. The pellet was resuspended in 5 ml of 0.1 mol/l sodium bicarbonate buffer, pH 8.3, containing 0.5 mol/l sodium chloride. The resulting solution was added to 3.5 ml of cyanogen bromide activated Sepharose 4B gel (Pharmacia, Sweden). 1 gram of the cyanogen bromide activated sepharose gel had previously been washed and swollen in 200 ml 0.001 mol/l hydrochloric acid to obtain 3.5 ml of gel.
The immunoglobulin solution was allowed to react with the gel overnight at 4°C. Following incubation, any unbound material was washed away with sodium bicarbonate coupling buffer. Remaining active groups on the gel were blocked by agitating the gel in 1 mol/l glycine buffer, pH 8.3 for 2 hours at room temperature. The gel was washed again with coupling buffer followed by 0.1 mol/l phosphate buffer pH 6.0 containing 0.5 mol/l sodium chloride. After a further wash with coupling buffer, the solid phase gel could be reacted with the granulosa cell conditioned media.
50 ml of granulosa cell conditioned media was concentrated to give a final volume of 3 ml in centrifugal filters (Millipore, Watford, UK).
A glass wool plug was inserted into the tip of a 5 ml fine capillary tipped glass pipette to make a small column. The anti-VEGF gel was shaken gently into a slurry and poured into the column. The column was washed under pressure with 100 ml of coupling buffer to pack the column tightly. The coupling buffer was replaced with 0.05

mol/l phosphate buffer, pH 7.4, by running 25 ml of phosphate buffer down the column. The immunoadsorbent was now ready for use.

The concentrated granulosa cell conditioned media was run into the column and left in the gel at room temperature overnight. The column was then washed with 100 ml of the coupling buffer. This was followed by 10 ml of 0.05 mol/l phosphate buffer, pH 6.0. 1 ml fractions of 0.1 mol/l glycine-hydrochloric acid buffer, pH 2.4, were then pipetted onto the gel and immediately forced into it by applying pressure with a teat fixed to the top of the column. Ten 0.5 ml fractions of the glycine buffer were run into the column and each 0.5 ml of solution was collected in a separate tube already containing 50 µl of 1 mol/l dipotassium hydrogen phosphate which neutralised the acid solution and gave a final pH of approximately 7.4.

Following glycine buffer elution of gel-bound products, the column was again washed with 0.05 mol/l phosphate buffer, pH 7.4, in which solution the gel was stored at 4°C for later use.

### 6.2.8 Western blotting.

SDS polyarylamide gel electrophoresis is the most popular method for estimating the size of a protein. This method of chromatography allows estimation of protein size by differential migration through the small pores of a gel matrix, smaller proteins migrating further than larger proteins. SDS binds to the proteins, disrupts their size and shape and imposes net charge densities on the proteins so the only variable determining migration is size. Comparison of the motility of an unknown protein with that of a set of standard marker proteins usually makes it possible to determine the molecular weight of the unknown. Following SDS polyacrylamide gel electrophoresis specific proteins can be identified immunochemically by western blotting. Proteins in samples are transferred from the gel in a way that retains the electrophoretic pattern, to a membrane to which the proteins bind tightly. The membrane is then treated with

specific antibodies for the protein of interest. Western blotting allows the detection of a single protein among a mass of other proteins in the sample. The protein band can be visualised in many ways one of which is the ECL-Plus western blotting system. This is a non-radioactive, chemiluminescent detection system for use with peroxidase labelled antibodies. The system is based on the enzymatic generation of an acridinium ester, which produces a signal. The combined peroxidase and peroxide catalysed oxidation of the Lumigen PS-3 acridan substrate generates thousands of acridinium ester intermediates per minute. These intermediates react with peroxide under slight alkaline conditions to produce a sustained, high intensity chemiluminescence with maximum emission at a wavelength of 430 nm.

30 µl of the sample to be tested (granulosa cell conditioned media, concentrated media and VEGF bound to the affinity chromatography column) with $VEGF_{165}$ and $VEGF_{121}$ standards were subjected to SDS-polyacrylamide gel electrophoresis using 6% resolving gels. Also run was a coloured kaleidoscope molecular weight marker (Bio-Rad, Hemel Hempstead, UK). Gels were run at 80 volts until the dye from the loading buffer had run off the end of the gel. The proteins on the gel were blotted on to polyvinylidene difluoride membranes using the Mini Trans-Blot Cell (Bio-Rad) in transfer buffer (25 mmol/l tris, 200 mmol/l glycine 20% v/v methonol). The membranes were blocked in tris-buffered saline with Tween (TBST; 0.05 mol/l tris-HCL, 0.15 mol/l NaCL, 0.1% Tween 20, pH 7.5) containing 10% dried milk powder. Blots were then exposed for 1 hour at room temperature to anti-human VEGF neutralizing antibody (1 µg/ml; R and D Systems) raised in goat, diluted in TBST containing 10% dried milk powder. After several washes in TBST the membranes were incubated with peroxide-conjugated rat anti goat secondary antibody (1:20,000 dilution; Sigma) diluted in TBST containing 10% dried milk powder. The membranes were developed using the ECL-plus system (Amersham Pharmacia Biotech, Little Chalfont, UK).

## 6.3 Results of granulosa cell cluster formation.

Granulosa cells were successfully isolated and cultured from tissue removed from the human ovary at the time of oocyte recovery. Cultures maintained with hCG in culture media were composed of large, round cells which and resembled 'bunches of grapes'. These could be maintained for over a week. The hCG appeared to have had a survival effect on the cells. Cultures without gonadotrophin undergo a form of degeneration which has not been clearly defined.

Studies looking at granulosa cell behaviour on extracellular matrices gave interesting results. Granulosa cells have the ability to form small cell clusters on Matrigel as shown in figure 6.1. which formed within 6 hours of culture. These clusters were also seen when granulosa cells were cultured on laminin, figure 6.2 and glass, figure 6.3. However, granulosa cells cultured on 3D collagen type I gels do not show this cluster formation, as shown in figure 6.4. On this matrix the granulosa cells adhered to the surface but no subsequent movement of cells was observed.

There were no apparent differences in the granulosa cell clusters forming on Matrigel or growth factor reduced Matrigel. Both formed identical clusters which could not be distinguished by light microscopy.

Although clusters formed on Matrigel, laminin and glass there were differences in the cluster formations. The clusters on Matrigel were much larger than those observed on the other matrices. The clusters were adhered to the Matrigel much more strongly than the other two matrices and the cells appeared to be clustered more tightly. Clusters could easily be dislodged from the laminin and glass surfaces and extreme care had to be taken during media changes.

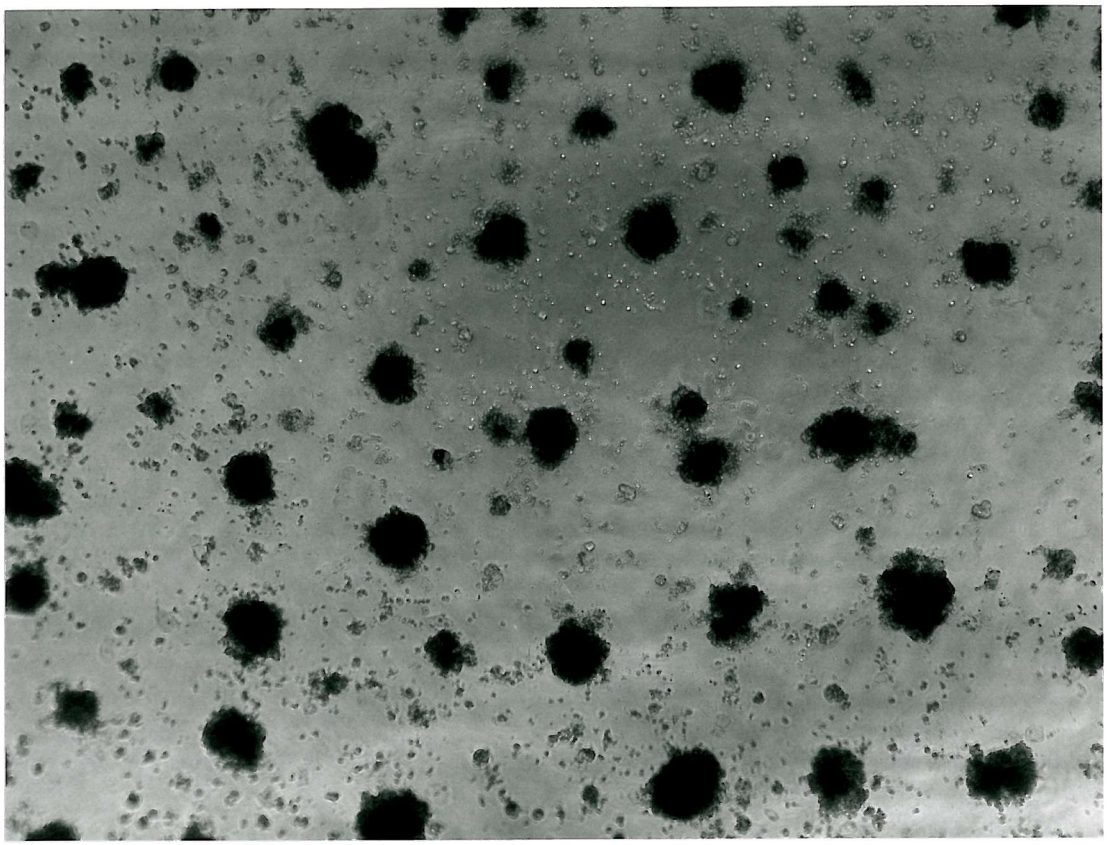

**Figure 6.1 Granulosa cell clusters on Matrigel.** Objective magnification x 4.

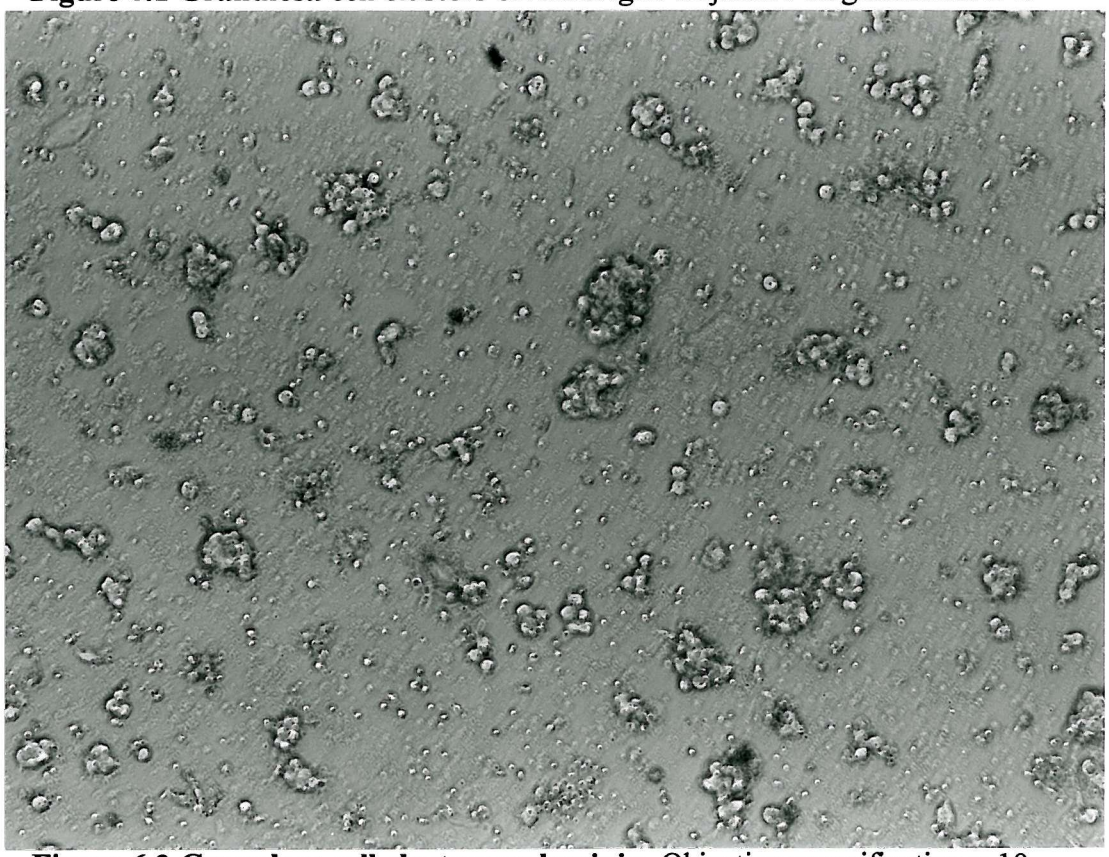

**Figure 6.2 Granulosa cell clusters on laminin.** Objective magnification x 10.

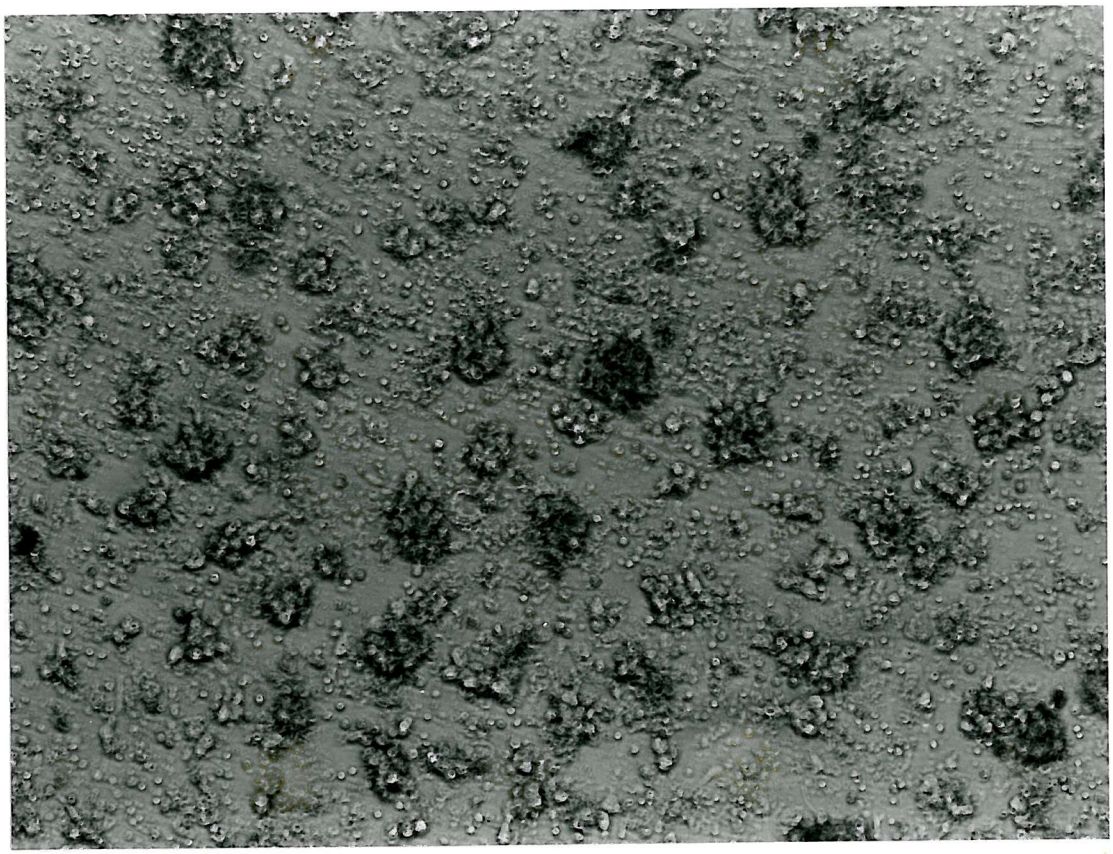

**Figure 6.3 Granulosa cell clusters on glass.** Objective magnification x 10.

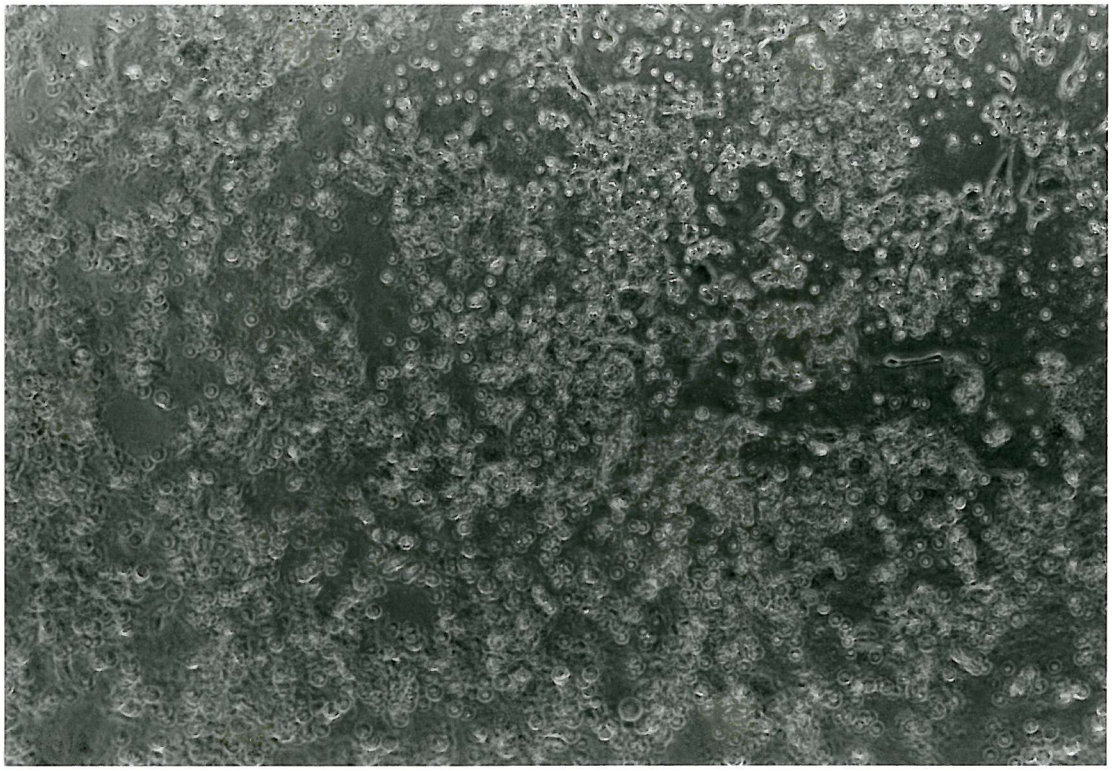

**Figure 6.4 Granulosa cells on 3D collagen type I gel.** Objective magnification x 10.

Immunocytochemical analysis for the laminin β1 antibody in cultures of granulosa cells which had clustered on Matrigel, showed that the granulosa cells appeared to gather the laminin as they moved towards each other to form clusters. Figure 6.4 shows the granulosa cells which can clearly be seen to be completely surrounded by laminin. The negative control showed no immunofluorescence.

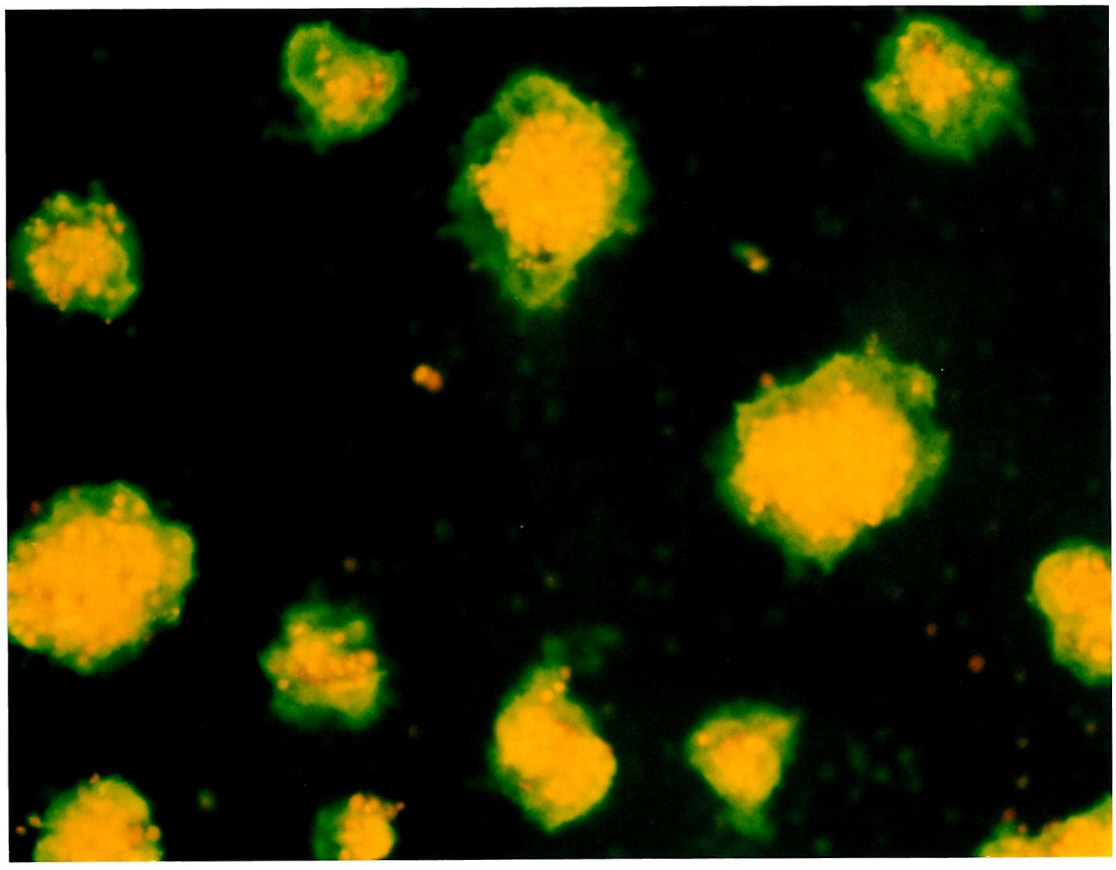

**Figure 6.5 Immunocytochemistry using the laminin β1 antibody.** Showing positive immunofluorescence for laminin β1 in granulosa cell clusters on Matrigel.

The results of the radioimmunoassay showed that granulosa cells maintained with hCG for a period of 4 days were producing detectable levels of VEGF.
Culture media from 10 different patients revealed that the average VEGF concentration produced was 10 ng/ml (ranging from 5-30 ng/ml). This included all

VEGF isoforms present as the assay did not discriminate between the different VEGF splice variants. All VEGF detected was produced by the granulosa cells as the cells were cultured on glass. Cultures on Matrigel would not have been appropriate for this study as this matrix is likely to contain VEGF due to its tumor origin which could have been released into the culture media (Boocock *et al.*, 1995).
In order to determine which VEGF isoforms were being produced by the granulosa cells, western blot analysis was performed.

The results of the western blot analysis, figure 6.5 showed that several VEGF isoforms were being produced by the granulosa cells in culture. Samples of unconcentrated media can be seen to produce both $VEGF_{165}$ and $VEGF_{121}$ but the larger isoforms are not concentrated enough to reveal bands on the gel. Attempts to concentrate the media with Ultrafree-MC Centrifugal filter units proved unsuccessful as the filters quickly became blocked and insufficient media could be concentrated.
The VEGF concentrated by affinity chromatography shows that $VEGF_{165}$ is the most abundant isoform produced by the granulosa cells. However, $VEGF_{121}$ and $VEGF_{189}$ are also both present in the media.

**Figure 6.6 Western blot analysis.** Showing the presence of VEGF isoforms produced by granulosa cells in culture. Lane 1, Synthetic $VEGF_{121}$ and $VEGF_{165}$ standards; Lanes 2-4, granulosa cell conditioned media. Lane 5, Synthetic $VEGF_{121}$ and $VEGF_{165}$ standards; Lanes 6-7 granulosa cell conditioned media; Lane 8, VEGF concentrated by affinity chromatography.

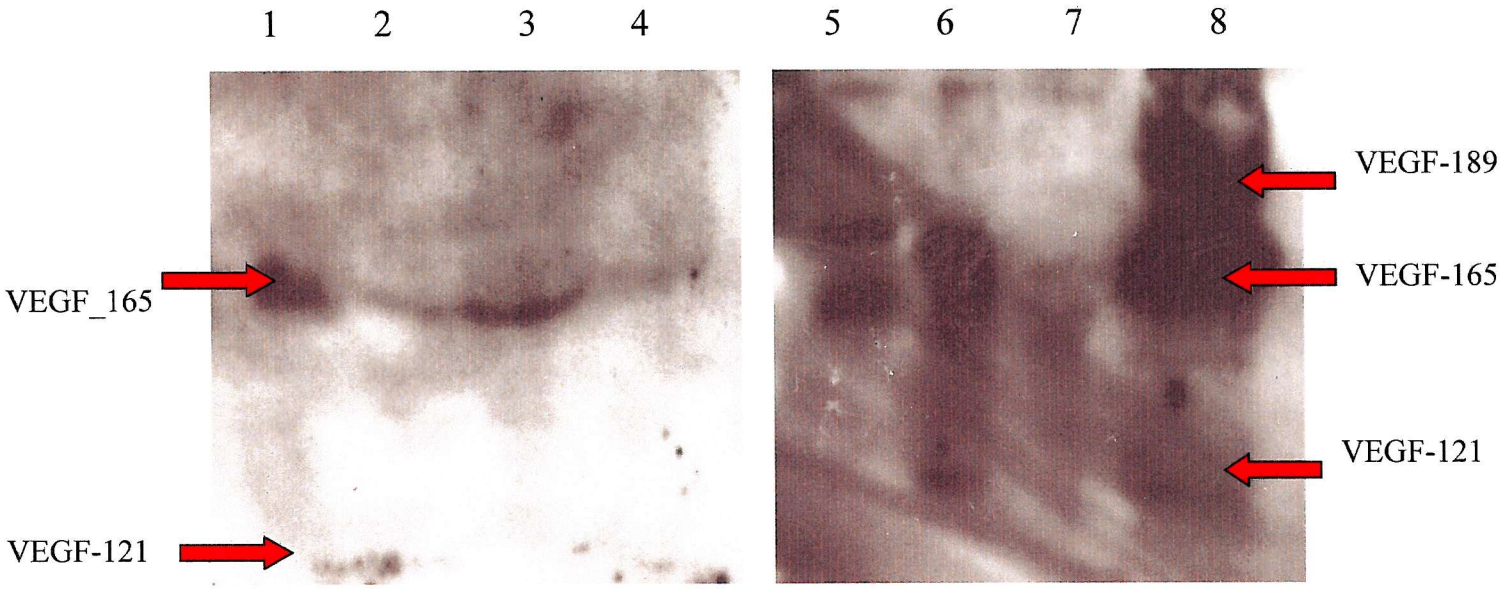
1
2
3
4
5
6
7
8
VEGF_165
VEGF-121
VEGF-189
VEGF-165
VEGF-121

## 6.4 Discussion.

The ability of granulosa cells to form clusters on extracellular matrix is an interesting feature of this cell type. The cluster formation has been shown to involve matrix remodelling as shown by the immunocytochemical analysis for the laminin β1 antibody on cultures on Matrigel. The granulosa cells appear to form the clusters by rolling across the surface of the Matrigel and gathering the laminin component with them. Recently it has been shown that granulosa cells in culture actually synthesise their own laminin (Richardson *et al.*, 1999). In the present study however, the laminin can be assumed to be from the Matrigel due to the short incubation time and the amount of laminin surrounding the granulosa cell clusters.

A recent report by Neulen *et al.*, 1998 has shown that granulosa cells obtained at oocyte recovery following IVF treatment express VEGF mRNA as part of an hCG mediated effect in culture. We have shown the presence of the VEGF protein with radioimmunoassay and that various VEGF isoforms are produced by the granulosa cells as shown by western blotting analysis. The major isoform is $VEGF_{165}$, then lower levels of $VEGF_{121}$ and $VEGF_{189}$.

# Chapter 7.

# Endothelial cell proliferation in response to VEGF, bFGF, VEGF receptor blocking antibodies and nitric oxide inhibitors.

## 7.1 Introduction.

As previously stated, VEGF has been shown to be a potent endothelial cell mitogen. VEGF is produced locally in the corpus luteum to stimulate the invasion of endothelial cells into the avascular granulosa layer (Kamat *et al.*, 1995).

VEGF is not the only endothelial cell mitogen, bFGF also has a mitogenic effect as do other numerous growth factors. bFGF has also been demonstrated to be produced by the granulosa cells during the formation of the corpus luteum (Doraiswamy *et al.*, 1998). However, VEGF is thought to be more specific for endothelial cells, but there are in fact synergistic effects between bFGF and VEGF (Yoshida *et al.*, 1996).

The mitogenic effects of VEGF on endothelial cells have in some circumstances been shown to be coupled to nitric oxide (NO) production (Papapetropoulos *et al.*, 1997). NO is produced mainly in endothelial cells through the endothelial NO synthase (eNOS) constitutively expressed in endothelial cells, which catalyses the conversion of L-arginine to L-citrulline. eNOS is calcium dependent and is mediated by calmodulin. VEGF has been shown to increase cytosolic calcium which promotes calmodulin binding. Therefore by inhibiting nitric oxide with inhibitors such as $N^{\omega}$-nitro-L-arginine methyl ester (L-NAME) it has been proposed that the mitogenic effect of VEGF can be blocked (Morbidelli *et al.*, 1996). Also it is thought that the KDR receptor is involved with cellular proliferation whilst flt-1 is involved with structure formation (Seetharam *et al.*, 1995; Waltenberger *et al.*, 1994). The use of blocking antibodies for

these receptors could demonstrate which receptor is involved with proliferation and if the proliferative effects of granulosa cell conditioned media are likely to be due to VEGF present in the media.

## 7.2 CellTitre 96 $Aq_{ueous}$ Non-Radioactive Cell Proliferation Assay.

The response of endothelial cells to various mitogenic substances was measured using a CellTitre 96 $Aq_{ueous}$ Non-Radioactive Cell Proliferation Assay. This is a colorimetric method for determining the number of viable cells in proliferation assays.

The advantages of this assay are;

1) **Non-radioactive**: requires no scintillation cocktail or radioactive waste disposal.

2) **Fast**: the assay can be performed in a 96 well plate with no plate washing or cell harvesting. The solubilisation step required with other reagents such as MTT are not needed because the MTS formazan product is soluble in tissue culture medium.

3) **Safe**: requires no volatile organic solvent to solubilize the formazan product (unlike MTT). The formazan product of MTT reduction is a crystalline precipitate that requires an additional step in the procedure to dissolve the crystals before recording absorbance readings at 570 nm.

4) **Convenient**: supplied as ready-to-use stable, frozen sterile solutions (unlike XTT). XTT, commonly used in cell proliferation assays, is a tetrazolium compound similar to MTS which is bioreduced into an aqueous soluble formazan product. Unlike MTS, XTT has limited solubility and is not stable in solution. Procedures using XTT require daily preparation of fresh solutions whereas MTS is a filter-sterilized solution in physiological buffered saline ready for use.

5) **Flexible**: plates can be read and returned to incubator for further colour development (unlike MTT).

The assay is composed of solutions of a novel tetrazolium compound (3-(4,5-dimethylthiazol-2-yl)-5-(3-carboxymethoxyphenyl)-2-(4-sulfophenyl)-2H-tetrazolium, inner salt: MTS) and an electron coupling reagent (phenazine methosulphate; PMS). MTS (Owen's reagent) is bioreduced by cells into a formazan that is soluble in tissue culture medium. The absorbance of the formazan at 490 nm can be measured directly from 96 well plates without additional processing. The conversion of MTS into the aqueous soluble formazan is accomplished by dehydrogenase enzymes found in metabolically active cells. The quantity of formazan product is directly proportional to the number of cells living in culture.

Figure 7.1 shows the structures of MTS tetrazolium and its formazan product.

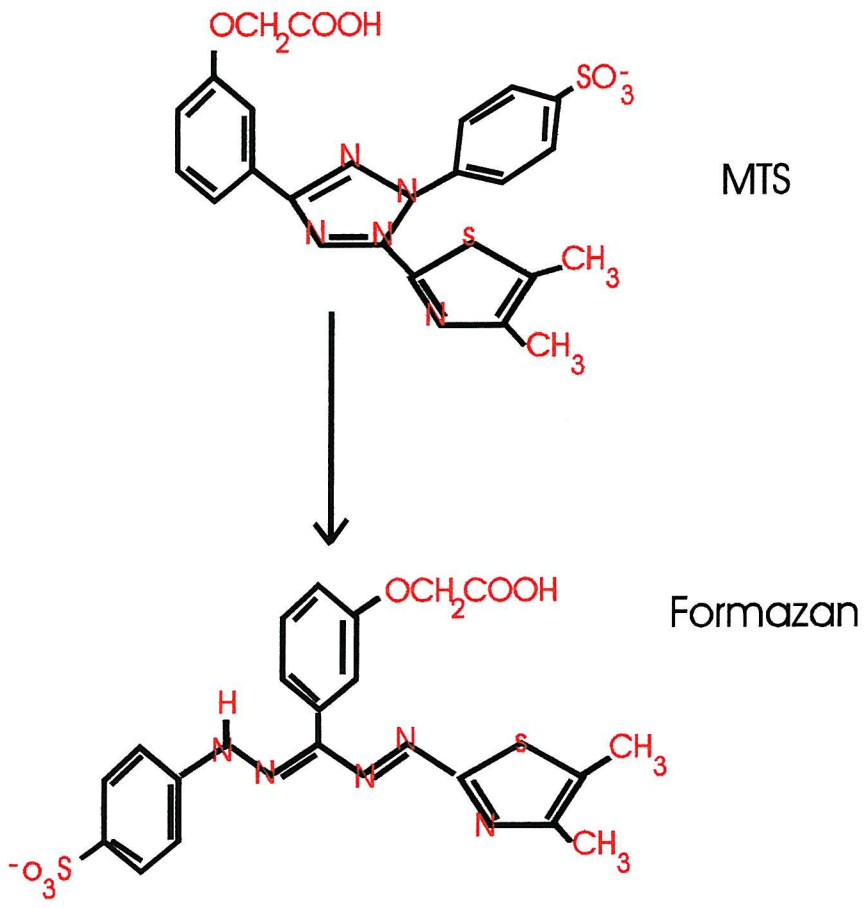


**Figure 7.1 Conversion of MTS into formazan** by the dehydrogenase enzyme in metabolically active cells.

## 7.3 Materials and methods.

### 7.3.1 Cell culture.

HOMEC and HUVEC were cultured as described in chapter 2 sections 2.4.3 and 2.4.8.

All cells in this assay were maintained in a basic Media 199 without phenol red supplemented with 10% fetal calf serum (heat inactivated), penicillin (100 units/ml), streptomycin (100 µg/ml), amphotericin B (2.5 µg/ml) and L-glutamine (2 µmol/ml). Any other supplements added to specific cultures are detailed in the relevant section. All additions were sterile filtered through a 0.44 µm sterile filter followed by a 0.22 µm sterile filter (Sartorius AG, Goettingen, Germany) before addition to the Media. Supplemented media was stored at 4°C and kept for no longer than 10 days following supplementation.

### 7.3.2 Cell proliferation assay.

10,000 HOMEC or HUVEC were added to wells of 96 well plates and incubated in 100 µl of M199. The 96 well plates had no gelatin coating or other matrix and were used as purchased (Falcon, Becton Dickinson Labware). 100 µl of the appropriate mitogenic solution (all reactions were performed in triplicate) was added to each well and the cells incubated at 37°C in 5% $CO_2$ in air for 96 hours.

Following 96 hours of incubation media were removed from each well and 100 µl of fresh M199 without phenol red was added to each well. 20 µl of PMS/MTS solution was added to each well and incubated at 37°C in 5% $CO_2$ in air for 3 hours to allow the colorometric change. Plates were read in an MRX Microplate reader (DYNEX Technologies, West Sussex, UK) and analysis of results was performed with Endpoint computer software.

## 7.3.3 Mitogenic solution preparation.

### 7.3.3.1 VEGF.

VEGF serial dilutions were prepared by the addition of VEGF in 0.1% BSA to M199 without phenol red to give a VEGF solution of 200 ng/ml. This solution was double diluted with M199 without phenol red to give a range of VEGF solutions that had final VEGF concentrations of;

| | |
|---|---|
| V6 | 100 ng/ml |
| V5 | 50 ng/ml |
| V4 | 25 ng/ml |
| V3 | 12.5 ng/ml |
| V2 | 6.25 ng/ml |
| V1 | 3.125 ng/ml |
| V0 | 0 ng/ml |

### 7.3.3.2 Granulosa cell conditioned media.

Granulosa cell conditioned media were collected from cultures with no added extracellular matrix and was sterile filtered through a 0.44 μM filter. The concentration of VEGF was detected by radioimmunoassay as described in section 6.2.6. For the experiment below the concentration was found to be 29.6 ng/ml. Serial dilutions were prepared by double dilution with M199 without phenol red to give a range of solutions that had final VEGF concentrations of;

| | |
|---|---|
| G6 | 14.8 ng/ml |
| G5 | 7.4 ng/ml |
| G4 | 3.7 ng/ml |
| G3 | 1.9 ng/ml |
| G2 | 0.9 ng/ml |
| G1 | 0.46 ng/ml |
| G0 | 0 ng/ml |

### 7.3.3.3 bFGF.

bFGF serial dilutions were prepared by the addition of bFGF in 0.1% BSA to M199 without phenol red to give a bFGF solution of 5 ng/ml. This solution was double diluted with M199 without phenol red to give a range of bFGF solutions that had final bFGF concentrations of;

| | |
|---|---|
| F6 | 2.50 ng/ml |
| F5 | 1.25 ng/ml |
| F4 | 0.62 ng/ml |
| F3 | 0.31 ng/ml |
| F2 | 0.15 ng/ml |
| F1 | 0.078 ng/ml |
| F0 | 0 ng/ml |

### 7.3.3.4 ECGS.

ECGS serial dilutions were prepared by the addition of ECGS to M199 without phenol red to give an ECGS solution of 1000 μg/ml. This solution was double diluted with M199 without phenol red to give a range of ECGS solutions that had a final concentration of;

| | |
|---|---|
| E6 | 500 μg/ml |
| E5 | 250 μg/ml |
| E4 | 125 μg/ml |
| E3 | 62.5 μg/ml |
| E2 | 31.3 μg/ml |
| E2 | 15.6 μg/ml |
| E1 | 0 μg/ml |

**7.3.3.5 $N^{\omega}$-nitro-L-arginine methyl ester.**

1) A stock solution of L-NAME was prepared (1000 μM). Dilutions were prepared by dilution with M199 (containing 12.5 ng/ml VEGF) without phenol red to give a range of L-NAME solutions with standard VEGF that had final concentrations of;

L6 500 μM L-NAME, 6.25 ng/ml VEGF

L5 250 μM L-NAME, 6.25 ng/ml VEGF

L4 200 μM L-NAME, 6.25 ng/ml VEGF

L3 150 μM L-NAME, 6.25 ng/ml VEGF

L2 100 μM L-NAME, 6.25 ng/ml VEGF

L1 50 μM L-NAME, 6.25 ng/ml VEGF

L0 0 μM L-NAME, 6.25 ng/ml VEGF

2) A stock solution of L-NAME was prepared (1000 μM) in M199. VEGF serial dilutions were prepared by the addition of VEGF in 0.1% BSA to M199 (1000 μM L-name) without phenol red to give a VEGF solution of 200 ng/ml. This solution was double diluted with M199 (1000 μM L-name) without phenol red to give a range of VEGF solutions that had final concentrations of;

V6 100 ng/ml VEGF, 500 μM L-NAME

V5 50 ng/ml VEGF, 500 μM L-NAME

V4 25 ng/ml VEGF, 500 μM L-NAME

V3 12.5 ng/ml VEGF, 500 μM L-NAME

V2 6.25 ng/ml VEGF, 500 μM L-NAME

V1 3.125 ng/ml VEGF, 500 μM L-NAME

V0 0 ng/ml VEGF, 500 μM L-NAME

### 7.3.3.6 Anti-VEGF neutralising antibody.

An anti-VEGF neutralising antibody (R and D systems) solution was prepared (2 µg/ml), 50 µl of this solution was incubated with 10,000 endothelial cells in 50 µl of M199 without phenol red in 96 well plates overnight at 37°C in 5% $CO_2$ in air. Following incubation VEGF serial dilutions were added as described in section 7.3.3.1.

### 7.3.3.7 Increasing anti-KDR antibody, constant VEGF.

A stock solution of anti-KDR monoclonal antibody was prepared (1000 ng/ml; sc-315; Santa Cruz Biotechnology, Inc., California, USA) in M199 (containing 25 ng/ml VEGF) without phenol red. Dilutions were prepared by dilution with M199 (containing 25 ng/ml VEGF) to give a range of anti-KDR solutions with standard VEGF that had final concentrations of;

| | |
|---|---|
| K6 | 500 ng/ml anti-KDR, 6.25 ng/ml VEGF |
| K5 | 200 ng/ml anti-KDR, 6.25 ng/ml VEGF |
| K4 | 150 ng/ml anti-KDR, 6.25 ng/ml VEGF |
| K3 | 100 ng/ml anti-KDR, 6.25 ng/ml VEGF |
| K2 | 50 ng/ml anti-KDR, 6.25 ng/ml VEGF |
| K1 | 0 ng/ml anti-KDR, 6.25 ng/ml VEGF |

### 7.3.3.8 Anti-KDR antibody, increasing VEGF.

An anti-KDR monoclonal antibody (200 ng/ml) solution was made up in M199, 50 µl of this solution was incubated with 10,000 endothelial cells in 50 µl of M199 without phenol red in 96 well plates overnight at 37°C in 5% $CO_2$ in air. Following incubation VEGF serial dilutions were added as described in section 7.3.3.1.

#### 7.3.3.9 Increasing anti-flt-1 antibody, constant VEGF.

A stock solution of anti-flt-1 monoclonal antibody was prepared (1000 ng/ml; sc-316; Santa Cruz Biotechnology, Inc., California, USA) in M199 (containing 25 ng/ml VEGF) without phenol red. Dilutions were prepared by dilution with M199 (containing 25 ng/ml VEGF) to give a range of anti-flt-1 solutions with standard VEGF that had final concentrations of;

| | |
|---|---|
| F6 | 500 ng/ml anti-flt-1, 6.25 ng/ml VEGF |
| F5 | 200 ng/ml anti-flt-1, 6.25 ng/ml VEGF |
| F4 | 150 ng/ml anti-flt-1, 6.25 ng/ml VEGF |
| F3 | 100 ng/ml anti-flt-1, 6.25 ng/ml VEGF |
| F2 | 50 ng/ml anti-flt-1, 6.25 ng/ml VEGF |
| F1 | 0 ng/ml anti-flt-1, 6.25 ng/ml VEGF |

#### 7.3.3.10 Anti-flt-1 antibody.

An anti-flt-1 monoclonal antibody (200 ng/ml) solution was made up in M199, 50 µl of this solution was incubated with 10,000 endothelial cells in 50 µl of M199 without phenol red in 96 well plates overnight at 37°C in 5% $CO_2$ in air. Following incubation VEGF serial dilutions were added as described in section 7.3.3.1.

### 7.3.4 Statistical Analysis.

The results that are shown are representative of analysis of three independent cell cultures for HUVEC and two independent cell cultures for HOMEC. Each determination was performed in triplicate (ie. n=3). P value represents the significance value determined in the single experiment shown. Significance value was determined using one-way analysis of variance technique using InStat computer software.

## 7.4 Results of cell proliferation assays.

The results of the cellular proliferation assay showed that VEGF stimulates an increase in the rate of endothelial cell proliferation. Both HOMEC and HUVEC responded by increased cellular proliferation in the presence of VEGF. Figure 7.2 shows the effect of a series of VEGF dilutions on HOMEC proliferation. Without the presence of VEGF the number of cells had doubled as expected (approximately $20x10^3$ cells at 0 ng/ml VEGF). The cell number actually shows a slightly higher number of cells than a doubling of the originally plated number ($10x10^3$ cells). The standard curve generated for conversion of the measured optical density into cell number was performed on a different day to the proliferation assay for practical reasons and therefore the precise evaluation of cell number may not be absolutely correct. Figure 7.2 shows that up to a concentration of 12.5 ng/ml VEGF there is an increase in the rate of HOMEC proliferation, from this concentration the rate of proliferation is sustained but no further increase in rate is seen. This data shows that the $ED_{50}$ of VEGF is ~6.25 ng/ml which corresponds to the manufactures guidelines for HUVEC. Statistical analysis of all of the VEGF concentrations showed the P value to be $< 0.0001$ which is considered to be extremely significant (analysis of variance).

Figure 7.3 shows that the HUVEC response to VEGF is very similar to that of HOMEC. VEGF increased the rate of cell proliferation up to a concentration of 12.5 ng/ml and the $ED_{50}$ of VEGF is ~6.25 ng/ml. Again, statistical analysis of the data revealed a P value of $< 0.0001$ which is considered highly significant.

Figure 7.4 shows that granulosa cell conditioned media increases the rate of HUVEC proliferation. VEGF was shown to be present in the granulosa cell conditioned media as detailed in chapter 6. The percentage increase in cell number is very similar to that seen with the synthetic $VEGF_{165}$, with a P value of $< 0.0001$.

An interesting finding of using granulosa cell conditioned media to stimulate endothelial cell proliferation, was that if the media was incubated for over five days with the granulosa cells it had an anti-mitogenic effect on endothelial cells, probably caused by inhibitors and toxic products accumulating in the media.

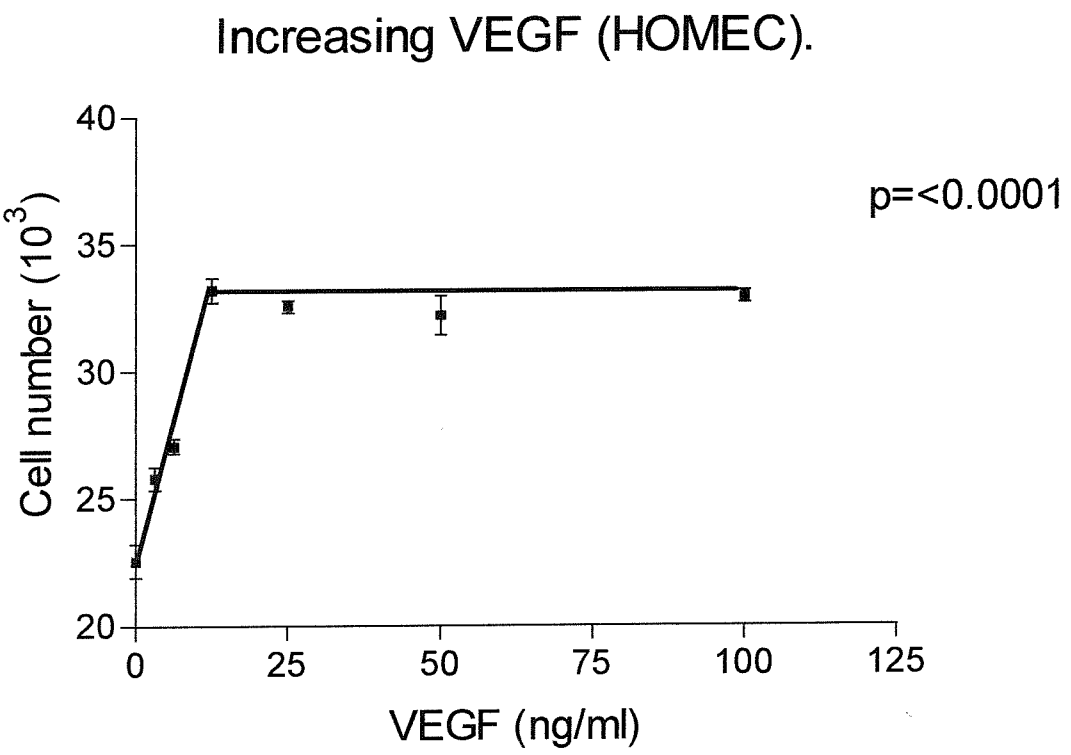


**Figure 7.2 VEGF mediated HOMEC proliferation.** A significant increase in HOMEC proliferation in response to increasing concentrations of VEGF is shown (triplicate determination at each concentration, mean +/- SEM; analysis of variance, $p < 0.0001$).

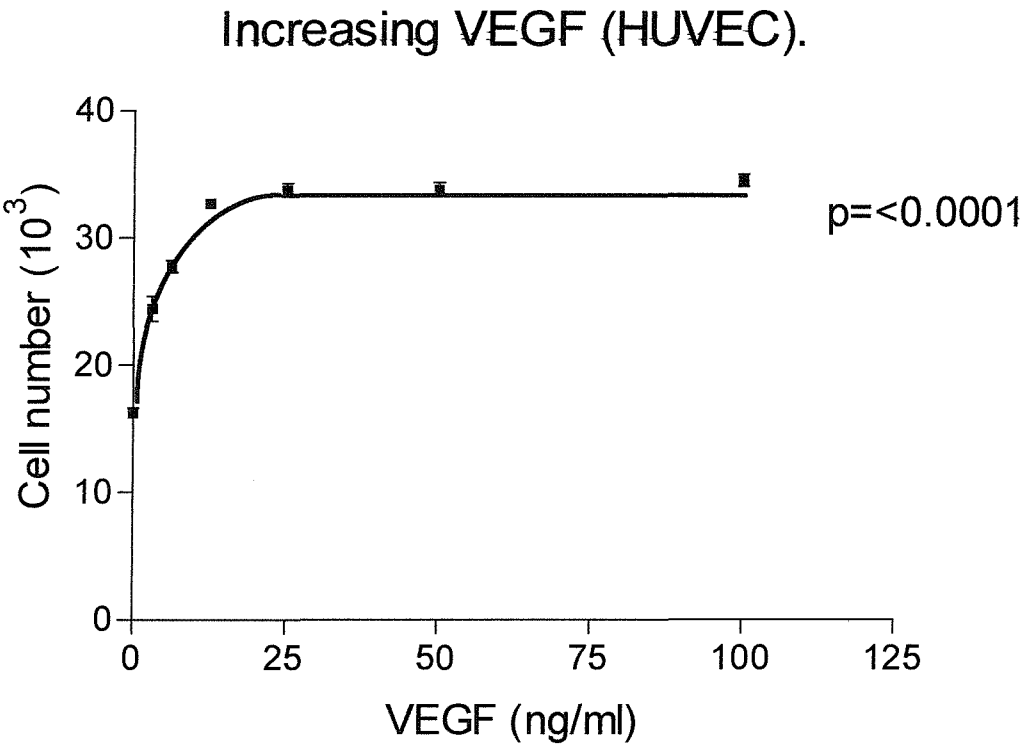


**Figure 7.3 VEGF mediated HUVEC proliferation.** A significant increase in HUVEC proliferation in response to increasing concentrations of VEGF is shown (triplicate determination at each concentration, mean +/- SEM; analysis of variance, $p < 0.0001$).

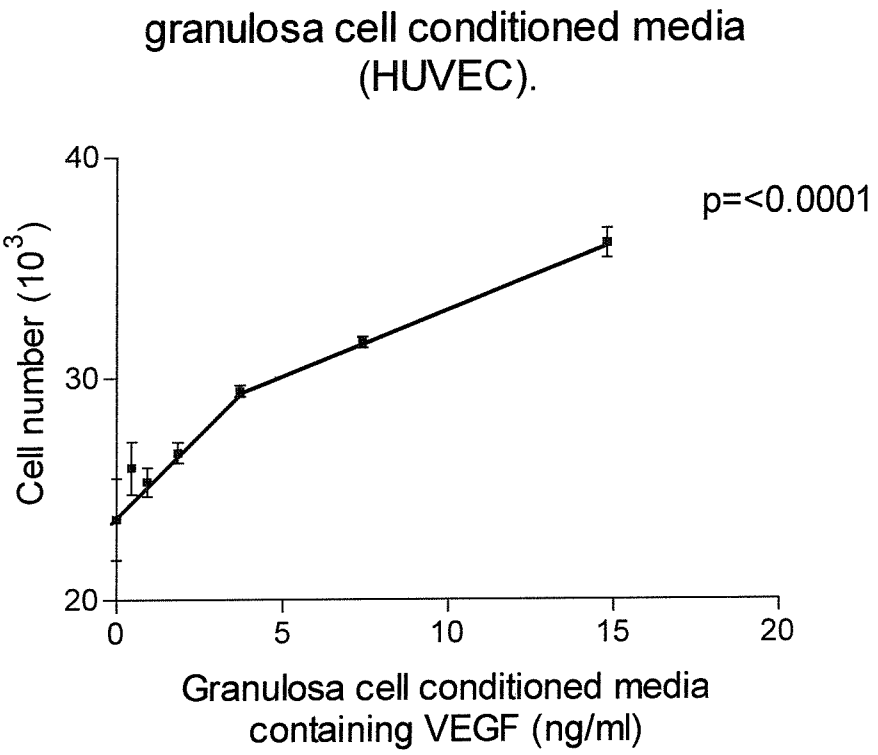


**Figure 7.4 VEGF/granulosa cell conditioned media mediated HUVEC proliferation.** A significant increase in HUVEC proliferation in response to increasing concentrations of VEGF in granulosa cell conditioned media is shown (triplicate determination at each concentration, mean +/- SEM; analysis of variance, $p < 0.0001$). Figure 7.5 shows that the HUVEC response to ECGS is similar to that seen with

VEGF. ECGS increased the rate of cell proliferation up to a concentration of 250 μg/ml after which the rate of proliferation was maintained. The $ED_{50}$ of ECGS is reported to be 75-300 μg/ml which is consistent with this data. Statistical analysis showed the P value to be significant at < 0.0001.

ECGS has been reported to contain bFGF although the quantities of this growth factor are not stated by the company. Figure 7.6 shows the rate of HUVEC proliferation in response to bFGF is similar to that seen with ECGS. Both growth factors increase the rate of proliferation at their highest concentration to give 10,000 more cells than when no growth factor was added. The $ED_{50}$ of bFGF is reported to be 0.1-0.25 ng/ml which is consistent with this data. However, statistical analysis revealed the P value to be 0.0546 which is just over the value which is considered to be significant.

Because the number of HOMEC was limited, certain studies were only performed on HUVEC rather than HOMEC. Antibodies to VEGF were only used with HUVEC. Anti-VEGF neutralising antibodies did not completely inhibit the effect of VEGF on HUVEC. The inhibition of HUVEC proliferation is shown in figure 7.7 and is most noticeable at the lower VEGF concentrations. The maximum increase in proliferation is not seen until 50 ng/ml VEGF is added as opposed to 12.5 ng/ml as shown in figure 7.3. Statistical analysis showed the P value to be 0.0066 which shows a significant increase in proliferation and indicates that the neutralizing antibody has only inhibited proliferation to a degree.

Figures 7.8 and 7.9 show the effect anti-flt-1 and anti-KDR on HUVEC proliferation. A standard VEGF concentration was maintained throughout the experiment so the only inhibition was caused by the antibodies. The results in figure 7.8 show that increasing levels of anti-flt-1 does not inhibit the proliferation of endothelial cells. The cellular proliferation does not decrease with increasing anti-flt-1. Inhibition of HUVEC proliferation was shown to be not significant with a P value of < 0.7578. A similar study using anti-KDR antibodies is shown in figure 7.9. Results show that increasing levels of anti-KDR inhibits the cellular proliferation of HUVEC in response to a standard concentration of VEGF. Inhibition of HUVEC proliferation was shown to be significant with a P value of < 0.0001.

From this data it was decided to study the effect of a standard concentration of 200 ng/ml of each of the antibodies for further studies, and to use a series of VEGF concentrations.

Anti-KDR and anti-flt-1 antibodies used to look for the receptor responsible for the VEGF mediated proliferation showed that anti-flt-1 antibodies had no effect on the proliferation of HUVEC in response to VEGF in granulosa cell conditioned media. Figure 7.10 shows the HUVEC proliferation in response to VEGF in the presence of anti-flt-1 antibodies, the increase in cellular proliferation is significant with a P value of $< 0.0001$. This data can be compared to that shown in Figure 7.4 to see that there is no inhibition in the mitogenic effect of VEGF. However, the same study performed with anti-KDR antibody showed a decrease in the level of endothelial cell proliferation in response to VEGF in the granulosa cell conditioned media. The cell number observed using anti-KDR only varies between 23,000 and 25,000, figure 7.11. Statistical analysis showed the increase in cell proliferation to have a P value of 0.7164 which is not significant. This data shows that anti-KDR antibodies inhibit the VEGF mediated proliferation of HUVEC.

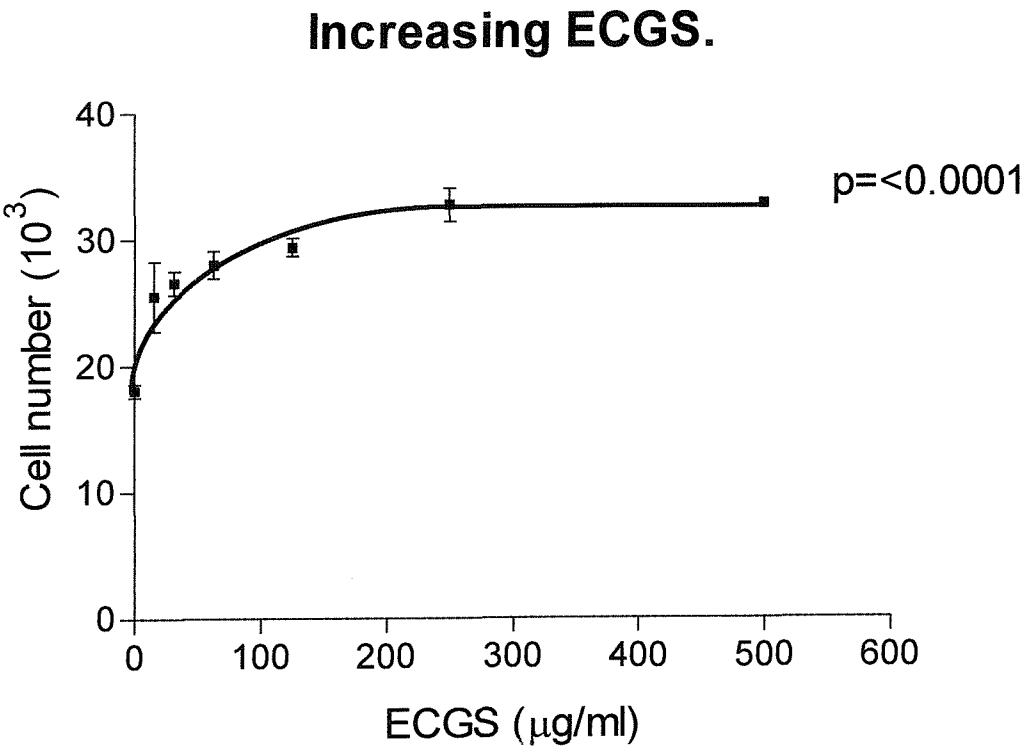


**Figure 7.5 ECGS mediated HUVEC proliferation.** A significant increase in HUVEC proliferation in response to increasing concentrations of ECGS is shown (triplicate determination at each concentration, mean +/- SEM; analysis of variance, $p < 0.0001$).

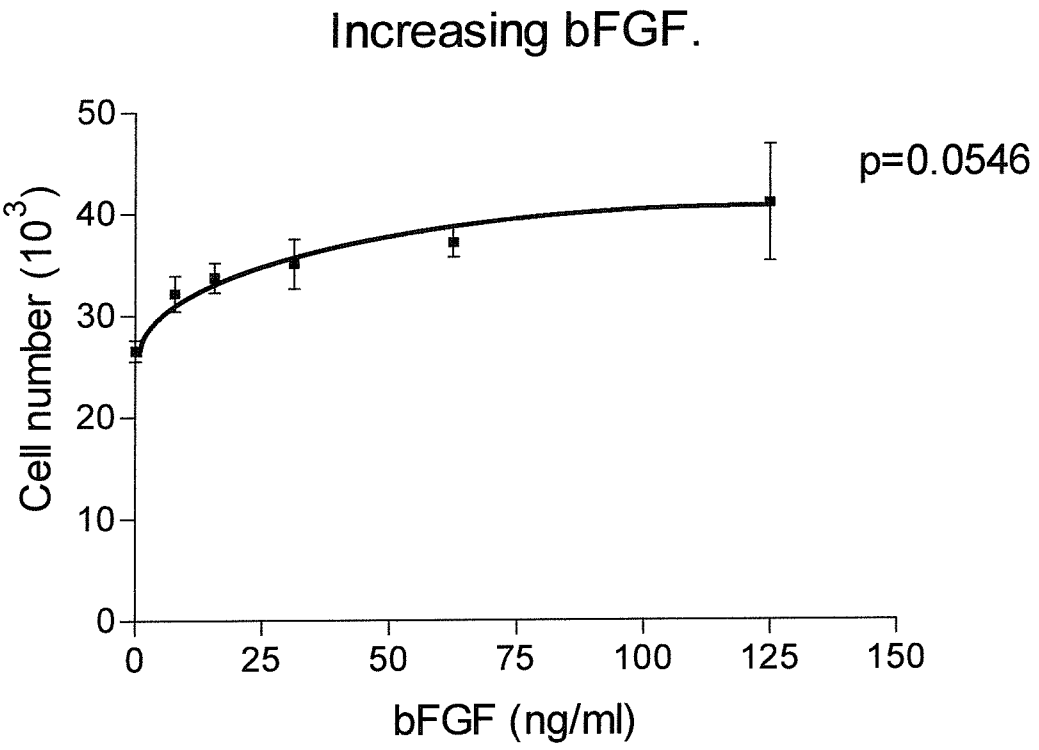


**Figure 7.6 bFGF mediated HUVEC proliferation.** An increase in HUVEC proliferation in response to increasing concentrations of bFGF is shown (triplicate determination at each concentration, mean +/- SEM; analysis of variance, p=0.0546).

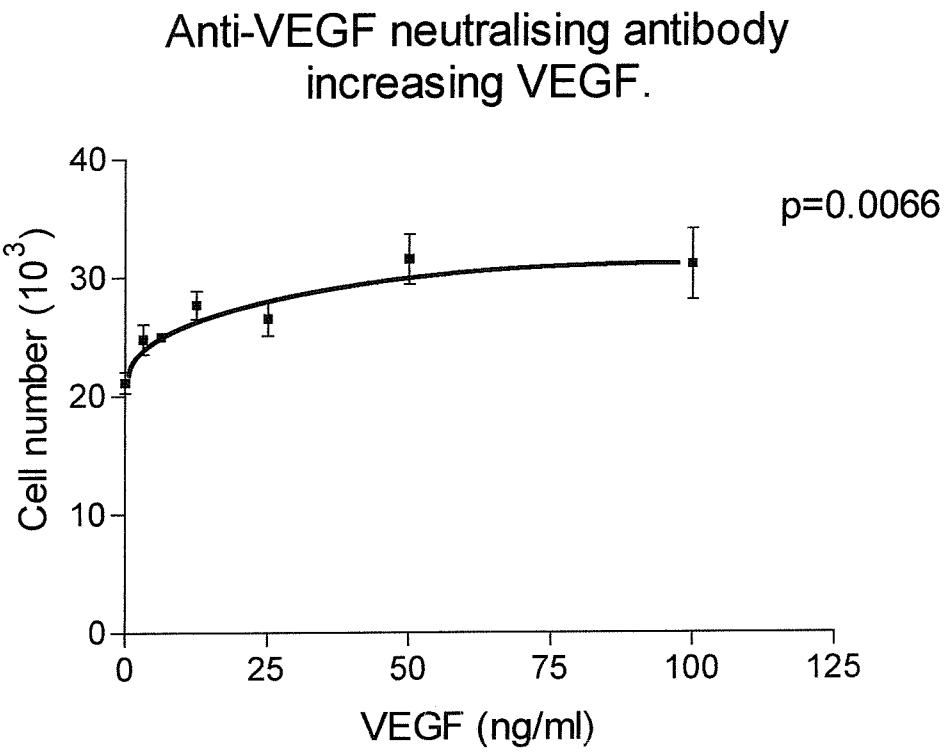


**Figure 7.7 Anti-VEGF neutralising antibody inhibition of VEGF mediated HUVEC proliferation.** An inhibition in the increase in HUVEC proliferation in response to increasing concentrations of VEGF is shown (triplicate determination at each concentration, mean +/- SEM; analysis of variance, p=0.0066).

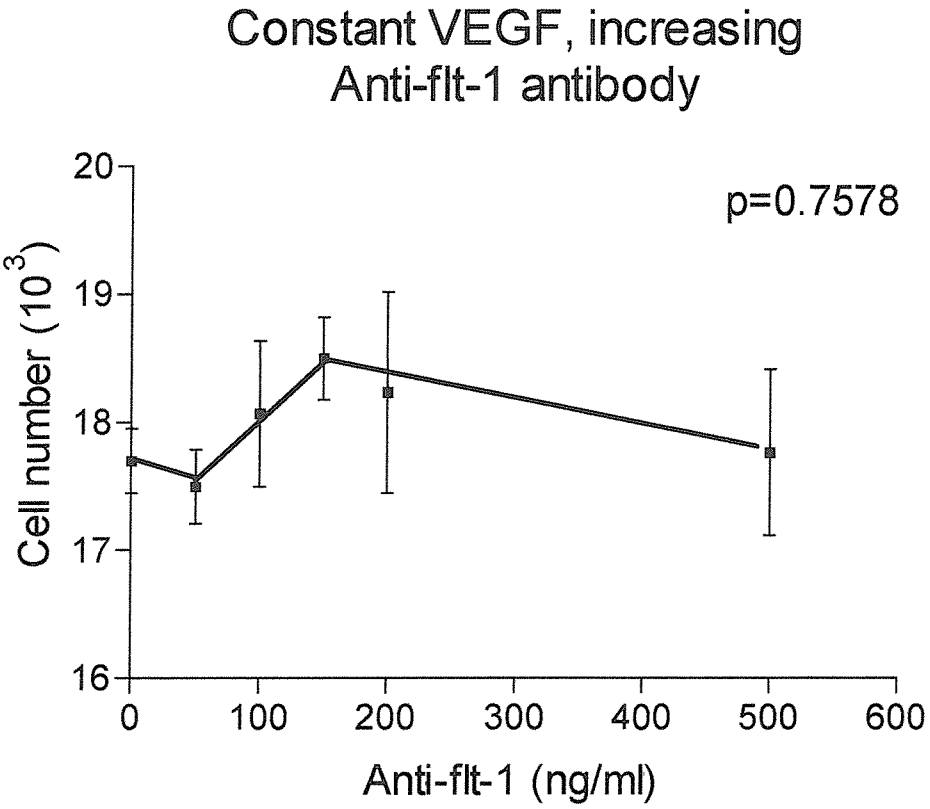


**Figure 7.8 Anti-flt-1 antibody inhibition of HUVEC proliferation.** A non significant increase in HUVEC proliferation in response to increasing concentrations of anti-flt-1 is shown (triplicate determination at each concentration, mean +/- SEM; analysis of variance, $p < 0.7578$).

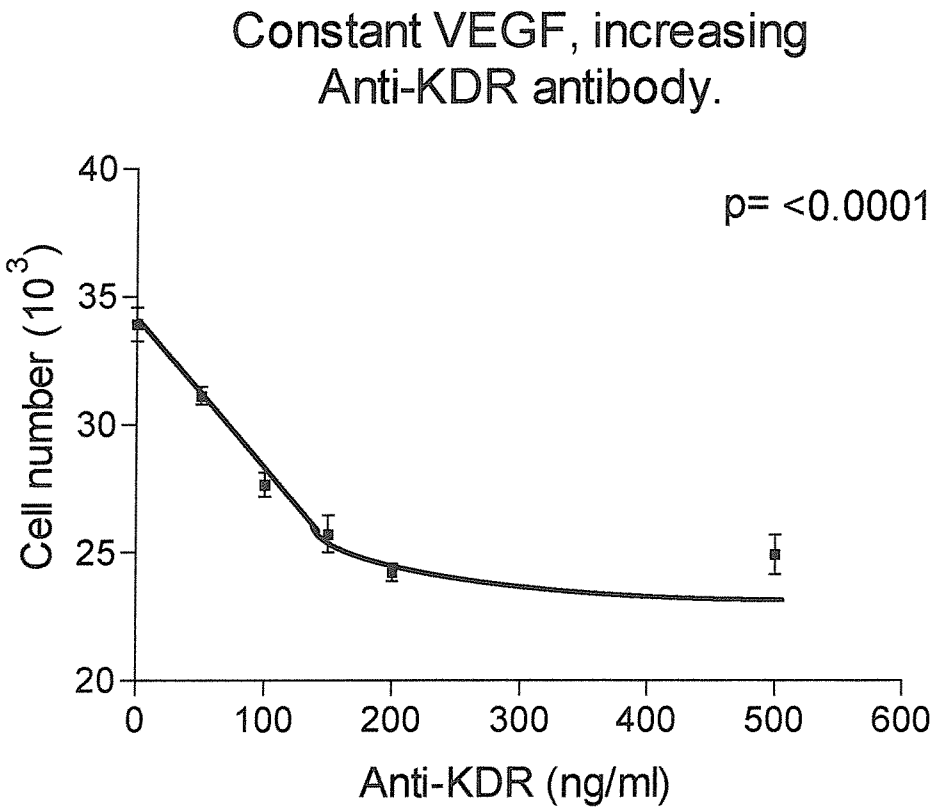


**Figure 7.9 Anti-KDR antibody inhibition of HUVEC proliferation.** A significant inhibition in the increase in HUVEC proliferation in response to increasing concentrations of anti-KDR is shown (triplicate determination at each concentration, mean /- SEM; analysis of variance, $p < 0.0001$).

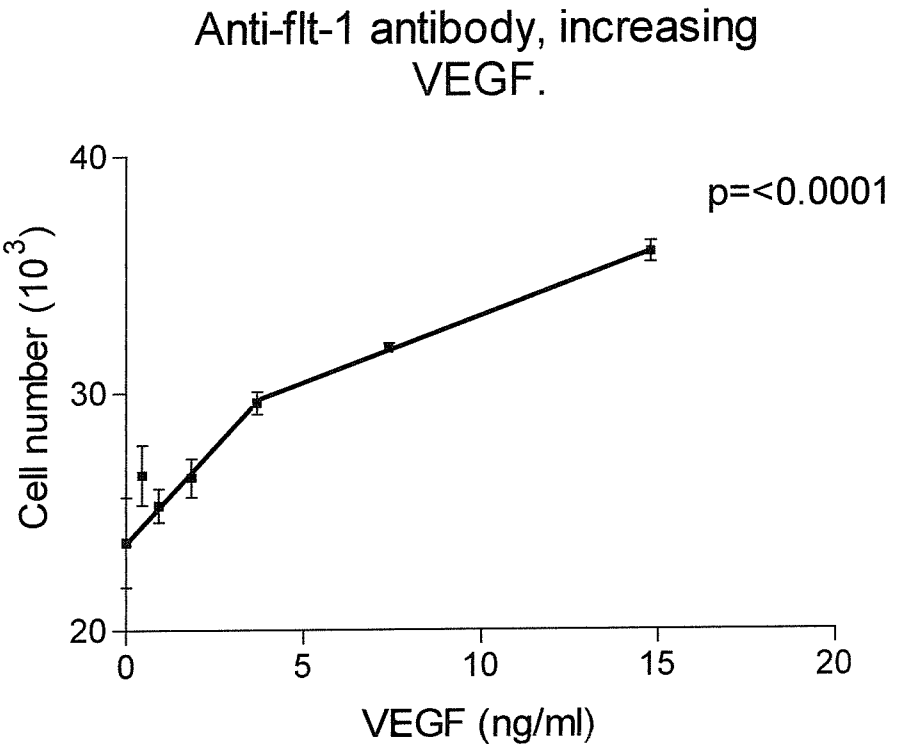


**Figure 7.10 Anti-flt-1 antibody inhibition of VEGF/granulosa cell conditioned media mediated HUVEC proliferation.** A significant increase in HUVEC proliferation in response to increasing concentrations of VEGF is shown (triplicate determination at each concentration, mean +/- SEM; analysis of variance, $p < 0.0001$).

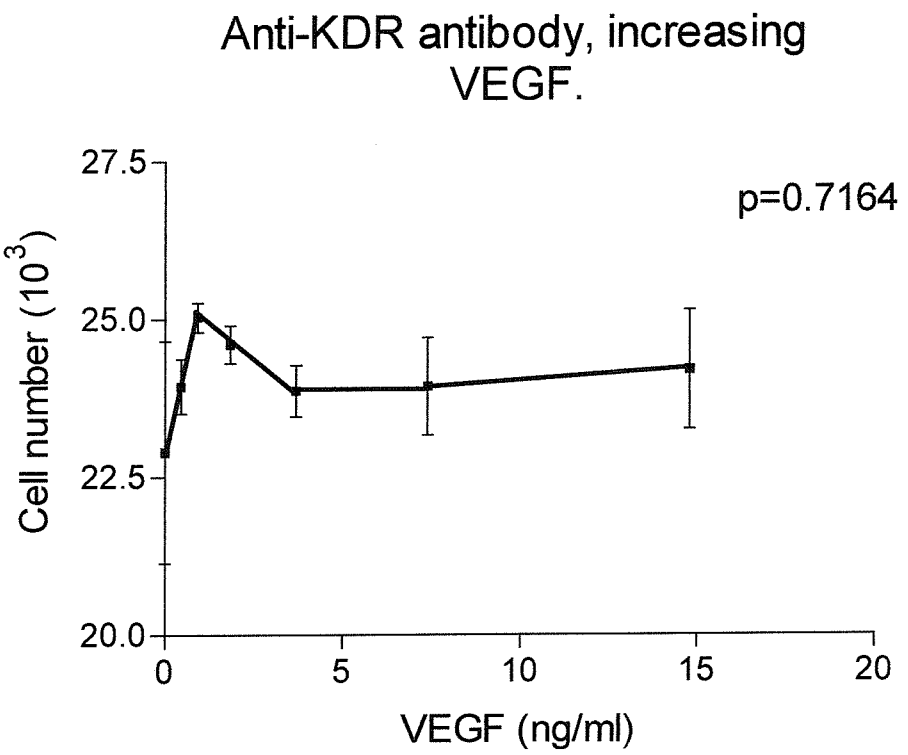


**Figure 7.11 Anti-KDR antibody inhibition of VEGF/granulosa cell conditioned media mediated HUVEC proliferation.** A significant inhibition in the increase in HUVEC proliferation in response to increasing concentrations of VEGF is shown (triplicate determination at each concentration, mean /- SEM; analysis of variance, $p < 0.7164$).

Figure 7.12 shows the effect of the nitric oxide synthase inhibitor L-NAME on HUVEC proliferation. A standard VEGF concentration was maintained throughout the experiment so the only inhibition was caused by L-NAME. The results show that increasing levels of L-NAME inhibit the proliferation of endothelial cells. Maximum inhibition is seen from L-NAME concentrations of 200 μM. This inhibition of HUVEC proliferation was shown to be significant with a P value of $< 0.0001$. From this data it was decided to study the effect of a standard concentration of 500 μM L-NAME and to use a series of VEGF concentrations.

Figure 7.13 shows the effects of VEGF on HOMEC in the presence of 500 μM L-NAME. There is no increase in the level of HOMEC proliferation at any VEGF concentration (P value is 0.5613).

Figure 7.14 shows the effects of VEGF on HUVEC in the presence of 500 μM L-NAME. There is no increase in the level of HUVEC proliferation at any VEGF concentration (P value is 0.4583)

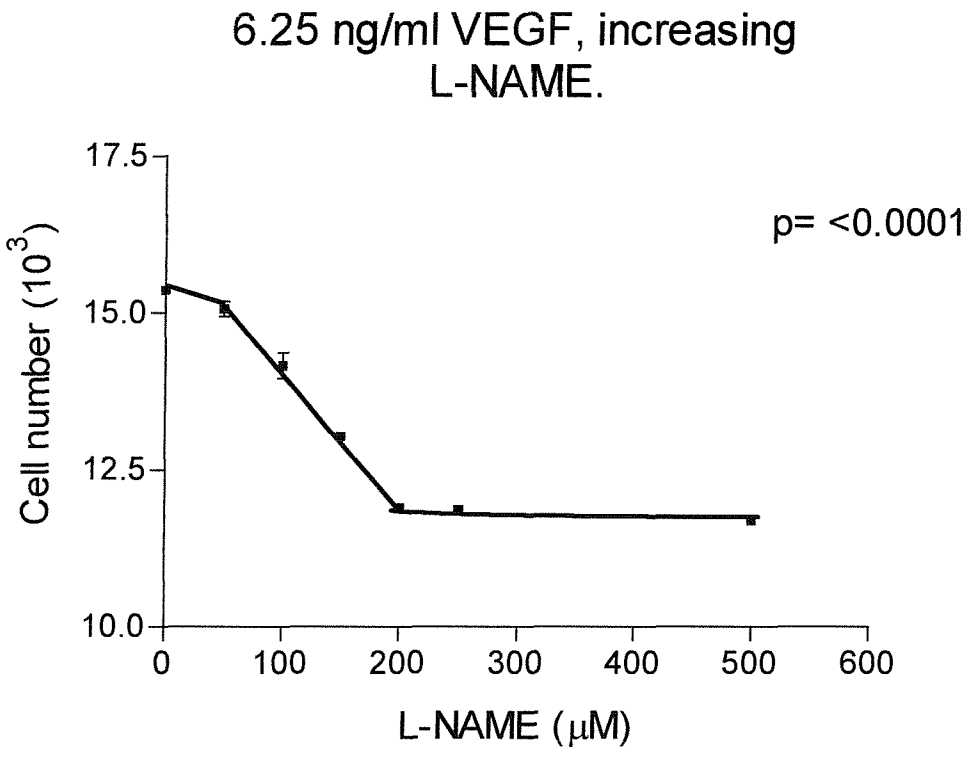


**Figure 7.12 L-NAME inhibition of HUVEC proliferation.** A significant inhibition of HUVEC proliferation with increasing concentrations of L-NAME is shown (triplicate determination at each concentration, mean +/- SEM; analysis of variance, $p < 0.0001$).

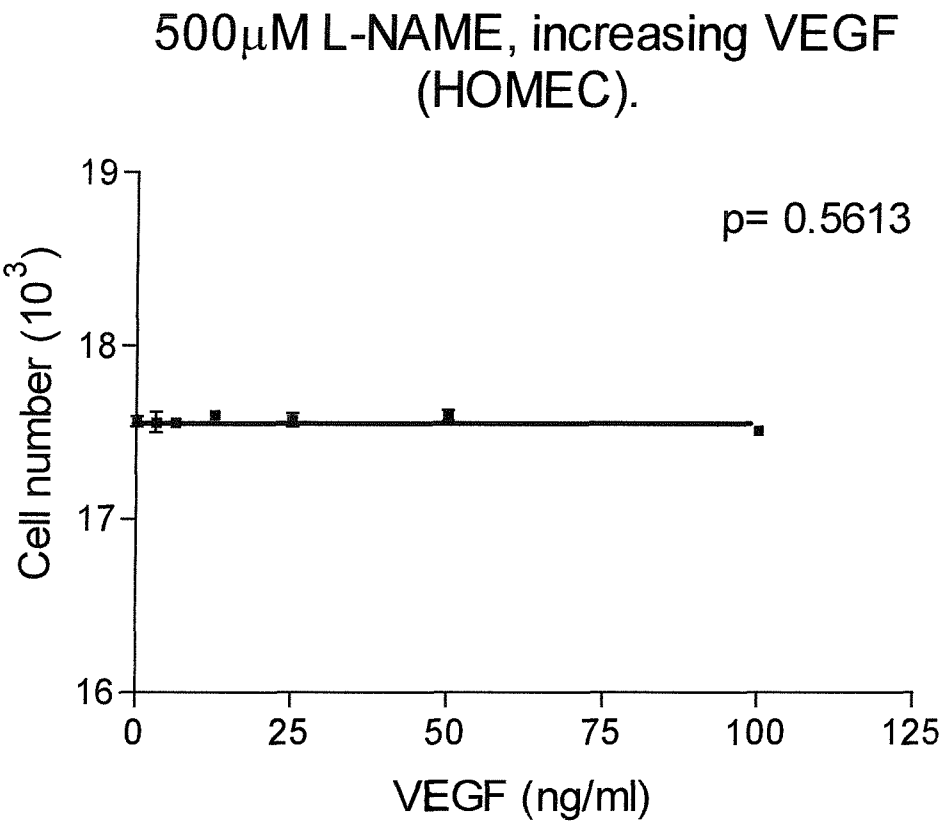


**Figure 7.13 L-NAME inhibition of VEGF mediated HOMEC proliferation.** A significant inhibition in the increase in HOMEC proliferation in response to increasing concentrations of VEGF is shown (triplicate determination at each concentration, mean +/- SEM; analysis of variance, p= 0.5613).

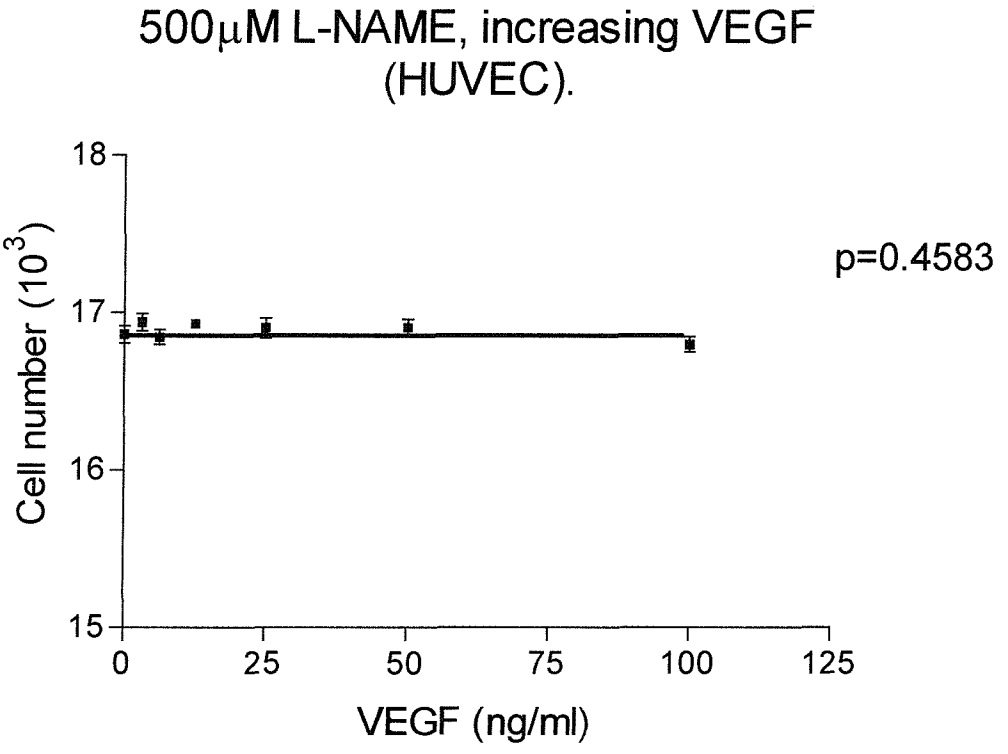


**Figure 7.14 L-NAME inhibition of VEGF mediated HUVEC proliferation.** A significant inhibition in the increase in HUVEC proliferation in response to increasing concentrations of VEGF is shown (triplicate determination at each concentration, mean +/- SEM; analysis of variance, p=0.4583).

## 7.5 Discussion.

Results of the cellular proliferation assays showed that VEGF increases the proliferation of both HOMEC and HUVEC in a dose dependant manner. The $ED_{50}$ for both cell types has been shown to 6.25 ng/ml which corresponds to the manufacturers guidelines for HUVEC. VEGF does not cause any further increase in proliferation from 12.5 ng/ml and the rate of proliferation remains at the same level after this concentration. The results of the HUVEC proliferation have also been shown by Papapetropoulos *et al.*, 1997.

The endothelial cell growth supplement which contains bFGF, increased the proliferation of HUVEC. Again, a maximum rate of proliferation was achieved which no further increase in ECGS could change. The increase in proliferation in response to both VEGF and ECGS was shown to be statistically significant. These results are also similar to those of Papapetropoulos *et al.*, 1997.

Surprisingly the effect of bFGF on HUVEC was not statistically significant although this was marginal.

Granulosa cell conditioned media increased the proliferation of HUVEC, this same increase was observed in the presence of anti-flt-1 antibodies but not in the presence of anti-KDR antibodies. This suggests that the flt-1 VEGF receptor is not actively involved in the proliferation of endothelial cells but has another function. However, the antibodies have not been formally demonstrated to be neutralizing antibodies and so further work would ne necessary to confirm this data. The ability of anti-KDR antibodies to inhibit the mitogenic effect of VEGF shows the vital role this receptor plays in angiogenesis. The evidence that the two receptors have different functions indicates that the events following binding of VEGF to the two receptors involve different intracellular signalling pathways.

The observation that anti-KDR antibodies inhibit VEGF mediated proliferation also indicate that it is the VEGF in the granulosa cell conditioned media which is upregulating HUVEC proliferation and not any other secreted growth factors.

The ability of L-NAME to inhibit the mitogenic effects of VEGF shows that NOS is important in the action of VEGF. By inhibiting the production of nitric oxide, the

mitogenic effects of VEGF can be inhibited. These results have also been demonstrated by Morbidelli *et al.*, 1996.

# Chapter 8.

# Endothelial/granulosa cell interactions in co-culture: formation of specific spatial inter-relationships.

## 8.1 Introduction.

A special feature of the ovary is the interaction between steroidogenic and vascular tissues.
VEGF production by granulosa cells in response to exposure to hCG has been shown to increase the rate of endothelial cell proliferation, as shown in chapter 7. Studies by Spanel-Borowski *et al.*, (1994) have shown that granulosa cells and endothelial cells in a co-culture environment survive well. However, in that study the cells were not in direct contact, but separated by a membrane which allowed the circulation of media. Their study showed an increase in the rate of endothelial cell proliferation which was proposed to be mediated by angiogenic growth factors produced by the granulosa cells.

Many studies have looked at the individual cell types from which the corpus luteum is composed. Chapter 5 details the complex capillary-like structural networks which form when endothelial cells are cultured on Matrigel, whilst chapter 6 shows the tight granulosa cell clusters which form on Matrigel. The effect of granulosa cell secreted mitogens has also been widely investigated but no studies have looked at the direct interactions when the two cell types are cultured together.

## 8.2 Materials and methods.

### 8.2.1 Cell culture.

HOMEC, HUVEC and ECV304 cells were isolated and cultured as described in chapter 2. Granulosa cells were isolated and cultured as described in chapter 6.

### 8.2.2 Endothelial/granulosa cell co-culture.

Cultures were prepared in three different ways,

1) granulosa cells were added to pre-formed endothelial cell capillary-like structure formations.
2) endothelial cells were added to pre-formed granulosa cell clusters.
3) endothelial cells and granulosa cells were added at the same time.

#### 8.2.2.1 Granulosa cells added to pre-formed endothelial cell capillary-like structure formations.

Lab-Tek II chamber slides were coated with 60 µl of Matrigel or growth factor reduced Matrigel. 40,000 HUVEC, HOMEC or ECV304 cells were added and left overnight at 37°C in M199 supplemented with ECGS (150 µg/ml) in 5% $CO_2$ in air to allow formation of capillary-like structures.
The following day 60,000 freshly isolated granulosa cells were added to the wells and cultures were maintained in 50:50 medium D with hCG (100 ng/ml): M199 with ECGS (150 µg/ml). Using 5% $CO_2$ in air at 37°C.
Cultures were monitored with phase contrast microscopy.

#### 8.2.2.2 Endothelial cells added to pre-formed granulosa cell clusters.

Lab-Tek II chamber slides were coated with 60 µl of Matrigel or growth factor reduced Matrigel.

60,000 freshly isolated granulosa cells were added and left overnight at 37°C in medium D with hCG (100 ng/ml) in 5% $CO_2$ in air to allow formation of clusters. The following day 40,000 HUVEC, HOMEC or ECV304 cells were added to the wells and cultures were maintained in 50:50 medium D with hCG (100 ng/ml): M199 with ECGS (150 µg/ml). Using 5% $CO_2$ in air at 37°C.
Cultures were monitored with phase contrast microscopy.

**8.2.2.3 Endothelial cells and granulosa cells added at the same time.**
Lab-Tek II chamber slides were coated with 60 µl of Matrigel or growth factor reduced Matrigel.
60,000 freshly isolated granulosa cells and 40,000 HUVEC, HOMEC or ECV304 cells were added to the wells and cultures were maintained in 50:50 medium D with hCG (100 ng/ml): M199 with ECGS (150 µg/ml). Using 5% $CO_2$ in air at 37°C.
Cultures were monitored with phase contrast microscopy.

**8.2.2.4 Granulosa cells added to endothelial cell monolayer.**
60,000 freshly isolated granulosa cells were added to an endothelial cell monolayer in a well of a 24 well plate. No matrix was used and cultures were maintained in 50:50 medium D with hCG (100 ng/ml): M199 with ECGS (150 µg/ml). Using 5% $CO_2$ in air at 37°C.
Cultures were monitored with phase contrast microscopy.

## 8.2.3 Blocking of network formation.

An attempt to block the formation of the specific cellular architecture was performed by addition of excess VEGF (250 ng/ml), or a combination of anti-human and anti-mouse VEGF neutralising antibodies (500 ng/ml; R and D Systems). Excess VEGF and neutralizing antibodies were pre-incubated with the Matrigel before addition of any cells and also added at the same time as the cells.

### 8.2.4 Time lapse video microscopy.

Individual wells of 24 well plates were separated using a heated scalpel. These single wells were then coated with 200 µl of standard Matrigel.
The variations of cell addition in the co-cultures described in section 8.2.2 were followed for cell additions to individual wells and the wells were transferred to a 50 $cm^2$ culture flask and gassed for 2 min with 5% $CO_2$ in air. The flask was sealed and transferred to the time lapse apparatus. This consisted of a microscope with a heated stage (37°C) linked to a JVC BR-9000 time lapse video recorder and monitor. Frames were taken over a period of time up to 60 hours.

### 8.2.5 Immunocytochemistry of endothelial/granulosa cell co-cultures for laminin β1 chain.

Cultures were prepared in Lab-Tek II chamber slides as detailed in section 8.2.2.3 on standard Matrigel.
Following formation of co-culture networks the cultures were fixed in ice cold methanol for 10 min and washed with PBS followed by a 30 min wash with 10% goat serum in PBS. A dilution of the primary antibody anti-laminin β1 was incubated overnight at room temperature. After 3 ten minute washes with 0.2% BSA in PBS, cultures were incubated with a fluorescein isothiocyanate conjugated secondary antibody (20 µm/ml) for 1 hour. Three further ten min washes with 0.2% BSA in PBS were followed by incubation with the nuclear counterstains propidium iodide (0.01 mg/ml). The chamber slides were disassembled to leave the bottom surface which was mounted with Moviol and imaged under ultraviolet light on an Olympus microscope. Photographs were taken with an Olympus camera using Ektachrome 400 film.

## 8.3 Results of endothelial/granulosa cell co-culture.

When endothelial cells were added to granulosa cells that had previously been allowed to cluster, specific cellular architecture was observed as shown in figure 8.1. The endothelial cells lined up to form capillary-like structures as previously shown in chapter 5, figure 5.3. However, in these cultures, the endothelial cells only appeared to form between granulosa cell clusters. The network of capillary-like structures appeared to be much more widely spaced that those seen previously and with the capillary-like structures being longer.

Granulosa cells which were added to pre-formed capillary-like structure networks again formed cultures as previously seen. However, granulosa cell clusters only formed in connection with the endothelial network. Generally the clusters formed at the junction of two or more capillary-like structures where there was a higher density of endothelial cells. Figure 8.2 shows this architecture and it can be observed that the granulosa clusters were not positioned along the length of the capillary-like structures, or anywhere but in association with the endothelial network.

Figure 8.3 shows the cellular architecture which formed when both endothelial and granulosa cells were plated at the same time. Once again there is a specific interaction between the cells to form a complex network where granulosa cell clusters are linked together by endothelial capillary-like structures.

An interesting finding was that when ECV304 cells were added at the same time as the granulosa cells the network was slightly different. The ECV304 cells did form bridges between clusters although they did not form such fine capillary-like structures. The cells appeared to remain separate and did not join together like HOMEC and HUVEC to form these fine structures. Figure 8.4 shows the formations with ECV304 cells.

Granulosa cells added to endothelial cell monolayers did not induce capillary-like structure formation at all. The endothelial cells remained in a monolayer and the granulosa cells clustered on top of them as shown in figure 8.5.

Attempts to inhibit the various formations which developed in co-culture using neutralising antibodies are shown in figure 8.6. There was no inhibition of the

architecture and cells organised themselves as when they were cultured under normal conditions. Excess VEGF also had no effect on the structure formations.

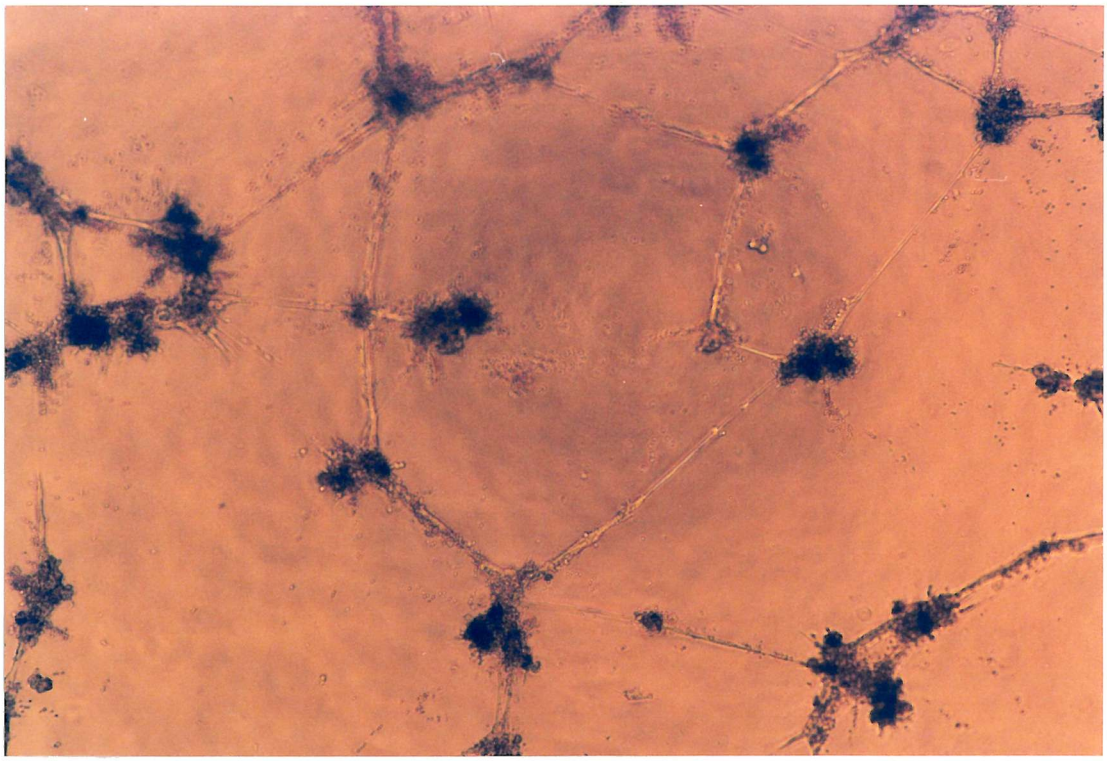

**Figure 8.1 HOMEC/granulosa cell co-culture on Matrigel.** Showing the formation of specific cellular architecture when endothelial cells were added to pre-formed granulosa cell clusters.

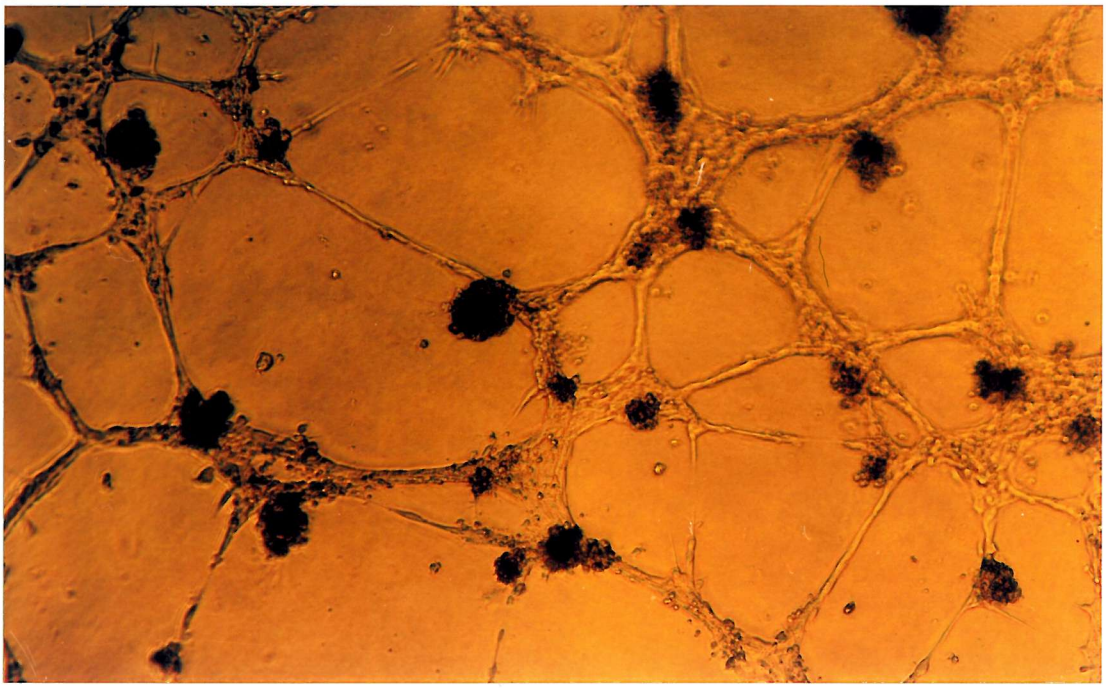

**Figure 8.2 HUVEC/granulosa cell co-culture on Matrigel.** Showing the formation of specific cellular architecture when granulosa cells were added to a pre-formed endothelial cell capillary-like structure network.

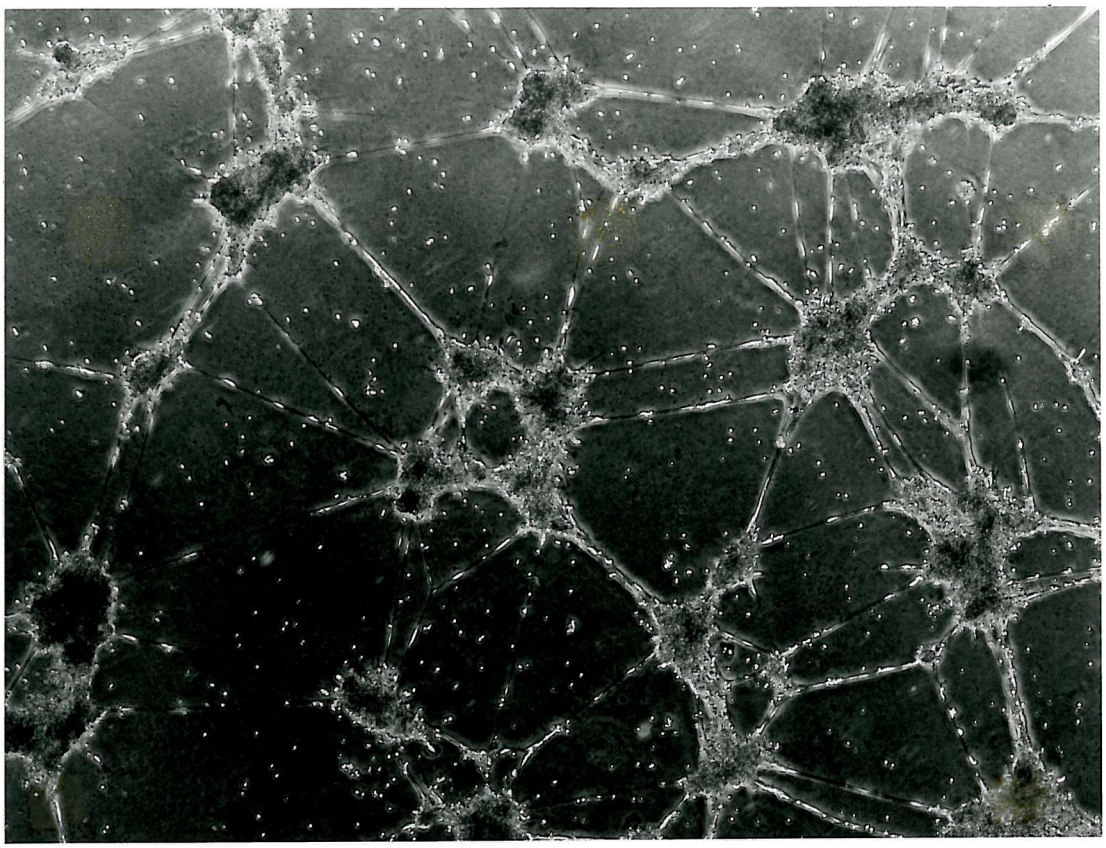

**Figure 8.3 HUVEC/granulosa cell co-culture on Matrigel.** Showing the formation of specific cellular architecture when both cell types were plated at the same time.

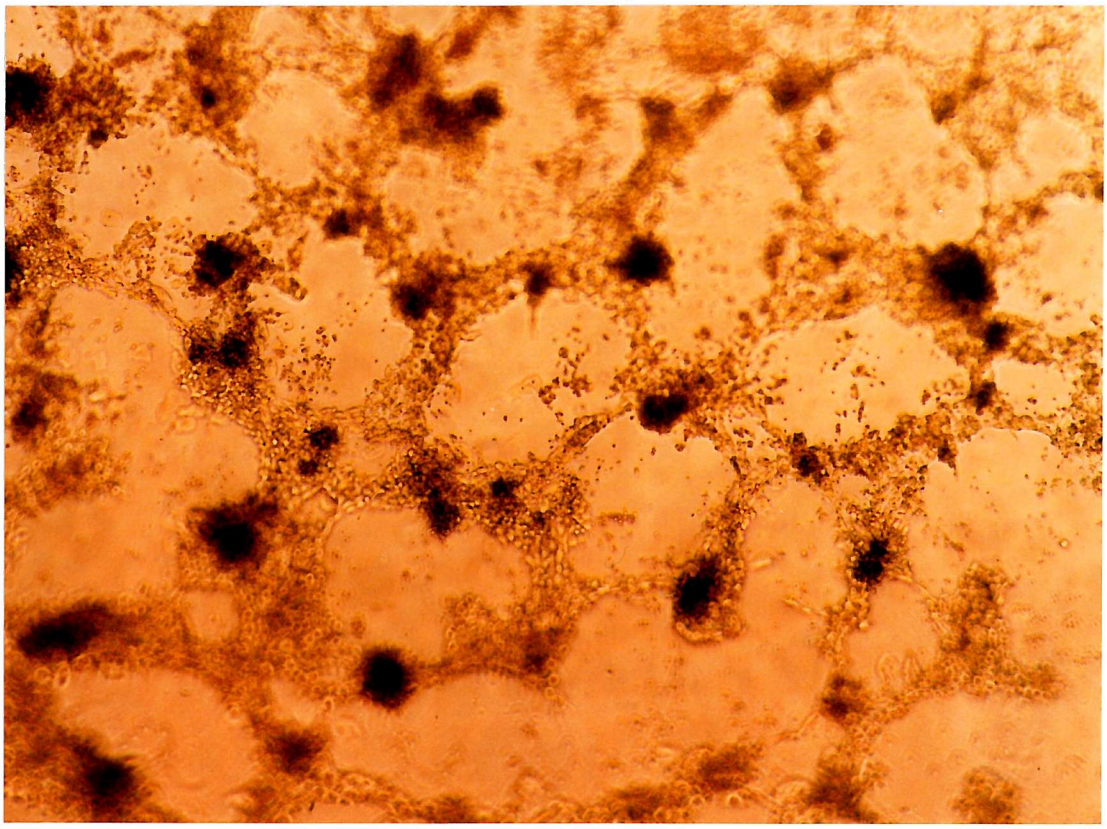

**Figure 8.4 ECV304/granulosa cell co-culture on Matrigel.** Showing the formation of specific cellular architecture when both cell types were plated at the same time.

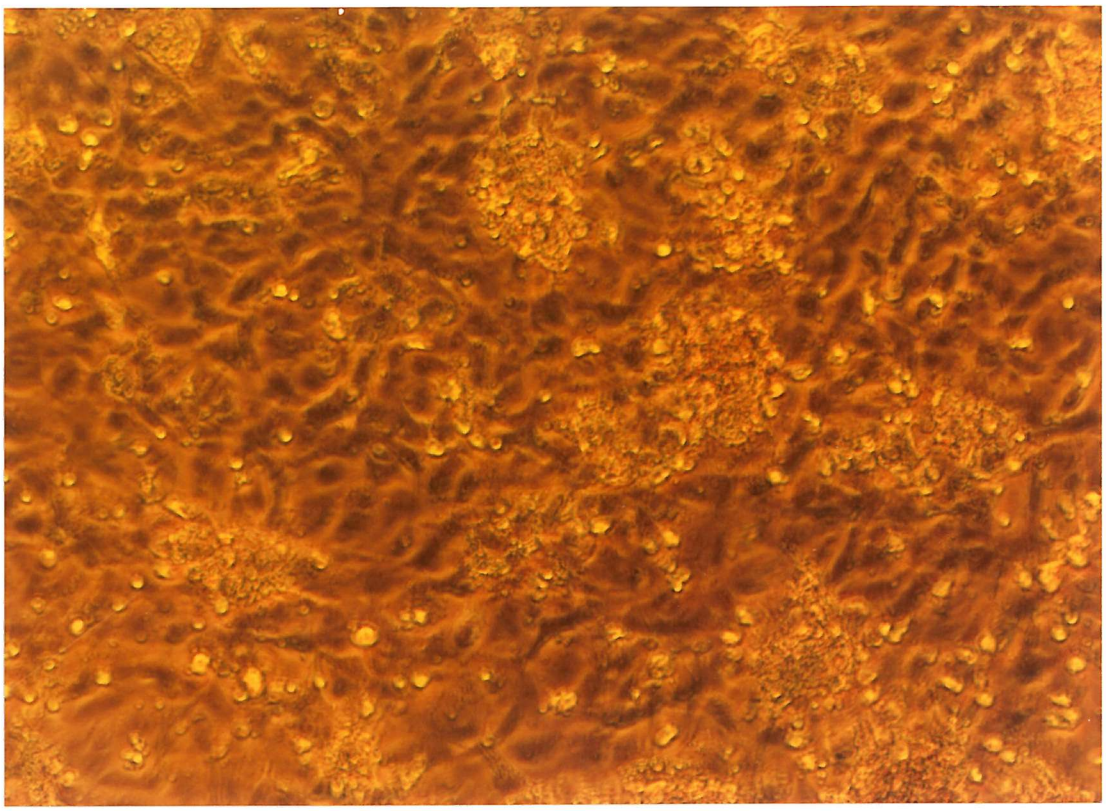

**Figure 8.5 HUVEC/granulosa cell co-culture.** Showing the formation of granulosa cell clusters on the surface of the HUVEC monolayer.

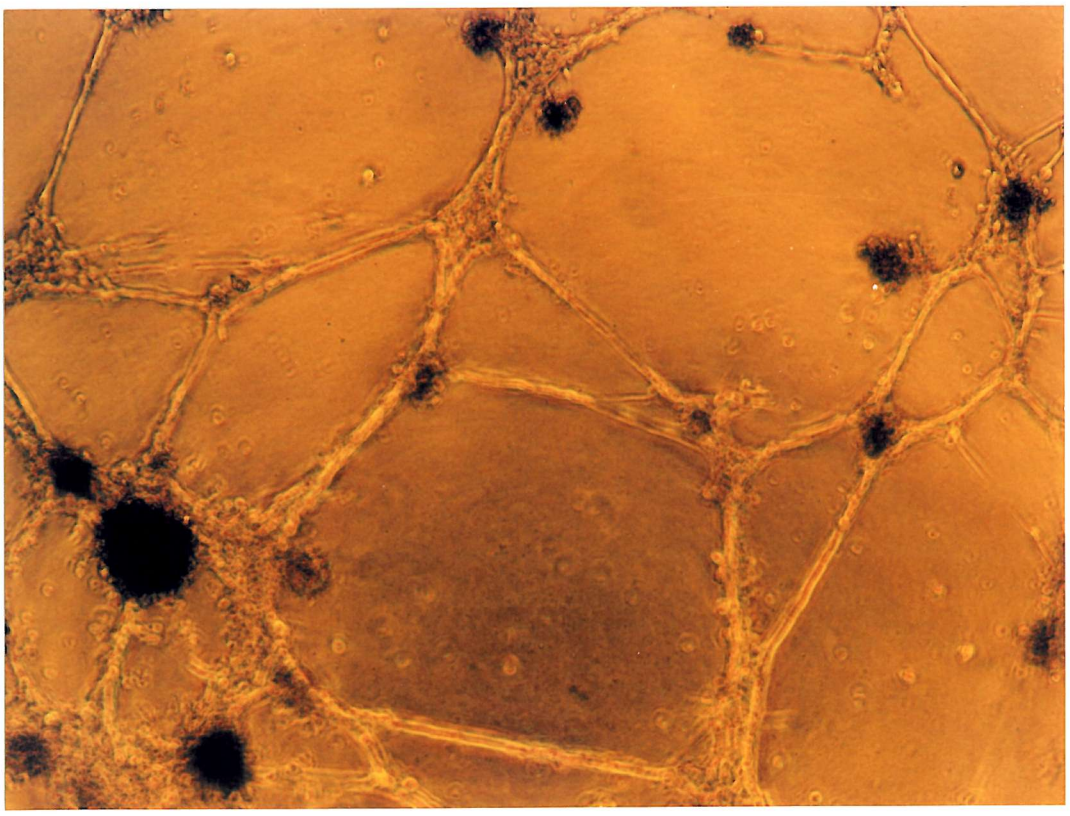

**Figure 8.6 HUVEC/granulosa co-culture on Matrigel.** Showing the formation of specific cellular architecture in the presence of anti VEGF neutralising antibodies.

Analysis of the formation of these complex cellular networks by time lapse video microscopy has shown how the structures are formed.

Figure 8.7 shows endothelial cells added to pre-clustered granulosa cells. The granulosa cell clusters can be clearly seen from the beginning of the timing. By two hours the endothelial cells appear to be beginning to align. An interesting feature here is that the cells which are lining up all appear to be at the periphery of the granulosa cell clusters. This is different to the formation of capillary-like structures shown in figure 5.7 where the endothelial cells all over the Matrigel appear to align at the same time and the complete network is discernable from four hours of culture. This observation of alignment around the granulosa clusters is more clearly seen by four hours of culture and by six hours capillary-like structures can clearly be seen to have formed between separate granulosa cell clusters. Further granulosa clusters appear to be involved in the network by eight hours of culture and from this point there do not appear to be any further developments within the cultures up to twelve hours.

Figure 8.8 shows granulosa cells added to pre-formed endothelial cell capillary-like structures. The endothelial cell network can be seen through the granulosa cell suspension at the beginning of the timing. There are a few small granulosa clusters that are already present in the suspension at the time of addition. It is difficult to see what is happening before eight hours of culture but from this point it can be seen that the junctions between the capillary-like structures are becoming larger as the granulosa cells cluster at these points. This observation is clearer at fourteen hours of culture when granulosa cell clusters can clearly be seen in association with the endothelial cell network. Over the next six hours of culture the granulosa clusters continue to increase in size. There is no change in the shape or organisation of the endothelial network itself, with the granulosa cells appearing to cluster at the junctions without causing any change in the overall structure.

Figure 8.9 shows the cellular architecture formed when both cell types were added at the same time. Again there are already a few small granulosa cell clusters in the cell suspension. As in figure 8.7, the endothelial cells are beginning to align by two hours of culture, however, in this case the beginning of granulosa cell clusters can be seen at the centre of these alignments. This observation is clearer at three hours of culture and

by four hours a fairly comprehensive endothelial cell network can be seen linking granulosa cell clusters. This endothelial cell network is refined over the next few hours and the granulosa clusters also increase in size. By eight hours a complete network can be seen which can be compared to figure 8.3, and there is very little further remodelling of the network after this point.

**Figure 8.7 Time lapse video microscopy of HUVEC/ granulosa cell co-culture on Matrigel.** Showing the formation of specific cellular architecture when endothelial cells were added to pre-formed granulosa cell clusters.

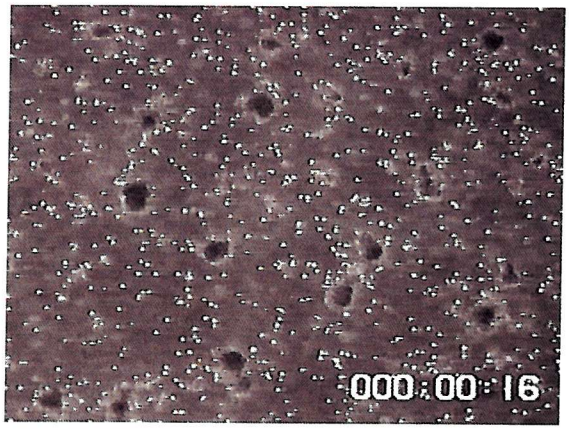
000:00:16

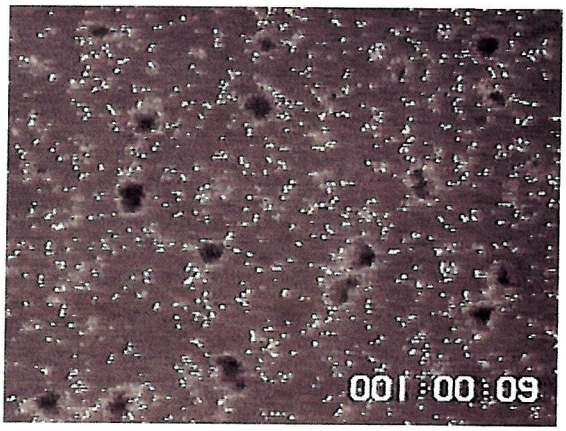
001:00:09

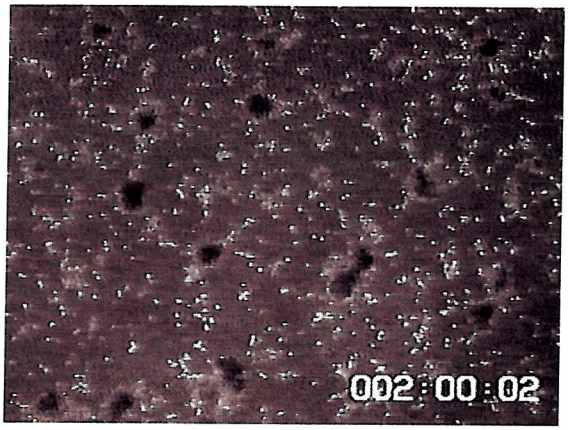
002:00:02

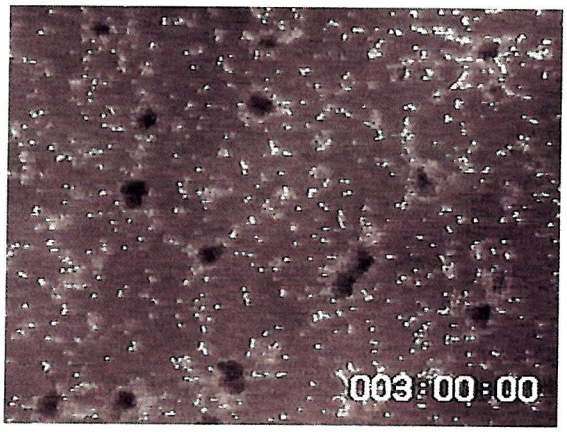
003:00:00

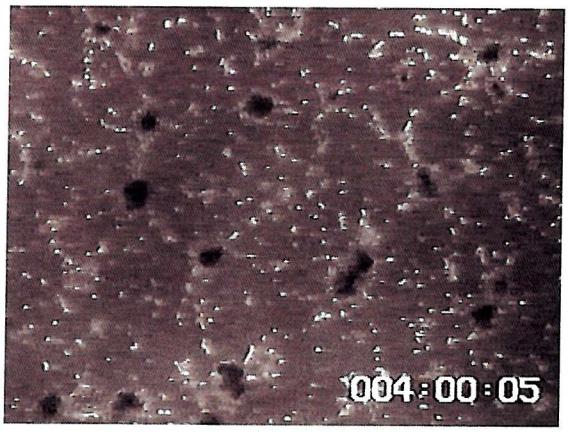
004:00:05

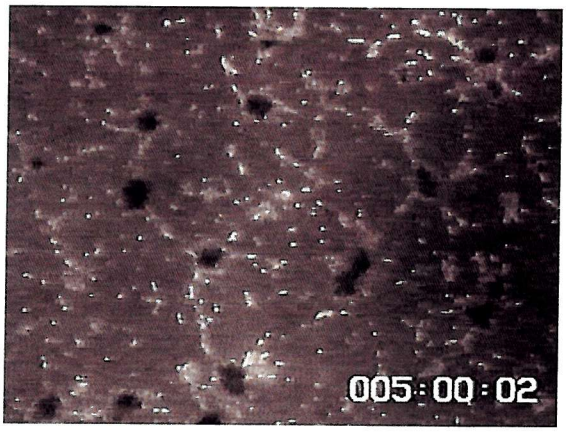
005:00:02

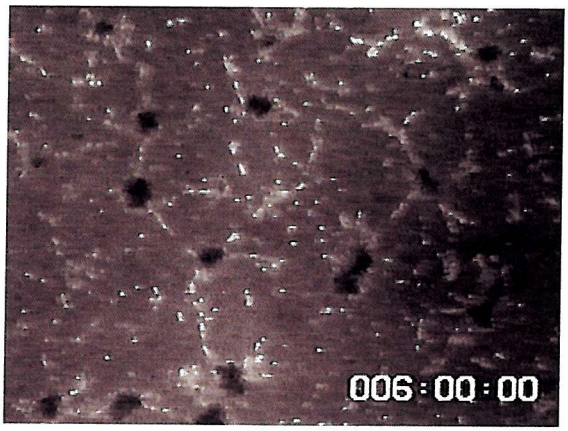
006:00:00

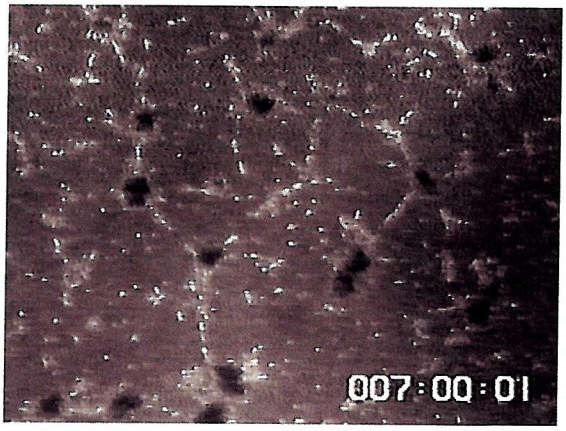
007:00:01

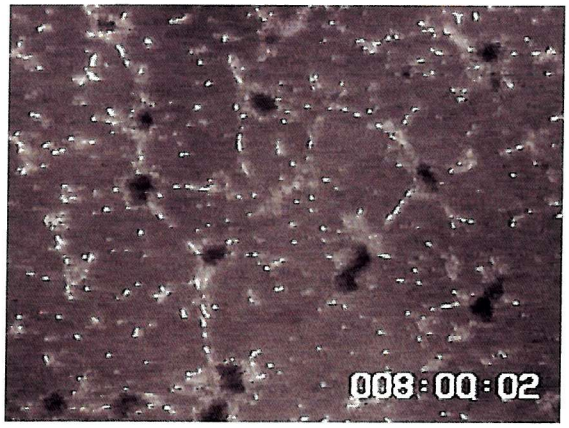
008:00:02

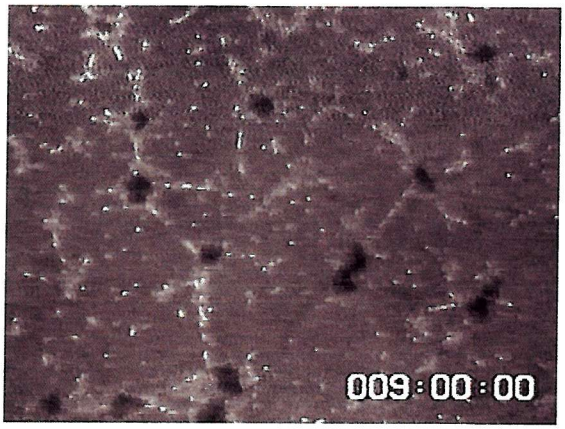
009:00:00

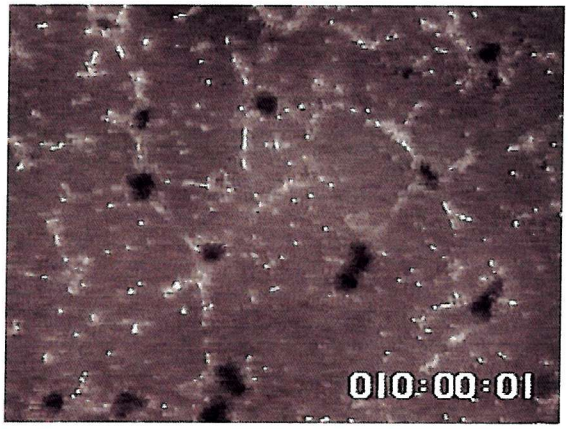
010:00:01


011:00:03

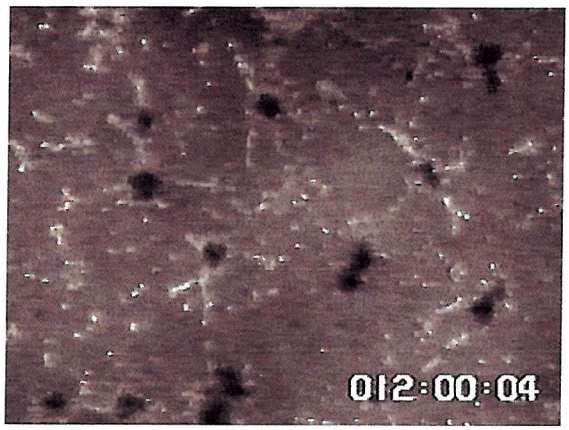
012:00:04

**Figure 8.8 Time lapse video microscopy of HUVEC/ granulosa cell co-culture on Matrigel.** Showing the formation of specific cellular architecture when granulosa cells were added to a pre-formed endothelial cell capillary-like structure network.

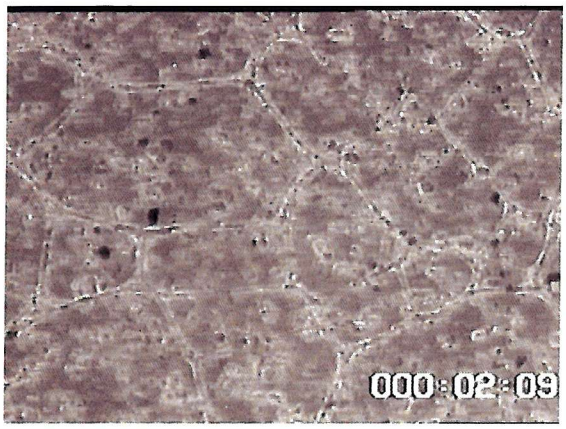
000:02:09

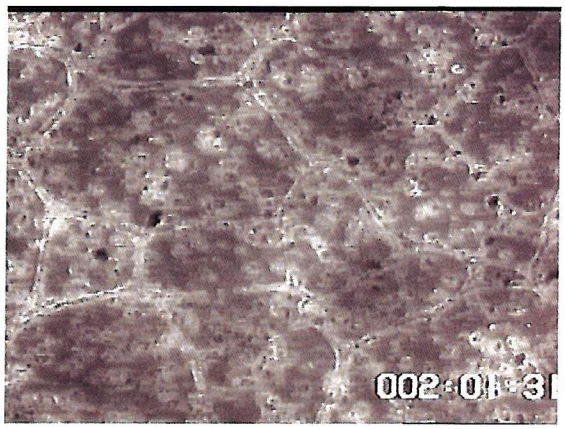
002:01:3

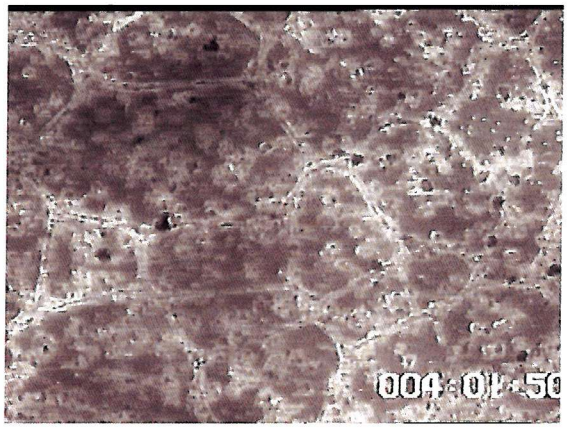
004:01:5

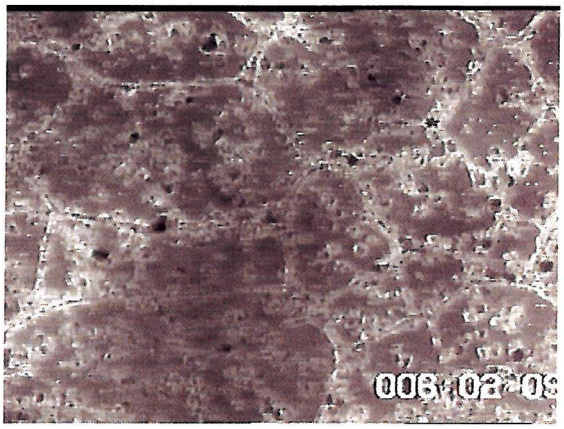
006:02:0

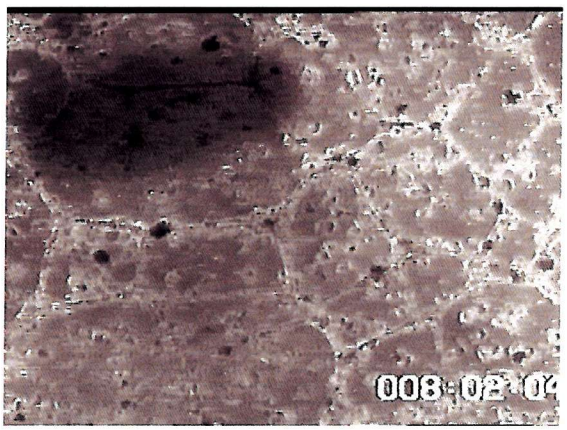
008:02:0

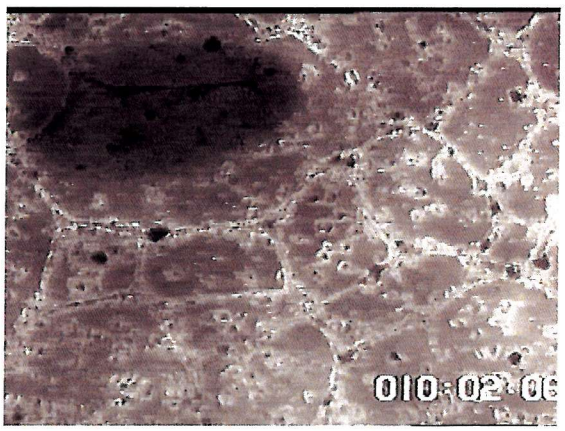
010:02:0

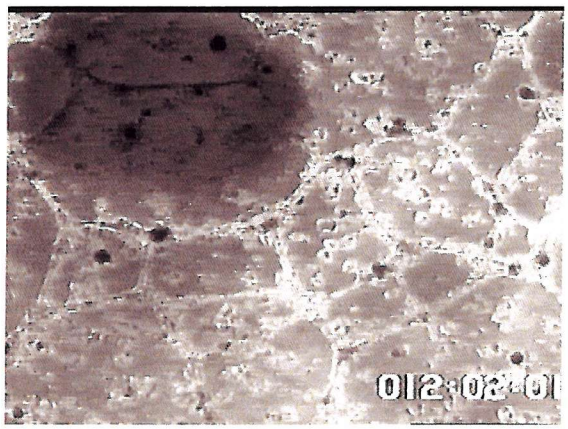
012:02:0

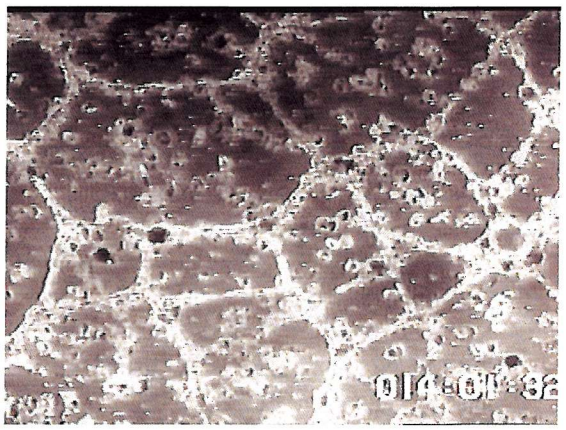
014:00:3

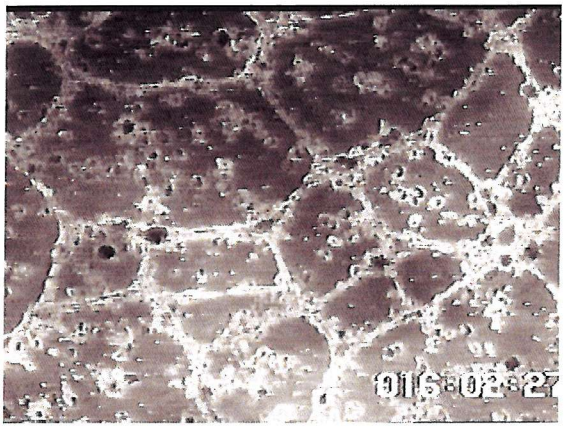

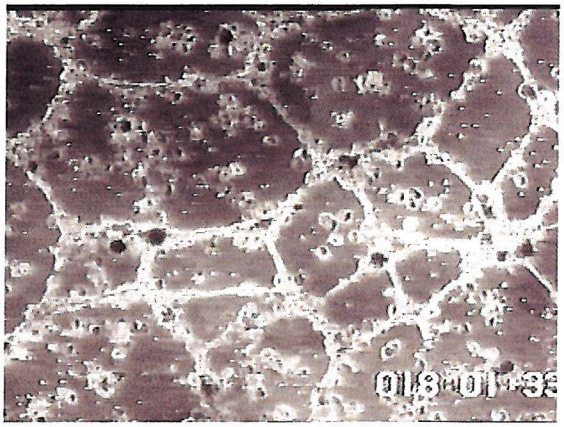

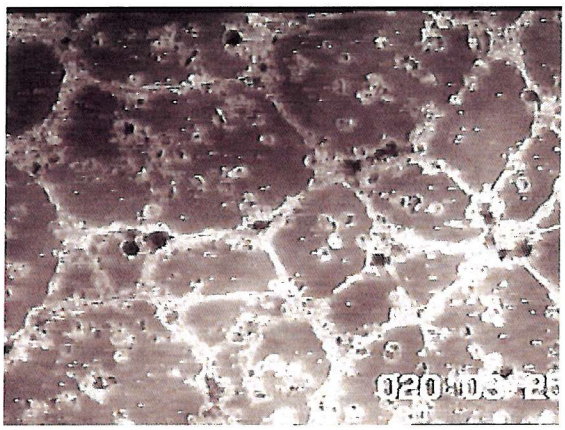

**Figure 8.9 Time lapse video microscopy of HUVEC/ granulosa cell co-culture on Matrigel.** Showing the formation of specific cellular architecture when both cell types were plated at the same time.

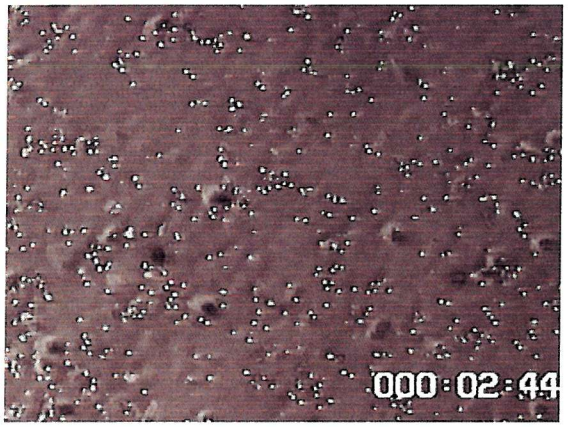
000:02:44

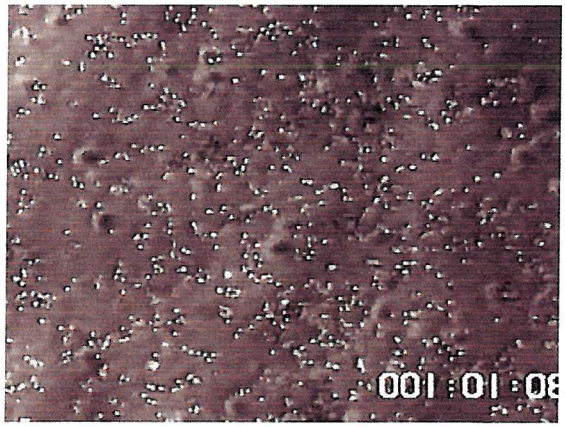
001:01:08

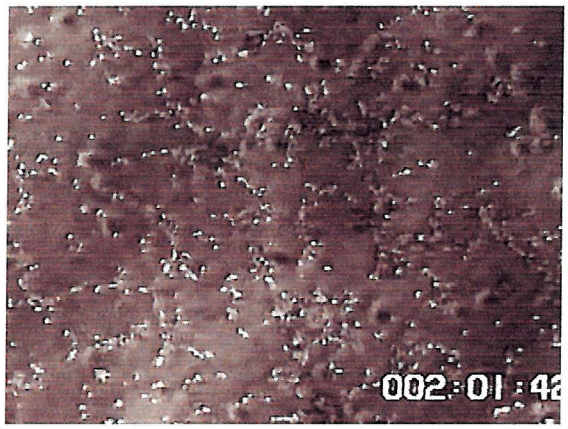
002:01:42

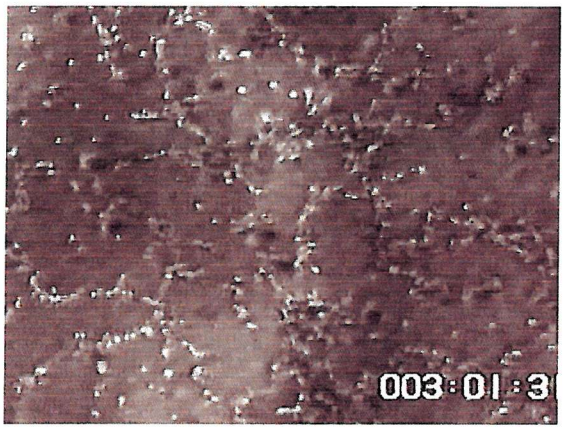
003:01:3

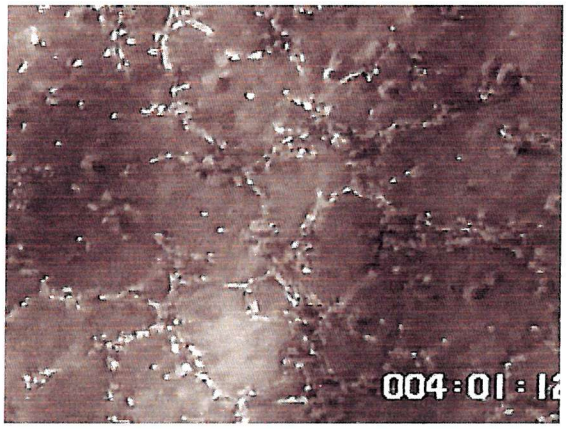
004:01:1

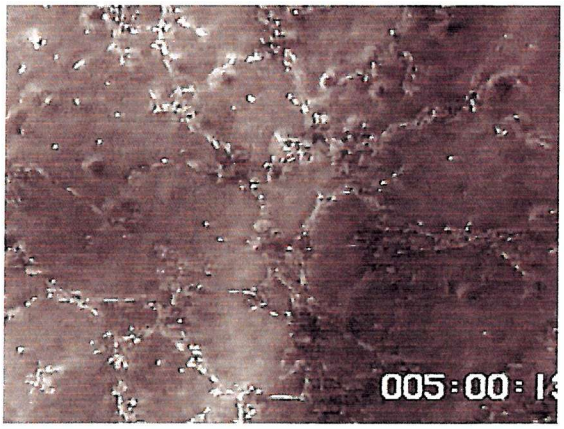
005:00:1

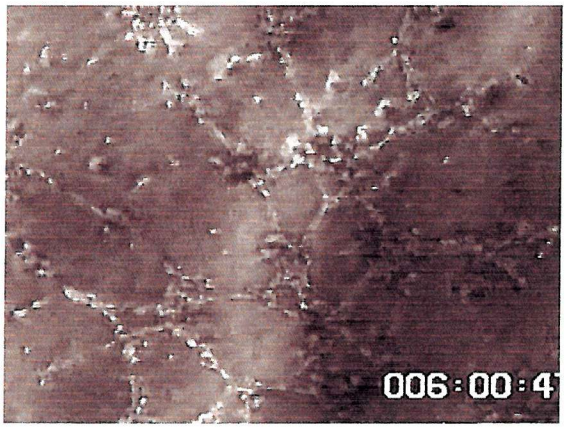
006:00:4

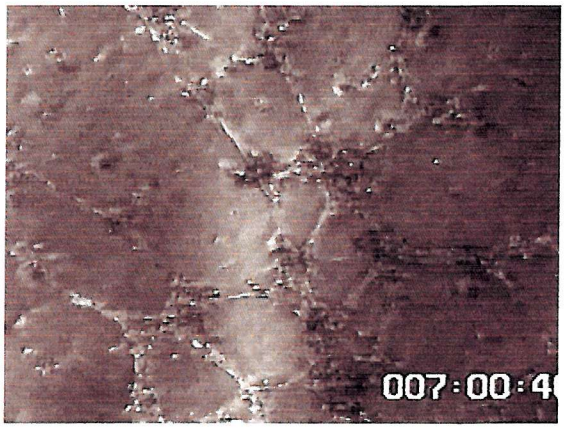
007:00:4

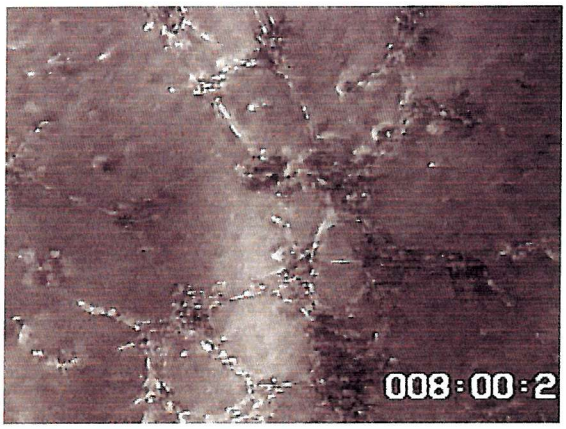
008:00:2

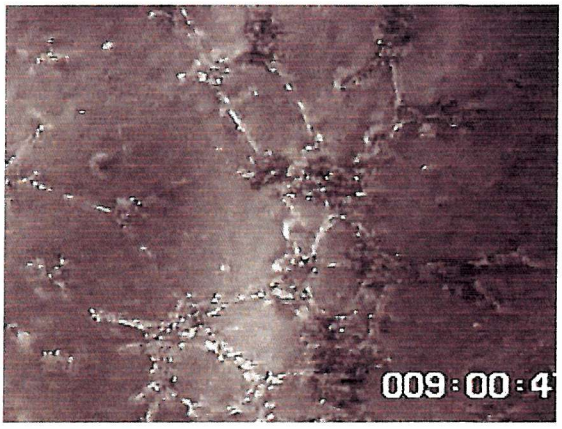
009:00:4

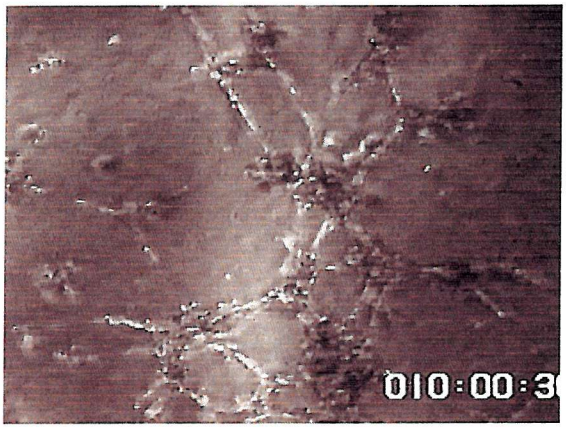
010:00:3

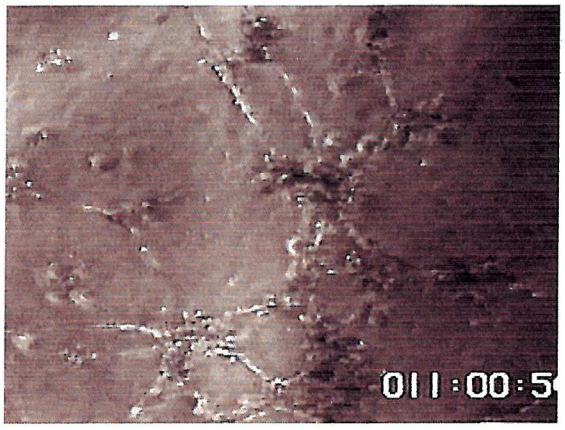
011:00:5

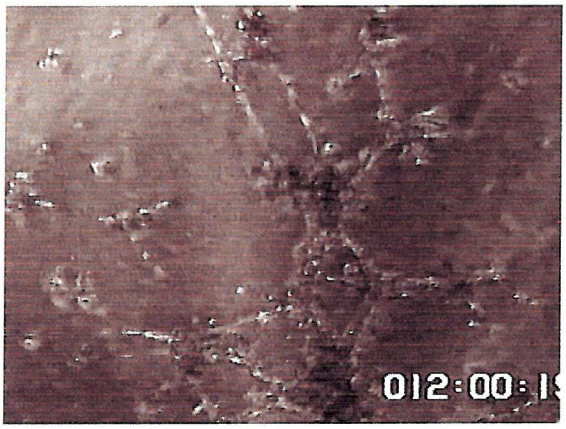
012:00:1

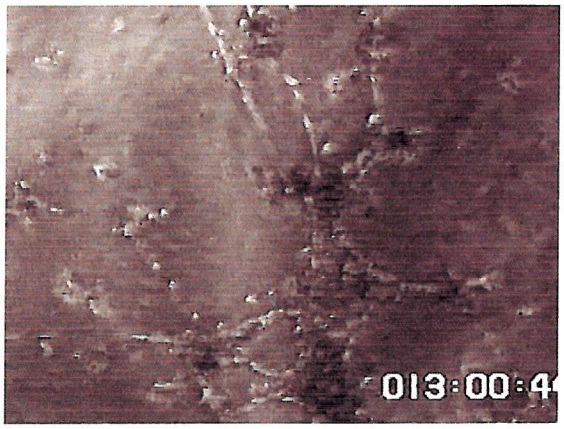
013:00:4

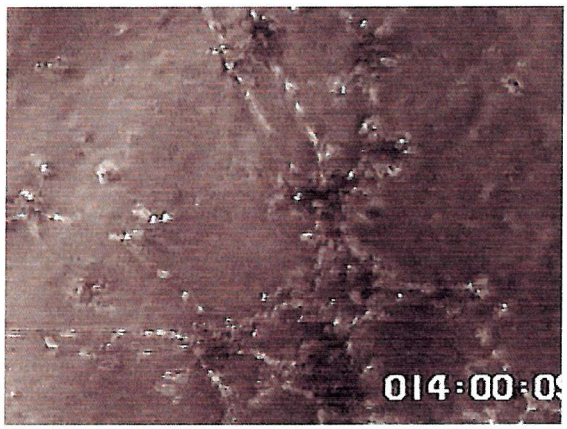
014:00:0

Immunocytochemistry for the Matrigel matrix component laminin β1 in endothelial/granulosa co-culture showed significant matrix remodelling, leaving areas of the original uniform Matrigel with areas completely free of laminin. Figure 8.10 shows part of the complex cellular network, with a) indicating granulosa clusters surrounded with laminin, b) showing HUVEC capillary-like structures coated in laminin, and c) showing areas of the Matrigel stripped of laminin.

The granulosa cells appeared to have gathered the laminin with them as they formed clusters and trails could be seen to radiate from the clusters.

Figure 8.11 shows a similar formation. Here granulosa clusters can clearly be seen to be surrounded by Matrigel, endothelial capillary-like structures are also coated in laminin and there are trails of laminin radiating from the granulosa cell clusters. The laminin does not appear as a uniform layer and extensive remodelling has been performed. This figure also further emphasises the specific nature in the interactions of the two cell types in structure formation.

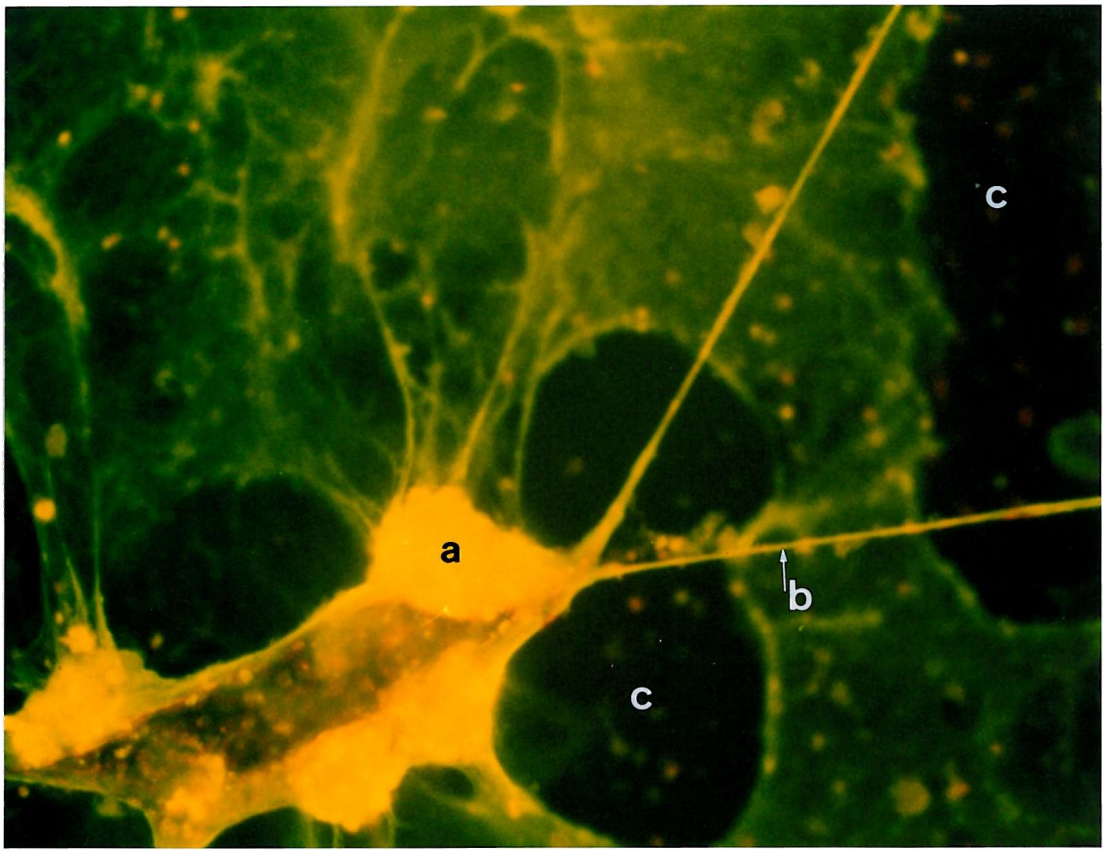


**Figure 8.10 Immunocytochemistry showing positive immunofluorescence using the anti-laminin β1.** a) indicating granulosa clusters surrounded with laminin, b) showing HUVEC capillary-like structures coated in laminin, and c) showing areas of the Matrigel stripped of laminin.

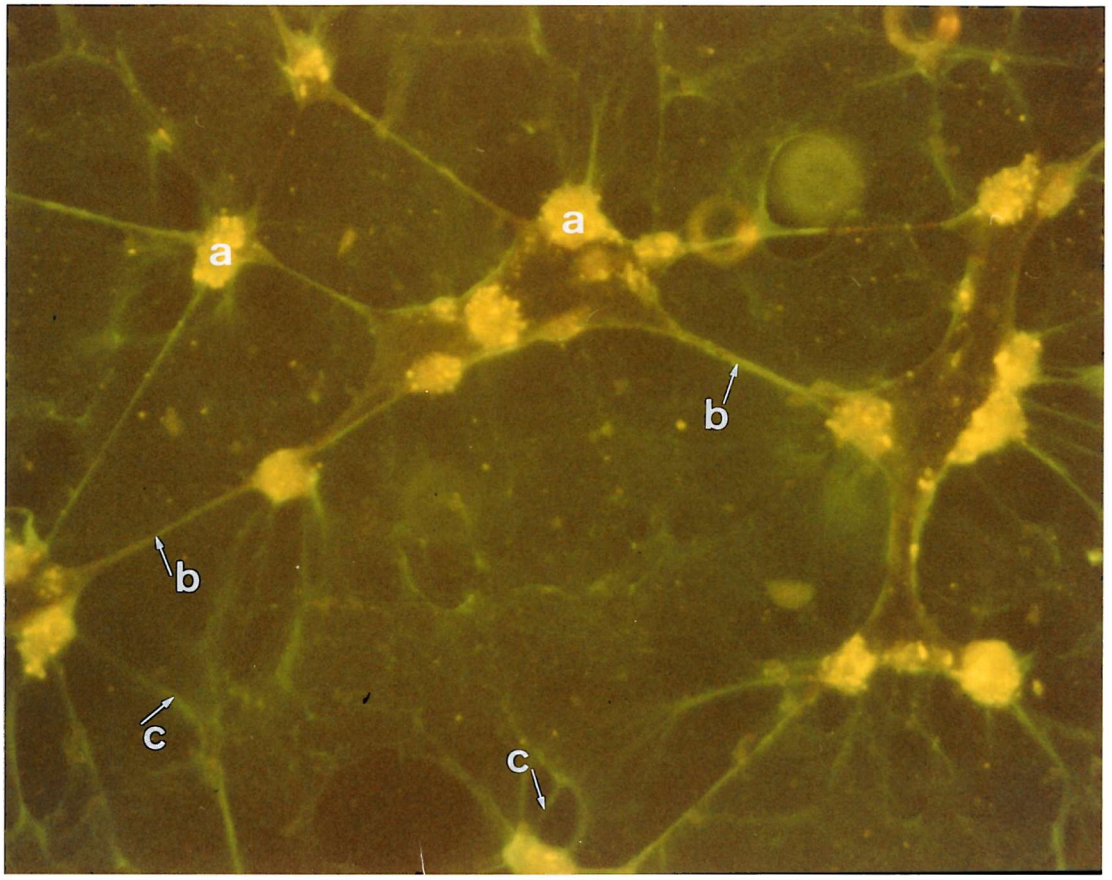


**Figure 8.11 Immunocytochemistry showing positive immunofluorescence using the anti-laminin β1.** a) indicating granulosa clusters surrounded with laminin, b) showing HUVEC capillary-like structures coated in laminin, and c) showing trails of laminin radiating from the granulosa cell clusters.

## 8.4 Discussion.

Angiogenesis is vital for the formation of the corpus luteum, this process involves considerable intercellular communication.

Previous studies have looked at the architecture of endothelial and granulosa cells on Matrigel but none have looked at the architecture when the two are cultured together. This finding of the cellular interactions of endothelial and granulosa cells when co-cultured on Matrigel is of great interest and may provide a model *in vitro* system for analysis of the cellular interactions which occur in the formation of the corpus luteum. The reasons for these cellular interactions have not been elucidated during the studies but there are numerous possible mechanisms. The structures form on both standard Matrigel and growth factor reduced Matrigel. However growth factors cannot be discarded as a possible cause because they are still present in growth factor reduced Matrigel. Integrins which have been shown to be involved in the formation of the capillary-like structures may play an important role as could any substance secreted by either cell type. The fact that these networks are formed regardless of the sequence of plating indicates that there is some form of intercellular signalling going on.

Within two hours of culture when endothelial cells are added to pre-clustered granulosa cells, and when both cell types are plated at the same time, endothelial cells appear to start the alignment process at the periphery of granulosa cells clusters. This may be due to the gathering of matrix components during the formation of these structures, with cells being attracted to the areas which are rich in ECM matrix components such as laminin.

# Chapter 9.

# Discussion.

This thesis has described the development of a novel method for the isolation and culture of human ovarian microvascular endothelial cells. The cell type was characterised by immunocytochemical studies, and observations of characteristic endothelial cell morphology. The studies performed on these cells showed the presence of both VEGF receptors, and a responsiveness to growth factors. Specific cellular interactions were seen in a co-culture model of endothelial and granulosa cells indicating the relationship of these two cell types in the corpus luteum.

Firstly, the research demonstrates that it is possible to culture cells from follicular material obtained from IVF aspirates. These aspirates would normally be discarded, however, the present study has shown that at least two cell types can be isolated and cultured from this material. The follicular fragments were cultured in Matrigel blobs which allowed the growth of endothelial cells from capillary fragments removed from the theca layer of the follicle wall. These cells formed capillary-like structures on the surface of the Matrigel and a characteristic endothelial cell cobblestone monolayer on the uncoated surface of the culture flask. Both of these features are characteristic of endothelial cells.

Further characterisation of the endothelial nature of the cells was by immunocytochemistry. The HOMEC possessed all of the endothelial specific markers, von Willebrand factor, UEA-1, PECAM-1, and E-selectin with at least the same level of positive immunofluorescence as that seen in HUVEC. The HOMEC however, constitutively expressed VCAM-1 unlike HUVEC. VCAM-1 expression is more typically seen in endothelial cells stimulated by cytokines (Haraldsen *et al.*, 1996). Its

expression in unstimulated HOMEC in the present study may reflect the special role of these cells in interacting with luteal cells and the tissue matrix during the rapid formation of the corpus luteum *in vitro*. The immunocytochemical studies also showed the HOMEC cultures to be very pure as there were very few cells in the cultures which did not show positive immunofluorescence for the endothelial cell specific markers.

These studies confirmed that the cells which had developed from follicular fragments were indeed endothelial cells. And further studies were facilitated by the fact that the cultures were very pure. However, the number of cells which were generated were not as large as those from other culture models such as HUVEC.

Development of RT and PCRs demonstrated the presence of both of the VEGF receptors flt-1 and KDR, as well as eNOS in HOMEC. These studies showed that the VEGF effects in the human corpus luteum could be mediated by either or both of the VEGF receptors on HOMEC. The effects of VEGF in endothelial cells has been shown in some circumstances to be coupled to the activation of eNOS (Morbidelli *et al.*, 1996). The present observations have shown that eNOS is expressed in HOMEC and therefore the constituents for important endothelial mechanisms in relation to VEGF action are in place in these cells.

Studies looking at the effect of VEGF showed a dose dependent increase in HOMEC proliferation in response to VEGF. This effect was also observed when HOMEC were cultured with granulosa cell conditioned media. The conditioned media was shown to contain VEGF by radioimmunoassay. Western blotting showed that the predominant isoform was $VEGF_{165}$, with lower levels of $VEGF_{121}$ and $VEGF_{189}$. Granulosa cells have also been shown to produce bFGF in culture, although bFGF did not have a statistically significant effect on endothelial cell proliferation in these studies.
An interesting observation of the VEGF proliferation assays with granulosa cell conditioned media was that the effects of VEGF on proliferation could be blocked with an anti-KDR antibody. These effects were not seen with an anti-flt-1 antibody indicating that the two VEGF receptors have different functions *in vivo*. This also

further confirmed that it was the VEGF in the granulosa cell conditioned media which was producing the mitogenic response. Further, the ability of L-NAME to inhibit endothelial cell proliferation in response to VEGF showed that NOS is important in the action of VEGF, and that by inhibiting the production of nitric oxide, the mitogenic effects of VEGF can be inhibited.

Finally, the ability of HOMEC and granulosa cells to form specific cellular architecture in co-culture is of great interest. Many previous studies have looked at the formation of endothelial capillary-like structures *in vitro*. However, there have been no other co-culture studies of this nature. The interactions of endothelial cells and granulosa cells via VEGF is not a new finding (Spanel-Borowski *et al.*, 1994). However, the fact that the cells interact structurally in culture may provide a model for further studies looking at the interactions of these cell types in the formation of the corpus luteum.
These structures formed on both standard and growth factor reduced Matrigel, irrespective of the order of plating. When fewer cells were involved in the cultures, it was possible to highlight the specificity of the interactions between the two cell types. The present study has not elucidated the mechanisms behind these interactions and this is an area of interest for future studies.

The studies presented in this thesis have shown the development of the first model for the isolation and culture of human ovarian microvascular endothelial cells. This model will provide a useful tool for researchers investigating the female reproductive system, enabling endothelial cells of the tissue of investigation to be used rather than cell lines or large vessel endothelial cells, as has previously been the case.

**Implications for clinical conditions.**

Angiogenesis has been reported to be a factor involved in many pathological conditions of the female reproductive system.
The mechanisms of selection during follicular development are as yet not completely

understood. The reason why one follicle proceeds to ovulate and form the corpus luteum whilst all other preovulatory follicles become atretic is unknown. A current opinion is that the development of the vasculature of the selected follicle is greater than that of the others. This increased vascularisation would lead to more nutrients reaching the follicle which may play a part in the selection process.

A condition related to the failure of the selection of a dominant follicle is polycystic ovary syndrome which in some circumstances is associated with anovulation and infertility. Patients with this condition have enlarged ovaries with a thickened capsule. Sectioning of the ovaries reveals multiple follicular subcapsular cysts which are lined with a few layers of granulosa cells and show hyperplasia of the theca interna with luteinization. Polycystic ovary syndrome results from a large number of small follicles developing, however, the normal path of folliculogenesis to ovulation rarely occurs. In this condition there is no selection of a dominant follicle and all of the preovulatory follicles become atretic (Franks, 1995).
There is evidence to suggest that polycystic ovary patients have increased ovarian vascularity. A recent study has shown higher serum VEGF concentrations and higher stromal blood flow in polycystic ovary patients than in women with normal ovaries. This increased vascularity caused by the increased amount of VEGF may result in a failure of diversion of blood flow away from the cohort of follicles to the leading follicle, thereby permitting uninhibited growth of other follicles and a multi follicular response (Agrawal *et al.*, 1998). A typical feature of polycystic ovary syndrome is elevation of follicular phase LH levels. LH has been shown to upregulate VEGF expression in granulosa cells and this raised LH level may play an important role in the increased vascularity of polycystic ovary syndrome (Neulen *et al.*, 1995). This finding of increased VEGF concentrations and ovarian vascularity suggests anti-angiogenic treatment may help as part of a treatment for this condition.

The recent finding that VEGF is essential for development of the follicles, and corpus luteum formation (Ferrara *et al.*, 1998) may provide new directions for research concerning anovulation and early pregnancy loss. It is possible that some causes of

human infertility are directly related to VEGF and follicular development and corpus luteum formation.

Ovarian hyperstimulation syndrome is a life threatening complication of superovulation and IVF treatment. One of the mechanisms responsible for ovarian hyperstimulation syndrome has been shown to be an increase in capillary permeability with acute fluid shift out of the intravascular space (Polishuk and Schenker, 1969) which results in marked ovarian enlargement, pleural effusion, electrolyte imbalance and hypotension (Schenker and Weinstein, 1978). This increase in capillary permeability is thought to be mediated by ovarian factors secreted in response to hCG hyperstimulation. VEGF is a major mediator of capillary leakage in ovarian hyperstimulation syndrome and can be detected at high levels in serum, peritoneal fluid and follicular fluid of patients (Agrawal *et al.*, 1999). This condition is a potential target for anti-VEGF therapy to reduce the high levels of VEGF and therefore reduce the increased permeability of the ovarian follicles.

Angiogenesis is also seen in pathological conditions such as tumours, diabetic retinopathy and rheumatoid arthritis.
Angiogenesis is a pre-requisite for solid tumour growth beyond a few millimetres, and capillary density of tumours has been linked with poor prognosis of the disease (Weidner and Folkman, 1996). Anti-VEGF therapy for the treatment of solid cancer has now become an area of extensive research. The growth of experimental tumours in mice can be inhibited by antibodies against VEGF (Kim *et al.*, 1993). As tumours develop and grow, areas become hypoxic and this hypoxia upregulates the expression of VEGF which in turn upregulates the expression of KDR in the developing endothelium (Plate *et al.*, 1992; Kremer *et al.*, 1997).
Karposi's sarcoma is the major neoplastic manifestation of the human immunodeficiency virus-induced AIDS. In Karposi's sarcoma the spindle cells have been identified as a source of VEGF (Cornali *et al.*, 1996), and the Karposi's sarcoma herpesvirus encoded G protein coupled receptor has been shown to induce VEGF, cell transformation and tumour formation in nude mice (Bais *et al.*, 1998). In addition, cell

lines derived from AIDS-linked Karposi's sarcoma express high levels of VEGF receptors (Masood *et al.*, 1997). As formation of a solid tumour is angiogenesis dependent, several strategies have been tested for targeting the endothelial compartment as part of anti-cancer therapy. Binding of VEGF to its receptors can be prevented by neutralising antibodies of soluble flt-1 (Kim *et al.*, 1993). Alternatively, tyrosine kinase inhibitors can be used to specifically block signalling downstream of the VEGF receptors (Strawn *et al.*, 1996).

Rheumatoid arthritis is characterised by chronic joint inflammation and infiltration of activated T cells and macrophages from the blood, together with the formation of new blood vessels. Cytokines have been shown to play a major role in rheumatoid arthritis in the stimulation of blood vessel development and recruitment of leucocytes to developing lesions (Paleolog, 1997). VEGF levels in the serum of patients with rheumatoid arthritis have been shown to be highly elevated, and it has been suggested that VEGF is involved in the pathogenesis of the disease (Harada *et al.*, 1998). Studies looking at targeting the individual cytokines involved in rheumatoid arthritis have shown that treatment with an antibody for tumour necrosis factor alpha (TNF alpha) result in the deactivation of the endothelium, leading to reduced transport of inflammatory cells to the joints. TNF alpha also decreases the levels of VEGF, suggesting that new blood vessel formation is also affected (Paleolog, 1997). These observations point towards anti-angiogenic therapies for the treatment of chronic inflammatory disease.

Proliferative diabetic retinopathy is a major cause of adult blindness. The condition is characterised by preretinal neovascularisation and fibrosis, which leads to haemorrhage and retinal detachment. The neovascularisation of the retina is thought to result from capillary closure which leads to areas of hypoxia and ischemia which induces angiogenesis (Kohner and Henkind, 1970; Bresnik *et al.*, 1977). There have been many angiogenic factors implicated in the neovascularisation of the retina of which VEGF is considered to be of major importance. VEGF levels have been shown to be upregulated in the aqueous fluid of patients with retinopathy (Shinoda *et al.*, 1999). It

is likely however, that VEGF is not the only angiogenic factor involved in proliferative diabetic retinopathy and that various factors may work together synergistically.

# References


Achen, M. G., Jeltsch, M., Kukk, E., Makinen, T., Vitali, A., Wilks, A. F., Alitalo, K., and Stacker, S. A. (1998). Vascular endothelial growth factor D (VEGF-D) is a ligand for the tyrosine kinases VEGF receptor-2 (Flk1) and VEGF receptor 3 (Flt4). *Proc. Natl. Acad. Sci. USA* **95**, 548-553.

Agrawal, R., Sladkevicius, P., and Engmann, L. (1998). Serum vascular growth factors concentrations and ovarian stromal blood flow are increased in women with polycystic ovaries. *Hum. Reprod.* **13**, 651-655.

Agrawal, R., Tan, S. L., Wild, S., Sladkevicius, P., Engmann, L., Payne, N., Bekir, J., Campbell, S., Conway, G., and Jacobs, H. (1999). Serum vascular endothelial growth factor concentrations in in vitro fertilization cycles predict the risk of ovarian hyperstimulation syndrome. *Fertil. Steril.* **71**, 287-293.

Aimes, R. T., and Quigley, J. P. (1995). Matrix metalloproteinase-2 is an interstitial collagenase. *J. Biol. Chem.* **270**, 5872-5876.

Aldred, L. F., and Cooke, B. A. (1983). The effect of cell damage on the density and steroidogenic capacity of rat testis leydig cells, using an NADH exclusion for determination of viability. *J. Steroid Biochem.* **18**, 411-414.

Amsterdam, A., Koch, Y., Lieberman, M. E., and Lindner, H. R. (1975). Distribution of binding sites for human chorionic gonadotropin in the preovulatory follicle of the rat. *J. Cell Biol.* **67**, 894.

Anderson, R. G. W. (1993). Caveolae: where incoming and outgoing messengers meet. *Proc. Natl. Acad. Sci. USA* **90**, 10909-10913.

Anthony, F. W., Evans, P. W., Wheeler, T., and Wood, P. J. (1997). Variation in detection of VEGF in maternal serum by immunoassay and the possible influence of binding proteins. *Ann. Clin. Biochem.* **34**, 276-280.

Aota, S., Nagai, T., and Yamada, K. M. (1991). Characterization of regions of fibronectin besides the arginine-glycine-aspartic acid sequence required for adhesive function of the cell-binding domain using site directed mutagenesis. *J. Biol. Chem.* **266**, 15938-15943.

Aten, R. F., Kolodecik, T. R., and Berhman, H. R. (1995). A cell adhesion receptor antiserum abolishes, whereas laminin and fibronectin pomote, luteinization of cultured rat granulosa cells. *Endocrinol.* **136**, 1753-1758.

Azmi, T. I., O'Shea, J. D., Bruce, N. W., and Rodgers, R. J. (1984). Morphometry of the functional and regressing corpus luteum of the guinea pig. *Anat. Rec.* **210**, 33-40.

Bacharach, E., Itin, A., and Keshet, E. (1992). In vivo patterns of expression of urokinase and its inhibitor PAI-1 suggest a concerted role in regulating physiological angiogenesis. *Proc. Natl. Acad. Sci. USA* **89**, 10686-10690.

Bagavandoss, P., and Wilks, J. W. (1991). Isolation and characterization of microvascular endothelial cells from developing corpus luteum. *Biol. Reprod.* **44**, 1132-1139.

Bais, C., Santomasso, B., Coso, O., Arvanitakis, L., Raaka, E. G., Gutkind, J. S., Asch, A. S., Cesarman, E., Gerhengorn, M. C., and Mesri, E. A. (1998). G protein-coupled receptor of Karposi's sarcoma-associated herpesvirus is a viral oncogene and angiogenesis activator. *Nature* **391**, 86-89.

Baragi, V. M., Fliszar, C. J., Conroy, M. C., Ye, Q. Z., Shipley, J. M., and Welgus, H. G. (1994). Contribution of the c-terminal domain of metalloproteinases to binding by tissue inhibitor of metalloproteinases, c-terminal truncated stromelysin and matrilysin exhibit equally compromised binding affinities as compared to full length stromelysin. *J. Biol. Chem.* **269**, 12692-12697.

Barleon, B., Sozzani, S., Zhou, D., Weich, H. A., Mantovani, A., and Marme, D. (1996). Migration of human monocytes in response to VEGF is mediated via the VEGF receptor flt-1. *Blood* **87**, 3336-3343.

Bassett, D. L. (1943). The changes in the vascular pattern of the ovary of the albino rat during the estrous cycle. *Am. J. Anat.* **73**, 251-292.

Beck, K., Hunter, I., and Engel, J. (1990). Structure and function of laminin, anatomy of a multidomain glycoprotein. *FASEB* **4**, 148-160.

Beers, W. H., Strickland, S., and Reich, E. (1975). Ovarian plasminogen activator: relationship to ovulation and hormonal regulation. *Cell* **6**, 387.

Behrman, H. R. (1979). Prostaglandins in hypothalamo-pituitary and ovarian function. *Ann. Rev. Physiol.* **41**, 685-700.

Behrman, H. R., Aten, R. F., and Pepperell, J. R. (1991). Cell-to-cell interactions in luteinization and luteolysis. In *Ovarian endocrinology*. Hillier, S. G. Blackwell Scientific Publications.

Behrman, H. R., Endo, T., Aten, R. F., and Musicki, B. (1993). Corpus luteum function and regression. *Reprod. Med. Rev.* **2**. 153-180.

Bjersing, L. (1967). The morphology and endocrine function of granulosa cells of ovarian follicles and corpora lutea. *Acta Endocrinol.* **125**, 5.

Blandau, R., and Rumery, R. (1963). Measurements of intrafollicular pressure in ovulatory and preovulatory follicles in the rat. *Fertil. Steril.* **14**, 330.

Boocock, C. A., Charnock-Jones, D. S., Sharkey, A. M., McLaren, J., Berker, P. J., Wright, K. A., Twentyman, P. R., and Smith, S. (1995). Expression of vascular endothelial growth factor and its receptors flt and KDR in ovarian carcinoma. *J. Natl. Cancer. Inst.* **87**, 469-476.

Bortolussi, M., Marini, G., and Dal Lago, A. (1977). Autoradiographic studies of the distribution of LH (hCG) receptors in the ovary of untreated and gonadotropin-primed immature rats. *Cell Tissue Res.* **183**, 329.

Bouck, N., Stellmach, V., and Hsu, S. C. (1996). How tumors become angiogenic. *Adv. Cancer Res.* **69**, 135-174.

Bresnik, G. H., David, M. D., and Myers, F. L. (1977). Clinicopathologic correlations in diabetic retinopathy. *Am. J. Opthalmol.* **95**, 1215-1220.

Brock, T. A., Dvorak, H. F., and Senger, D. R. (1991). Tumor-secreted vascular permeability factor increases cytosolic Ca2+ and von willebrand factor release in human endothelial cells. *Am. J. Pathol.* **138**, 213-221.

Brown, K. J., Maynes, S. F., Bezos, A., Maguire, D. J., Ford, M. D., and Parish, C. R. (1996). A novel in vitro assay for human angiogenesis. *Lab. Invest.* **75**. 539-555.

Broxmeyer, H. E., Cooper, S., Li, Z. H., and Song, H. Y. (1995). Myeloid progenitor cells regulatory effects of vascular endothelial growth factor. *Int. J. Haem.* **62**, 203-215.

Bruce, N. W., and Moor, R. M. (1976). Capillary blood flow to ovarian follicles, stroma and corpora lutea of anethetized sheep. *J. Reprod. Fertil.* **46**, 299-304.

Burr, J. J., and Davies, J. I. (1951). The vascular system of the rabbit ovary and its relationship to ovulation. *Anat. Rec.* **111**, 273-297.

Cao, J., Sato, H., Takino, T., and Selki, M. (1995). The C-terminal region of membrane-type matrix metalloproteinase is a functional transmembrane domain required for protein-gelatinase A activation. *J. Biol. Chem.* **270**, 801-805.

Carmeliet, P., Schoonjans, L., Kieckens, L., Ream, B., Degen, J., Bronson, R., De Vos, R., van den Oord, J. J., Collen, D., and Mulligan, R. C. (1994). Physiological cosequences of loss of plasminogen activator gene function in mice. *Nature* **368**, 419-424.

Charnoch-Jones, D. S., Sharkey, A. M., Boocock, C. A., Ahmed, A., Plevin, R., Ferrara, N., and Smith, S. K. (1994). Vascular endothelial growth factor receptor localization and activation in human trophoblast and choriocarcinoma cells. *Biol. Reprod.* **51**, 524-530.

Chin, J. R., Murphey, G., and Werb, Z. (1985). Stromelysin, a connective tissue-degrading metalloendopeptidase secreted by stimulated rabbit synovial fibroblasts in parallel with collagenase. *J. Biol. Chem.* **260**, 12367-12376.

Chin, K., Kurashima, Y., Ogura, T., Tajiri, H., Yoshida, S., and Esumi, H. (1997). Induction of vascular endothelial growth factor by nitric oxide in human glioblastoma and hepatocellular carcinoma cells. *Oncogene* **15**, 437-442.

Christenson, L. K., and Stouffer, R. L. (1995). Isolation and culture of primate luteal endothelial cells. *Biol. Reprod.* **52**, 68.

Christenson, L. K., and Stouffer, R. L. (1996). Proliferation of microvascular endothelial cells in the primate corpus luteum during the menstrual cycle and simulated early pregnancy. *Endocrinol.* **137**, 367-374.

Christenson, L. K., and Stouffer, R. L. (1996). Isolation and culture of microvascular endothelial cells from the primate corpus luteum. *Biol. Reprod.* **55**, 1397-1404.

Clauss, M., Gerlarch, M., gerlarch, H., Brett, J., Wang, F., Familletti, P. C., Pan, Y. C., Olander, J. V., Connolly, D. T., and Stern, D. (1990). Vascular permeability factor: a tumor-derived polypeptide that induces endothelial cell and monocyte procoagulant activity, and promotes monocyte migration. *J. Exp. Med.* **172**, 1535-1545.

Coggi, G., Dell'Orto, P., and Viale, G. (1986). Avidin-biotin methods. In *Immunocytochemistry, modern methods and applications*, (2nd edn), Polak, J.M., and Van Noorden, S. 54-70. Jonh Wright & sons, Bristol.

Cohen, T., Gitay-Goren, H., Sharon, R., Shibuya, M., Halaban, R., Levi, B., and Neufeld, G. (1995). VEGF-121, a vascular endothelial growth factor (VEGF) isoform lacking heparin binding ability, requires cell surface heparan sulfates for efficient binding to the VEGF receptors of human melanoma cells. *J. Biol. Chem.* **270**, 11322-11326.

Collier, I. E., Wilhelm, S. M., Eisen, A. Z., Marmer, B. L., Grant, G. A., Seltzer, J. L., Kronberger, A., He, C., Bauer, E. A., and Goldberg, G. I. (1988) H-ras oncogene-transformed human bronchial epithelial cells (TBE-1) secrete a single matrix metalloproteinase capable of degrading basement membrane collagen. *J. Biol. Chem.* **263**, 6579-6587.

Coons, A. H., Creech, H. J., and Jones, R. N. (1941). Immunological properties of an antibody containing a fluorescent group. *Proc. Soc. Exp. Biol. Med.* **47**, 200-202.

Conley, A. J., Kaminski, M. A., Dubowski, S. A., Jablonka-Shariff, A., Redmer, D. A., and Reynolds, L. P. (1995). Immunolocalization of 3β-hydroysteroid dehydrogenase and P450 17α-hydroxylase during follicular and luteal development in pigs, sheep and cows. *Biol. Reprod.* **52**, 1081-1094.

Connolly, D.T., Olander, J. V., Heunelman, D., Nelson, R., Monsell, R., Siegel, N., Haymore, B. L., Leimgruber, R. M., and Feder, J. (1998). Human vascular permeability factor. *J. Biol. Chem.* **264**, 20017-20024.

Cornali, E., Zietz, C., Benelli, R., Weninger, W., Breier, G., Tschachler, E., Albini, A., and Sturzl, M. (1996). Vascular endothelial growth factor regulates angiogenesis and vascular permeability in Karposi's sarcoma. *Am. J. Pathol.* **149**, 1851-1869.

Craig, L. E., Spelman, J. P., Strandberg, J. D., and Zink, M. C. (1998). Endothelial cells from diverse tissues exhibit differences in growth and morphology. *Microvasc. Res.* **55**, 65-76.

Curry, T. E., Dean, D. D., Woessner, J. F., and Le Maire, W. J. (1985). The extraction of a tissue collagenase associated with ovulation in the rat. *Biol. Reprod.* **33**, 981-991.

Curry, T. E., Manns, J. S., Huang, M. H., and Keeble, S. C. (1992). Gelatinase and proteoglycans activity during the periovulatory period in the rat. *Biol. Reprod.* **46**, 256-264.

Damber, J. E., Cajander, S., Gafvels, M., and Selstam, G. (1987). Blood flow changes and vascular appearance in preovulatory follicles and corpora lutea in immature, pregnant mare's serum gonadotropin-treated rats. *Biol. Reprod.* **37**, 651-658.

Davis, S., Aldrich, T. H., Jones, P. F., Acherson, A., Compton, D. L., Jain, V., Ryan, T. E., Bruno, J., Radziejewski, C., Maisonpierre, P. C., and Yancopoulos, G. D. (1996). Isolation of angiopoietin-1, a ligand for the tie-2 receptor, by secretion-trap expression cloning. *Cell* **87**, 1161-1169.

DeLisser, H. M., Newman, P. J., and Albelda, S. M. (1993). Platelet endothelial cell adhesion molecule (CD31). *Curr. Top. Microbiol. Immunol.* **184**, 37-43.

Dembinskakiec, A., Dulak, J., Partyka, L., Huk, I., and Mailnski, T. (1997). VEGF-nitric oxide reciprocal regulation. *Nature Med.* **3**, 1177.

Deroanne, C. F., Hajitou, A., Calberg-Bacq, C. M., Nusgens, B. V., and Lapiere, C. M. (1997). Angiogenesis by fibroblast growth factor 4 is mediated through an autocrine up-regulation of vascular endothelial growth factor expression. *Cancer Res.* **57**, 5590-5597.

De vries, C., Escobedo, J. A., Ueno, H., Houck, K., Ferrara, N., and Williams, L. T. (1992). The fms-like tyrosine kinase, a receptor for vascular endothelial growth factor. *Science* **255**, 989-991.

DeZerega, G. S., Richardson, C. M., Davis, T. F., Hodgen, G. D., and Catt, K. J. (1980). Fluorescence localization of luteinizing hormone/human chorionic gonadotropin uptake in the primate ovary: characterization of the preovulatory ovary. *Fertil. Steril.* **34**, 379-385.

Dharmarajan, A. M., Bruce, N. W., and Meyer, G. T. (1985). Quantitative ultrastructural characteristics relating to transport between luteal cell cytoplasm and blood in the corpus luteum of the pregnant rat. *Am. J. Anat.* **172**, 87-99.

Dharmarajan, A. M., Bruce, N. W., and McArdle, H. J. (1986). Comparison of flow rates and composition of ovarian lymph and blood in the day-16 pregnant rat. *J Reprod. Fertil.* **77**, 169-76.

Dissen, G. A., Lara, H. E., Fahrenbach, W. H., Costa, M. E., and Ojeda, S. R. (1994). Immature rat ovaries become revascularised rapidly after autotransplantation and show a gonadotrophin-dependent increase in angiogenic factor gene expression. *Endocrinol.* **134**, 1146-1154.

Doraiswamy, V., Knutson, D. L., Grazul-Bilska, A. T. Redmer, D. A., and Reynolds, L. P. (1998). Fibroblast growth factor receptor-1 and -2 in the ovine corpus luteum throughout the estrous cycle. *Growth Factors* **16**, 125-135.

Doyle, J. B. (1951). Exploratory culdotomy for observation of tuboovarian physiology at ovulation time. *Fertil. Steril.* **2**, 475.

Dveksler, G. S., Baslie, A. A., and Dieffenbach, C. W. (1992). Analysis of gene expression: use of oligonucleotide primer for glyceraldehyde-3-phosphate dehydrogenase. *PCR Methods and Applications* **1**, 283-285.

Dvorak, H. F. (1986). Tumors: wounds that do not heal. Similarity between tumor stroma generation and wound healing. *New Eng. J. Med.* **315**, 1650-1658.

Dvorak, H. F., Nagy, J. A., Berse, B., Brown, L. F., Yeo, K. T., Yeo, T. K., Dvorak, A. M., Vanderwater, L., Sioussat, T. M., and Senger, D. R. (1992). Vascular permeability factor, fibrin, and the pathogenesis of tumor stroma formation. *Ann. N.Y. Acad. Sci.* **667**, 110-111.

Dvorak, A. M., Kohn, S., Morgan, E. S., Fox, P., Nagy, J. A., and Dvorak, H. F. (1996). The vesiculo-vacuolar organelle (VVO): a distinct endothelial cell structure that provides a transcellular pathway for macromolecular extravasation. *J. Leukocyte Biol.* **59**, 100-115.

Egan, S. E., Giddings, B. W., Brooks, M. W., Bunday, L., Sizeland, A. M., and Weinberg, R. A. (1993). Association of sos ras exchange protein with GRB2 is implicated in tyrosine kinase signal transduction and transformation. *Nature* **363**, 45-51.

Enders, A. C. (1973). Cytology of the corpus luteum. *Biol. Reprod.* **8**, 158-182.

Enholm, B., Paavonen, K., Ristimaeki, A., Kumar, V., Gunji, Y., Klefstrom, J., Kivinen, L., Laiho, M., Olofsson, B., Joukov, V., Eriksson, U., and Alitalo, K. (1997). Comparison of VEGF, VEGF-B, VEGF-C and Ang-1 mRNA regulation by serum, growth factors, oncoproteins and hypoxia. *Oncogene*. **14**, 2475-2483.

Ercolani, L., Florence, B., Denaro, M., and Alexander, M. (1998). Isolation and complete sequence of a functional human glyceraldehyde-3-phosphate dehydrogenase gene. *J. Biol. Chem.* **263**, 15335-15341.

Ericson, G. F., Wang, C., and Hsueh, A. J. W. (1979). FSH induction of functional LH receptors in granulosa cells cultured in a chemically defined medium. *Nature* **279**, 336.

Espey, L. L., and Lipner, H. (1963). Measurements of intrafollicular presures in the rabbit ovary. *Am. J. Physiol.* **205**, 1067.

Espey, L. L. (1992). Ovulation as an inflammatory process. In *Local regulation of ovarian function* 183-200. Eds Sjoberg, N., Hamberger, L., Janson, P., Owman, C., and Coelingh-Bennink, H. Parthenon Publishing group, Park Ridge.

Espey, L. L. (1994). Current status of the hypothesis that mammalian ovulation is comparable to an inflammatory reaction. *Biol. Reprod.* **50**, 233-238.

Esser, S., Wolburg, K., Wolburg, H., Breier, G., Kurzchalia, T., and Risau, W. (1998). Vascular endothelial growth factor induces endothelial fenestrations in vitro. *J. Cell Biol.* **140**, 947-959

Eyster, K. M., Ottobre, J. S., Stouffer, R. L. (1985). Adenylate cyclase in the corpus luteum of the rhesus monkey. Changes in basal and gonadotropin-sensitive activities during the luteal phase of the menstrual cycle. *Endocrinol.* **117**, 1571-1577.

Fajardo, L. F. (1989). The complexity of endothelial cells. *Am. J. Clin. Pathol.* **92**, 241-250.

Fenyves, A. M., Behrens, J., and Spanel-Borowski, K. (1993). Cultured microvascular endothelial cells (mvec) differ in cytoskeleton, expression of cadhedrins and fibronectin matrix - a study under the influence of interferon-gamma. *J. Cell Sci.* **106**, 879-890.

Feron, O., Belhassen, L., Kobzik, L., Smith, T. W., Kelly, R. A., and Michel, T. (1996). Endothelial nitric oxide synthase targeting to caveolae-specific interactions with caveolin isoforms in cardiac myocytes and endothelial cells. *J. Biol. Chem.* **271**, 22810-22814.

Ferrara, N., and Henzel, W. J. (1989). Pituitary follicular cells secrete a novel heparin-binding growth factor specific for vascular endothelial cells. *Biochem. Biophys. Res. Com.* **161**, 851-858.

Ferrara, N., Leung, D. W., Cachianes, G., Winer, J., and Henzel, W. J. (1991). Purification and cloning of vascular endothelial growth factor secreted by folliculostellate cells. *Methods Enzymol.* **198**, 391-405.

Ferrara, N., Chen, H., Davis-Smyth, T., Gerber, H., Nguyen, T., Peers, D., Chisholm, V., Hillian, K., and Schwall, R. H. (1998). Vascular endothelial growth factor is essential for corpus luteum angiogenesis. *Nature Med.* **4**, 336-340.

Finkenzeller, G., Sparacio, A., Technau, A., Marme, D., and Siemeister, G. (1997). Sp1 recognition sites in the proximal promoter of the human vascular endothelial growth factor gene are essential for platelet-derived growth factor-induced gene expression. *Oncogene* **15**, 669-676.

Flaumenhaft, R., and Rifkin, D. B. (1992). The extracellular regulation of growth factor action. *Mol. Biol. Cell* **3**, 1057-1065.

Folkman, J. (1985). Tumor angiogenesis. *Adv. Cancer Res.* **43**, 175-203.

Folkman, J. (1995). Clinical applications of research on angiogenesis. *N. Eng. J. Med.* **333**, 1757-1763.

Fortune, J. E. (1994). Ovarian follicular growth and development in mammals. *Biol. Reprod.* **50**, 225-232.

Franks, S. (1995). Medical progress article: Polysistic ovary syndrome. *N. Engl. J. Med.* **333**, 853-861.

Fraser, H. M., Lunn, S. F., Harrison, D. J., and Kerr, J. B. (1999). Luteal regression in the primate: different forms of cell death during natural and gonadotropin-releasing hormone antagonist or prostaglandin analogue induced luteolysis. *Biol. Reprod.* **61**, 1468-1479.

Freije, J. M. P., Diez-Itza, I., Balbin, M., Sanchez, L. M., Blasco, R., Tolivia, J., and Lopez-Otin, C. (1994). Molecular cloning and expression of collagenase-3, a novel human matrix metalloproteinase produced by breast carcinomas. *J. Biol. Chem.* **269**, 16766-16773.

Garcia-Cardena, G., Oh, P., Liu, J., Schnitzer, J. E., and Sessa, W. C. (1996). Targeting of nitric oxide synthase to endothelial cell caveolae via palmitoylation: implications for nitric oxide signaling. *Proc. Natl. Acad. Sci. USA* **93**, 6448-6453.

Garrido, C., Saule, S., and Gospodarowicz, D. (1993). Transcriptional regulation of vascular endothelial growth factor gene expression in ovarian bovine granulosa cells. *Growth Factors* **8**, 109-117.

Ghinea, N., Hai, M. T. V., Groyer-Picard, M., and Milgrom, E. (1994). How protein hormones reach their target cells. Receptor-mediated transcytosis of hCG through endothelial cells. *J. Cell Biol.* **125**, 87-97.

Gitay-Goren, H., Soker, S., Vlodavsky, I., and Neufeld, G. (1992). The binding of vascular endothelial growth factor to its receptors is dependent on cell surface-associated heparin-like molecules. *J. Biol. Chem.* **267**, 6093-6098.

Golay, J., Passerini, F., and Introna, M. (1991). A simple and rapid method to analyse specific mRNAs from few cells in a semi-quantitative way using the polymerase chain reaction. *PCR Methods and Applications* **1**, 144-145.

Goldberg, G. I., Wilhelm, S. M., Kronberger, A., Bauer, E. A., Grant, G. A., and Eisen, A. Z. (1986). Human fibroblast collagenase. Complete primary structure and homology to an oncogene transfomation-induced rat protein. *J. Biol. Chem.* **261**, 6600-6605.

Gordon, J. D., Mesiano, S., Zaloudek, C. J., and Jaffe, R.B. (1996). Vascular endothelial growth factor localization in human ovary and fallopian tubes: possible role in reproductive function and ovarian cyst formation. *J. Clin. Endocrinol. Metab.* **81**, 353-359.

Gorlin, R. J. (1997). Fibroblast growth factors, their receptors and receptor disorders. *J. Cranio-Maxillo-Facial Surg.* **25**, 69-79.

Goto, F., Goto, K., Weindel, K., and Folkman, J. (1993). Synergistic effect of vascular endothelial growth factor and basic fibroblast growth factor on the proliferation and cord formation of bovine capillary endothelial cells within collagen gels. *Lab. Invest.* **69**, 508-517.

Gougeon, A. (1996). Regulation of ovarian folliclular development in primates: Fact and hypotheses. *Endocrin. Rev.* **17**, 121-155.

Groome, N. P., Illingworth, P. J., O'Brien, M., Pai, R., Rodger, F. E., Mather, J., and McNeilly, A. S. (1996). Measurement of dimeric inhibin B throughout the human menstrual cycle. *J. Clin. Endocrinol. Metab.* **81**, 1401-1405.

Gross, J. L., Moscatelli, D., Jaffe, E. A., and Rifkin, D. (1982). Plasminogen activator and collagenase production by cultured capillary endothelial cells. *J. Cell Biol.* **95**, 974-981.

Gupta, K., Ramakrishnan, S., Browne, P. V., Solovey, A., and Hebbel, R. P. (1997). A novel technique for culture of human dermal microvascular endothelial cells under either serum-free or serum-supplemented conditions: Isolation by panning and stimulation with vascular endothelial growth factor. *Exp. Cell Res.* **230**, 244-251.

Haas, T. L., Davis, S. J., and Madri, J. A. (1998). Three-dimensional type I collagen lattices induce coordinate expression of matrix metalloproteinases MT1-MMP and MMP-2 in microvascular endothelial cells. *J. Biol. Chem.* **273**, 3604-3610.

Harada, M., Mitsuyama, K., Yoshida, H., Sakisaka, S., Taniguchi, E., Kawaguchi, T., Ariyoshi, M., Saiki, T., Sakamoto, M., Nagata, K., Sata, M., Matsuo, K., and Tanikawa, K. (1998). Vascular endothelial growth factor in patients with rheumatoid arthritis. *Scandinavian J. Rheumatol.* **27**, 377-380.

Haraldsen, G. (1996). Cytokine regulated expression of E-selectin, intercellular adhesion molecule-1 (ICAM-1), and vascular cell adhesion molecule-1 (VCAM-1) in human intestinal microvascular endothelial cells. *J. Immunol.* **156**, 2558-2565.

He, Z., and Tessier-Lavigne, M. (1997). Neuropilin is a receptor for the axonal chemorepellent semaphorin III. *Cell* **90**, 739-751.

Hendrick, J., de Groot, P. G., Sixma, J. J., and van Mourik, J. A. (1988). Storage and secretion of von Willebrand factor by endothelial cells. *Haemostasis.* **18**, 246-261.

Hillier, S. G., Reichert, L. E., and Van Hall, E. V. (1981). Control of preovulatory follicular estrogen biosynthesis in the human ovary. *J. Clin. Endocrinol. Metab.* **52**, 799.

Hillier, S. G. (1985). Sex steroid metabolism and follicular development in the ovaries. *Oxf. Rev. Reprod. Biol.* 7, 168-222.

Hillier, S. G., Whitelaw, P. F., and Smyth, C. D. (1994). Follicular estrogen synthesis-the 2-cell, 2-gonadotropin model revisited. *Mol. Cell. Endocrinol.* **100**, 51-54.

Hirsch, B., Leonhardt, S., Jarry, H., Reich, R., Tsafriri, A., and Wuttke, W. (1993). In vivo measurement of rat ovarian collagenolytic activities. *Endocirnol.* **133**, 2761-2765.

Holthofer, H., Virtanen, I., Kariniemi, L., Hormia, M., Linder, E., and Miettinen, A. (1982). Ulex europaeus-1 lectin as a marker for vascular endothelium in human tissues. *Lab. Invest.* **47**, 60-66.

Hood, J. D., Meininger, C. J., Ziche, M., and Granger, H. J. (1998). VEGF upregulates ecNOS message, protein, and NO production in human endothelial cells. *Am. J. Physiol.* **274**, H1054-H1058.

Houck, K. A., Ferrara, N., Winer, J., Cachianes, G. Li, B., and Leung, D. W. (1991). the vascular endothelial growth factor family-identification of a fourth molecular species and characterization of alternative splicing of RNA. *Mol. Endocrinol.* **5**, 1806-1814.

Houck, K. A., Leung, D. W., Rowland, A. M., Winer, J., and Ferrara, N. (1992). Dual regulation of vascular endothelial growth factor bioavailability by genetic and proteolytic mechanisms. *J. Biol. Chem.* **267**, 26031-26037.

Hu, D. E., and Fan, T. P. (1995). Protein kinase C inhibitor calphostin C prevenys cytokine-induced angiogenesis in the rat. *Inflammation* **19**, 39-54.

Huang, L., Turck, C. W., Rao, P., and Peters, K. G. (1995). GRB2 and SH-PTP2: Potentially important endothelial signaling molecules downstream of the TEK/TIE2 receptor tyrosine kinase. *Oncogene* **11**, 2097-2103.

Hughes, S. E., Crossman, D., and Hall, P. A. (1993). Expression of basic and acidic fibroblast growth factors and their receptors in normal and atherosclerotic human arteries. *Cardiovasc. Res.* **27**, 1214-1219.

Hughes, S. E. (1996). Functional characterization of the spontaneously transformed human umbilical vein endothelial cell line ECV304: Use in an in vitro model of angiogenesis. *Exp. Cell Res.* **225**, 171-185.

Hurwitz, A., Dushnik, M., Solomon, H., Ben-Chetrit, A., Finci-Yeheskel, Z., Milwidski, A., Mayer, M., Adashi, E. Y., and Yagel, S. (1993). Cytokine mediated regulation of rat ovarian function: interleukin-1beta stimulates the accumulation of a 92 kilodalton gelatinase. *Endocrinol.* **132**, 2709-2714.

Ilan, N., Mahooti, S., and Madri, J. A. (1998). Distinct signal transduction pathways are utilized during the tube formation and survival phases of in vitro angiogenesis. *J. Cell. Sci.* **111**, 3621-3631.

Innis, M. A., Gelfand, D. H., Sninsky, J. J., and White, T. J. (1990). *PCR Protocols: A guide to Methods and Applications.* **Part 1**, pp 1-166. Academic Press, Inc.

Jablonka-Shariff, A., Grazul-Bilska, A. T., Redmer, D. A., and Reynolds, L. P. (1993). Growth and cellular proliferation of ovine lutea throughout the estrous cycle. *Endocrinol.* **133**, 1871-1879.

Jaffe, E. A., Nachman, R. L., Becker, C. G., and Minidi, C. R. (1973). Culture of human endothelial cells derived from umbilical veins: identification by morphological and immunological criteria. *J. Clin. Invest.* **52**, 2745-2756.

Jeltsch, M., Kaipainen, A., Joukov, V., Meng, X. J., Lakso, M., Rauvala, H., Swartz, M., Fukumura, D., Jain, R. K., and Alitalo, K. (1997). Hperplasia of lymphatic vessels in VEGF-C transgenic mice. *Science* **276**, 1423-1425.

Jenkins, J. M., Davies, D. W., Devonport, H., Anthony, F. W., Gadd, S. C., Watson, R. H., Masson, G. M. (1991). Comparison of poor responders with good responders using a standard buserelin human menopausal gonadotropin regime for in vitro fertilization. *Human Reprod.* **6**, 918-921.

Jocelyn, H. D., and Setchell, B. P. (1972). Regneir de Graaf on the human reproductive organs. *J. Reprod. Fertil.* **17**, 131-135.

Jones, J. I., and Clemmons, D. R. (1995). Insulin-like growth factors and their binding proteins-biological actions. *Endocrine Rev.* **16**, 3-34.

Jones, M. K., Sarfeh, I. J., and Tarnawski, A. S. (1998). Induction of in vitro angiogenesis in the endothelial-derived cell line, EA hy926, by ethanol is mediated through PKC and MAPK. *Biochem. Biophys. Res. Com.* **249**, 118-123.

Joukov, V., Pajusola, K., Kaipainen, A., Chilov, D., Lahtinen, I., Kukk, E., Saksela, O., Kalkkinen, N., and Alitalo, K. (1996). A novel vascular endothelial growth factor, VEGF-C is a ligand for the flt-4 (VEGFR-3) and KDR (VEGFR-2) receptor tyrosine kinase. *The EMBO Journal* **15**, 290-298.

Ju, H., Zou, R., Venema, V. J., and Venema, R. C. (1997). Direct interaction of endothelial nitric oxide synthase and caveolin-1 inhibits synthase activity. *J. Biol. Chem.* **272**, 18522-18525.

Kacemi, A., Challier, J. C., Galtier, M., and Olive, G. (1996). Culture of endothelial cells from placental microvessels. *Cell and Tissue Res.* **283**, 183-190.

Kaipainen, A., Korhonen, J., Pajusola, K., Aprelikova, O., Persico, M. G., Terman, B. I., and Alitalo, K. (1993). The related flt-4, flt-1 and KDR receptor tyrosine kinases shoe distinct expression patterns in human fetal endothelial cells. *J. Exp. Med.* **178**, 2077-2088.

Kamat, B. R., Brown, L. F., Manseau, E. J., Senger, D. R., and Dvorak, H. F. (1995). Expression of vascular permeability factor/vascular endothelial growth factor by human granulosa and theca lutein cells. Role in corpus luteum development. *Am. J. Pathol.* **146**, 157-165.

Keck, P. J., Hauser, S. D., Krivi, G., Sanzo, K., Warren, T., Feder, J., and Connolly, D. T. (1989). Vascular permeability factor, an endothelial cell mitogen related to PDGF. *Science* **246**, 1309-1312.

Kendall, R. L., Wang, G., and Thomas, K. A. (1996). Identification of a natural soluble form of the vacular endothelial growth factor receptor, flt-1, and its heterodimerization with KDR. *Biochem. Biophys. Res. Com.* **226**, 324-328.

Kennedy, S. H., Rouda, S., Quin, H., Aho, S., Selber, J., and Tan, E. M. (1997). Acidic FGF regulates intestitial collagenase gene expression in human smooth muscle cells. *J. Cell. Biochem.* **65**, 32-41.

Kerr, J. F. R., Wyllie, A. H., and Currie, A. R. (1972). Apoptosis: a basic biological phenomenon with wide-ranging implications in tissue kinetics. *Br. J. Cancer* **26**, 239-257.

Keyt, B. A., Nguyen, H. V., Berleau, L. T., Duarte, C. M., Park, J., Chen, H., and Ferrara, N. (1996). Identification of vascular endothelial growth factor determinants for binding KDR FLT-1 receptors-generation of receptor-selective VEGF variants by site-directed mutagenesis. *J. Biol. Chem.* **271**, 5638-5646.

Kim, S. J., Glick, A., Sporn, M. B., and Roberts, A. B. (1989). Charcterisation of the promoter region of the human transforming growth factor-beta 1 gene. *J. Biol. Chem.* **264**, 402-408.

Kim, K. J., Li, B., Winer, J., Armanini, M., Gillett, N., Phillips, H. S., and Ferrara, N. (1993). Inhibition of vascular endothelial growth factor induced angiogenesis suppresses tumour growth in vivo. *Nature* **362**, 841-844.

Kitsukawa, T., Shimizu, M., Sanbo, M., Hirata, T., Taniguchi, M., Bekku, Y., Yagi, T., and Fujisawa, H. (1997). Neuropilin semaphorin III/D-mediated chemorepulsive signals play a crucial role in peripheral nerve projection in mice. *Neuron* **19**, 995-1005.

Klagsbrun, M., and D'Amore, P. A. (1991). Regulators of angiogenesis. *Ann. Rev. Physiol.* **53**, 217.

Kleinman, H. K., McGarvey, M. L., Liotta, L. A., Robey, P. G., Tryggvason, K., and Martin, G. R. (1982). Isolation and characterization of type-IV procollagen, laminin, and heparan-sulfate proteoglycan from the EHS sarcoma. *Biochem.* **21**, 6188-6193.

Knobil, E. (1973). On the regulation of the primate corpus luteum. *Biol. Reprod.* **8**, 246-258.

Kohn, S., Nagy, J. A., Dvorak, H. F., and Dvorak, A. M. (1992). Pathways of macromolecular tracer transport across venules and small veins: structural basis for the hyperpermeability of tumor blood vessels. *Lab. Invest.* **67**, 596-607.

Kohner, E., and Henkind, P. (1970). Correlation of fluorescein angiogram and retinal digest in diabetic retinopathy. *Am. J. Opthalmol.* **69**, 403-414.

Konttinen, Y. T., Nykanen, P., Nordstrom, D., Saari, H., Sandelin, J. (1989). DNA synthesis in prolyl 4-hydroxylase positive fibroblasts in-situ in synovial tissue, an autoradiography immunoperoxidase double labelling study. *J. Rheumatol.* **16**, 339-345.

Koolwijk, P., van Erck, M. G. M., de Vree, W. J. A., Vermeer, M. A., Weich, H. A., Hanemaaijer, R., and van Hinsberg, V. W. M. (1996). Cooperative effect of TNFα, bFGF, and VEGF on the formation of tubular structures of human microvascular endothelial cells in a fibrin matrix. Role of urokinase activity. *J. Cell Biol.* **132**, 1177-1188.

Kraling, B. M., and Bischoff, J. (1998). A simplified method for growth of human microvascular endothelial cells results in decreased senescence and continued responsiveness to cytokines and growth factors. *In Vitro Cell. Dev. Biol.* **34**, 308-315.

Kremer, C., Breier, G., Risau, W., and Plate, K. H. (1997). Up-regulation of flk-1/ vascular endothelial growth factor receptor 2 by its ligand in a cerebral slice culture system. *Cancer Res.* **57**, 3852-3859.

Kroll, J., and Waltenberger, J. (1997). The vascular endothelial growth factor receptor KDR activates multiple signal transduction pathways in porcine aortic endothelial cells. *J. Biol. Chem.* **272**, 32521-32527.

Ku, D. D. Zaleski, J. K., Liu, S., and Brock, T. A. (1993). Vascular endothelial growth factor induces EDRF-dependent relaxation in coronary arteries. *Am. J. Pathol.* **265**, H586-H592.

Kubota, Y., Kawa, Y., and Mizoguchi. M. (1996). Cdw49b/CD29 integrin complex mediates the differentiation of human endothelial cells into capillary-like structures in vitro. *J. Dermatol. Sci.* **12**, 36-43

Kuhn, K. (1987). Type I, II and III. In *structure and function of collagen types.* 1-42. Eds. Mayne, R., and Burgeson, R. E. Academic Press.

Lamszuz, K., Schmid, N. O., Ergun, S., and Westphal, M. (1999). Isolation and culture of human neuromicrovascular endothelial cells. *J. Neuro. Res.* **55**, 370-381.

Lee, J., Gray, A., Yuan, J., Luoh, S. M., Avraham, H., and Wood, W. I. (1996). Vascular endothelial growth factor-related protein: a ligand and specific activator of the tyrosine kinase receptor flt-4. *Proc. Natl. Acad. Sci. USA* **93**, 1988-1992.

Lei, Z. M., Chegini, N., and Rao, C. V. (1991). Quantitative cell composition of human and bovine corpora lutea from various reproductive states. *Biol. Reprod.* **44**, 1148-1156.

Leonard, S., Luthman, D., Logel, J., Luthman, J., Antle, C., Freedman, R., and Hoffer, B. (1993). Acidic and basic fibroblast growth factor mRNAs are increased in striatum following MPTP-induced dopamine neurofiber lesion. *Mol. Brain Res.* **18**, 275-284.

Leung, D. W., Cachianes, G., Kuang, W. J., Goeddel. D, V., and Ferrara, N. (1989). Vascular endothelial growth factor is a secreted angiogenic mitogen. *Science* **246**, 1306-1309

Levy, A. P., Levy, N. S., Wegner, S., and Goldberg, M. A. (1995). Transcriptional regulation of the rat vascular endothelial growth factor gene by hypoxia. *J. Biol. Chem.* **270**, 13333-13340.

Levy, A. P., Levy, N. S., and Goldberg, M. A. (1996). Hypoxia-inducible protein binding to vascular endothelial growth factor mRNA and its modulation by the von Hippel-Lindau protein. *J. Biol. Chem.* **271**, 25492-25497.

Li, J. H., Wei, Y. Z., and Wagner, T. E. (1999). In vitro endothelial differentiation of long-term cultured murine embryonic yolk sac cells induced by Matrigel. *Stem Cells* **17**, 72-81.

Lindner, V., and Reidy, M. (1993). Expression of fibroblast growth factor and its receptor by smooth muscle cells and endothelium in injured rat arteries. An en face study. *Circ. Res.* **73**, 589-595.

Lindner, V. (1995). Role of basic fibroblast growth factor and platlet-derived growth factor (B-chain) in neointima formation after arterial injury. *J. Cardiol.* **4**, 137-144.

Liotta, L. A., Goldfarb, R. H., Brundage, R., Siegal, G. P., Terranova, V., and Garbisa, S. (1981). Effect of plasminogen activator (urokinase), plasmin, and thrombin on glycoprotein and collagenous components of the basement membrane. *Cancer Res.* **41**, 4629-4636.

Lisanti, M. P., Scherer, P. E., Tang, Z., and Sargiacomo, M. (1994). Caveolae, caveolin and caveolin-rich membrane domains: a signalling hypothesis. *Trends Cell Biol.* **4**, 231-235.

Liu, K., Brandstrom, A., Lui, Y. X., Ny, T., and Selstam, G. (1996). Coordinated expression of tissue type plasminogen activator type I during corpus luteum formation and luteolysis in the adult pseudopregnant rat. *Endocrinol.* **137**, 2126-2132.

Loskutoff, D. J., and Edington, T. E. (1979). Synthesis of a fibrinolytic activator by endothelial cells. *Proc. Natl. Acad. Sci. USA* **74**, 3903-3907.

Lui, Y. X., Cox, S. R., Morita, T., and Kourembanas, S. (1995). Hypoxia regulates vascular endothelial growth factor gene expression in endothelial cells-identification of a 5' enhancer. *Circ. Res.* 77, 638-643.

Maisonpierre, P. C. (1997). Angiopoietin-2, a natural antagonist for Tie-2 that disrupts in vivo angiogenesis. *Science* **227**, 55-60.

Maglione, D., Guerriero, V., Viglietto, G., Delli-Bovi, P., and Persico, M. G. (1991). Isolation of a human placenta cDNA coding for a protein related to the vascular permeability factor. *Proc. Natl. Acad. Sci. USA* **88**, 9267-9271

Maglione, D., Guerriero, V., Viglietto, G., Ferraro, M. G., Aprelikova, O., Alitalo, K., Vecchio, S. D., Lei, K. J., Chou, J. Y., and Persico, M. G. (1993). Two alternative mRNAs encoding for the angiogenic factor, placenta growth factor (PIGF) are transcribed from a single gene of chromosome 14. *Oncogene* **8**, 925-931.

Malvern, F., and Sawyer, C. H. (1966). A luteolytic action of prolactin in hypophysectomised rats. *Endocrinol.* **79**, 268-274.

Malvern, P. V. (1969). Hypophysial reulation of luteolysis in the rat. In *The gonads*. 367-382. McKerns, K. W. Meredith corporation.

Mann, J. S., Kinkey, M. S., Edwards, D. R., and Curry, T. E. (1991). Hormonal regulation of matrix metalloproteinase inhibitors in rat granulosa cells and ovaries. *Endocrinol.* **128**, 1825-1832.

Marshall, C. J. (1995). Specificity of receptor tyrosine kinase signaling: transient versus sustained extracellular signal-related kinase activation. *Cell* **80**, 179-185.

Masood, R., Cai, J., Zheng, T., Smith, D. L., Naidu, Y., and Gill, P. S. (1997). Vascular endothelial growth factor/vascular permeability factor is an autocrine growth factor for AIDS-Karposi sarcoma. *Proc. Natl. Acad. Sci. USA* **94**, 979-984.

Matthews, W., Jordan, C. T., Weigand, G. W., Pardoll, D., and Lemischka, I. R. (1991). A receptor tyrosine kinase specific to hematopoietic stem cells and progenitor cell enriched populations. *Cell* **65**, 1143-1152.

McCarron, R. M., Wang, L., Stanimirovic, D. B., and Spatz, M. (1995). Differential regulation of adhesion molecule expression by human cerebrovascular and umbilical vein endothelial cells. *Endothelium* **2**, 339-346.

McClure, N., Healy, D. L., Rogers, P. A., Sullivan, J., Beaton, L., Haning, R. V., Connolly, D. T., and Robertson, D. M. (1994). Vascular endothelial growth factor as a capillary permeability agent in ovarian hyperstimulation syndrome. *Lancet* **344**, 235-236.

McIntush, E. W., and Smith, M. F. (1998). Matrix metalloproteinases and tissue inhibitors of metalloproteinases in ovarian function. *Rev. Reprod.* **3**, 23-30.

Midgley, A. R. (1973). Autoradiographic analysis of gonadotropin binding to rat ovarian tissue sections. *Adv. Exp. Med. Biol.* **36**, 365.

Mignatti, P., and Rifkin, D. B. (1993). Biology and biochemistry of proteinases in tumor invasion. *Physiol. Rev.* **73**, 161-195.

Millauer, B., Wizigman-Voos, S., Schnurch, H., Martinez, R., Moller, N. P. H., Risau, W., and Ullrich, A. (1993). High affinity VEGF binding and development suggests flk-1 as a major regulator of vasculogenesis and angiogenesis. *Cell* **72**, 835-846.

Miller, E. J., Harris, E. D., Chung, E., Finch, F. E., McCroskery, P. A., and Butler, W. T. (1976). Cleavage of type II and III collagens with mammalian collagenase: Site of cleavage and primary structure of the NH-2-terminal portion of the smaller fragment released from both collagens. *Biochem.* **15**, 787-792.

Montesano, R., Roth, J., Robert, A., and Orci, L. (1982). Non-coated membrane invaginations are involved in binding and internalization of cholera and tetanus toxins. *Nature*. **296**, 651-653.

Montesano, R., Pepper, M. S., Vassalli, J. D., and Orci, L. (1992). Modulation of angiogenesis in vitro. *EXS*. **61**, 129-136.

Morbidelli, L., Chang, C. H., Douglas, J. G., Granger, H. J., Ledda, F., and Ziche, M. (1996). Nitric oxide mediates mitogenic effect of VEGF on coronary venular endothelium. *Am. J. Physiol.* **270**, H411-H415.

Morbidelli, L., Orlando, C., Maggi, C. A., Ledda, F., and Ziche, M. (1995). Proliferation and migration of endothelial cells is promoted by endothelins via activation of Etb receptors. *Am. J. Physiol. (Heart Circ. Physiol.)* **296**, H686-H695.

Morris, B., and Sass, M. B. (1966). The formation of the lymph in the ovary. *Proc. R. Soc. Br.* **164**, 577-591.

Moscatelli, D., and Rifkin, D. B. (1988). Membrane and matrix localization of proteinases: A common theme in tumor cell invasion and angiogenesis. *Biochem. Biophys. Acta*. **948**, 67-85.

Moses, M. A., Klagsbrun, M., and Shing, Y. (1995). The role of growth factors in vascular cell development and differentiation. *Int. Rev. Cytol.* **161**, 1-48.

Mukhopadhyay, D., Tsiokas, L., and Sukhatme, V. P. (1995). Wild-type p53 and v-Src exert opposing influences on human vascular endothelial growth factor gene expression. *Cancer Res.* **55**, 6161-6165.

Muller, Y. A., Christinger, H. W., Keyt, B. A., and Devos, A. M. (1997). The crystal structure of vascular endothelial growth factor (VEGF) refined to 1.93 angstrom resolution: multiple copy flexibility and receptor binding. *Structure* **5**, 1325-1338.

Murdoch, W. J., and McCormick, R. J. (1992). Enhanced degradation of collagen within apical versus basal wall of ovulatory ovine follicles. *Am. J. Physiol.* **263**, E221-E225.

Murohara, T., Horowitz, J. R., Silver, M., Tsurumi, Y., Chen, D. F., Sullivan, A., and Isner, J. M. (1998). Vascular endothelial growth factor permeability factor enhances vascular permeability via nitric oxide and prostacyclin. *Circulation* **97**, 99-107.

Murphy, G., Willenbrock, F., Ward, R. V., Cockett, M. I., Eaton, D., and Docherty, A. J. P. (1992). The c-terminal domain of 72kD gelatinase A is not required for catalysis, but essential for membrane activation and modulates interactions with tissue inhibitors of metalloproteinases. *Biochem. J.* **283**, 637-641.

Murphy, G., Segain, J. P., O'Shea, M., Cocket, M., Ioannou, O., Lefebvre, O., Chambon, P., and Basset, P. (1993). The 28-kD N-terminal domain of mouse stromelysin-3 has the general properties of a weak metalloproteinase. *J. Biol. Chem.* **268**, 15435-15441.

Myoken, Y., Kayada, Y., Okamoto, T., Kan, M., Sato, G. H., and Sato, J. D. (1991). Vascular endothelial growth factor (VEGF) produced by A-431 human epidermoid carcinoma cells and identification of VEGF membrane binding sites. *Proc. Natl. Acad. Sci. USA* **82**, 6133-6137.

Neeman, M., Abramovitch, R., Schiffenbauer, Y. S., and Tempel, C. (1997). Regulation of angiogenesis by hypoxic stress: from solid tumours to the ovarian follicle. *Int. J. Exp. Pathol.* **78**, 57-70.

Neulen, J., Yan, Z., Raczek, S., Weindel, K., Keck, C., Weich, H. A., Marme, D., and Breckwoldt, M. (1995). Human chorionic gonadotropin-dependent expression of vascular endothelial growth factor/vascular permeability factor in human granulosa cells: importance in ovarian hyperstimulation syndrome. *J. Clin. Endocrin. Metab.* **80**, 1967-1971.

Neulen, J., Raczek, J., Pogorzelski, M., Grunwald, K., Yeo, T. K., Dvorak, H. F., Weich, H. A., and Breckwoldt, M. (1998). Secretion of vascular endothelial growth factor vascular permeability factor from human luteinized granulosa cells is human chorionic gonadotrophin dependent. *Mol. Human. Reprod.* **4**, 203-206.

Newton, C. R., and Graham, A. (1994). *PCR.* 1-36. Bios Scientific Publishers Limited, Oxford.

Nicholson, R., Murphy, G., and Breathnach, R. (1989). Human and rat malignant-tumor-associated mRNAs encode stromelysin-like metalloproteinases. *Biochem.* **28**, 5195-5203.

Nicosia, R. F., and Madri, J. A. (1987). The microvascular extracellular matrix: Developmental changes during angiogenesis in the aortic-ring plasma clot model. *Am. J. Pathol.* **128**, 78-90.

Nicosia, S. V., Diaz, J., Nicosia, R. F., Saunders, B. O., and Murocacho, C. (1995). Cell proliferation and apoptosis during development and aging of the rabbit corpus luteum. *Ann. Clin. Lab. Sci.* **25**, 143-157.

Nishizuka, Y. (1993). Intracellular signaling by hydrolysis of phospholipids and activation of protein kinase C. *Science* **258**, 607-614.

Nothnick, W. B., Edwards, D. R., Leco, K. J., and Curry, T. E. (1995). Expression and activity of ovarian tissue inhibitors of metalloproteinases during pseudopregnancy in the rat. *Biol. Reprod.* **53**, 684-691.

Oh, S. J., Jeltsch, M. M., Birkenhager, R., McCarthy, J. E. G., Weich, H. A., Christ, B., Alitalo, K., and Wilting, J. (1998). VEGF and VEGF-C: specific induction of angiogenesis and lymphangiogenesis in the differentiated avian chorioallantoic membrane. *Dev. Biol.* **188**, 96-109.

Olofsson, B., Korpelainen, E., Mandriota, S., Pepper, M. S., Aase, K., Kumar, V., Gunji, Y., Jeltsch, M. M., Shibuya, M., Alitalo, K., and Eriksson, U. (1996). Vascular endothelial growth factor (VEGF) B binds to VEGF receptor-1 and regulates plasminogen activator activity in endothelial cells. *Proc. Natl. Acad. Sci. USA* **95**, 11709-11714.

Olah, I., Kendall, C., and Glick, B. (1992). Anti-vimentin monoclonal antibody recognises a cell with dendritic appearance in the chicken's bursa fabricus. *Anat. Rec.* **232**, 121-125.

Olofsson, B., Korpelainen, E., Mandriota, S., Pepper, M. S., Aase, K., Kumar, V., Gunji, Y., Jeltsch, M. M., Shibuya, M., Alitalo, K., and Eriksson, U. (1998). Vascular endothelial growth factor (VEGF) B binds to VEGF receptor-1 and regulates plasminogen activator activity in endothelial cells. *Proc. Natl. Acad. Sci. USA* **95**, 11709-11714.

Orlandini, M., Marconcini, L., Ferruzzi, R., and Olivero, S. (1996). Identification of a c-fos-induced gene that is related to the platelet-derived growth factor/vascular endothelial growth factor family. *Proc. Natl. Acad. Sci. USA* **93**, 11675-11680.

O'Sullivan, M. J. B., Stamouli, A., Thomas, E. J., and Richardson, M. C. (1997). Gonadotropin regulation of production of tissue inhibitor of MMP-1 by luteinized human granulosa cells: a potential mechanism for luteal rescue. *Mol. Hum. Reprod.* **3**, 405-410.

Page, C., Rose, M., Yacoub, M., and Pigott, R. (1992). Antigenic heterogeneity of vascular endothelium. *Am. J. Pathol.* **141**, 673-683.

Pajusola, K. (1993). Two human flt-4 receptor tyrosine kinase isoforms with distinct carboxy-terminal tails are produced by alternative processing of primary transcripts. *Oncogene* **8**, 2931-2937.

Paleolog, E. (1997). Target effector role of vascular endothelium in the inflammatory response: insights from the clinical trial of anti-TNF alpha antibody in rheumatoid arthritis. *J. Clin. Pathol.* **50**, 225-233.

Papapetropoulos, A., Garcia-Cardena, G., Madri, J. A., and Sessa, W. C. (1997). Nitric oxide production contributes to the angiogenic properties of vascular endothelial growth factor in human endothelial cells. *J. Clin. Invest.* **100**, 3131-3139.

Parton, R. G. (1994). Ultrastructural localization of gangliosides: GM1 is concentrated in caveolae. *J. Histochem. Cytochem.* **42**, 115-126.

Parton, R. G. (1996). Caveolae and caveolins. *Curr. Opin. Cell Biol.* **8**, 542-548.

Pederson, E. S. (1951). Histogenesis of lutein tissue of the rat. *Am. J. Anat.* **1**, 397-427.

Pepper, M. S., Ferrara, N., Orci, L., and Montesano, R. (1991). VEGF induces plasminogen activators and plasminogen activator inhibitor-1 in microvascular endothelial cells. *Biochem. Biophys. Res. Com.* **181**, 902-906.

Pepper, M. S., Ferrara, N., Orci, L., and Montesano, R. (1992). Potent synergism between vascular endothelial growth factor in the induction of angiogenesis in vitro. *Biochem. Biophys. Res. Com.* **198**, 824-831.

Pertovaara, L., Kaipainen, A., Mustonen, T., Orpana, A., Ferrara, N., Saksela, O., Alitalo, K. (1994). Vascular endothelial growth factor is induced in response to transforming growth factor-beta in fibroblastic and epithelial cells. *J. Biol. Chem.* **269**, 6271-6274.

Philips, H. S., Hains, J., Leung, D. W., and Ferrara, N. (1990). Vascular endothelial growth factor is expressed in rat corpora lutea. *Endocrinol.* **127**, 965-967.

Plate, K. H., Breier, G., Weich, H. A., and Risau, W. (1992). Vascular endothelial growth factor is a potential tumour angiogenesis factor in human gliomas in vivo. *Nature* **359**, 845-848.

Plendl, J., Neumuller, C., Vollmar, A., Auerbach, R., and Sinowatz, F. (1996). Isolation and characterization of endothelial cells from different organs in fetal pigs. *Anatomy and Embryology* **194**, 445-456.

Plouet, J., and Moukadiri, H. (1990). Characterization of the receptor to vasculotropin on bovine adrenal cortex-derived capillary endothelial cells. *J. Biol. Chem.* **265**, 22071-22074

Polishuk, W. Z., and Schenker, J. G. (1969). Ovarian overstimulation syndrome. *Fertil. Steril.* **20**, 443-450.

Ponce, M. L., Nomizu, M., Delgado, M. C., Kuratomi, Y., Hoffman, M. P., Powell, S., Yamada, Y., Kleinman, H. K., and Malinda, K. M. (1999). Identification of endothelial cell binding sites on the laminin gamma-1 chain. *Circ. Res.* **84**, 688-694.

Puri, M. C., Rossant, J., Alitalo, K., Bernstein, A., and Partanen, J. (1995). The receptor tyrosine kinase TIE is required for integrity and survival of vascular endothelial cells. *EMBO J.* **14**, 5884-5891.

Quinn, C. O., Scott, D. K., Brinckerhoff, C. E., Matrisian, L. M., Jeffery, J. J., and Partridge, N. C. (1990). Rat collagenase: Cloning, amino acid sequence comparison and parathyroid hormone regulation in osteoblastic cells. *J. Biol. Chem.* **265**, 13521-13527.

Quinn, T. P., Peters, K. G., DeVries, C., Ferrara, N., and Williams, L. T. (1993). Fetal liver-kinase 1 is a receptor for vascular endothelial growth factor and is selectively expressed in vascular endothelium. *Proc. Natl. Acad. Sci. USA* **90**, 7533-7537.

Rajaniemi, H. J., Midgley, A. R., Duncan, J. A., and Reichert, L. E. (1977). Gonadotropin receptors in rat ovarian tissue. Binding sites for luteinizing hormone and differentiation of granulosa cells to luteal cells. *Endocrinol.* **101**, 898.

Ray, J. M., and Stetler-Stevenson, W. G. (1994). The role of matrix metalloproteinases and their inhibitors in tumor invasion, metastasis and angiogenesis. *Eur. Respir. J.* **7**, 2026-2072.

Ravindranath, N., Little-Ihrig, L., Phillips, H. S., Ferrary, N., and Zeleznik, A. J. (1992). Vascular endothelial growth factor messenger RNA expression in the primate ovary. *Endocrinol.* **131**, 254-260.

Redmer, D. A., Dai, Y., Li, J., Charnock-Jones, D. S., Smith, S. K., Reynolds, L. P., and Moor, R. M. (1996). Characterization and expression of vascular endothelial growth factor (VEGF) in the ovine corpus luteum. *J. Reprod. Fertil.* **108**, 157-165.

Redmer, D. A., and Reynolds, L. P. (1996). Angiogenesis in the ovary. *Rev. Reprod.* **1**, 182-192.

Reich, R., Miskin, R., and Tsafriri, A. (1985). Follicular plasminogen activator: involvement in ovulation. *Endocrinol.* **116**, 516-521.

Reich, R., Miskin, R., and Tsafriri, A. (1986). Intrafollicular distribution of plasminogen activators and their hormonal regulation in vitro. *Endocrinol.* **119**, 1588-1601.

Reynolds, L. P., Killilea, S. D., and Redmer, D. A. (1992). Angiogenesis in the female reproductive system. *FASEB J.* **6**, 886-892.

Reynolds, L. P., Killilea, S. D., Grazul-Bilska, A. T., and Redmer. (1994). Mitogenic factors of corpora lutea. *Prog. Growth Factor Res.* **5**, 159-175.

Richard, L., Velasco, P., and Detmer, A. (1998). A simple immunomagnetic protocol for the selective isolation and long term culture of human dermal microvascular endothelial cells. *Exp. Cell Res.* **240**, 1-6.

Richardson, M. C., Davies, D. W., Watson, R. H., Dunsford, M. L., Inman, C. B., and Masson, G. M. (1992). Cultured granulosa cells as a model for corpus luteum function-relative roles of gonadotrophin and low density lipoprotein studied under defined culture conditions. *Hum. Reprod.* 7, 12-18.

Richardson, M. C., Slack, C., and Stewart, I. J. (1999). Rearrangement of extracellular matrix during cluster formation by luteinising granulosa cells in culture. *J. Anat.* in press.

Roberts, W. G., and Palade, G. E. (1997). Neovasculature induced by vascular endothelial growth factor is fenestrated. *Cancer Res.* **57**, 765-772.

Robinson, L. J., Pang, S. P., Harris, D. S., Heuser, J., and James, D. E. (1992). Translocation of the glucose transporter (GLUT 4) to the cell surface in permeabilized 3T3-L1 adipocytes. *J. Cell Biol.* **117**, 1181-1196.

Rojas, F. J., Moretti-Rojas, I. M., Balmaceda, J. P., and Asch, R. H. (1989). Changes in adenylate cyclase activity of the human and nonhuman primate corpus luteum during the menstrual cycle and pregnancy. *J. Clin. Endocrinol. Metab.* **68**, 379-385.

Root, L. L., and Shipley, G. D. (1991). Human dermal fibroblasts express multiple bFGF and aFGF proteins. *In Vitro cell. Dev. Biol.* **27A**, 815-822.

Rosnet, O., Marchetto, S., De Lapeyriere,O., and Birnbaum, D. (1991). Murine flt-3, a gene encoding a novel tyrosine kinase receptor of the PDGFR/CSF-1R family. *Oncogene* **6**, 1641-1650.

Roush, W. (1998). Receptor links blood vessels, axons. *Science* **279**, 2042.

Ruco, L. P., Pomponi, D., Pigott, R., Gearing, A. J. H., Biaocchini, A., and Baroni, C. D. (1992). Expression and cell distribution of the intercellular adhesion molecule, vascular cell adhesion molecule, endothelial leukocyte adhesion molecule, and endothelial cell adhesion molecule (CD31) in reactive human lymph nodes and in Hodgkin's disease. *Am. J. Pathol.* **140**, 1337-1343.

Russell, D. L., Salamonsen, L. A., and Findlay, J. L. (1995). Immunization against the N-terminal peptide of the inhibin alpha 43 subunit (alpha N) disrupts tissue remodelling and the increase in matrix metalloproteinase-2 during ovulation. *Endocrinol.* **136**, 3657-3664.

Ryuto, M., Ono, M., Izumi, H., Yoshida, S., Weich, H. A., Kohno, K., and Kuwano, M. (1996). Induction of vascular endothelial growth factor by tumor necrosis factor alpha in human glioma cells-possible roles of SP-1. *J. Biol. Chem.* **271**, 28220-28228.

Saiki, R. K., Scharf, S., Faloona, F., Mullis, K. B., Horn, G. T., Erlich, H. A., and Arnheim, N. (1985). Enzymatic amplification of beta-globin genomic sequences and restriction site analysis for diagnosis of sickle cell anemia. *Science* **230**, 1350.

Sander, P., Wolf, K., Bergmaier, U., Gess, B., and Kurtz, A. (1997). Molecular heterogeneity of basal laminae: isoforms of laminin and collagen IV at the neuromuscular junction and elsewhere. *J. Cell Biol.* **111**, 1685-1699.

Sato, Y., Shimada, T., and Takaki, R. (1991). Autocrinological role of basic fibroblast growth factor on tube formation of vascular endothelial cells in vitro. *Biochem. Biophys. Res. Com.* **180**, 1098-1102.

Sato, H., Takino, T., Okada, Y., Cao, J., Shinagawa, A., Yamamoto, E., and Seiki, M. (1994). A matrix metalloproteinase expressed on the surface of invasive tumor cells. *Nature* **370**, 61-65.

Sato, T. N., Tozawa, Y., Deutsch, U., Wolberg-Bulcholz, K., Fujiwara, Y., Gendron-Maguire, M., Gridley, T., Wolberg, H., Risau, W., and Qin, Y. (1995). Distinct roles of the receptor tyrosine kinases Tie-1 and Tie-2 in blood vessel formation. *Nature* **376**, 70-74.

Savard, K., Marsh, J. M., and Rice, B. F. (1965). Gonadotropins and ovarian steroidogenesis. *Recent Prog. Horm. Res.* **21**, 285-365.

Sawano, A., Takahashi, T., Yamaguchi, S., Aonuma, M., and Shibuya, M. (1996). Flt-1 but not KDR-flk-1 tyrosine kinase is a receptor for placenta growth factor, which is related to vascular endothelial growth factor. *Cell Growth Diff.* 7, 213-221.

Schenker, J. G., and Weinstein, D. (1978). Ovarian hyperstimulation syndrome: a current survey. *Fertil. Steril.* **30**, 255-268.

Schlessinger, J., and Ullrich, A. (1992). Growth factor signaling by receptor tyrosine kinases. *Neuron* **9**, 383-391.

Schmid, T. M., Mayne, R., Jeffery, J. J., and Lisenmayer, T. F. (1986). Type X collagen contains two cleavage sites for a vertebrate collagenase. *J. Biol. Chem.* **261**, 4184-4189.

Schwachula, A., Riemann, D., Kehlen, A., and Langer, J. (1994). Characterisation of the immunophenotype and functional properties of fibroblast-like synoviocytes in comparison to skin fibroblasts and umbilical vein endothelial cells. *Immunobiology* **190**, 67-92.

Schweigerer, L., Neufeld, G., Friedman, J., Abraham, J. A., Fiddes, J. C., and Gospodarowicz, D. (1997). Capillary endothelial cells express basic fibroblast growth factor, a mitogen that stimulates their own growth. *Nature* **325**, 257.

Seetharam, L., Gotoh, N., Maru, Y., Neufeld, G., Yamaguchi, S., and Shibuya, M. (1995). A unique signal transduction from FLT tyrosine kinase, a receptor for vascular endothelial growth factor (VEGF). *Oncogene* **10**, 135-147

Senger, D. R., Galli, S. J., Dvorak, A. M., Perruzzi, C. A., Harvey, V. S., and Dvorak, H. F. (1983). Tumor cells sectrete a vascular permeability factor that promotes accumulation of ascites fluid. *Science* **219**, 983-985.

Shaul, P. W., Smart, E. J., and Robinson, L. J. (1996). Acylation targets endothelial nitric-oxide synthase to plasmalemmal caveolae. *J. Biol. Chem.* **271**, 6518-6522.

Shibuya, M., Yamaguchi, S., Yamane, A., Ikeda, T., Tojo, A., Matsushima, H., and Sato, M. (1990). Nucleotide sequence and expression of a novel human receptor type tyrosine kinase gene (flt) closely related to the fms family. *Oncogene* **5**, 519-524.

Shibuya, M. (1995). Role of VEGF-FLT receptor system in normal and tumour angiogenesis. *Ad. Cancer Res.* **67**, 281-316.

Shinoda, K., Ishida, S., Kawashima, S., Wakabayashi, T., Matsuzaki, T., Takayama, M., Shinmura, K., and Yamada, M. (1999). Comparison of the levels of hepatocyte growth factor and vascular endothelial growth factor in aqueous fluid and serum with grades of retinopathy in patients with diabetes mellitus. *Br. J. Opthalmol.* **83**, 834-837.

Shweiki, D., Itin, A., Soffer, D., and Keshet, E. (1992). Vascular endothelial growth factor induced by hypoxia may mediate hypoxia-initiated angiogenesis. *Nature (London)* **359**, 845-848

Soker, S., Takashima, S., Miao, H. Q., Neufeld, G., and Klagsbrun, M. (1998). Neuropilin-1 is expressed by endothelial and tumor cells as an isoform specific receptor for vascular endothelial growth factor. *Cell* **92**, 735-745.

Spanel-Borowski, K., Ricken, A. M., Saxer, M., and Huber, P. R. (1994). Long-term coculture of bovine granulosa cells with microvascular endothelial cells - effect on cell growth and cell death. *Mol. Cell Endocrinol.* **104**, 11-19.

Spies, H. G., and Niswender, G. D. (1971). Levels of prolactin, LH and FSH in the serum of intact and pelvic-neuroectomised rats. *Endocrinol.* **88**, 937-943.

Stamer, W. D., Roberts, B. C., Howell, D. N., and Epstein, D. L. (1998). Isolation, culture, and characterization of endothelial cells from Schlemm's canal. *Invest. Opthalmol. Vis. Sci.* **39**, 1804-1812.

Strawn, L. M., McMahon, G., App, H., Schreck, R., Kuchler, W. R., Longhi, M. P., Hui, T. H., Tang, C., Levitzki, A., Gazit, A., Chen, I., Keri, G., Orfi, L., Risau, W., Flamme, I., Ullrich, A., Hirth, K. P., and Shawver, L. K. (1996). Flk-1 as a target for tumour growth inhibition. *Cancer Res.* **56**, 3540-3545.

Suri, C., Jones, P. F., Patan, S., Bartunkova, S., Maisonpierre, P. C., Davis, S., Sato, T. N., and Yancopoulos, G. (1996). Requisite role of angiopoitin-1, a ligand for the TIE2 receptor, during embryonic angiogenesis. *Cell* **87**, 1171-1180.

Tadakuma, H., Okamura, H., Kitaoka, M., Iyama, K. (1993). Association of immunolocalization of matrix metalloproteinase 1 with ovulation in hCG treated rabbit ovary. *J. Reprod. Fertil.* **98**, 503-508.

Tamura, T., Nakano, H., and Nagase, H. (1995). Early activation signal transduction pathways. *J. Immunol.* **155**, 4692-4701.

Tanaka, T., Andoh, N., Takeya, T., and Sato, E. (1992). Differential screening of ovarian cDNA libraries detected the expression of porcine collagenase inhibitor gene in functional corpora lutea. *Mol. Cell. Endocrinol.* **83**, 65-71.

Tao, Y. X., Lei, Z. M., Hofmann, G. E., and Rao, C. V. (1995). Human intermediate trophoblasts expresss chorionic gonadotropin/luteinizing hormone. *Biol. Reprod.* **53**, 899-904.

Terman, B. I., Carrion, M. E., Kovacs, E., Rasmussen, B. A., Eddy, R. L., and Shows, T. B. (1991). Identification of a new endothelial cell growth factor receptor tyrosine kinase. *Oncogene* **6**, 1677-1683.

Terman, B. I., Dougher-Vermazen, M., Carrion, M. E., Dimitrov, D., Armellino, D. C., Gospodarowicz, D., and Bohlen, P. (1992). Identification of the KDR tyrosine kinase as a receptor for vascular endothelial growth factor. *Biochem. Biophys. Res. Com.* **187**, 1579-1586.

Terman, B. I., Khandke, L., Doughervermazan, M., Maglione, D., Lassam, N. J., Gospodarowicz, D., Persico, M. G., Bohlen, P., and Eisinger, M. (1994). VEGF receptor subtypes KDR and FLT1 show different sensitivities to heparin and placenta growth factor. *Growth Factors* **11**, 187-195.

Tischer, E., Mitchell, R., Hartman, T., Silva, M., Gospodarowicz, D., Fiddes, J. C., and Abraham, J. A. (1991). The human gene for vascular endothelial growth factor. *J. Biol. Chem.* **266**, 11947-11954.

Tolsma, S. S., Stack, M. S., and Bouck, N. (1997). Lumen formation and other angiogenic activities of cultured capillary endothelial cells are inhibited by thrombospondin-1. *Microvasc. Res.* **54**, 13-26.

Tonnesen, M. G., Jenkins, D., Siegal, S., Lee, L. A., Huff, J. C., and Clark, R. A. F. (1985). Expression of fibronectin, laminin, and factor VIII-related antigen during development of the human cutaneous microvasculature. *J. Invest. Dermatol.* **85**, 564-568.

Tortora, G. J., and Anagnostakos, N. P. (1987). *Principles of anatomy and physiology*. (5th edn). 719-725, Harper and Row.

Trochan, V., Mabilat, C., Bertrand, P., Legrand, Y., Smadjajoffe, F., Soria, C., Delpech, B., and Lu, H. (1996). Evidence of involvement of CD44 in endothelial cell proliferation, migration and angiogenesis in vitro. *Int. J. Cancer* **66**, 664-668.

Tsafriri, A., Chun, S. Y., and Reich, R. (1993). Follicle rupture and ovulation. In *The ovary*. 227-244. Adashi, E., Leung, P. C. K. Eds. Raven Press New York.

Tsang, P. C. W., Poff, J. P., Boulton, E. P., and Condon, W. A. (1995). Four day old bovine corpus luteum: progesterone production and identification of matrix metalloproteinase activity. *Biol. Reprod.* **53**, 1160-1168.

Tuder, R. M., Flook, B. E., and Voelkel, N. F. (1995). Increased gene expression for VEGF and the VEGF receptors KDR/Flk and Flt in lungs exposed to acute or to chronic hypoxia-modulation of gene expression by nitric oxide. *J. Clin. Invest.* **95**, 1798-1807.

Ullrich, A., and Schlessinger, J. (1990). Signal transduction by receptors with tyrosine kinase activity. *Cell* **61**, 203.

Unemori, E. N., Ferrara, N., Bauer, E. A., and Amento, E. P. (1992). VEGF induces interstitial collagenase expression in human endothelial cells. *J. Cell Physiol.* **153**, 557-562.

Utoguchi, N., Dantakean, A., Makimoto, H., Wakai, T., Tsutsumi, Y., Nakagawa, S., and Mayumi, T. (1995). Isolation and properties of tumor-derived endothelial cells from rat KMT-17 fibrosarcoma. *Japanese J. Cancer Res.* **86**, 193-201.

Vaisman, N., Gospodarowicz, D., and Neufeld, G. (1990). Characterization of the receptors for vascular endothelial growth factor. *J. Biol. Chem.* **265**, 19461-19466

Venema, V. J., Zou, R., Ju, H., Marrero, M. B., and Venema, R. C. (1996). Caveolin-1 detergent solubility and association with endothelial nitric oxide synthase is modulated by tyrosine phosphorylation. *Biochem. Biophys. Res. Com.* **236**, 155-161.

Villaschi, S., and Nicosia, R. F. (1993). Angiogenic role of endogenous basic fibroblast growth factor released by rat aorta after injury. *Am. J. Pathol.* **143**, 181-190.

Vincenti, V., Cassano, C., Rocchi, M., and Persico, G. (1996). Assignment of the vascular endothelial growth factor gene to human chromosome 6P21.3. *Circ.* **93**, 1493-1495.

Waltenberger, J., Claessonwelsh, L., Siegbahn, A., Shibuya, M., and Heldin, C. H. (1994). Differential signal transduction properties of KDR and Flt-1, two receptors for VEGF. *J. Biol. Chem.* **269**, 26988-26995.

Wang, L., and Semenza, G. L. (1993). General involvement of hypoxia-inducible factor-1 in transcriptional response to hypoxia. *Proc. Natl. Acad. Sci. USA* **90**, 4303-4308.

Weidner, N., and Folkman, J. (1996). Tumoral vascularity as a prognostic factor in cancer. *Important Adv. Oncol.* 167-190.

Wellicome, S. (1993). Detection of a circulatory form of vascular cell adhesion molecule-1 with raised levels in rheumatoid arthritis and systemic lupus erythmatosus. *Clin. Exp. Immunol.* **92**, 412-418.

Wellner, M., Maasch, C., Kupprion, C., Lindschau, C., Luft, F., and Haller, H. (1999). The proliferative effect of vascular endothelial growth factor requires protein kinase C-α and protein kinase C-ζ. *Arterioscler. Thromb. Vasc. Biol.* **19**, 178-185.

Wilhelm, S. M., Collier, I. E., Kronberger, A., Eisen, A. Z., Marmer, B. L., Grant, G. A., Bauer, E. A., and Goldberg, G. I. (1987). Human skin fibroblast stromelysin: structure, glycosylation, substrate specificity, and differential expression in normal and tumorgenic cells. *Proc. Natl. Acad. Sci.* **84**, 6725-6729.

Wilhelm, S. M., Collier, I. E., Marmer, B. L., Eisen, A. Z., Grant, G. A., and Goldberg, G. I. (1989). SV40-transformed human lung fibroblasts secrete a 92-kD type IV collagenase which is identical to that secreted by normal human macrophages. *J. Biol. Chem.* **264**, 17213-17221.

Williams, G. M., Kemp, S. J. G., and Brindle, N. P. J. (1996). Involvement of protein tyrosine kinases in regulation of endothelial cell organization by basement membrane proteins. *Biochem. Biophs. Res. Com.* **229**, 375-380.

Woessner, J. F. (1994). The family of matrix metalloproteinases. *Ann. N. Y. Acad. Sci.* **732**, 11-21.

Wu, H. M., Huang, Q., Yuan, Y., and Granger, H. J. (1996). VEGF induces NO-dependent hyperpermeability in coronary venules. *Am. J. Physiol.* **271**, H2735-H2739.

Wyllie, A. H., Keer, J. F. R., and Currie, A. R. (1980). Cell death: the significance of apoptosis. *Int. Rev. Cytol.* **68**, 251-306.

Yamada, Y., Nezu, J., Shimane, M., and Hirata, Y. (1997). Molecular cloning of a novel vascular endothelial growth factor, VEGF-D. *Genomics* **42**, 483-488.

Yamomoto, S., Konishi, I., Nanbu, K., Komatsu, T., Mandai, M., Kuroda, H., Matsushita, K., and Mori, T. (1997a). Immunohistochemical localization of basic fibroblast growth factor during folliculogenesis in the human ovary. *Gynecol. Endocrinol.* **11**, 223-230.

Yamomoto, S., Konishi, I., Tsuruta, Y., Nanbu, T., Mandai, M., Kuroda, H., Matsushita, K., Hamid, A. A., Yura, Y., and Mori, T. (1997b). Expression of vascular endothelial growth factor during folliculogenesis and corpus luteum formation in the human ovary. *Gynecol. Endocrinol.* **11**, 371-381.

Yoshida, A., Anand-Apte, B., and Zetter, B. R. (1996). Differential endothelial migration and proliferation to basic fibroblast growth factor and vascular endothelial growth factor. *Growth Factors* **13**, 57-64.

Yu, Y., and Sato, D. (1999). MAP kinases, phosphatidylinositol 3-kinase, and p70 S6 kinase mediate the mitogenic response of human endothelial cells to vascular endothelial growth factor. *J. Cell. Physiol.* **178**, 235-246.

Yuan, W., and Giudice, L. C. (1997). Programmed cell death in human ovary is a function of follicle and corpus luteum status. *J. Clin. Endocrinol. Metab.* **82**, 3148-3155.

Zeleznik, A. J., Schuler, H. M., and Reichert, L. E. (1981). Gonadotropin-binding sites in the rhesus monkey ovary: role of the vasculature in the selective distribution of hCG to the preovulatory follicle. *Endocrinol.* **109**, 356-362.

Zheng, J., Redmer, D. A., and Reynolds, L. P. (1993). Vascular development and heparin-binding growth factors in the bovine corpus luteum at several stages of the estrous cycle. *Biol. Reprod.* **49**, 1177-1189.

Zheng, J., Fricke, P. M., Reynolds, L. P., and Redmer, D. A. (1994). Evaluation of growth, cell proliferation and cell death in bovine corpora lutea throughout the estrous cycle. *Biol. Reprod.* **51**, 623-632.

Ziche, M., Morbidelli, L., Choudhuri, R., Zhang, H., Donnini, S., Granger, H. J., and Bicknell, R. (1997). Nitric oxide synthase lies downstream from vascular endothelial growth factor-induced but not basic fibroblast growth factor-induced angiogenesis. *J. Clin. Invest.* **99**, 2625-2634.